TE
5092
.M8A3
no.
71-1
c.2

2856

JUN 30 1973

COOPERATIVE HIGHWAY RESEARCH PROGRAM
REPORT 71-1

Property of
MoDOT TRANSPORTATION LIBRARY

# TIME-DEPENDENT DEFORMATIONS OF CONCRETE

MISSOURI STATE HIGHWAY DEPARTMENT
FEDERAL HIGHWAY ADMINISTRATION
UNIVERSITY OF MISSOURI, COLUMBIA

## List of Previous Reports for this Project

Meyers, B.L., "A Review of Literature Pertaining to Creep and Shrinkage of Concrete," University of Missouri, Engr. Exp. Station Bul. No. 56 Feb. 26, 1963.

Pauw, A., and Meyers, B.L., "Apparatus and Instrumentation for Creep and Shrinkage Studies," MCHRP Report, (also in Highway Research Record No. 34, Publication 1154), University of Missouri, 1963.

Buettner, Donald R., and Hollrah, Ronald L., "Creep Recovery and Creep of Preshrunk Concrete," MCHRP Report, University of Missouri, 1965.

Long, Jack R., and Buettner, Donald R., "Deflections of Prestressed Concrete Beams" MCHRP Report, University of Missouri, 1966.

Buettner, Donald R., and Bhavsar, Pravin D., "Creep and Damping Characteristics of Concrete," MCHRP Report, University of Missouri, 1966.

Pauw, Adrian, and Chai, James Wen-Yu, "Creep and Creep Recovery for Plain Concrete," MCHRP Report 67-8, 1967.

Pauw, Adrian, and Sherkat, A. Akbar, "Time-Dependent Deflection of a Box Girder Bridge," MCHRP Report 67-9, 1967.

Bayazid, Hakam, and Pauw, Adrian, "Creep and Shrinkage of Eccentrically Loaded Prisms," MCHRP Report 68-15, 1968.

## Unpublished Thesis Reports Related to this Project

McCafferty, Robert M., "Sustained-Load Deflections of Concrete Beams," M.S. Thesis, University of Missouri, August 1963.

Brautigam, Paul A., "Deflections and Strains in Reinforced Concrete Bridges," M.S. Thesis, University of Missouri, 1965.

Jones, Myron L., "Deflection of Concrete Beams due to Sustained Load," M.S. Thesis, University of Missouri, January 1966.

Hollrah, Ronald L., "Rheological Models for the Deformation of Concrete", Ph.D. Thesis, University of Missouri, May 1971.

TF
5092
.M8A3
no. 71-1

TECHNICAL REPORT STANDARD TITLE PAGE

DEPARTMENT OF
JUN 29 1973

| | | |
|---|---|---|
| 1. Report No. | 2. Government Accession No. | 3. Recipient's Catalog No. |
| 4. Title and Subtitle<br>Time-Dependent Deformations of Concrete | | 5. Report Date<br>September 1971<br>6. Performing Organization Code |
| 7. Author(s)<br>Adrian Pauw, Professor | | 8. Performing Organization Report No.<br>MCHRP 71-1 |
| 9. Performing Organization Name and Address<br>University of Missouri - Columbia<br>Department of Civil Engineering<br>Columbia, Missouri | | 10. Work Unit No.<br>11. Contract or Grant No.<br>60-2 |
| 12. Sponsoring Agency Name and Address<br>Missouri State Highway Department<br>Jefferson City, Missouri 65101 | | 13. Type of Report and Period Covered<br>Final<br>14. Sponsoring Agency Code<br>2856 |

15. Supplementary Notes

In cooperation with U. S. Department of Transportation, Federal Highway Administration

16. Abstract

This final project report summarizes the research efforts on a Missouri Cooperative Highway Research Project initiated in 1959 to study the effects of creep and shrinkage on the deflection of reinforced concrete bridges. The results of the experimental phase of the program are summarized and compared with the theories and observations of other researchers.

Methods for predicting the elastic and time-dependent properties of concrete based on the concrete constituents are developed. Methods of analysis for predicting the structural behavior of plain and reinforced concrete members based on assumed load history and elastic and time-dependent properties of concrete are also presented. Finally, design recommendations are summarized for estimating material properties and for calculating time-dependent stresses and strains in reinforced concrete beams and columns.

| | | | |
|---|---|---|---|
| 17. Key Words<br>concrete creep, concrete shrinkage, time dependent properties of concrete, deflections of concrete structures | | 18. Distribution Statement | |
| 19. Security Classif. (of this report)<br>Unclassified | 20. Security Classif. (of this page)<br>Unclassified | 21. No. of Pages<br>297 | 22. Price |

Form DOT F 1700.7 (8-69)

## Abstract

This final project report summarizes the research efforts on a Missouri Cooperative Highway Research Project initiated in 1959 to study the effects of creep and shrinkage on the deflection of reinforced concrete bridges. The results of the experimental phase of the program are summarized and compared with the theories and observations of other researchers.

Methods for predicting the elastic and time-dependent properties of concrete based on the concrete constituents are developed. Methods of analysis for predicting the structural behavior of plain and reinforced concrete members based on assumed load history and elastic and time-dependent properties of concrete are also presented. Finally, design recommendations are summarized for estimating material properties and for calculating time-dependent stresses and strains in reinforced concrete beams and columns.

Acknowledgements

The work described in this report was initially proposed by the author in 1958. The experimental phase was initiated in September 1959 with Dr. Bernard L. Meyers as project engineer. Upon Dr. Meyers' departure from the University of Missouri, the experimental phases were completed under the direction of Prof. Donald R. Buettner, presently Professor of Civil Engineering, University of Wisconsin at Milwaukee. The analytical work was performed under the direction of the author of this final report.

Sincere appreciation is expressed to the personnel of the Missouri State Highway Commission and of the Federal Highway Administration, associated with this project, for their many suggestions, interest and encouragement and for providing the financial resources to support the university staff and graduate students employed on this project. The author is also indebted to the College of Engineering for the release time and staff assistance provided the past three years to complete this final report. The contributions of Messrs H. Bayazid, P.D. Bhavsar, P.A. Brautigam, Wen-Yu Chai, R.L. Hollrah, M.L. Jones, J.R. Long, R.M. McCafferty, and A.A. Sherkat, graduate research assistants employed on this project, is also acknowledged.

TIME-DEPENDENT DEFORMATIONS

OF CONCRETE

TABLE OF CONTENTS


Chapter Page

I. SUMMARY OF CREEP RESEARCH PROGRAM

1.1 Introduction . . . . . 1
1.2 Scope and Objectives . . . . . 1
1.3 Literature Review. . . . . 2
1.4 Creep Laboratory . . . . . 3
1.5 Phenomenological Studies . . . . . 3
1.6 Structural Response to Creep and Shrinkage . . . . . 5
1.7 Objective of Summary Report. . . . . 8

II. DEFORMATIONS OF CONCRETE UNDER CONSTANT SUSTAINED COMPRESSIVE STRESS

2.1 Introduction . . . . . 9
2.2 Components of Strain . . . . . 10
2.3 Instantaneous Strains. . . . . 14
2.4 Level of Stress. . . . . 17
2.5 Modulus of Elasticity. . . . . 17
2.6 Age at Time of Loading . . . . . 18
2.7 Creep Recovery . . . . . 20

III. DEFORMATION PROPERTIES OF PLAIN CONCRETE - STATE OF THE ART

3.1 Introduction . . . . . 22
3.2 Compressive Strength . . . . . 23
3.3 Modulus of Rupture and Tensile Strength. . . . . 25
3.4 Elastic Modulus. . . . . 26
3.5 Factors Influencing Shrinkage Strains in Plain Concrete . . . . . 31
3.6 Prediction of Shrinkage Strains. . . . . 35
3.7 Creep Characteristics. . . . . 45
3.8 Creep Prediction . . . . . 47
3.9 Temperature Effects. . . . . 58

IV. PREDICTION OF AXIAL DEFORMATION UNDER TIME-DEPENDENT COMPRESSIVE STRESS

4.1 Introduction . . . . . 59
4.2 The Effective Modulus Method . . . . . 60
4.3 The Method of Superposition. . . . . 62
4.4 The Rate-of-Creep Method . . . . . 63

Chapter Page

4.5 Comparison of Analytical Results with Experimental Data. . . . . 66
4.6 The Rate-of-Flow Method. . . . . 70
4.7 The Residual Creep Limit Method. . . . . 76
4.8 Modified Effective Modulus Method. . . . . 82

V. ELASTIC AND TIME-DEPENDENT DEFORMATIONS OF CONCENTRICALLY LOADED COLUMNS

5.1 Introduction . . . . . 83
5.2 Basic Analysis Assumptions . . . . . 83
5.3 Section Rigidity Profile . . . . . 84
5.4 Shrinkage Strains by the Section - Rigidity Method. . . . . 85
5.5 Comparison of Computed Shrinkage Values with Test Data. . . . . 88
5.6 Elastic and Creep Strains by the Section-Rigidity Method. . . . . 88
5.7 Creep and Shrinkage Strains by the Rate-of-Creep Method . . . . . 94
5.8 The Modified Rate-of-Creep Method. . . . . 99
5.9 Comparison of Analysis Methods . . . . . 102
5.10 Analysis for Variable Loading. . . . . 104
5.11 Stress-Time and Strain-Time Relationships . . . . . 108
5.12 Prestress Losses in Uniformly Prestressed Elements . . . . . 109

VI. ELASTIC AND TIME DEPENDENT DEFORMATIONS OF FLEXURAL MEMBERS

6.1 Introduction . . . . . 110
6.2 Basic Assumptions-Moment Curvature and Deflection Calculations. . . . . 112
6.3 Calculation of Section Rigidity - Section Moulding . . . . . 118
6.4 Section Properties - Rectangular Beams with Tension Reinforcement Only. . . . . 127
6.5 Section Properties - Flanged Beams and Beams with Compression Reinforcement . . . . . 138
6.6 Analysis of Shrinkage and Temperature Effects. . . . . 146
6.7 Typical Computations . . . . . 151
6.8 Summary and Conclusions. . . . . 155

VII. SUMMARY AND RECOMMENDATIONS

7.1 Summary. . . . . 157
7.2 Design Recommendations - Material Properties . . . . . 157
7.2.1 Strength of Concrete. . . . . 158
7.2.2 Elastic Modulus . . . . . 159
7.2.3 Shrinkage . . . . . 160
7.2.4 Creep . . . . . 162
7.3 Design Recommendations - Concentrically Loaded Columns . . . . . 165

Chapter Page

7.3.1 Section Rigidity Method . . . . . 165
7.3.2 Rate-of-Creep Method. . . . . 168
7.4 Design Recommendations - Flexural Members. . . . . 168
7.4.1 Flexural Stressed Due to Load . . . . . 169
7.4.2 Effect of Member Geometry and Support Constraints . . . . . 171
7.4.3 Section Properties. . . . . 172
7.4.4 Stress and Deflection Augmentation Factors . . . . . 176
7.4.5 Shrinkage Stresses and Deflections. . . . . 177
7.5 Analysis for Delayed Load Application. . . . . 179
7.6 Recommendations for Further Research . . . . . 179

BIBLIOGRAPHY. . . . . 181

Appendix

I-A PHENOMENOLOGICAL STUDIES . . . . . 187
Introduction. . . . . 187
Objectives and Scope of Test Program. . . . . 187
Analysis of Test Data . . . . . 188
Test Specimens. . . . . 189
Fabrication and Curing of Test Specimens. . . . . 190
Loading Procedure and Instrumentation . . . . . 190
Shrinkage Measurements. . . . . 197
Test Results. . . . . 197
Variation in Measured Data. . . . . 197
Influence of Mix Constituents . . . . . 201
Creep and Shrinkage Prediction Formulas . . . . . 213
Conclusions . . . . . 214

I-B RHEOLOGICAL MODELS . . . . . 215

II-A THE EFFECT OF AGGREGATE CONTENT ON THE ELASTIC AND CREEP STRAINS OF MORTAR AND CONCRETE . . . . . 233
Mechanical Model. . . . . 233
Rheological Model . . . . . 237

II-B THE EFFECT OF AGGREGATE CONTENT ON THE SHRINKAGE OF CONCRETE. . . . . 243
Introduction. . . . . 243
The Model . . . . . 243
Analysis. . . . . 243
Conclusions . . . . . 248

II-C RELEVANT PROVISIONS REGARDING CREEP AND SHRINKAGE IN THE PROPOSED REVISED CEB CODE . . . . . 251
Linear Deformations . . . . . 251
Shrinkage . . . . . 252
Creep . . . . . 255
Total Deformation . . . . . 259
Determination of Deformation Modulus for Axial Strains . . . . . 260

Appendix | Page


III-A THE RATE-OF-CREEP METHOD FOR PREDICTING COLUMN STRAINS . . . . . 261
Introduction . . . . . 261
Derivation of Time-Dependent Stress-Strain Equations. . . . . 261
Shrinkage. . . . . 264

IV-A BEAMS WITH PIECEWISE CONSTANT MOMENTS OF INERTIA . . . . . 267
Piecewise Constant Section Approximation . . . . . 267
Location of Points of Inflection . . . . . 267
Centerline Deflection. . . . . 269
Computation of Support Moments . . . . . 272
Iterative Computation. . . . . 274

LIST OF FIGURES


| Figure | | Page |
|---|---|---|
| 1 | Strain Components | 12 |
| 2 | Strains in a Loaded Concrete Specimen in a Drying Environment | 13 |
| 3 | Idealized Representation of a Cyclic Stress-Strain Diagram | 16 |
| 4 | Idealized Stress-Strain Diagram Recommended by CEB | 16 |
| 5 | Specific Creep Surface | 19 |
| 6 | Residual Creep Limit Curve | 21 |
| 7 | Time Dependent Strain Variables | 24 |
| 8 | Mechanical Model of Concrete | 27 |
| 9 | Effect of Water-Cement Ratio and Age on the Secant Modulus of Elasticity of Cement Paste | 29 |
| 10 | Shrinkage Constants Determined by the Hyperbolic Equation (Typical) | 37 |
| 11 | Variation of the Degree of Hydration with Curing Time | 39 |
| 12 | Effect of Aggregate Concentration on Shrinkage | 39 |
| 13 | "Standard" Specific Creep Curve for a Typical Lightweight Aggregate Concrete | 51 |
| 14 | Correction-Factors for Modifying "Standard" Creep Curve | 52 |
| 15 | Relationship Between Percent Creep and Paste Ratio | 55 |
| 16 | Effective Modulus-$E_{ce}$ | 61 |
| 17 | Superposition Principle, Sum of Elastic and Creep Strain | 64 |
| 18 | Creep Recovery for Mature Concrete | 65 |
| 19 | Approximation of Stress History | 65 |
| 20 | Rate-of-Creep Method | 67 |
| 21 | Comparison of Creep Analysis Methods | 68 |
| 22 | Strain Components for Rate-of-Flow Method | 71 |
| 23 | Basic Creep Data for Rate-of-Flow Method | 74 |
| 24 | Plot for Determining Q-Values | 75 |
| 25 | Total Creep and Creep Limit Curves | 77 |
| 26 | Characteristic Age | 79 |
| 27 | Limiting Total Creep and Flow Ratios | 79 |
| 28 | Column Shrinkage, Section Rigidity Method | 89 |
| 29 | Prediction of Column Shrinkage | 90 |
| 30 | Elastic and Creep Column Stress, Section Rigidity Method | 92 |
| 31 | Design Aid for Rate-of-Creep Method | 97 |
| 32 | Moment-Couple in Reinforced Concrete Beam | 111 |
| 33 | Moment and Section Rigidities for Haunched Beam | 115 |
| 34 | Flexural Rigidity as Function of Modular Ratio - Interior Span of a Box Girder Bridge [19] | 117 |
| 35 | Section Moulding | 119 |
| 36 | T-Beam | 121 |

| Figure | | Page |
|---|---|---|
| 37 | Transformed Area, Rectangular Beam with Tension Reinforcement Only | 128 |
| 38 | Depth of Compression Zone as Function of Transformed Steel Area | 130 |
| 39 | Moment of Inertia Coefficient | 130 |
| 40 | Concrete Stress Coefficient | 131 |
| 41 | Steel Stress Coefficient | 131 |
| 42 | Steel Stress Multiplier | 133 |
| 43 | Concrete Stress Multiplier | 133 |
| 44 | Deflection Multiplier | 134 |
| 45 | Rectangular Beam-Tension Reinforcement Only | 135 |
| 46 | Flanged Beams and Beams with Compression Reinforcement | 139 |
| 47 | Equilibrium Conditions for Flanged Beams | 140 |
| 48 | Compression Zone Depth Ratio Flanged Beams | 142 |
| 49 | Warping Analysis for Uniform Shrinkage | 147 |
| 50 | Shrinkage Coefficient - Rectangular Beams, Tension Reinforcement Only | 149 |


Appendix I-A


| | | |
|---|---|---|
| 1 | Typical Creep and Shrinkage Strains | 198 |
| 2 | Spectrum of Creep vs. Age | 200 |
| 3 | Spectrum of Shrinkage vs. Age | 200 |
| 4 | One Year Creep as Function of Stress-Strength Ratio | 205 |
| 5 | One Year Creep as Function of Paste Volume Ratio | 205 |


Appendix I-B


| | | |
|---|---|---|
| 1 | The Burgers Body | 216 |
| 2 | Model Suggested by Flugge | 216 |
| 3 | Elementary Model, Torroja and Paez | 217 |
| 4 | Complete Model, Torroja and Paez | 217 |
| 5 | Non-Linear Maxwell Model Suggested by Chang | 219 |
| 6 | Model Suggested by Freudenthal and Roll | 219 |
| 7 | Model Suggested by Hansen | 220 |
| 8 | Simplified Model Suggested by Hansen | 220 |
| 9 | Models by Glucklich (First Theory) | 222 |
| 10 | Model by Flucklich (Second Theory) | 223 |
| 11 | Creep Strain - Time Curve (Glucklich) | 223 |
| 12 | Model Proposed by Constantinescu-Catunesti | 225 |
| 13 | Model Proposed by Glucklich and Ishai | 225 |
| 14 | Another Model by Glucklich and Ishai | 226 |
| 15 | Model for Prestressed Concrete (Hansen) | 228 |
| 16 | Second Model for Prestressed Concrete (Hansen) | 228 |
| 17 | Non-Linear Maxwell Model Proposed by Desayi and Sen | 229 |

Figure | Page

Appendix II-A


1 England's Mechanical Model. . . . . 234
2 Force System. . . . . 234
3 Burgers Body. . . . . 240
4 Hollrah's Rheological Model . . . . . 240
5 Creep and Shrinkage Strain Response . . . . . 242


Appendix II-B


1 Body-Centered Aggregate-Paste Model . . . . . 244
2 Free Shrinkage of Shell Compensated by Negative Hydrostatic Pressure. . . . . 244
3 Equilibrium Restoring Forces. . . . . 246
4 Equilibrium of Paste Shell. . . . . 246


Appendix II-C


Coefficient $\psi$ (Environment). . . . . 253
Coefficient $\alpha_s$ (Dimensions) . . . . . 253
Coefficient $\beta_s$ (Composition). . . . . 254
Coefficient $\rho^*$ (Age). . . . . 255
Coefficient $\phi_o$ (Climatic Condition) . . . . . 257
Coefficient $\alpha_f$ (Effective Thickness). . . . . 258
Coefficient $\zeta$ (Age at Loading) . . . . . 258


Appendix IV-A


1 Assumed Regions of Piecewise Constant Section Rigidity . . . . . 268
2 Location of Point of Contraflexure. . . . . 270
3 Stiffness Parameters A, B, and C. . . . . 271
4 Stiffness Parameter D . . . . . 273

LIST OF TABLES


| Table | | Page |
|---|---|---|
| I | Constants for Time-Dependent Strength Relationship | 25 |
| II | Elastic Modulus of Aggregates | 30 |
| III | Average Increase in Creep | 47 |
| IV | Comparison of Observed and Computed Results, Section-Rigidity Method | 95 |
| V | Comparison of Observed and Computed Results, Rate-of-Creep Method | 100 |
| VI | Comparison of Observed and Computed Results, Modified Rate-of-Creep Method | 103 |
| VII | Comparison of Results from Three Methods of Analysis | 104 |
| VIII | Comparison of Methods of Analysis | 105 |
| IX | T-Beam Section Properties by Section Moulding | 124 |
| | Appendix I-A | |
| I | Concrete Mix Data | 191 |
| II | Creep | 202 |
| III | Shrinkage | 207 |
| IV | Time-Dependent Strains in Reinforced Concrete | 212 |
| | Appendix II-A | |
| I | Ratio-Predicted/Observed Values | 238 |

## Notation

Reference shows where symbol is first defined. Where symbol has more than one meaning separate references are given.

| | | | Reference |
|---|---|---|---|
| $A$ | = | time dependent coefficient | Eq. 2 |
| $A$ | = | constant ranging between 0 and 1 | Eq. 8 |
| $A$ | = | empirical constant | Eq. 15,30,42,49 |
| $A_g$ | = | gross area of section | Eq. 56 |
| $A_{gcu}$ | = | gross area of section transformed to equivalent concrete after creep | Eq. 56 |
| $A_i$ | = | beam stiffness parameter, i=1,2 | Eq. 86 |
| $A_j$ | = | total area of first j sections | Eq. 87 |
| $A_s$ | = | area of tensile reinforcement | Eq. 92 |
| $A'_s$ | = | area of compressive reinforcement | Eq. 103 |
| $B$ | = | time dependent coefficient | Eq. 2 |
| $B$ | = | empirical constant | Eq. 15,30,40 |
| $B_i$ | = | beam stiffness parameter, i=1,2 | Eq. 86 |
| $C$ | = | empirical constant | Eq. 30 |
| $C_{fr}$ | = | Constant relating creep to paste ratio | Eq. 35 |
| $C_i$ | = | beam stiffness parameter, i=1,2 | Eq. 86 |
| $C_{ij}$ | = | moment carry-over factor, i to j | App. IV-A |
| $C_t$ | = | creep ratio, ($t_\ell$ days after loading) | Eq. 29 |
| $C_u$ | = | limiting value of $C_t$ | Eq. 29 |
| $C_{ud}$ | = | modified limiting creep ratio | Eq. 81 |
| $(C.F.)_{cp}$ | = | creep correction factor | Eq. 33 |

| | | Reference |
|---|---|---|
| $(C.F.)_{sh}$ | = shrinkage correction factor | Eq. 28 |
| $D_i$ | = beam stiffness parameter, i=1,2 | App. IV-A |
| $E$ | = modulus of elasticity | Eq. 82 |
| $E$ | = beam stiffness parameter | App. IV-A |
| $E_a$ | = modulus of elasticity of aggregate | Eq. 8 |
| $E_c$ | = modulus of elasticity of concrete | Eq. 3 |
| $E_{ca}$ | = modulus of elasticity of coarse aggregate | App. II-A |
| $E_{cc}$ | = creep strain modulus of concrete (CEB) | App. II-C |
| $E_{cd}$ | = effective delayed elastic modulus | Eq. 79 |
| $E_{ce}$ | = effective modulus of elasticity of concrete | Eq. 41 |
| $E_{cu}$ | = limiting value of $E_{ce}$ | Eq. 54 |
| $E_{fa}$ | = modulus of elasticity of fine aggregate | App. II-A |
| $E_m$ | = modulus of elasticity of mortar | App. II-A |
| $E_{ma}$ | = modulus of elasticity of matrix | App. II-A |
| $E_{mu}$ | = limiting effective value of $E_m$ | App. II-A |
| $E_p$ | = modulus of elasticity of paste | Eq. 8 |
| $E_{pu}$ | = limiting effective value of $E_p$ | App. II-A |
| $E_s$ | = modulus of elasticity of reinforcement | Eq. 53 |
| $F$ | = force | App. II-A |
| $F_i$ | = beam stiffness parameter, i=1,2 | App. IV-A |
| $F_{mp}$ | = parallel force component | App. II-A |
| $F_{ms}$ | = series force component | App. II-A |
| $F_s$ | = effective shrinkage force | Eq. 118 |
| $G_i$ | = beam stiffness parameter, i=1,2 | App. IV-A |
| $G_k$ | = spring constant | App. I-B |
| $G_m$ | = spring constant | App. I-B |

| | | Reference |
|---|---|---|
| $H$ | = relative humidity | Eq. 17 |
| $I$ | = moment of inertia | Eq. 82 |
| $I_e$ | = effective I of reinforced section transformed to equivalent concrete after creep | Eq. 128 |
| $I_i$ | = moment of inertia of beam section at end i | App. IV-A |
| $I_j$ | = centroidal moment of inertia of area $A_j$ | Eq. 90 |
| $K_b$ | = beam section rigidity ($K_b = EI$) | Eq. 82 |
| $K_{be}$ | = effective value of $K_b$ after creep | Eq. 82 |
| $K_{bi}$ | = initial value of $K_b$ | Eq. 84 |
| $K_{bu}$ | = ultimate value of $K_b$, $t \to \infty$ | Eq. 84 |
| $K_c$ | = section rigidity at center of beam | Eq. 86 |
| $K_{ei}$ | = section rigidity at end i of beam | Eq. 86 |
| $K_i$ | = stiffness factor at end i | App. IV-A |
| $M$ | = bending moment | Eq. 82 |
| $M_{d\ell}$ | = dead load moment | p. 152 |
| $M_{\ell i}$ | = end support moment, i=1,2 | Eq. 85 |
| $M_i^{FE}$ | = fixed end moment, i=1,2 | App. IV-A |
| $M_{\ell\ell}$ | = live load moment | p. 152 |
| $M_{max}$ | = maximum positive bending moment | Eq. 83 |
| $M_o$ | = simple beam moment | Eq. 85 |
| $M_s$ | = shrinkage or warping moment | Eq. 120 |
| $P$ | = total axial column load | Eq. 59 |
| $Q$ | = empirical constants, rate of flow method | Eq. 45 |
| $R_p$ | = elastic modulus for plain strain | App. II-B |
| $S$ | = surface area | Eq. 13 |
| $T$ | = temperature, (deg.C, CEB) | App. II-C |

| | | Reference |
|---|---|---|
| $V$ | = volume | Eq. 13 |
| $V_a$ | = volumetric fraction of aggregate | Eq. 8 |
| $V_c$ | = volume of cement | Eq. 14 |
| $V_{ch}$ | = volume concentration of hydrated cement | Eq. 15 |
| $V_{cu}$ | = volume concentration of unhydrated cement | Eq. 14 |
| $V_{fa}$ | = volume ratio of fine aggregate in mortar | App. II-B |
| $V_p$ | = volumetric fraction of paste | Eq. 8 |
| $V_s$ | = volume of solids | Eq. 14 |
| $W$ | = unit weight of concrete, pcf | Eq. 3 |
| $W_r$ | = ratio of evaporable water to evaporable water content at saturation | App. I-B |
| $a$ | = empirical constant | Eq. 5,11,39 |
| $a$ | = deflection | Eq. 85 |
| $a_i$ | = initial or elastic deflection | Eq. 84 |
| $a_{max}$ | = maximum deflection | Eq. 83 |
| $a_s$ | = deflection due to shrinkage | Eq. 122 |
| $a_u$ | = ultimate deflection after creep | Eq. 84 |
| $b$ | = empirical constant | Eq. 5,11,39 |
| $b$ | = total beam width | Eq. 92 |
| $b_f$ | = net flange width, $b=b-b_w$ | Eq. 101 |
| $b_w$ | = web width | Eq. 101 |
| $d$ | = empirical constant | Eq. 13 |
| $d$ | = effective depth of R/C beam | Eq. 92 |
| $d'$ | = depth of compression reinforcement | Eq. 105 |
| $e$ | = base of Naperian logarithm | Eq. 4 |
| $e$ | = empirical exponent | Eq. 12 |

| | | Reference |
|---|---|---|
| $e_s$ | = eccentricity of warping force | Eq. 119 |
| $f'_c$ | = compressive strength (28-day cylinder) | Eq. 3 |
| $f_{cr}$ | = modulus of rupture | Eq. 6 |
| $f'_c(t)$ | = compressive strength at age t days | Eq. 5 |
| $f_{ct}$ | = tensile strength | Eq. 7 |
| h | = degree of hydration | Eq. 14 |
| $h_m$ | = effective depth, cm (CEB) | Eq. 26 |
| $h_x$ | = depth of prism | Eq. 31 |
| k | = age at time of initial load application, days | Eq. 4 |
| k' | = age k for reference specimen | Eq. 52 |
| k | = compression zone depth ratio | Eq. 92 |
| $k_e$ | = compression zone depth ratio after creep | Eq. 128 |
| $k_{ef}$ | = effective flange area ratio | Eq. 105 |
| $k_{efu}$ | = limiting value of $k_{ef}$ after creep | Eq. 121 |
| $k_i$ | = initial value of k, before creep | Eq. 96 |
| $k_t$ | = uncracked tension zone depth ratio | Eq. 130 |
| $k_u$ | = limiting value of k, after creep | Eq. 96 |
| $\ell$ | = length of span | Eq. 83 |
| m | = time dependent coefficient | Eq. 2 |
| m | = empirical constant | Eq. 4, App. I-B |
| $m_i$ | = end moment ratio, i=1,2 | Eq. 86 |
| n | = exponent | App. 1-B |
| p | = empirical constant | Eq. 4 |
| p | = perimeter | App. II-C |
| r | = empirical constant | Eq. 4 |

| | | Reference |
|---|---|---|
| $r$ | = radius of curvature | Eq. 82 |
| $r_{su}$ | = radius of curvature due to shrinkage | Eq. 121 |
| $s_j$ | = distance between centroids of area $A_j$ and $\Delta A_j$ | Eq. 88 |
| $t$ | = total depth of beam | Fig. 46 |
| $t$ | = age from time of casting, days | Eq. 4 |
| $t_c$ | = characteristic time factor | Eq. 33 |
| $t_{ck}$ | = characteristic creep time (half-life), days | Eq. 48 |
| $t_d$ | = time after drying, days | Eq. 9 |
| $t_e$ | = effective time (CEB) | Eq. 26 |
| $t_f$ | = flange thickness | Eq. 101 |
| $t_i$ | = age at time load is removed, days (CEB) | App. II-C |
| $t_\ell$ | = time after loading, days | Eq. 29 |
| $t_n$ | = age of concrete (CEB) | App. II-C |
| $t_r$ | = age modified for curing temperature (CEB) | App. II-C |
| $t_{sk}$ | = characteristic shrinkage time (half-life), days | Eq. 9 |
| $t_1$ | = age at time of loading, days (CEB) | App. II-C |
| $w$ | = uniformly distributed load | Eq. 85 |
| $x_e$ | = eccentricity of load | Eq. 31 |
| $x_i$ | = end distance to point of inflection | Eq. 86 |
| $\bar{y}_j$ | = distance of centroid of area $A_j$ from reference axis | Eq. 88 |
| $\alpha$ | = empirical constant | Eq. 4 |
| $\alpha_c$ | = empirical constant (for creep magnitude) | Eq. 526 |
| $\alpha_{ct}$ | = empirical constant (for modifying $t_c$) | Eq. 127 |
| $\alpha_{cu}$ | = empirical coefficient (for estimating creep) | Eq. 36) |

| | | Reference |
|---|---|---|
| $\alpha_{ef}$ | = effective flange area ratio | Eq. 104 |
| $\alpha_{efu}$ | = value of $\alpha_{ef}$ after creep | Eq. 121 |
| $\alpha_f$ | = creep multiplier for member size (CEB) | App. II-C |
| $\alpha_{fa}$ | = flange area ratio | Eq. 101 |
| $\alpha_{gc}$ | = transformed area ratio | Eq. 56a |
| $\alpha_{gcu}$ | = value of $\alpha_{gc}$ after creep | Eq. 56 |
| $\alpha_i$ | = haunch flexibility ratio, $K_c/K_{ei}$, i=1,2 | Eq. 86 |
| $\alpha_m$ | = correction factor for member size | Eq. 13 |
| $\alpha_{oy}$ | = slope of elastic strain gradient | Eq. 32 |
| $\alpha_r$ | = coefficient for modulus of rupture | Eq. 6 |
| $\alpha_s$ | = shrinkage correction factor for member size (CEB) | Eq. 24 |
| $\alpha_{sk}$ | = factor to compute $t_{sk}$ | Eq. 27 |
| $\alpha_t$ | = tensile strength coefficient | Eq. 7 |
| $\alpha_{ty}$ | = elastic strain gradient | Eq. 31 |
| $\alpha_1$ | = spring compliance factor | Eq. 38 |
| $\alpha_2$ | = spring compliance factor | Eq. 38 |
| $\beta$ | = empirical constant | Eq. 4 |
| $\beta$ | = gel compliance factor | Eq. 38 |
| $\beta_a$ | = aggregate size ratio | App. II-B |
| $\beta_{a1}$ | = value of $\beta_a$ for mortar | App. II-B |
| $\beta_{a2}$ | = value of $\beta_a$ for concrete | App. II-B |
| $\beta_c$ | = limiting creep ratio | Eq. 52 |
| $\beta_d$ | = delayed elastic strain ratio | Eq. 79 |
| $\beta_e$ | = tee beam parameter | Eq. 109 |
| $\beta_f$ | = mix composition parameter for creep (CEB) | App. II-C |
| $\beta_s$ | = mix composition parameter for shrinkage (CEB) | Eq. 24 |
| $\beta_t$ | = coefficient for modifying $t_c$ | Eq. 127 |

| | | Reference |
|---|---|---|
| $\gamma_e$ | = tee-beam parameter | Eq. 110 |
| $\gamma_{vs}$ | = mass factor | Eq. 13 |
| $\delta_a$ | = deflection multiplier | Eq. 83 |
| $\delta_r$ | = strain multiplier, function of reinforcement | Eq. 60 |
| $\delta_{rc}$ | = value of $\delta_r$ after creep | Eq. 60 |
| $\delta_{rs}$ | = restrained shrinkage coefficient | Eq. 55 |
| $\varepsilon$ | = strain | Eq. 2 |
| $\varepsilon'$ | = specific strain ($\varepsilon$ per unit stress) | Eq. 30 |
| $\varepsilon_a$ | = aggregate strain due to shrinkage | App. II-B |
| $\varepsilon_{bc}$ | = basic creep strain | Eq. 38 |
| $\varepsilon_c$ | = creep strain | Eq. 1 |
| $\varepsilon_{cr}$ | = restrained creep strain | App. I-A |
| $\varepsilon_{cs}$ | = creep plus shrinkage strain, $\varepsilon_c+\varepsilon_s$ | Eq. 38 |
| $\varepsilon_{csu}$ | = limiting value of $\varepsilon_{cs}$, $t\to\infty$ | App. I-A |
| $\varepsilon_{ct}$ | = specific creep strain, $\varepsilon_c$, at age t days | Eq. 4 |
| $\varepsilon_{cu}$ | = limiting value of $\varepsilon_c$, $t\to\infty$ | Eq. 48 |
| $\varepsilon_{c1}$ | = $\varepsilon_c$ for t = one year | Eq. 35 |
| $\varepsilon_d$ | = delayed elastic strain | Eq. 45 |
| $\varepsilon_{ds}$ | = value of $\varepsilon_d$ at beginning of interval | Eq. 47 |
| $\varepsilon_{dsu}$ | = limiting value of slow delayed elastic strain | Eq. 47 |
| $\varepsilon'_{du}$ | = specific delayed elastic strain recovery | Eq. 50 |
| $\varepsilon_{et1}$ | = instantaneous elastic deformation (CEB) | App. II-C |
| $\varepsilon'_f$ | = specific creep flow | Eq. 45 |
| $\varepsilon'_{fu}$ | = limiting value of $\varepsilon'_f$ , $t\to\infty$ | Eq. 50 |
| $\varepsilon_i$ | = instantaneous (elastic) strain | Eq. 1 |
| $\varepsilon_p$ | = strain in paste shell | App. II-B |
| $\varepsilon_{pr}$ | = radial strain in paste shell | App. II-B |

| | | Reference |
|---|---|---|
| $\varepsilon_{pt}$ | = tangential strain in paste shell | App. II-B |
| $\varepsilon_r$ | = strain restrained by reinforcement | Eq. 63 |
| $\varepsilon_{rc}$ | = value of $\varepsilon_r$ after creep | Eq. 63b, 74 |
| $\varepsilon_{rcs}$ | = restrained creep plus shrinkage strain | App. I-A |
| $\varepsilon_{rs}$ | = shrinkage restrained by reinforcement | Eq. 55, 71 |
| $\varepsilon_{rt}$ | = total strain recovery at age t days | Eq. 51 |
| $\varepsilon_{ru}$ | = limiting value of $\varepsilon_r$ after creep and shrinkage | Eq. 66, 77 |
| $\varepsilon_s$ | = shrinkage strain | Eq. 9 |
| $\varepsilon_{sh}$ | = free drying shrinkage at 50% R.H. | Eq. 17 |
| $\varepsilon_{sp}$ | = free drying shrinkage of paste | Eq. 20 |
| $\varepsilon_{st}$ | = value of $\varepsilon_s$ at time t | App. III-A |
| $\varepsilon_{su}$ | = value of $\varepsilon_s$ as $t \to \infty$ | Eq. 9 |
| $\varepsilon_{tn}$ | = total deformation at time $t_n$ (CEB) | App. II-C |
| $\varepsilon_{to}$ | = average time dependent strain | Eq. 31 |
| $\varepsilon_{t\infty}$ | = limiting strain value as $t \to \infty$ | App. I-B |
| $\varepsilon_v$ | = hygro-thermal volume change | Eq. 1 |
| $\varepsilon_z$ | = delayed strain yet to be developed | Eq. 45 |
| $\zeta$ | = age at time of loading coefficient (CEB) | App. II-C |
| $\eta$ | = modular ratio | Eq. 53 |
| $\eta_d$ | = modular ratio modified for delayed elasticity | Eq. 80 |
| $\eta_e$ | = effective modular ratio, $(C_t+1)\eta$ | Eq. 53 |
| $\eta_m$ | = fluidity | App. I-B |
| $\eta_u$ | = limiting value of $\eta_e$ as $t \to \infty$ | Eq. 54 |
| $\nu$ | = Poisson's ratio | Eq. 20 |
| $\nu_a$ | = Poisson's ratio for aggregate | Eq. 20 |
| $\nu_p$ | = Poisson's ratio for paste | Eq. 20 |

| | | Reference |
|---|---|---|
| $\xi$ | = reinforcement parameter (CEB) | App. II-B |
| $\rho$ | = reinforcement ratio, columns | Eq. 55 |
| $\rho$ | = tensile reinforcement ratio, beams | Eq. 92, 102 |
| $\rho'$ | = compression reinforcement ratio, beams | Eq. 103 |
| $\rho^*$ | = creep and shrinkage age factor (CEB) | Eq. 25 |
| $\rho_e$ | = effective transformed area reinforcement ratio | Eq. 68 |
| $\rho_f$ | = flange area reinforcement ratio | Eq. 107 |
| $\rho_w$ | = web area reinforcement ratio | Eq. 106 |
| $\sigma$ | = stress level | Eq. 2 |
| $\sigma_a$ | = stress in aggregate core due to shrinkage of paste | App. II-B |
| $\sigma_{ac}$ | = average compressive stress level | Eq. 32 |
| $\sigma_{ave}$ | = average stress gross section, $p/A_g$ | Eq. 59 |
| $\sigma_c$ | = concrete stress | Eq. 62a, 94 |
| $\sigma_{ci}$ | = initial stress in concrete | Eq. 97 |
| $\sigma_{cr}$ | = R/C column, concrete stress after creep | Eq. 61b, 72 |
| $\sigma_{cs}$ | = R/C column, concrete stress due to restrained shrinkage | Eq. 58, 69 |
| $\sigma_{ct}$ | = R/C column, concrete stress at time t | App. III-A |
| $\sigma_{cu}$ | = concrete stress after creep and shrinkage | Eq. 64,75,97 |
| $\sigma_{pt}$ | = biaxial tensile stress in paste shell | App. II-B |
| $\sigma_s$ | = steel stress | Eq. 62a, 95 |
| $\sigma_{se}$ | = effective shrinkage stress | Eq. 37, 67 |
| $\sigma_{si}$ | = initial value of $\sigma_s$ | Eq. 46 |
| $\sigma_{sp}$ | = unrestrained shrinkage stress equivalent for paste shell | App. II-B |
| $\sigma_{sr}$ | = R/C column, steel stress after creep | Eq. 62b, 73 |

| | | Reference |
|---|---|---|
| $\sigma_{ss}$ | = R/C column, steel stress due to shrinkage | Eq. 57, 70 |
| $\sigma_{st}$ | = R/C column, steel stress at time t | App. III-A |
| $\sigma_{su}$ | = steel stress after creep and shrinkage | Eq. 65,76,96 |
| $\tau_1, \tau_2$ | = time factors | Eq. 30, 38 |
| $\tau_f$ | = flange thickness to depth ratio | Eq. 114 |
| $\phi$ | = tee-beam parameter for moment of inertia | Eq. 115 |
| $\phi_a$ | = deflection multiplier | Eq. 84, 100 |
| $\phi_{as}$ | = shrinkage deflection multiplier | Eq. 124 |
| $\phi_c$ | = concrete stress multiplier | Eq. 97 |
| $\phi_f$ | = fluidity of dashpot | Eq. 38 |
| $\phi_n$ | = ultimate creep coefficient (CEB) | App. II-C |
| $\phi_o$ | = creep correction factor for environment (CEB) | App. II-C |
| $\phi_t$ | = tensile reinforcement stress multiplier | Eq. 96 |
| $\chi_i$ | = length ratio $x_i/\ell$, i=1,2 | Eq. 86 |
| $\psi$ | = shrinkage correction factor for environment (CEB) | Eq. 24 |

Prefixes

| | |
|---|---|
| $\Delta$ | = increment |
| d | = differential |
| $\Sigma$ | = sum |
| $\int$ | = integral |
| F( ) | = function of ( ) |
| ln | = natural logarithm (base e) |
| log | = Briggs logarithm (base 10) |

# CHAPTER I

# SUMMARY OF CREEP RESEARCH PROGRAM

## 1.1 Introduction

In early 1958 the Highway Department of the State of Missouri had begun building continuous "hollow slab" and box girder bridges for many of their interchange bridges. These structures, having center spans ranging from 60 to 150 feet, were recognized to be subject to both elastic and extended creep deflection due to sustained dead loads. They were therefore provided with an estimated camber. Upon completion of some of the earlier of these structures it was observed that in some cases the full amount of the initial dead load deflection did not occur and it became evident that some bridges might retain an excessive amount of their "Ultimate Camber" (1)*.

## 1.2 Scope and Objectives

The interest in this problem led to the initiation, in September 1959, of an extensive cooperative research program to study the effects of creep and shrinkage on the deflection of reinforced concrete bridges. The study originally proposed included the following phases:

1. A survey of available literature and preparation of an annotated bibliography on creep and shrinkage phenomena in concrete;
2. A testing program to study the effect of the aggregate and cement on creep and shrinkage;

---

*Number in parentheses refer to references listed.

3. Studies of the effect of member size and of reinforcement on the time rate and ultimate magnitude of creep and shrinkage strains;
4. Studies of the effect of creep and shrinkage on stress redistribution and of the effect of local cracking on the deflection of simple and continuous spans.

The stated ultimate objective was the development of a rational procedure for computing shrinkage and creep deflections for both simple and complex structures.

Subsequently, by mutual agreement, the initial scope was expanded to include a field testing program to correlate developed estimation procedures with actual field performance and a series of correlary studies to evaluate such factors as effect of age of concrete at time of loading on ultimate creep magnitudes, the effect of cyclic loading, the magnitude of creep recovery as a function of age of concrete and time under load, the effect of load reversal, the relationship between the creep and shrinkage characteristics of paste and aggregate constituents to that of the concrete, and the relationship between the creep and shrinkage characteristics and internal damping of a concrete.

## 1.3 Literature Review

Phase 1 was formally completed in February 1963 with the publication by Professor Meyers of "A Review of Literature Pertaining to Creep and Shrinkage of Concrete" (2). The literature has been continuously monitored to this date for current developments. This effort was also extended by Prof. Meyers in his capacity as chairman of the Bibliography Subcommittee of ACI Committee 209, "Creep and Volume Changes in Concrete". This committee published a very extensive bibliography in 1965, including over 400 annotated items as well as some 300 non-annotated references of lesser interest and a supplemental reference list of some 650 items (3). Professor

Meyers was also invited to coauthor, with Professor A.M. Neville, a "state of the art" paper on influences on creep for the 1964 ACI Symposium on Creep of Concrete (4).

## 1.4 Creep Laboratory

The testing program for phase 2 and 3 required the development of a special humidity and temperature controlled laboratory, loading racks to maintain the specimens under controlled stress, casting beds for the preparation of the specimens and special instrumentation for the measurement and recording of strains. A detailed description of this laboratory was included in a report entitled "Apparatus and Instrumentation for Creep and Shrinkage Studies". This report was subsequently published in the Highway Research Record (5).

## 1.5 Phenomenological Studies

The design of the initial test series was based on the phenomenological approach, and was an effort to isolate the effect of mix constituents (i.e. of such variables as water-cement ratio, paste content, type of aggregate, etc.) on the magnitude and rate of development of creep and shrinkage. Unfortunately, it is not possible to alter one constituent of concrete without altering at least one other. For example, a change in the water-cement ratio is accompanied by a change in the cement paste content or in workability, or in both. As a result, the interpretation of data from such tests requires considerable skill, and is sometimes impossible, because very subtle effects may become completely overshadowed by instrumentation and other limitations. Thus, for example, it was found that shrinkage strains of unloaded specimens prepared from the same batch, under as near as possible uniform procedures and subjected to the same environmental conditions, might vary as much as fifty per cent from the mean. Because of this difficulty and other problems, the report for these phases

was never released. Some of the more significant data and conclusions from these phase 2 and phase 3 studies are therefore attached in an appendix to this report. These studies, however, pointed out the need for a series of correlary studies.

The first of these correlary studies dealt with the phenomena of creep recovery and creep of preshrunk specimens. Very little data appeared to be available in the literature for creep recovery of concrete subjected to a load sustained for a prolonged time. Use was therefore made of the test specimens previously loaded under the phase 2 and 3 studies. Similarly, the shrinkage specimens from these studies were available for further studies. These specimens were in hygral equilibrium with their environment and they could therefore be used to study basic creep properties without complicating influences due to shrinkage. The results of this phase were reported by Prof. Donald R. Buettner and Mr. Ronald L. Hollrah in a report entitled "Creep Recovery and Creep of Preshrunk Concrete" (6).

The second of these studies was undertaken to determine the effect of cyclical loading on creep and creep recovery as well as the effect of the age of the concrete at time of initial load application. This study phase was initiated by Professor James Lane and carried out by Mr. James Wen-Yu Chai. The findings from this study were reported in MCHRP Report 67-8, "Creep and Creep Recovery for Plain Concrete." (7)

The third and last of the correlary studies on plain concrete had as its objective an evaluation of the effect of stress gradients on creep magnitudes and time rates, including the effect of stress gradient reversal. Test results for the later effect were inconclusive but this study did lead to a technique whereby shrinkage and creep may be determined from a single loaded specimen. The findings from this study phase were reported in MCHRP Report 68-15, "Creep and Shrinkage of Eccentrically Loaded Prisms" (8).

In addition to the phenomenonlogical studies, an attempt was made to predict basic creep and shrinkage behavior of plain concrete using rheological models. An effort to reproduce the findings of Vaishnav and Kesler (9), linking the damping characteristics to the shrinkage and creep of a given concrete, was not successful. This study was reported by Professor Donald R. Buettner and Pravin D. Bhavsar in a report entitled "Creep and Damping Characteristics of Concrete" (10). The study on "Creep Recovery and Creep of Preshrunk Concrete" (6) also included an attempt to obtain rheological model constants for basic creep to fit the model proposed by Ali and Kesler (11). The primary conclusion was that the Ali and Kesler model predicted a basic or viscous creep from two to three times higher than that obtained by loading the preshrunk concrete prisms. Thus it appears that basic creep also is dependent on the age of the concrete at loading. The possibility of using rheological models to predict creep and shrinkage behavior was further studied by Hollrah for his Ph.D. dissertation topic. The prediction of creep and shrinkage characteristics based on a composite model consisting of rheological models for the paste, and mortar has shown some promise of success. This approach would permit estimation of the creep and shrinkage characteristic for any concrete mix for which the rheological model constants for the paste, and the elastic properties of the sand and coarse aggregate are known. The composite model is built up on the basis of the volumetric proportions of the paste and mortar. This study is still incomplete but a brief summary of the results obtained to date, is included in an appendix to this report.

## 1.6 Structural Response to Creep and Shrinkage

In parallel with the studies for plain concrete, theoretical and experimental studies were initiated to develop reliable methods for predicting deflection behavior based on known or presumed shrinkage and creep characteristics of the concrete. The theoretical

studies were based on an extension of a previously developed concept for a controlled-deflection design method for reinforced concrete beams and slabs (12). The initial laboratory study consisted of four simply supported rectangular beams. This work was carried out by Mr. Robert M. McCafferty and was reported in an MS Thesis in August 1963 (13). McCafferty attempted the development of a rational analysis using a modified creep coefficient to determine an effective modulus. Meyers and Pauw further developed this method for a report entitled "Effect of Creep and Shrinkage on the Behavior of Reinforced Concrete Members" presented at the ACI Symposium on Creep of Concrete in 1964 (14). An additional series of laboratory beam specimens was tested and analyzed by Jones (15). This series included 6 rectangular beams and two T-beams. Half the beams were fabricated with normal weight concrete and the other half with lightweight concrete. Jones' results indicated that for uncracked beams the effective-modulus method of analysis based on a fully cracked section gave somewhat conservative results. The computed deflections for the T-beams were in excellent agreement with observed deflections.

The deflection of prestressed beams was also studied. Two methods of analysis were compared (viz. the effective modulus method and a method proposed by Branson, Scordelis and Sozen (16)), with the observed deflections of four test beams. For the beams in this study, reported by Long and Buettner (17), the method of analysis proposed by Branson, Scordelis and Sozen consistently predicted lower sustained load deflections when it was assumed that the creep deflection due to prestress was fully recoverable. This finding provided the impetus for the study of the effect of stress gradient reversal by Bayazid (8). The effective-modulus method predicted somewhat greater sustained load deflections when prestress creep deflections were assumed to be fully recoverable. From these results and the somewhat inconclusive results of the stress gradient reversal studies it appears that only part of the

prestress creep strain can be considered recoverable. This point is discussed in more detail in the section on design recommendations.

As a further evaluation of the methods of analysis available, field deflection measurements were made on three highway bridges (18). Considerable difficulty was encountered in the interpretation of these measurements, partly because of geometrical complications but primarily due to instrumentation difficulties and the effect on deflection of temperature and humidity fluctuations. Nevertheless, a detailed analysis of the structure with the most regular geometry was made and the deflections predicted were found to correlate reasonably well with the observed range of deflection values obtained from field measurements. The results of this study were reported by Pauw and Sherkat in MCHRP Report 67-9 (19). The principal findings were that under continuous sustained load, section rigidity is not very sensitive to either the magnitude of the creep strain potential or the degree of cracking, provided the section is reinforced with a normal percentage of steel and provided that the dead-load stress levels represent a significant fraction of the total design service-load stress. Hence, the effective-modulus method can be expected to give reasonable sustained-load deflection predictions both for simple and continuous reinforced concrete bridges even though the creep and shrinkage characteristics of the concrete cannot be predicted exactly.

Concrete is not truly a material but rather a complex material system wherein aggregate particles are held together by a cement paste which bond these particles together into a structural system which collectively behaves much as though it were a uniform isotropic material having certain specific properties of elasticity, creep and shrinkage. Being a composite or conglomerate material, there is a wide variation in the ways the discrete pieces of aggregate are loaded and in the way the system deforms with time under the influence of internal and external forces. The forces in the paste and mortar surrounding the larger pieces of aggregate are by no means uniform. Creep is the result of flow of the paste under these

forces and results in a redistribution of loads and deformations in the system without causing failure. Creep is therefore, a beneficial and valuable property of concrete.

The structural designer is primarily interested in designing a safe and serviceable structure. With a basic understanding of the behavior of concrete as a material system, the designer actually gains a great deal of flexibility, for through creep a concrete structure actually tries to adapt itself to the constraints assumed in the design. Sections and regions highly stressed will tend to yield and thus redistribute their loads to other sections or regions which will accept these loads, within the limits of their own strength.

## 1.7 Objective of Summary Report

The ultimate objective of the research in this project was to provide the designer with some useful guide lines for design. In this summary report, the "State of the Art", with respect to our present knowledge regarding the mechanism of the phenomena of creep and shrinkage is therefore limited to a brief review. Hopefully, this summary will be sufficiently adequate to help the designer identify those relatively few cases where creep and/or shrinkage can cause major difficulties and where an effort to limit these strains through rigid material specifications can thus be justified. More often a reasonable estimate of these properties under actual field conditions will suffice to give the designer enough information to predict the probable deflection behavior under normal service loads, and design sections can be adjusted if necessary to keep deformations within reasonable limits. Some suggested guide lines are therefore proposed whereby these properties can be estimated under assumed environmental and service conditions and several methods of analysis for predicting time-dependent response are reviewed and evaluated.

# CHAPTER II

# DEFORMATIONS OF CONCRETE UNDER CONSTANT SUSTAINED COMPRESSIVE STRESS

## 2.1 Introduction

The physical structure of concrete is extremely complex and as yet a general theory of deformation has not been developed which incorporates all the experimental observations on the deformation properties of concrete. Deformations of concrete of a given composition and age depend on hygro-thermal history and current environmental conditions of temperature and humidity, prior load history, rate of loading, state of stress and other secondary factors (20). For the purpose of designing for strength it is convenient to characterize concrete as a material with a single-valued relationship between stress and strain, independent of load or environment history or of changes with age in the physical structure and properties of the concrete itself. Such a simplistic approach, however, may be inadequate when design is governed by permissible deformations.

The designer of concrete structures is faced with many complex problems. Not only are there complexities in the very nature of concrete considered as a material, further complexities are introduced when it is combined with reinforcing and/or prestressing steel and other complexities arise from the nature of loading and the environment to which structures may be subjected during their lifetime.

Concrete considered as a structural system undergoes complex physical and chemical changes during its lifetime. In its infancy, as it cures and gains strength, it also tends to shrink due to evaporation of moisture. This early tendency to shrink is moderated by thermal expansion due to the heat of hydration of the cement. During this early stage, if unrestrained, concrete may either shrink or expand depending on the characteristics of the cement, the mix proportions and the rate of heat dissipation. If the concrete is

restrained, large stresses may be introduced which will ultimately be reflected in changes in deformations when hygro-thermal and stress equilibrium are restored. Later, upon maturing, the concrete is exposed to variations in humidity, temperature and loading conditions, producing stresses and strains which may have significant effects on the serviceability of the structure (20).

Two kinds of stresses are induced by restraints to volume changes in concrete. The first kind of stress is found in all reinforced concrete structures and is due to internal restraints offered by the reinforcement and, to a degree, by the concrete itself, as in the case of non-uniform shrinkage. The second kind of stress is found only in statically indeterminate structures and results from external restraints offered by various elements of the structure to length and angle changes in component members.

The design of most structures generally reduces to a decision-making process based on satisfying certain empirical design requirements. Discrepancies between actual and ideal elastic stresses and deformations computed by rational analysis may amount to as much as fifty percent, or even more, and these discrepancies may be especially significant in young concrete. While for most structures a refined analysis may not be warranted, the availability of such analysis is necessary if more realistic empirical requirements are to be developed for conventional designs. Such refined methods of analysis can vary greatly in degree of sophistication. The more highly sophisticated analyses are normally only justified if the material properties of the concrete can be formulated with a high degree of reliability.

## 2.2 Components of Strain

When it is necessary to consider the effect of the actual behavior of concrete in a real structure over an extended period of time the assumption of a single-valued stress-strain relationship becomes inadequate. Realistic evaluation of time-dependent performance requires the formulation of a more general definition of

the stress-strain relationship. To permit a reasonably simple formulation, albeit not entirely accurate, it is common practice to consider the phenomena of elastic deformation, shrinkage and creep to be additive (4). The total strain $\varepsilon_{\Sigma}$ may be defined as the sum of three components as summarized in Figs. 1 and 2 (4,7). Thus

$$\varepsilon_{\Sigma} = \sum \varepsilon_i + \sum \varepsilon_c + \sum \varepsilon_v \qquad (1)$$

where:

$\sum \varepsilon_i$ = the strains resulting from instantaneous response to loading both recoverable (elastic) and irrecoverable (plastic);

$\sum \varepsilon_c$ = the time-dependent strains caused by creep for a given stress history and under given hygro-thermal conditions;

$\sum \varepsilon_v$ = the time-dependent strains caused by volume changes due to changes in the hygro-thermal state and physico-chemical changes such as shrinkage or swelling due to moisture changes, thermal expansion or contraction and chemical expansion or contraction.

The over-all, time-dependent increase in strains of a stressed and drying member is assumed to consist of shrinkage (equal to the strain in a similar unstressed member) and of creep due to stress. This assumption is convenient but inaccurate because creep and shrinkage are not independent phenomena to which the principle of superposition can be applied. In fact, the effect of shrinkage on creep is to increase the magnitude of creep. For analysis, separation is desirable although in some empirical methods of analysis it is actually convenient to treat the two phenomena together (4).

Since most of the available data on creep and shrinkage were obtained on the assumption of additive properties of creep and shrinkage, creep is normally considered as the time-dependent deformation in excess of shrinkage. Where a more fundamental approach is warranted, a distinction is made between creep under conditions of hygral equilibrium (no moisture movement to or from the ambient medium), called basic creep, and the additional creep caused by

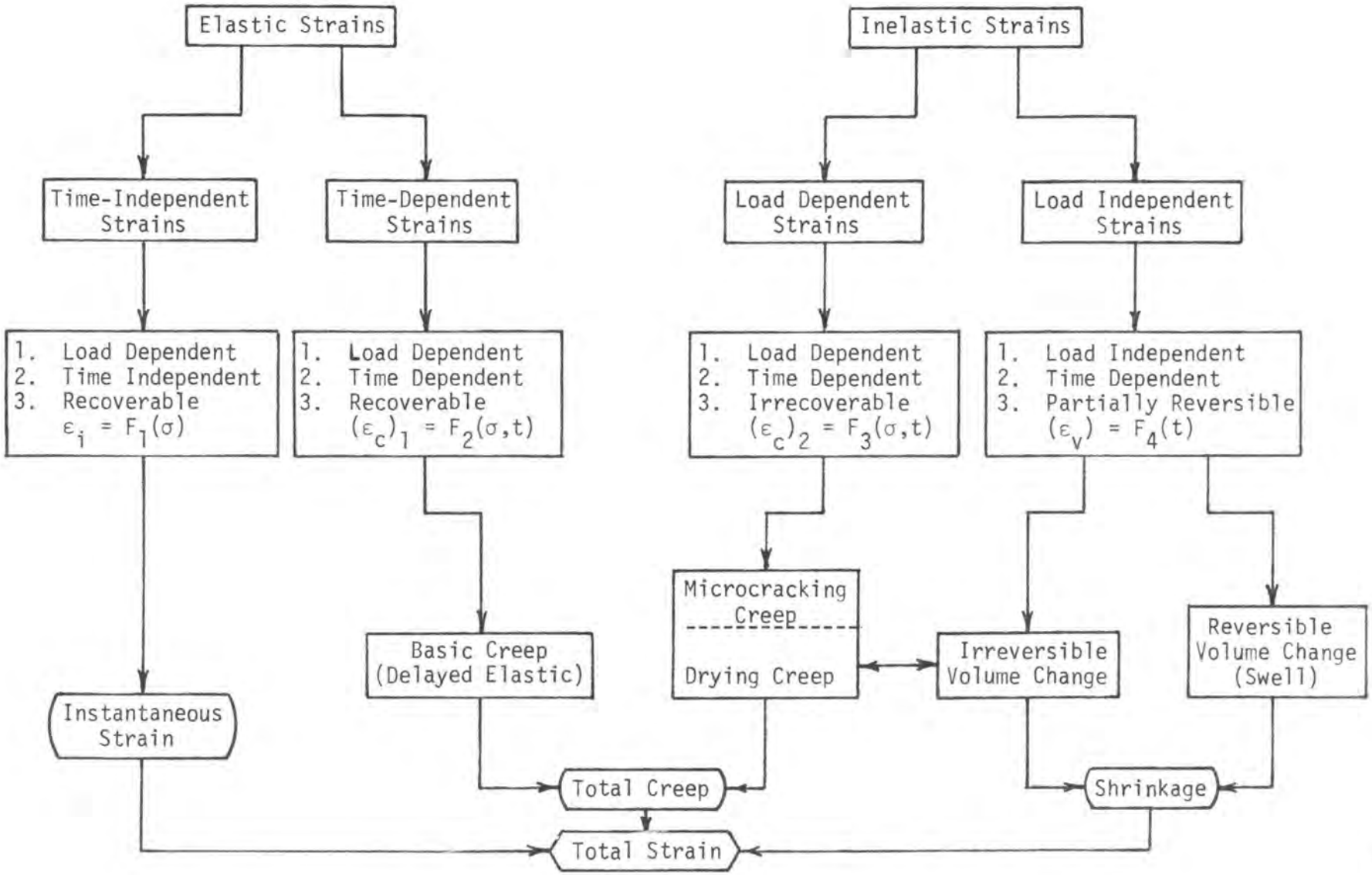


FIG. 1 STRAIN COMPONENTS

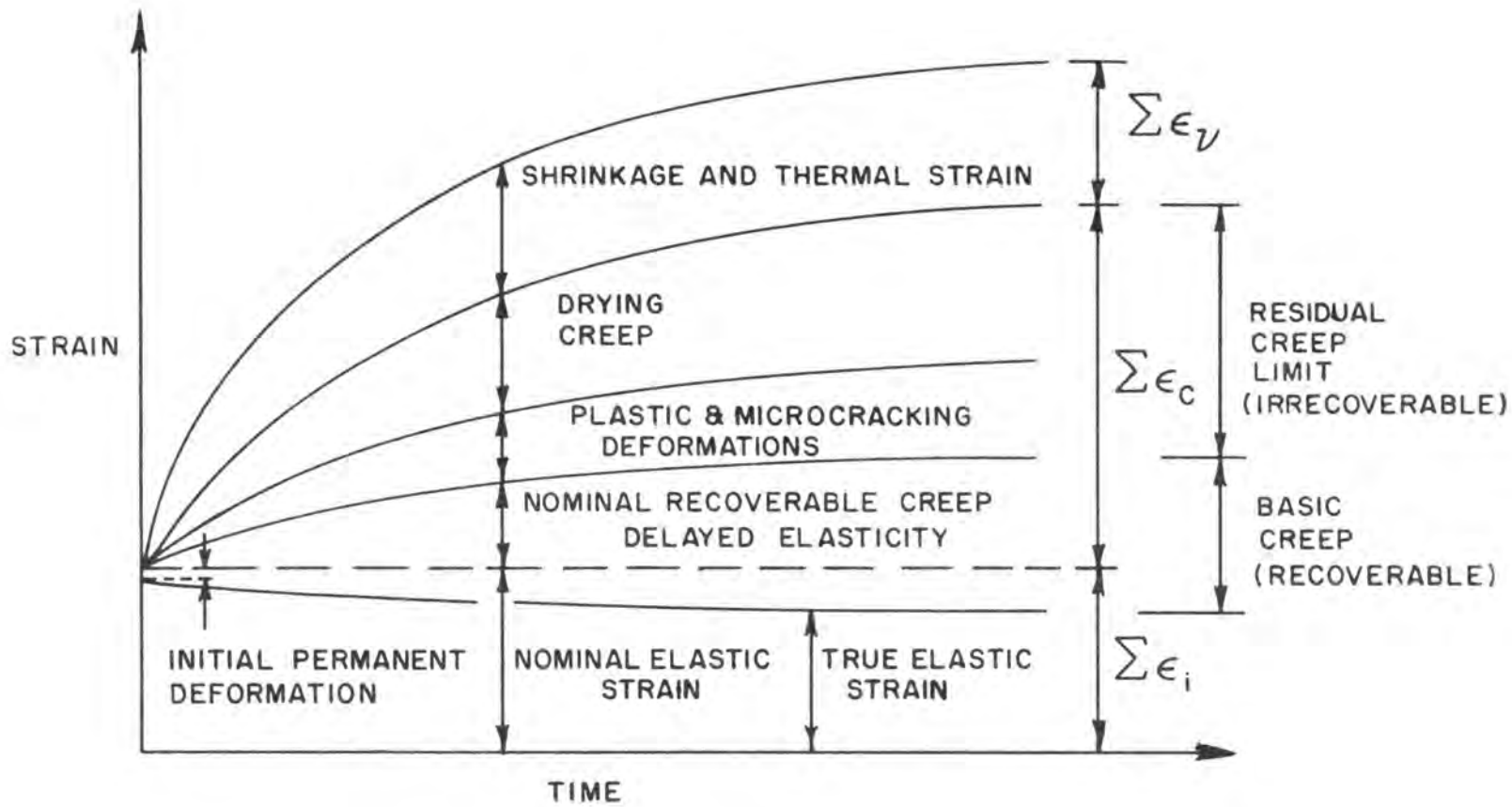


FIG. 2 - STRAINS IN A LOADED CONCRETE SPECIMEN IN A DRYING ENVIRONMENT

drying, called drying creep. Many researchers have considered basic creep to be recoverable and have treated it as delayed elasticity. In fact, however, only part of this creep appears to be recoverable (6) possibly due to micro-cracking and/or intercrystalline plastic flow in the hardened paste. Alternately, basic creep is defined as the recoverable creep as shown in Fig. 2.

There is always the question whether the elastic strain after a period of sustained load should be calculated on the basis of an increasing elastic modulus or on the original value at the time of first loading. Hollrah's tests, of both loaded and unloaded specimens indicated a marked decrease in elastic modulus after several years (6). The elastic modulus tends to decrease with a decrease in moisture content and increase with increased strength. At early ages, before complete hydration, the effect of increase in strength overrides the effect of decrease in moisture content. The elastic modulus tends to increase as the concrete matures. The rate of increase decreases, and under exceptional conditions there may even be a slight decrease in modulus. Strictly speaking, creep at a given time should be reckoned as the strain in excess of the elastic strain at that time. In the case of a constant sustained load the point is only a matter of definition since if the elastic strain diminishes with time, the creep strain may be assumed to be correspondingly increased for the same total strain. Under varying stress the problem is only of secondary importance since changes in elastic strain are small compared to the sum of the time-dependent strains. The terms and definitions involved are illustrated in Fig. 2.

## 2.3 Instantaneous Strains

While this report is primarily concerned with time-dependent strains, the nature of the instantaneous strains and deformations should be clarified in that they constitute a part of the total strain or deformation. The compression stress-strain diagram of a loading-unloading cycle on a concrete element forms an open

hysteresis loop. The virgin loading branch of the curve is convex with respect to the strain axis and the unloading branch is concave. A residual permanent set results, upon complete unloading, as shown in an idealized representation in Fig. 3. It should be noted that this compression stress-strain diagram is dependent on the rate of loading and unloading and therefore is not truly time independent. Bresler and Selna (20) in their studies on time dependent behavior have assumed a parabolic stress-strain relationship defined by

$$\sigma = A\varepsilon - B\varepsilon^m \tag{2}$$

where:

$\sigma$ = compressive stress level

$\varepsilon$ = compressive strain

A,B,m = time dependent coefficients

The ascending branch of the virgin stress-strain curve can be expressed by Eq. 2 with a reasonable degree of accuracy. The descending branch however is very sensitive to the stress rate and it is difficult to represent actual behavior with accuracy. Fortunately, in most practical cases stress levels are relatively low and only the ascending branch of the curve is of primary interest.

The ACI building code provisions assume a linearized instantaneous stress-strain relationship (21), where the slope of the stress-strain curve given by the secant modulus at 0.45 $f'_c$ may be approximated by the formula:

$$E_c = 33\sqrt{W^3 f'_c} \tag{3}$$

In Eq. 3,

$E_c$ = secant modulus, psi

W = unit weight of concrete, pcf

$f'_c$ = 28-day compressive strength, psi

The European Committee on Concrete (CEB) recommends a parabolic relationship as shown in Fig. 4. The initial slope is approximately

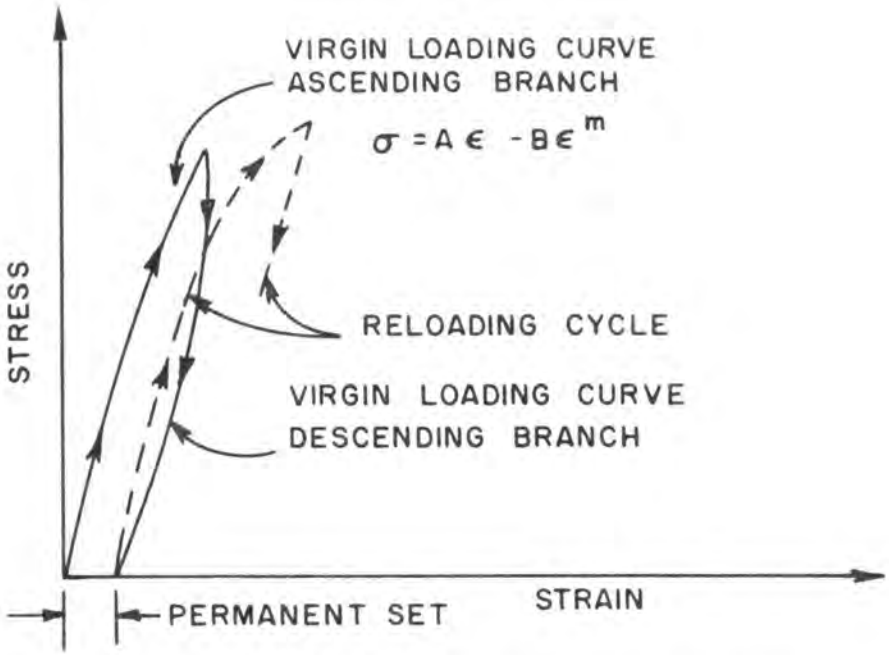


FIG. 3 - IDEALIZED REPRESENTATION OF CYCLIC STRESS - STRAIN DIAGRAM.

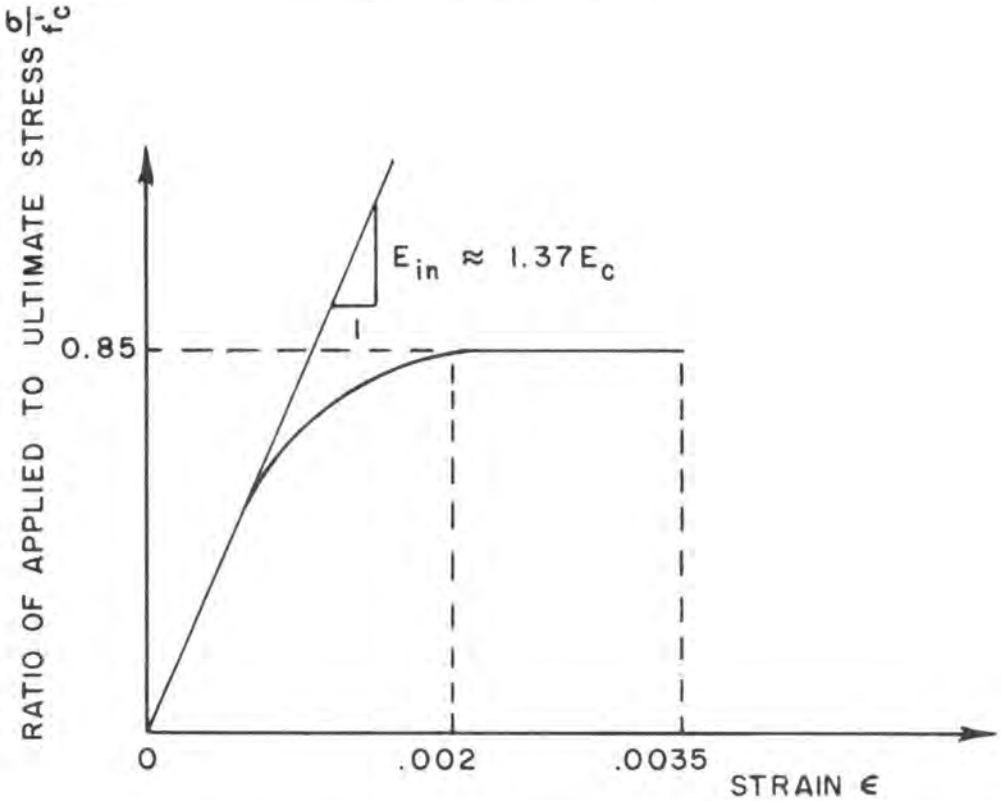


FIG 4 - IDEALIZED STRESS - STRAIN DIAGRAM RECOMMENDED BY CEB (24)

1.37 times the value given by the ACI formula and for rapid load application (to failure in 2 minutes) the apex is located at a stress of 0.85 $f'_c$ and a strain of 0.002 (24).

## 2.4 Level of Stress

Based on experimental results of many researchers there exists substantial evidence that, with the possible exception of concrete loaded at a very early age, creep is proportional to the applied stress, at least for stresses in the normal service range (23,25, 26,29). There is some uncertainty as to the upper stress limit of proportionality but it normally falls somewhere between 25 to 75 percent of the stress-strength ratio (4,23,27,28). There is evidence that for the recoverable creep component the proportional limit is near the upper range; the limit of proportionality therefore is a function of the age of the concrete at loading. Within the limit of proportionality, it is convenient to define the creep per unit stress as specific creep (29).

Almost all creep experiments have been performed using cylindrical or prismatic specimens subjected to a constant uniform compressive stress. Since creep is due, in part, to a migration of moisture there has been conjecture as to the effect of a stress gradient on the specific creep. The studies by H. Bayazid (8) did not reveal any detectable trend in average values. The use of a sustained modulus of elasticity, as defined below, therefore appears warranted for analysis of members subjected to a sustained eccentric compressive load.

## 2.5 Modulus of Elasticity

McHenry (22) defines the ratio of stress to instantaneous axial strain, in a cylinder subjected to a uniformly distributed load over the ends, as the "instantaneous modulus of elasticity". The ratio of a constant sustained stress to the total strain (elastic plus creep) which it has produced at any time is defined as the "sustained

modulus of elasticity". This sustained modulus reduces in value continuously with time but the rate of change diminishes in such a way that a limiting value is approached.

Still another "modulus" is commonly used relating ultimate strain to ultimate stress values. In reinforced concrete flexural members there is an internal redistribution of stress with time due to the stiffening action of the reinforcement. Under a sustained load the ultimate stresses in the concrete compression zone may be approximated by the use of a fictitious "effective modulus". This modulus should not be confused with the sustained modulus although, for members subjected to a gradually decreasing stress level, these modulus values may not be significantly different.

## 2.6 Age at Time of Loading

The state of strain of concrete at any time is not only a function of the forces acting at that time but of the entire past stress history. Not only the creep potential (the ultimate creep developed for a sustained stress) but also the rate of creep decreases with increased age of concrete at time of initial load application. The effect of age at time of loading can be exhibited graphically by a specific creep surface as shown in Fig. 5. McHenry (22) suggests the following formula for approximating the specific creep surface:

$$\varepsilon'_{ct} = \alpha(1-e^{r(t-k)}) + \beta e^{-pk}(1-e^{-m(t-k)}) \qquad (4)$$

where:

$\varepsilon'_{ct}$ = specific creep (creep due to a sustained unit load from time $t = k$)

$k$ = age of concrete at time of loading

$t$ = time from day of casting (age of concrete)

$\alpha, \beta, m, p, r$ = constants to be determined from laboratory tests.

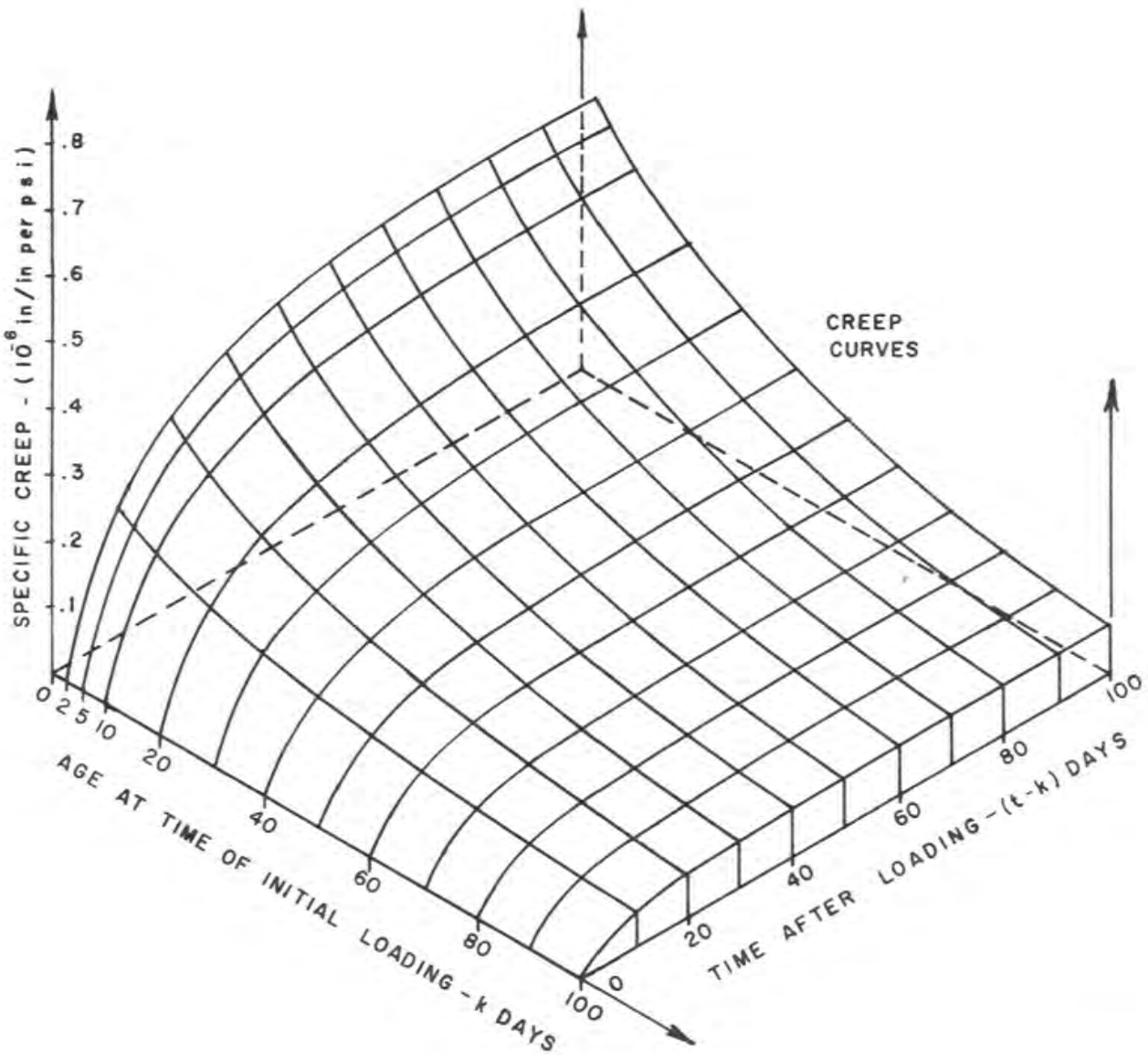


FIG. 5 - SPECIFIC CREEP SURFACE

It readily becomes apparent that the measurement of the creep characteristics of a concrete, even for a constant sustained load and a fixed hygro-thermal environment, requires an extensive laboratory program. A minimum of three creep curves for three distinct ages at time of loading are required to define the specific creep surface with reasonable accuracy.

## 2.7 Creep Recovery

Under practical conditions, stresses are not constant but may either increase or decrease with time. Clearly the elastic strains are recovered when a specimen is unloaded but only a portion of the creep strain is recovered. Chai's tests (7) indicate that for concrete initially loaded at a relatively early age (12 to 28 days), recovery of ten to twenty percent of the creep experienced can be expected, with both absolute and percentage values increasing with an increase in the loading time. For very long sustained load periods, the creep recovery appears to again decrease (6).

Creep recovery expressed as a percentage of the creep strain also appears to increase with increased age at time of loading. Absolute creep recovery values, however, decrease since creep also decreases with age at time of loading. It has been found convenient to define a residual creep limit as a function of age at time of unloading as shown in Fig. 6 (7). The potential creep recovery is then obtained by subtracting the residual creep limit from the total creep, assuming the elastic strain to be invariant with time.

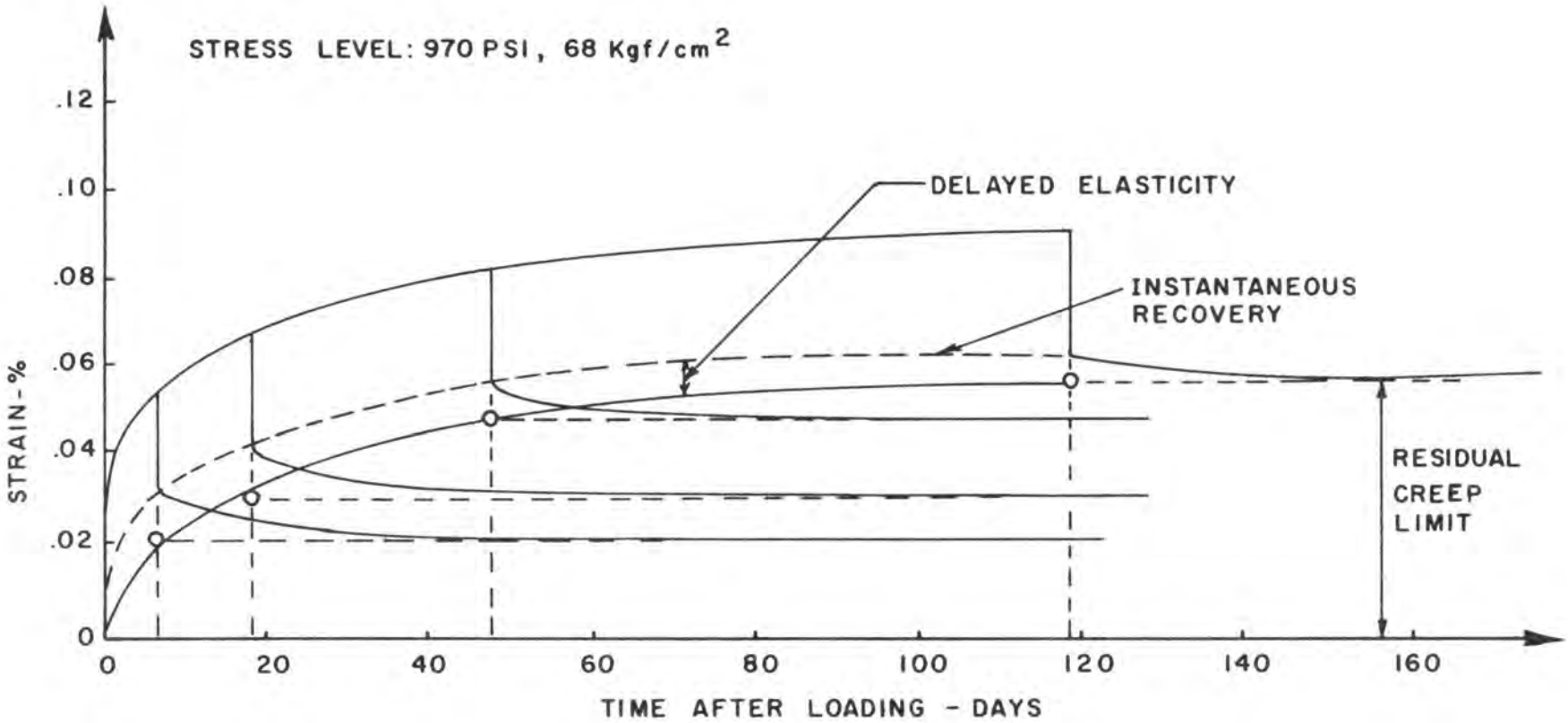


FIG. 6 - RESIDUAL CREEP LIMIT CURVE

# CHAPTER III

# DEFORMATION PROPERTIES OF PLAIN CONCRETE-

# STATE OF THE ART

## 3.1 Introduction

In predicting and controlling elastic and time-dependent deformations and their consequences, the structural designer is faced with an exceedingly complex problem. Not only is the material response dependent on a large number of interrelated parameters, but at the time of design these parameters themselves can not be established with absolute confidence. The ultimate solution of this problem might well be based on a statistical approach to design whereby designs can be optimized on the basis of confidence intervals for governing design parameters.

Present design procedures are primarily deterministic in nature. The designer needs a set of functional relationships which take into account all of the more pertinent factors. A design can then be analyzed and modified, if need be, by using these relationships as fixed constraints. Fortunately reinforced concrete is a most accommodating material indeed. Large discrepancies between assumed material response and the actual behavior are readily accommodated by internal stress redistribution and relaxation of both internal and external constraints.

The more important functional relationships for the material response of plain concrete needed for a deterministic analysis are listed below:

1. Time-dependent compressive strength relationship, $f'_c$ (t)
2. Tensile strength relationship, $f_{ct}$
3. Elastic (instantaneous) deformation characteristics, i.e., elastic modulus, $E_c$

4. Shrinkage characteristics, $\varepsilon_s$
5. Creep characteristics.

Items 1, 2, and 3 are governed primarily by the mix proportions and the properties of the constituent materials and to a lesser degree by the hygro-thermal ambient conditions subsequent to the curing period. Items 3 and 4, in addition to being governed by these factors, can be significantly modified by ambient environmental conditions, by stress conditions, and by the prior stress history. The more significant parameters affecting these time-dependent strains are summarized in Fig. 7.

The formulas discussed in this chapter represent some efforts to provide the designer a guide in developing the required functional constraints governing his design.

## 3.2 Compressive Strength

The 28-day compressive strength of concrete is normally specified in design since it is the parameter most readily controlled by test. Test values, however, only represent the potential performance of the material when consolidated and cured under standard controlled conditions. The actual field strength of the concrete may deviate markedly from test values depending on such factors as field conditions of consolidation and curing, size of the member, and age of the concrete. From a behavioral point of view it is fortunate that strains are not directly proportional to strength but vary more nearly as the square root of the strength. Thus a discrepancy of say twenty percent in strength would only be reflected in a change of about ten percent in elastic modulus. An estimate of the time-dependent strength relationship is needed by the designer to estimate not only the elastic deformations but also the magnitude of creep strains, since creep appears to be almost linearly proportional to the stress-strength ratio (4).

Branson (31) proposed the following empirical hyperbolic relationship for predicting the compressive strength at anytime, given the 28-day compressive strength:

PARAMETERS AFFECTING STRAIN

| | | | |
|---|---|---|---|
| 1. Geometry of Member | 5. Length of Curing | 9. Environment Humidity | 13. Duration of Unloading Period |
| 2. Water-Cement Ratio | 6. Curing Temperature | 10. Time of Initial Load | 14. Stress Distribution |
| 3. Mix Proportions | 7. Curing Humidity | 11. Duration of Load Period | 15. Stress Magnitude |
| 4. Type of Aggregate | 8. Environment Temper- | 12. Number of Load Cycles | 16. Stress Rate |

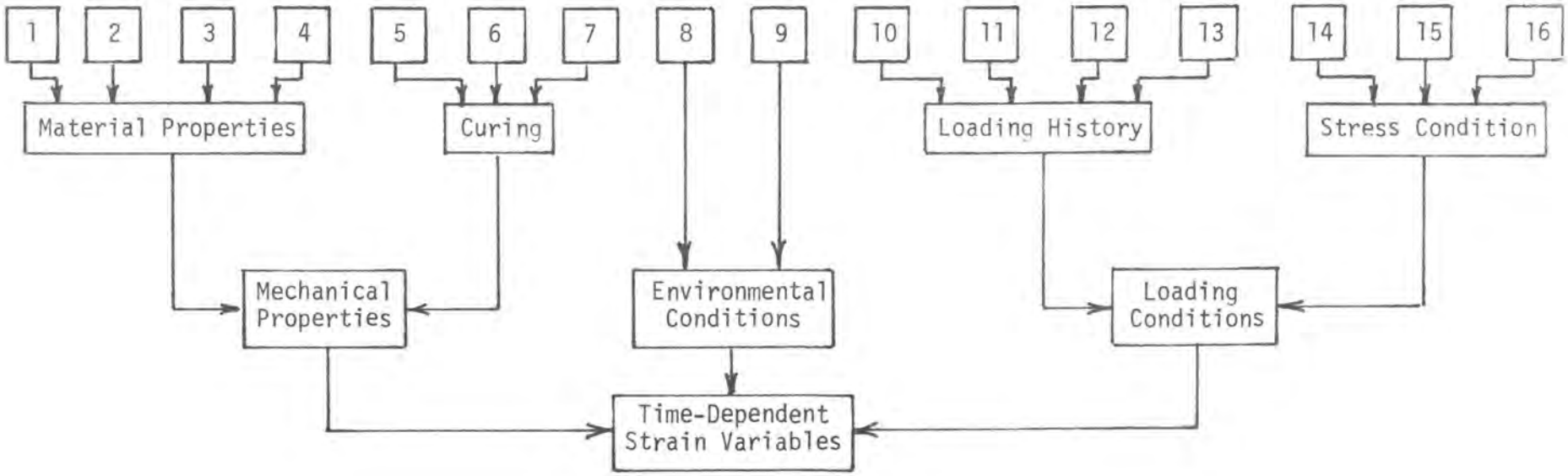


FIG. 7. TIME-DEPENDENT STRAIN VARIABLES

$$f_c'(t) = \frac{t}{a + bt} f_c'(28) \tag{5}$$

In Eq. 5:

$f_c'(t)$ = compressive strength at age t days

$t$ = days after casting

$f_c'(28)$ = 28-day compressive strength for the given mix

$a,b$ = constants determined experimentally

The constants a and b are primarily functions of the type of cement and type of curing and do not appear to be significantly affected by the type of aggregate. Table I shows the constants suggested by Branson for both Type I and Type III cements and for both moist and steam curing. These constants are applicable for normal weight concrete as well as sanded and all lightweight concretes. The ratio of early strength and ultimate strength to the 28-day strength based on this formula are also shown in Table I.

TABLE I

CONSTANTS FOR TIME-DEPENDENT STRENGTH RELATIONSHIP

| Cement Type | Type of Curing | a | b | t days | $\frac{f_c'(t)}{f_c'(28)}$ | $\frac{f_c'(\infty)}{f_c'(28)}$ |
|---|---|---|---|---|---|---|
| I | moist | 4.00 | 0.85 | 7 | .70 | 1.18 |
| III | moist | 2.30 | 0.92 | 7 | .80 | 1.09 |
| I | steam | 1.00 | 0.95 | 2.5 | .74 | 1.05 |
| III | steam | 0.70 | 0.98 | 2.5 | .80 | 1.02 |

### 3.3 Modulus of Rupture and Tensile Strength

An estimate of the modulus of rupture and/or the tensile strength is of value in predicting the degree of cracking in flexural members and members stressed in tension. Very little information appears to be available regarding the time-dependent characteristics of these strengths although it has been observed

that the tensile strength of lightweight concrete decreases with age as the specimen dries out. Generally, both the modulus of rupture, $f_{cr}$, and the tensile strength, $f_{ct}$, are assumed to be proportional to the square root of the compressive strength and to be lower for lightweight aggregate concretes than for normal weight concretes. In general, the modulus of rupture may be estimated by the relationship:

$$f_{cr} = \alpha_r \sqrt{W f_c'} \tag{6}$$

and the tensile strength by:

$$f_{ct} = \alpha_t \sqrt{W f_c'} \tag{7}$$

The constants $\alpha_r$ and $\alpha_t$ have to be determined by test for a given aggregate, mix proportions, and specified ambient conditions of temperature and humidity. For $f_c'$ in psi, and W in pcf, $\alpha_r$ will range between 0.60 to 0.95, with the smaller values tending to apply to higher strength concretes and vice-versa. The constant $\alpha_t$ can be expected to have a value of about 1/3 for both normal and lightweight aggregate concretes.

## 3.4 Elastic Modulus

The ACI-318 formula for secant modulus given in Eq. 3 in the previous chapter is an empirical relationship based on reported test results by a large number of researchers and represents a very wide range of compressive strengths and aggregate types. In recent years several mechanical models (32,33) have been proposed to predict the elastic modulus of concrete on the basis of the elastic moduli of the cement matrix and the aggregate constituents and on the mix proportions. Regardless of the assumptions made, these models tend to be equivalent to combinations of elementary series and parallel arrangements of the laminated structural models proposed by Dantu as shown in Fig. 8.

The modulus of elasticity, $E_c$, of the concrete is given by:

COMPOSITE SOLID CONSISTING OF LAMINATIONS OF PASTE AND AGGREGATE

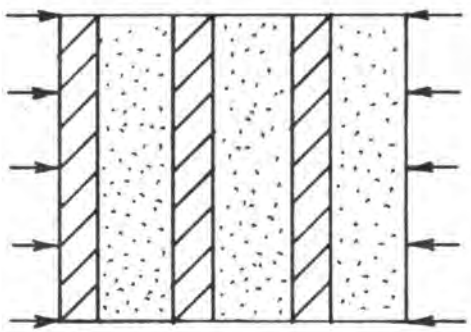

LOADING PERPENDICULAR TO LAMINATIONS

COMPOSITE SOLID OF TWO DIFFERENT MATERIALS

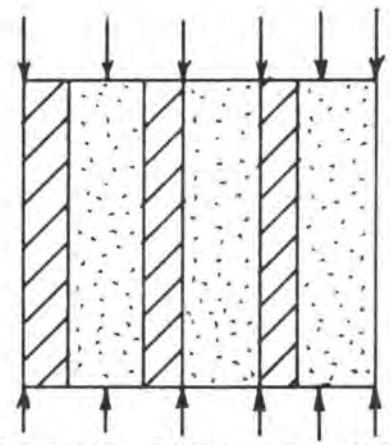

LOADING PARALLEL TO LAMINATIONS

$$\frac{1}{E_c} = \frac{V_a}{E_a} + \frac{V_p}{E_p}$$

$$E_c = V_a E_a + V_p E_p$$

FIG. 8 - MECHANICAL MODEL OF CONCRETE [33]

$$\frac{1}{E_c} = \frac{V_a E_p + V_p E_a}{E_p E_a} (1-A) + \left(\frac{1}{V_p E_p + V_a E_a}\right) A \qquad (8)$$

where:

$E_p$ = modulus of elasticity of the cement paste

$E_a$ = modulus of elasticity of the aggregate

$V_p$ = volumetric fraction of the cement paste

$V_a$ = volumetric fraction of the aggregate

A = a constant whose value ranges between 0 and 1.

T.C. Hansen (34) has suggested that "A" depends on the ratio of the moduli of the cement and aggregate phase. "A" approaches a value of zero if the "soft" case (loading perpendicular to the laminations) dominates, and unity if the "hard" case dominates. For isotropy Dougill (33) and Hirsch (32) use a value of one half.

Pauw and Hollrah have studied a similar model consisting of a cube of aggregate centered in a cubical shell of cement paste. The functional relationships for this model are slightly more complex than that given by Eq. 8. For the data tested, this model predicts about the same or slightly lower values than Eq. 8 with A=0.5. The equations for this model are given in Appendix II-A. It should be noted that in all these models, the effect of Poisson's ratio is ignored.

Application of these equations presumes that the moduli of the concrete paste and of the aggregate are known or can be established. The relationship between the secant modulus of the paste and the water-cement ratio for several concrete ages as given by Hirsch (33), is shown in Fig. 9. The modulus of a given aggregate may be difficult to determine by direct test. Some typical values reported in Hirsch's paper (33) and in the discussions of this paper are given in Table II.

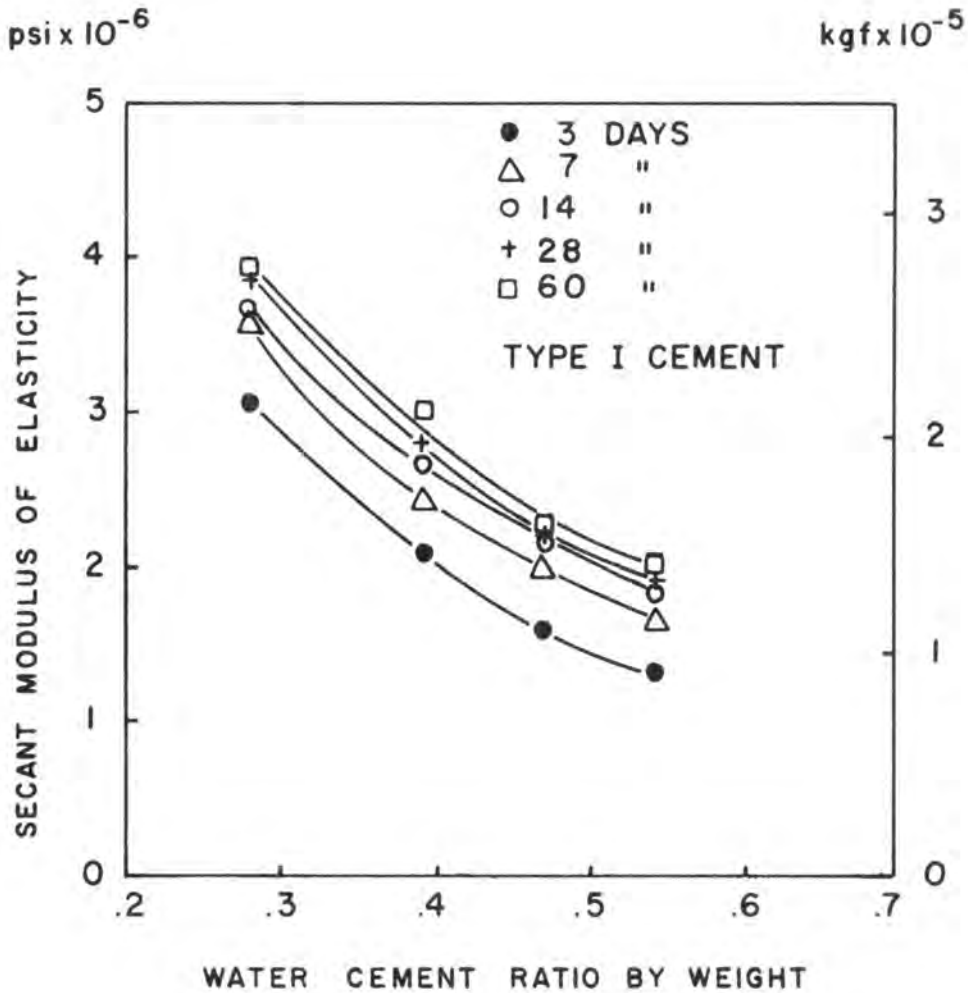


FIG. 9 - EFFECT OF WATER - CEMENT RATIO AND AGE ON THE SECANT MODULUS OF ELASTICITY OF CEMENT PASTE [32]

TABLE II

ELASTIC MODULUS OF AGGREGATES

| Type of Aggregate | Secant Modulus x $10^{-6}$psi |
|---|---|
| Ottawa Sand | 11.0 |
| Glass | 10.3 to 10.5 |
| Gravel | 9.0 |
| Limestone | 1.9 to 11.4 |
| Chert | 6.8 to 14.4 |
| Quartzite | 6.7 to 8.6 |
| Diorite | 14.8 |
| Flint | 8.0 |
| Basalt | 10.9 |
| Granite | 3.3 to 10.2 |
| Trachyte | 10.5 |

Where the aggregate modulus can not be determined directly by test it can be determined indirectly by solving Eq. 8 for $E_p$ for a given concrete for which the modulus has been determined experimentally. Eq. 8 is useful for predicting the effect on the modulus of a change in mix proportions. In a discussion of Hirsch's paper, Ishai points out that Eq. 8 is inapplicable for the limiting case $E_a$=0, representing a porous cement paste. Substitution of $E_a$=0, gives $E_c$=0 for all values of $V_a/V_p$. This contradicts the obvious fact that a porous material has a definite modulus which decreases with increasing voids ratio. The Pauw-Hollrah model is subject to the same limitations. In spite of obvious limitations, these models presently offer about the best alternative available if the elastic modulus can not be determined directly by test. These models can also be used to predict the ultimate creep. By substituting the sustained load modulus of the cement paste the ultimate effective modulus of the concrete can be computed, (35). The creep factor (i.e., the elastic plus creep strain divided by the elastic strain) is then given by dividing the instantaneous or elastic modulus by the computed ultimate effective modulus. This result tends to confirm the experimentally determined relationship between creep and elastic modulus reported by Hickey (36).

## 3.5 Factors Influencing Shrinkage Strains in Plain Concrete

The structural engineer needs an estimate of the shrinkage properties of concrete, not only to predict time-dependent deflections due to shrinkage, but also to estimate the magnitude of drying creep under stress. Shrinkage of concrete is attributable to chemical and physical causes and may be classified into the following three categories:

a. Plastic Shrinkage
b. Drying Shrinkage
c. Carbonization Shrinkage

Plastic shrinkage occurs while the concrete is still in the plastic state and can cause shrinkage cracks in the exposed surface of freshly placed concrete. This shrinkage process is irreversible and is caused by a rapid evaporation of water from the surface of the exposed concrete. While such plastic shrinkage cracks can have serious structural consequences, they can be avoided by proper field procedures. An excellent discussion of these problems can be found in a paper by Lerch (37) which includes recommendations for corrective measures.

Carbonization shrinkage is due to a reaction between carbon dioxide in the air with certain components of the hydrated cement paste. The reaction can take place even for very small concentrations of $CO_2$ in the atmosphere and is sensitive to the ambient humidity in the range from 25 to 100 percent with a maximum at about 50 percent. This shrinkage is also irreversible but is normally limited to a thin layer of about 1/2 to 3/4 inch adjacent to the exposed surface of the concrete member. Carbonization shrinkage is, therefore, only of serious structural consequence in relatively thin slabs exposed to an unusual environment.

In estimating time-dependent structural behavior, the designer is primarily concerned with the phenomenon of drying shrinkage. Drying shrinkage appears to be primarily due to a loss of adsorbed water from the cement gel resulting in a reduction of volume. Some researchers have advanced the theory that drying shrinkage is

due to a progressive increase in the meniscular curvature of the capillary water caused by dessication. The surface tension at the free water surface in the capillaries subjects the gel solids to increasingly greater compressive stresses which in turn result in a volume reduction (26).

Regardless of which theory may be correct, shrinkage is accompanied by a moisture migration from the core of the member to the exposed surface. Hence, both the magnitude and rate of shrinkage development are strongly influenced by the shape and size of the member as well as by the relative humidity of the environment. Shrinkage ceases when the member is in hygral equilibrium with its environment and is partially reversible (swell) if water is re-adsorbed by the cement gel.

In addition to the above parameters, the factors which determine the terminal magnitude and rate of shrinkage development include:

a. The cement paste content
b. The water-cement ratio
c. The type of cement
d. The characteristics of the aggregate
e. The presence of admixtures
f. The degree of compaction
g. The type of curing
h. The ambient temperature.

Of the above, the first two factors are most significant. It is generally agreed that the seat of time-dependent deformations lies in the cement gel, hence, most researchers have assumed that shrinkage of concrete is proportional to the cement-paste content. With an increase in the water-cement ratio there is a linear increase in the excess of water over and above that required for hydration of the cement. Since this excess water increases the porosity and decreases the strength and modulus of the cement gel as well as the volume of aggregate restraining shrinkage, shrinkage of concrete increases with an increase in the water-cement ratio.

The type of cement used appears to have only an indirect effect on shrinkage. High early strength cement (type III) exhibits

somewhat greater shrinkage than standard cement (type I); and type II and type IV cements, somewhat less. This result is due in part to the fineness of grinding. The adsorbed water for a given degree of fluidity of the cement paste is a function of the specific surface and hence, concretes using type III cements require somewhat more water for the same workability (26). The heat of hydration for type III cement is also greater and this may result in increased shrinkage if the heat of hydration is not completely dissipated by the end of the curing period.

With the possible exception of lightweight aggregates, concrete aggregates which are normally acceptable for the manufacture of structural quality concrete do not appreciably influence the shrinkage because the modulus of the aggregate is several times that of the paste. Aggregates, and especially porous aggregates, which themselves are subject to shrinkage, however, will increase shrinkage of the concrete. T.C. Hansen has demonstrated that aggregates which exhibit even a moderate shrinkage can cause a serious increase in concrete shrinkage which can not be controlled by merely adjusting the mix proportions (38). Hveem and Tremper have stressed the importance of clean aggregates. Colloidal impurities, primarily clay, not only in lumps but also in the form of coatings and small discrete particles, can have a very marked effect. Such particles adsorb water during the mixing period and swell to several times their dry volume (39).

There is considerable difference of opinion as to the effect of admixtures. In the University of Missouri test program it was found that their effect was masked by changes in mixing water requirements resulting from their use. Calcium chloride is definitely known to substantially increase shrinkage even when used in normal amounts. Air entrainment in normal percentages appears to have little or no effect. In general, admixtures should be used with caution if shrinkage is critical and then their effect should be established by comparative tests. Continued mixing and retempering may increase shrinkage. This may be explained by the additional water introduced in retempering.

Shrinkage has been found to be very sensitive to the degree of compaction. Incompletely compacted specimens in the test program at the University of Missouri exhibited shrinkage strains as much as twice as those of properly compacted specimens when subjected to the same environmental conditions. In fact, large variations in shrinkage were encountered in the companion shrinkage specimens for the creep studies. These variations could only be attributed to minor differences in the surface texture of the specimens. This phenomenon can be expected to be more pronounced for small specimens with a small volume to surface ratio.

Steam curing at moderate or low temperatures and for short periods does not appear to significantly alter the shrinkage characteristics of a concrete. For specimens steam cured at high temperature and prolonged periods, shrinkage may be reduced as much as fifty percent.

Both the terminal magnitude and the rate of shrinkage increase with temperature. Ishai attributes this increase primarily to a decrease in adhesive forces between solid particles and confined liquid layers in the cement gel (40).

"Prepacked" concrete has been shown to exhibit less shrinkage than normally placed concrete. This phenomenon appears to be due to the increased restraint of the aggregate "skeleton" to shrinkage of the cement gel. This restraint may result, however, in the development of microcracking in the cement paste matrix. Shrinkage can of course be controlled by the use of shrinkage compensated cements. With the present pricing structure most designers do not feel that specification of shrinkage compensated cement is warranted except under unusual circumstances as in the case of water containment structures.

Drying shrinkage is very sensitive to ambient humidity. Most testing programs have been performed at an ambient temperature of 72°F and a relative humidity of 50 percent. Such data must be adjusted to correct for actual environmental conditions. It has been found that where humidity fluctuates the minimum rather than the average relative humidity tends to control.

Since shrinkage is related to moisture movement and surface evaporation it is quite sensitive to the geometry of the specimen.

Hansen and Mattock (45) and Keeton (46) have found that the mass factor (i.e. the volume to surface relationship) is a convenient parameter for adjusting test values to actual structural members.

## 3.6 Prediction of Shrinkage Strains

From the above discussion of factors affecting shrinkage, it is evident that the designer can not arbitrarily select a uniform shrinkage value that is representative of the potential shrinkage in all elements of a given structure and under all conditions. In designing individual structural elements, for which the effects of shrinkage must be considered, the basic shrinkage properties of the concrete specified should be adjusted to reflect geometric proportions and the probable environmental conditions. The most reliable method of predicting the basic shrinkage properties of a particular quality concrete is to determine these properties experimentally over a short period, perferably at least ninety days, and extrapolating these data to predict terminal shrinkage values. Data may be fitted to empirical equations of various forms. The Lorman or Ross hyperbolic form is generally most convenient since it lends itself particularly well to predicting terminal values (4). In the Lorman equation the shrinkage at any time $t_d$ days after drying is initiated is given by:

$$\varepsilon_s = \frac{\varepsilon_{su}\, t_d}{t_{sk} + t_d} \tag{9}$$

where:

$\varepsilon_{su}$ = the terminal shrinkage at $t=\infty$

$t_{sk}$ = the time for which the shrinkage is one half the ultimate or terminal value.

Eq. 9 may be written in the linear form:

$$t_d = \varepsilon_{su} \left(\frac{t_d}{\varepsilon_s}\right) - t_{sk} \tag{10}$$

Thus when the data is plotted with $t_d$ as ordinates and $t_d/\varepsilon_s$ as abscissas the zero intercept gives the value of $t_{sk}$ and the slope of

the line is equal to the ultimate shrinkage. A typical plot for shrinkage determination is shown in Fig. 10. Ross' equation is essentially the same as Lorman's equation.

$$\varepsilon_s = \frac{t_d}{a + bt_d} \tag{11}$$

where a and b are constants to be determined from experimental data. It is readily seen that $\varepsilon_{su}$ in Lorman's equation corresponds to 1/b and $t_{sk}$ to a/b.

An analysis by Meyers and Neville of creep and shrinkage test data from tests made at the University of Missouri revealed that one-year creep and shrinkage values could be predicted with a coefficient of variation of 15 percent from test data for a period of only about 60 days. Increasing the test period to half a year reduced the coefficient of variation to about 10 percent (4). While the Lorman or Ross equations provide a reasonable estimate of the ultimate shrinkage they generally give a poor approximation at the beginning of the drying period. For that, and other reasons, many researchers prefer an exponential form of equation. Typical is the equation suggested by Aroutionian and used in modified form by Inge Lyse (41).

$$\varepsilon_s = \varepsilon_{su}(1-e^{-\alpha_m t_d^{\,e}}) \tag{12}$$

where:

$\varepsilon_{su}$ = ultimate shrinkage

$t_d$ = time in days from day drying was initiated

e = a constant exponent, independent of mix proportions.

In Eq. 12, $\alpha_m$ is a constant which can be adjusted for the appropriate mass factor, $\gamma_{vs}$, of the member.

$$\alpha_m = d\left(\frac{S}{V}\right) = d/\gamma_{vs} \tag{13}$$

where:

d = constant, independent of mix proportions

$\gamma_{vs}$ = mass factor, volume to surface area ratio.

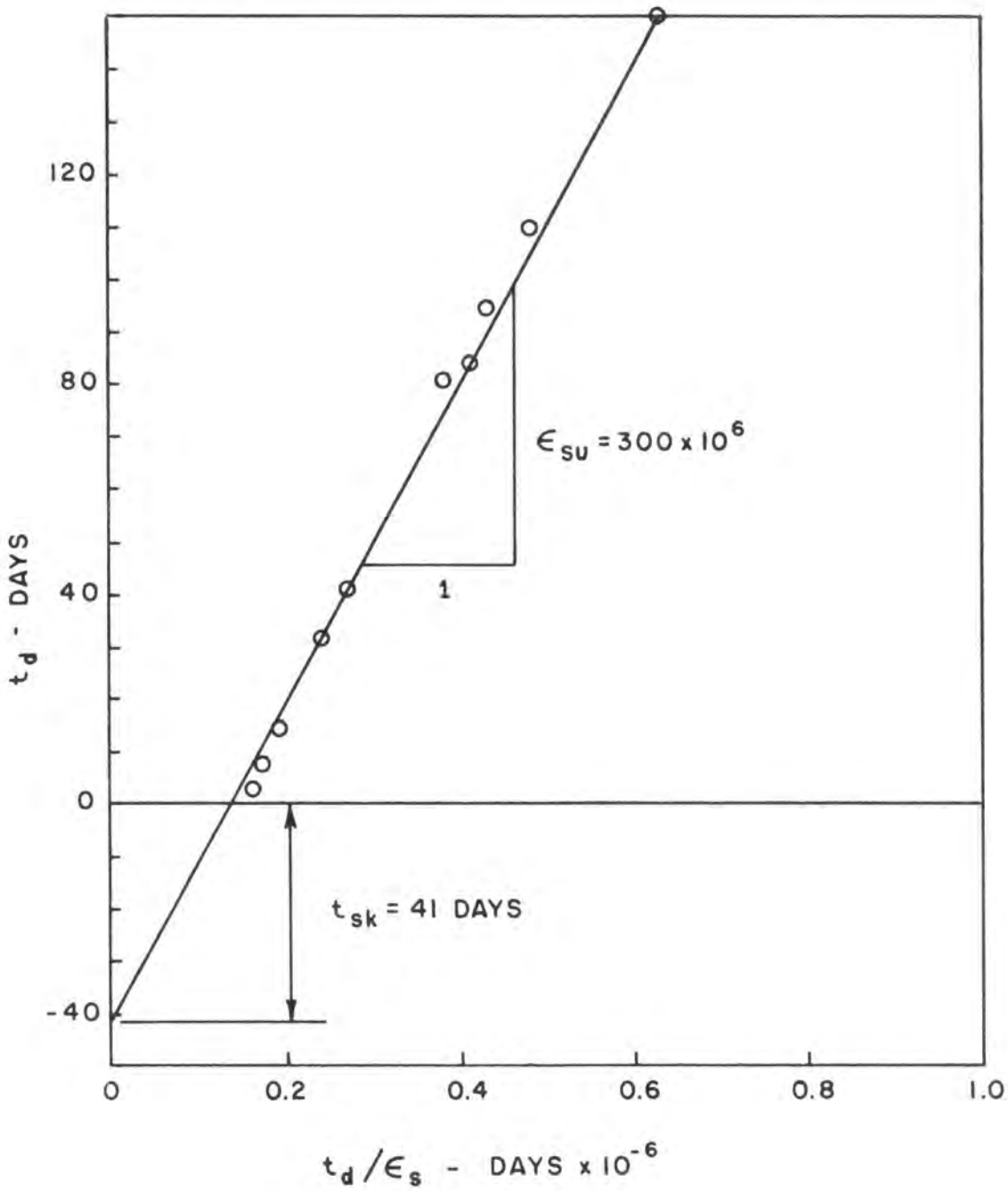


FIG. 10 - SHRINKAGE CONSTANTS DETERMINED BY THE HYPERBOLIC EQUATION (TYPICAL)

When the basic shrinkage properties cannot be determined on the basis of tests, an analytical prediction can be resorted to. The reliability of these predictions are somewhat doubtful. Several of these prediction formulas are discussed below.

Wallo and Kesler (40) have developed a formula based on the assumption that the ultimate shrinkage, $\varepsilon_{su}$, is proportional to the concentration of the restraining particles at a particular relative humidity. The concentration of restraining particles is given by the volume of solids:

$$V_s = V_a + V_{cu} = V_a + (1-h)V_c \tag{14}$$

where:

$V_a$ = volume concentration of aggregate

$V_c$ = volume of cement

$V_{cu}$ = volume concentration of unhydrated cement

$h$ = degree of hydration.

The degree of hydration is a function of the curing time. The values established by Verbeck (42) are shown in Fig. 11. The ultimate shrinkage is given by the relationship

$$\varepsilon_{su} = (A-B\ V_{ch})\ (1-V_s)\ F(H) \tag{15}$$

where:

$\varepsilon_{su}$ = ultimate free drying shrinkage strain at $t=\infty$

A,B = constants independent of mix proportions

$V_{ch}$ = volume concentration of hydrated cement including the gel pores

F(H) = a function to account for the effects of ambient relative humidity on shrinkage.

The volume concentration of hydrated cement is given by:

$$V_{ch} = 2.2\ h\ V_c \tag{16}$$

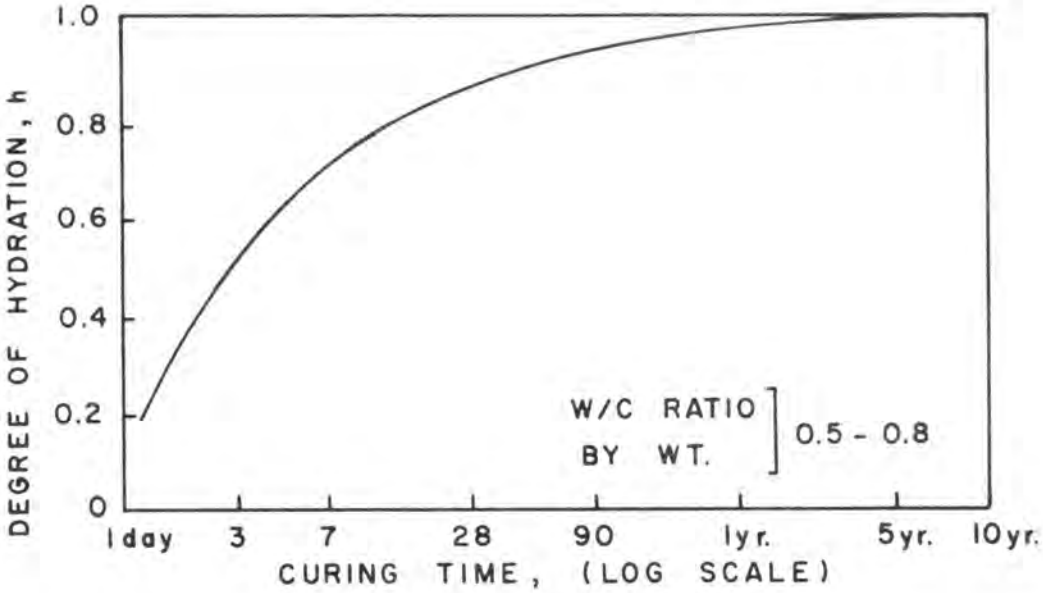


FIG. 11 - VARIATION OF THE DEGREE OF HYDRATION WITH CURING TIME [40]

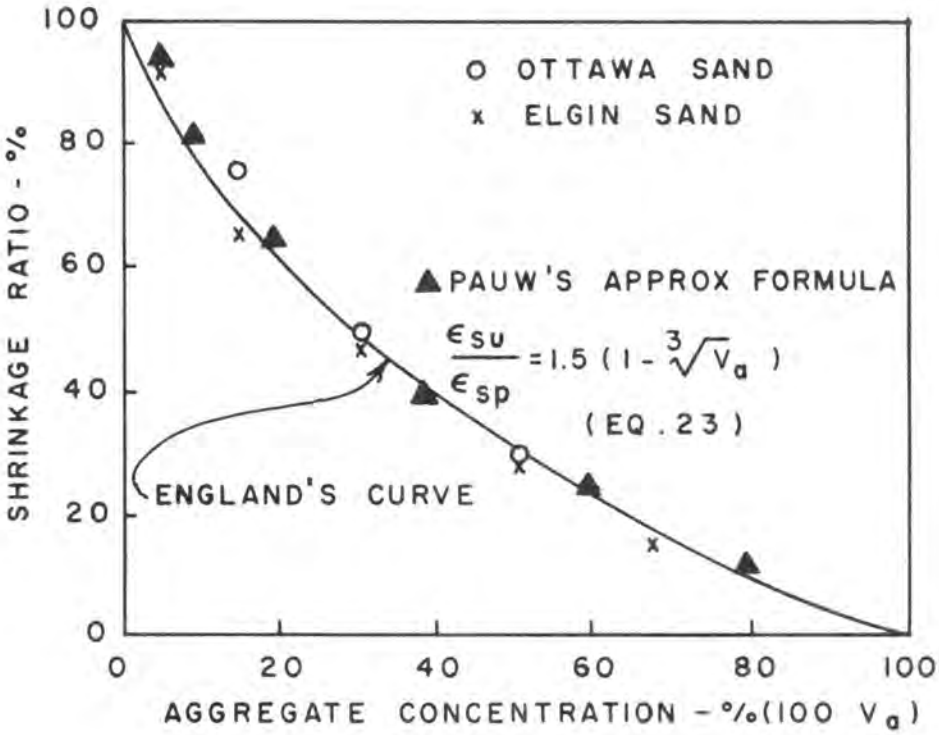


FIG. 12 - EFFECT OF AGGREGATE CONCENTRATION ON SHRINKAGE [44]

For F(H), Wallo and Kesler recommend an equation developed by Dutron relating the shrinkage at 50 percent relative humidity and the shrinkage at any other relative humidity, all at about 70° F.

$$\varepsilon_s = \varepsilon_{sh} \left(0.96 \log \frac{105-H}{5}\right) \tag{17}$$

where:

$\varepsilon_{sh}$ = free drying shrinkage strain in a 50 percent relative humidity environment

H = ambient relative humidity, in percent.

The values of A and B which gave the best fit to available data was found to be $A = 2400 \times 10^{-6}$ and $B = 2100 \times 10^{-6}$. The relationship for ultimate free shrinkage developed by Wallo and Kesler thus reduces to

$$\varepsilon_{su} = (2400-2100V_{ch})\ (1-V_s)\ \left(0.96\log \frac{105-H}{5}\right)\ 10^{-6} \tag{18}$$

Wallo and Kesler also recommend the use of Eq. 12 to depict the shrinkage-time relationship as a function of the volume to surface ratio. For the ratio $\gamma_{vs}$ in inches, a value of d equal to 0.1 and the exponent, e, equal to 0.65 is recommended, thus

$$\varepsilon_s = \varepsilon_{su}\ (1-e^{0.1t_d\ 0.65/\gamma_{vs}}) \tag{19}$$

A somewhat different approach based on mechanical models of the concrete as a two-phase system has been used by Pickett, T. C. Hansen, England and Pauw. Pickett (43) uses as his model a spherical paste shell surrounding a spherical aggregate particle. Only the paste shell is assumed to shrink and both the aggregate and cement phase are assumed to be elastic. Pickett's equation relating the shrinkage of the concrete to the shrinkage of the paste under equivalent conditions of drying is as follows:

$$\log \frac{\varepsilon_{sp}}{\varepsilon_s} = \frac{3(1-\nu_p)}{1+\nu_p + 2(1-\nu_a)\ \frac{E_p}{E_a}}\ \log \frac{1}{1-V_a} \tag{20}$$

where:

$\varepsilon_{sp}$ = free shrinkage of the cement paste at time $t_d$

$\varepsilon_s$ = free shrinkage of the concrete at time $t_d$

$\nu_p$ = Poisson's ratio for the paste

$\nu_a$ = Poisson's ratio for the aggregate

$E_p$ = modulus of elasticity of the paste

$E_a$ = modulus of elasticity of the aggregate

$V_a$ = aggregate volume ratio, i.e., volume of aggregate per unit volume of concrete.

Hansen (38) extended Pickett's solution to take into account the possibility of shrinkage of the aggregate. England (44) uses a solid model consisting of staggered aggregate cubes separated by cement paste layers. A numerical analysis requiring the use of a computer was employed to predict the structural response of the model. The effect of Poisson's ratio was not included. England concludes that creep or shrinkage strains of concretes made from different aggregates will differ only slightly from one another if the elastic moduli of the aggregates are greater than $5 \times 10^6$ psi, whatever the aggregate concentration. A plot of the shrinkage ratio in terms of the shrinkage of the cement paste versus the aggregate-volume ratio as reported by England is shown in Fig. 12 (44). Pauw and Hollrah have also studied a rheological model simulating the condition of an elastic aggregate particle embedded in a matrix shell. The analysis developed based on this model (Appendix II-A) gives a reasonable prediction of the elastic, creep and shrinkage properties using measured elastic and visco-elastic constraints for the cement and aggregate constituents. A recently completed unpublished study incorporating the effect of Poisson's ratio, but based on a cubical rather than the spherical model used by Pickett, has resulted in the following expression for predicting the shrinkage in terms of the shrinkage of the cement paste:

$$\varepsilon_s = \frac{(1-V_a^{2/3})(1-2\nu_a) + V_a^{2/3}(1-V_a^{1/3})(1+\nu_p)\frac{E_a}{E_p}}{(1-V_a^{2/3})(1-2\nu_a) + V_a^{2/3}(1-\nu_p)\frac{E_a}{E_p}}\,\varepsilon_{sp} \tag{21}$$

The variables in Eq. 21, are as defined for Eq. 20. The derivation of this equation is given in Appendix II-B. Since shrinkage and creep go hand in hand, the effective modulus of the paste, $E_p$, is time-dependent and decreases rapidly due to the sustained shrinkage stress. Hence, for most aggregates, the ratio $E_a/E_p$ becomes quite large and the second term in both the numerator and demoninator is dominant, provided $V_a$ is greater than zero. Thus the terminal shrinkage ratio is given approximately by the relatively simple relationship:

$$\varepsilon_{su} = \frac{1+\nu_p}{1-\nu_p}\,(1-\sqrt[3]{V_a})\,\varepsilon_{sp}\ ,\quad V_a>0 \tag{22}$$

For $\nu_p = 0.2$

$$\frac{\varepsilon_{su}}{\varepsilon_{sp}} = 1.5\,(1-\sqrt[3]{V_a})\ ,\qquad V_a>0 \tag{23}$$

This relationship is in close agreement with England's results as shown in Fig. 12 except for extremely small values of $V_a$.

The relative simplicity of Eq. 22 makes its use attractive for prediction of the ultimate shrinkage. Unfortunately there is a paucity of information on the shrinkage characteristics of cement paste both as a function of the water-cement ratio and of the geometric and ambient humidity conditions of drying. It should also be noted that Eq. 22 is quite sensitive to the effect of Poisson's ratio for the paste.

All of the presently available prediction formulas for shrinkage of plain concrete incorporate two basic parameters:

1. A parameter which determines the ultimate shrinkage
2. A parameter which determines the time-rate of shrinkage development.

The first parameter is primarily a function of the properties of the mix constituents, the geometry and size of the member and the environmental conditions. The second parameter is a function of the member geometry only. A reasonable approximation of the time-rate of shrinkage development can be obtained either by a hyperbolic type formula, such as Eq. 9; a modified hyperbolic form with a modified time parameter $t' = t^e$, where e is a suitably selected exponent; or by an exponential formula such as Eq. 12. There seems to be a consensus of opinion that the ultimate shrinkage of a standard size specimen in a standard environment (50 percent relative humidity and 70°F) is governed primarily by the characteristics of the paste and the volume concentration of the aggregate restraining the free shrinkage of the paste. There also appears to be agreement that the mass factor (volume to surface ratio, or alternately, the cross-sectional area to perimeter ratio) is a suitable parameter for determining the effect of the geometry of the member (45,46). The effect on the ultimate shrinkage of the ambient humidity is generally taken into account by Dutrons' formula, Eq. 17. The ultimate shrinkage of concrete in an environment wherein the relative humidity fluctuates tends to be determined by the minimum, rather than the average, value of the relative humidity.

Information on the effect of temperature is primarily limited to the effect on creep (47,48). Shrinkage of concrete exposed to abnormally high temperatures should be determined by a test program relevant to the condition of exposure.

The proposed C.E.B. specifications (24)* gives the ultimate shrinkage of plain concrete as the product of three factors, viz.:

$$\bar{\varepsilon}_{su} = \psi \, \alpha_s \, \beta_s \tag{24}$$

---

*A translation of the relevant C.E.B. provisions for creep and shrinkage is given in Appendix II-C.

where:

$\psi$ = a function of the climatic or environmental conditions

$\alpha_s$ = a function of the dimensions of the member

$\beta_s$ = a function of the physical composition of the concrete.

$\psi$ is given by a graph which appears to be based on Dutron's formula and is referenced to a normal shrinkage of 0.0275 percent at a relative humidity of 70 percent and for an effective thickness of 10 cm (4 inches). The effective thickness is defined as the ratio of the area by one-half the perimeter (hydraulic radius). The coefficient $\alpha_s$ is defined by a hyperbolic type curve and decreases from a value of 1.0 for an effective thickness of 10 cm to 0.5 for an effective thickness of 50 cm. The parameter $\beta_s$ ranges from about 0.6 to 1.6 and is shown as a function of the water-cement ratio and the strength of the concrete.

The shrinkage as a function of time is given by

$$\epsilon_s = \epsilon_{su}\,\rho^* \tag{25}$$

where $\rho$ is defined by a standard curve and is plotted as a function of the effective time $t_e$. The concept of an effective time is introduced to account for the effect of member geometry by defining

$$t_e = t_d\sqrt{\frac{10}{h_m}} \tag{26}$$

where $h_m$ is the effective thickness in cm.

When the hyperbolic type formula, Eq. 9, is used to define the time-rate of shrinkage, the shape of the curve is characterized by the age $t_{sk}$ when the shrinkage is one-half the ultimate value. Hansen and Mattock (45) reported values ranging from 37 to 216 days for 4 inch to 24 inch diameter specimens, respectively. Based on their test data the value of $t_{sk}$ is given by the empirical relationship

$$t_{sk} = \alpha_{sk}e^{0.36\,\gamma_{vs}} \tag{27}$$

where the mass factor, $\gamma_{vs}$(volume to surface ratio, V/S), is given in inches and the coefficient $\alpha_{sk}$ has a value of 26.0.

Branson also favors the hyperbolic form and recommends values of $t_{sk}$ of 35 and 55 days for seven-day moist cured, and 2-3 day dry-steam cured concretes, respectively, for a forty percent or less relative humidity environment. For relative humidities between 40 and 80 percent the estimated shrinkage may be reduced by multiplying by the coefficient

$$(C.F.)_{sh} = 1.40 - 0.01H, \; 40 \leq H \leq 80$$

Hence, for moist cured concrete, the shrinkage strain at any time $t_d$ days after drying is initiated may be estimated by the relationship

$$\varepsilon_s = \frac{(1.40 - 0.01H)\, t_d}{35 + t_d} \; \varepsilon_{su} \tag{28}$$

## 3.7 Creep Characteristics

It has already been noted that creep and shrinkage are not independent phenomena and that, in fact, the effect of shrinkage on creep is to increase the magnitude of creep. Nevertheless, since creep is stress dependent, for purposes of analysis, it is convenient to consider shrinkage and creep to be additive properties, i.e., to consider creep as deformation in excess of shrinkage. However, where a more fundamental approach is warranted, a distinction must be made between creep of concrete in hygral equilibrium (i.e., creep of concrete under conditions of no moisture movement to or from the ambient medium) defined as basic creep and the additional creep caused by drying, defined as drying creep (4).

Both Inge Lyse (41) and Ali and Kesler (11) consider drying creep to be proportional to the corresponding free shrinkage following time of loading, as well as to the stress level, within normal stress ranges. There exists substantial evidence of the proportionality between both basic and drying creep and the applied stress, the only possible exception being specimens loaded at an early age. There is, however, some uncertainty as to the upper limit of proportionality. Values

ranging from as low as 23 percent to as high as 85 percent of the compressive strength have been reported. For purposes of design analysis the assumption of an upper limit of 30 percent for sustained load stresses is reasonably conservative.

Since drying creep is proportional to shrinkage, the factors determining the terminal magnitude of shrinkage also apply to creep. Drying creep magnitudes are extremely sensitive to age at time of loading. If the time when the load is applied does not coincide with the time drying is initiated, drying creep is proportional to the shrinkage increment developed subsequent to the time of loading.

The basic creep component is normally considered to be equivalent to the creep of concrete in hygral equilibrium with the ambient environment and is, therefore, independent of the geometry of the member. Hollrah's study of creep of aged specimens (6) indicate that basic creep also is dependent on the age of concrete at time of loading. Hence, the visco-elastic properties as well as strength and modulus appear to change with age. While independent of the humidity of the ambient environment and of the geometry of the member, basic creep, in addition to age at time of loading and magnitude of stress level, is also dependent on the mix constituents, the degree of consolidation and type of curing, and on the ambient temperature. Recoverable creep may be treated as delayed elasticity but, as shown in Fig. 2, this recovery is in part offset by the increase in elastic modulus due to changes in the gel structure as the concrete continues to cure.

Whereas, the drying shrinkage of members with a reasonably low volume to surface ratio tends to stabilize by the end of one year, creep deformations appear to increase indefinitely, albeit at a diminishing rate. This increase appears to be due to a plastic or viscous flow of the hardened cement paste. Troxell, Raphael and Davis (49) report detectable increases in creep up to thirty years as shown in Table III.

The preponderance of experimental data available is restricted to uniform uniaxial compression. The limited amount of data available for non-uniform loads indicates that specific creep is somewhat greater for concrete subjected to a stress gradient as a result of moisture movement away from the more highly stressed areas toward lower stressed

TABLE III

AVERAGE INCREASE IN CREEP

| | |
|---|---|
| Creep after 1 year | 1.00 |
| Creep after 2 years | 1.14 |
| Creep after 5 years | 1.20 |
| Creep after 10 years | 1.26 |
| Creep after 20 years | 1.33 |
| Creep after 30 years | 1.36 |

areas. Creep under uniaxial tension has been found to be essentially of the same order of magnitude as under compression. Drying enchances tensile creep even somewhat more than it does creep in compression. Very little data is available for creep in torsion. There is some conjecture that, since concrete in pure torsion is not subjected to a volume change, torsional creep is independent of shrinkage. Creep in a direction normal to the applied load can be expressed in terms of a creep Poisson's ratio. There are strong indications that this ratio is zero, i.e., that axial creep does not produce an increase in the lateral deformation for stresses in the normal service-load range. These measurements are extremely difficult. Not only are the Poisson's ratio strains an order of magnitude smaller than the direct axial strains, for compression specimens they are further reduced by shrinkage. Clearly the effect of different states of stress on creep is a subject deserving further study.

One of two methods is generally employed for calculating creep strains. The first method uses the concept of specific creep, $\varepsilon_c'$, i.e., creep per unit stress. This method is useful in applying the rate of creep method discussed in the next chapter. The second method uses the concept of a creep coefficient or creep ratio, $C_t$, i.e., the ratio of creep strain divided by the elastic strain. This method is most convenient when the effect of creep is determined by the use of a sustained or effective modulus. In effect the elastic strains are augmented by a multiplier to take into account the increase due to creep.

## 3.8 Creep Prediction

As in the case of shrinkage, the most practical and reliable method for predicting the creep characteristics of a particular concrete is

based on short-time experimental data. These data must be extrapolated to predict terminal creep values under standard conditions of the test and further modified to reflect field environmental conditions and actual member geometry. The ultimate creep values can best be estimated by the use of the Lorman or Ross Hyperbolic formula. Thus

$$C_t = \frac{C_u \, t_\ell}{t_{ck} + t_\ell} \tag{29}$$

where:

$C_u$ = the ultimate creep strain ratio at $t = \infty$

$t_\ell$ = the time in days after load is applied ($t_\ell = t - k$)

$t_{ck}$ = the time in days after load is applied for which the creep is one half the ultimate value

As previously noted, creep tends to increase indefinitely with time as indicated by Table III. Hence, the Lorman approximation tends to underestimate the creep at ages in excess of say one or two years. It also has been observed that the Lorman approximation tends to underestimate the creep at early ages. Branson has suggested the use of a modified time t in the hyperbolic approximation formula by substituting $t^e$ for t, where e is a fractional exponent. A value of e equal to 0.6 has been found to be suitable for most approximations.

Some researchers prefer the use of an exponential form to fit the experimental data. An equation of the form

$$\varepsilon_c' = A + B\, e^{-t/\tau_1} + C\, e^{-t/\tau_2} + \ldots \tag{30}$$

can be made to fit a given set of data with any desired precision by suitable adjustments of the coefficients A, B, C, ..., and $\tau_1$, $\tau_2$ .... It has been observed that, except for concretes loaded at very early ages, two exponential terms will usually give a fit well within the limits of normal experimental variations.

When concentrically loaded compression cylinders are used to experimentally determine the creep characteristics of a particular concrete,

comparison shrinkage specimens are required to separate the creep strains from the combined creep and shrinkage strains. Care must be taken that these specimens are stored under identical environmental conditions, since even small variations in environment can result in significant discrepancies. Bayazid and Pauw developed an experimental procedure whereby creep and shrinkage strains may be determined from strain measurements on a single eccentrically loaded specimen (8). For prisms of depth h, loaded with an average applied stress $\sigma_{ave}$, at an eccentricity $x_e$, it was shown that the shrinkage strain is given by:

$$\varepsilon_s = \varepsilon_{to} - \frac{h_x^2}{12\ x_e}\ \alpha_{ty} \tag{31}$$

and the specific creep by

$$\varepsilon_c' = \frac{\frac{h_x^2}{12\ x_e}\ (\alpha_{ty} - \alpha_{oy})}{\sigma_{ac}} \tag{32}$$

where:

$\varepsilon_{to}$ = average time dependent strain at the centroid of the specimen

$h_x$ = depth of prism (x-dimension)

$x_e$ = eccentricity of applied load

$\alpha_{oy}$ = slope of the elastic strain gradient (i.e., the slope of the initial strain gradient at time of load application)

$\alpha_{ty}$ = slope of the strain gradient at time $t_\ell$ after application of load

$\sigma_{ac}$ = average compressive stress level.

A minimum of two sets of strain measurements must be made to determine the strain gradient required to separate creep strains from the shrinkage strains. This test procedure is based on the assumption that creep strains

are proportional to stress, i.e., that specific creep is independent of stress level. It has already been noted that this is a reasonable assumption for normal sustained stress levels.

About the most that can be expected from any reasonable laboratory program are creep curves for loads applied at two or three different ages for one type of specimen and one set of environmental conditions. This data must, therefore, be interpolated and extrapolated to provide the information on the creep properties required for analysis for any age at time of loading and for any geometrical configuration and environmental condition. Experimentally determined correction factors have been proposed by Jones, Hirsch and Stephenson and by Wagner (4) which may be used to modify a "standard" creep curve determined under controlled conditions.

The curves developed by Hirsch, Jones, and Stephenson were based on test results for lightweight concrete. While the "standard" curve is primarily a function of the property of the aggregate, the correction curves appear to be generally valid for both normal weight as well as lightweight concrete. The "standard" specific creep curve shown in Fig. 13 was developed for a lightweight concrete conforming to the following standard conditions:

| | |
|---|---|
| Cement content | = 540 lb. per cu yd |
| Entrained air | = 6 percent |
| Slump | = 2 in. |
| Stress level | = 1420 psi |
| Relative humidity | = 60 percent |
| Age at time of loading | = 14 days for Type I cement; 7 days for Type III cement. |

The values given in Fig. 13 may be multiplied by the appropriate correction factors given in the curves in Fig. 14 to modify the "standard" values for the particular slump, air content, cement type and content, percent of fines, relative humidity of storage, thickness of member and age at loading.

Research by Bureau of Reclamation engineers (36) and others, has shown that creep strains are proportional to elastic strains and it is

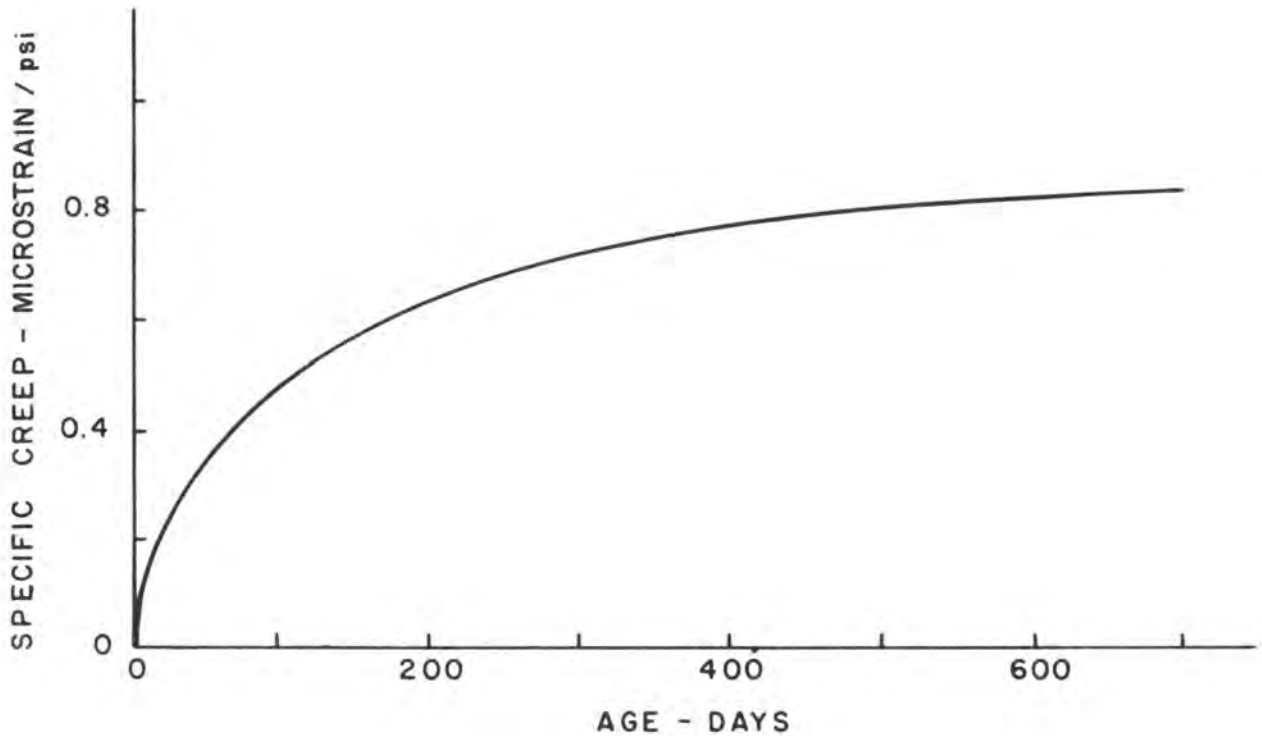


FIG. 13. "STANDARD" SPECIFIC CREEP CURVE FOR A TYPICAL LIGHTWEIGHT AGGREGATE CONCRETE

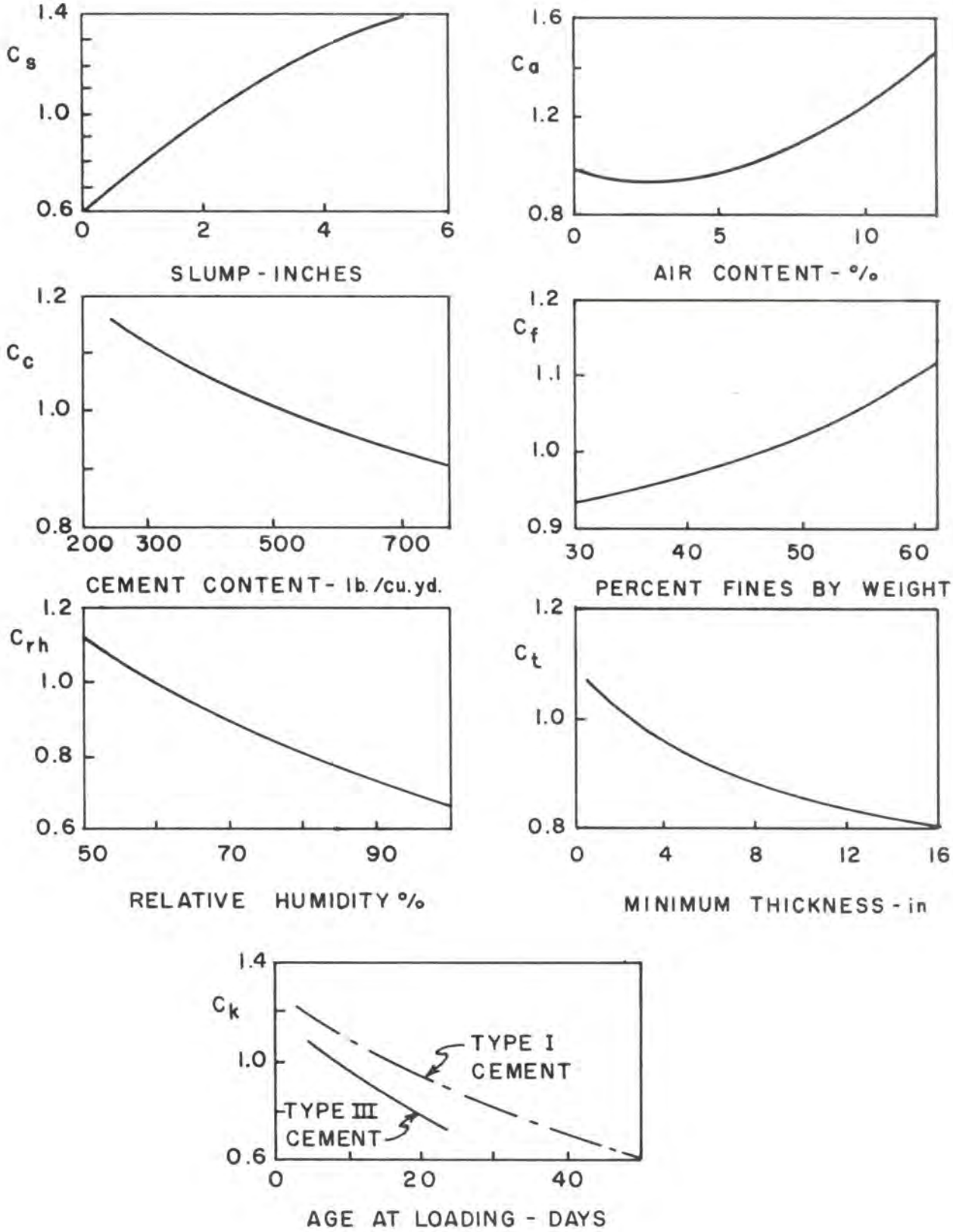


FIG. 14. CORRECTION-FACTORS FOR MODIFYING "STANDARD" CREEP CURVE (4)

therefore, often convenient to express creep as a ratio of the creep/elastic strain. Branson (31) has recommended the use of the following expression for predicting creep strain:

$$C_t = \frac{t_\ell^{0.60}}{t_c + t_\ell^{0.60}} \; C_u \tag{33}$$

where:

$C_t$ = ratio of creep to elastic strain

$t_c$ = characteristic time factor ($t_c \doteq 10$)

$t_\ell$ = age in days after loading

$C_u$ = ultimate or limiting creep ratio

The value of $C_u$ has been found to range from a low of 1.3 to a high of 4.2 depending on conditions of environment, age at time of loading, type of aggregate, type and amount of cement, etc. In the absence of specific creep data, Branson recommends a value of $C_u = 2.35$ for a relative humidity environment of 40 percent. For greater relative humidity values $C_u$ may be estimated by multiplying by the correction factor

$$(C.F.)_{cp} = 1.27 - 0.0067\,H \;,\; H > 40\%$$

where:

H = relative humidity in percent

Thus:

$$C_t \doteq (3 - 0.016H)\,\frac{t^{0.6}}{10 + t^{0.6}} \tag{34}$$

The approach followed by the European Committee on Concrete (C.E.B.) is very similar (24). Their recommendation is that creep be computed as the product of the elastic deformation by three factors, $\phi_n = \phi_o\,\alpha_c\,\beta_c$, a factor to correct for environmental conditions, member size and composition of the concrete; $\zeta$, a coefficient which is a function of age at time stress is applied; and $\rho^*$, a coefficient which is a function of the duration of the applied load. The details of the recommendations are given in Appendix II-C.

Other researchers (4) have found a relationship between creep, the stress-strength ratio, $\sigma/f'_c$, and the paste content. Fig. 15 shows a plot of one year creep at a stress-strength ratio of fifty percent vs. paste content, for a number of different concretes, both normal weight and lightweight. These experimental values are reasonably well defined by the relationship

$$\varepsilon_{c_1} = C_{fr} V_p \tag{35}$$

where:

$\varepsilon_{c_1}$ = one year creep in percent for a stress-strength ratio $\sigma/f'_c = 0.50$

$V_p$ = paste volume ratio

$C_{fr}$ = constant ranging from 0.36 to 0.54

From Eq. 33 it follows that the ultimate creep, $\varepsilon_{cu}$, is approximate thirty percent greater than the one-year creep, $\varepsilon_{cr}$. Also, from Eq. 3, for $\sigma/f'_c$ equal to one half, the elastic strain is approximately

$$\varepsilon_i \doteq \frac{1}{66}\sqrt{\frac{f'_c}{W^3}}$$

Combining, the estimated value of the limiting or ultimate creep ratio, $C_u$, is found to be:

$$C_u = \alpha_{cu} V_p \sqrt{W^3/f'_c} \tag{36}$$

where:

$\alpha_{cu}$ = a constant ranging between 0.30 and 0.50, when

$W$ = the unit weight of concrete in pcf

$f'_c$ = the nominal 28-day compressive strength of the concrete, psi

The above concept is consistent with Inge Lyse's conclusion that creep, while proportional to the applied stress, is primarily governed

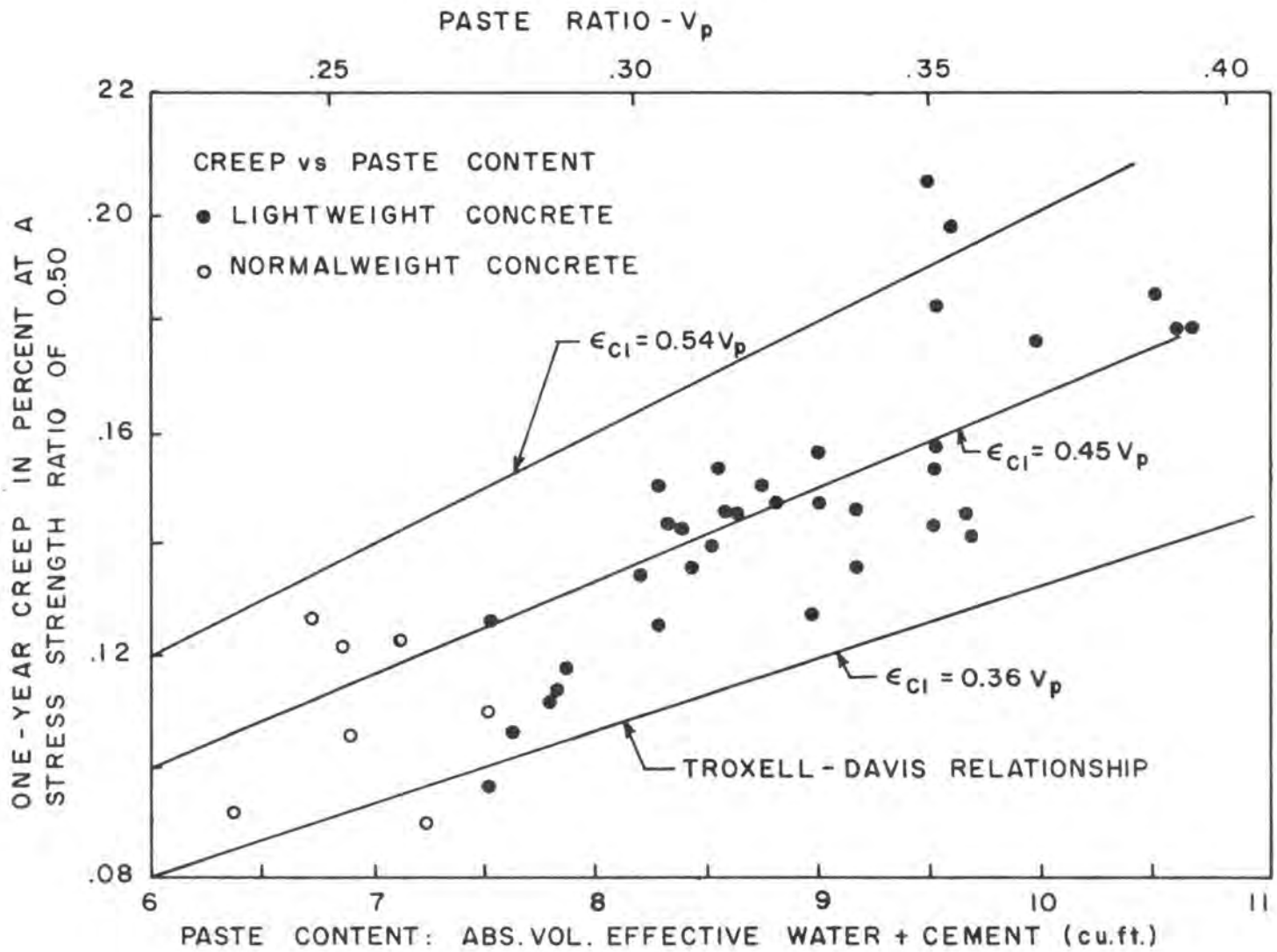


FIG. 15. RELATIONSHIP BETWEEN PERCENT CREEP AND PASTE RATIO

by the shrinkage characteristics of the concrete (41). Thus creep can be computed from the shrinkage by multiplying by the ratio of the applied sustained stress, $\sigma$, to the stress, $\sigma_{se}$, which would give a creep strain equal to the shrinkage strain at the particular relative humidity. Hence, the total creep may be determined from Eq. 12, viz.

$$\varepsilon_c = \varepsilon_s \frac{\sigma}{\sigma_{se}}$$

$$= \varepsilon_{su}(1-e^{-\alpha_m t_d^e}) \frac{\sigma}{\sigma_{se}} \qquad (37)$$

The prediction method recommended by Wallo and Kesler is based on the assumption that creep consists of two components, basic creep and drying creep (40). Basic creep is assumed to be recoverable whereas drying creep is not. The equation for basic creep has been developed on the basis of a rheological model conforming to the viscoelastic nature of creep in concrete. Wallo and Kesler's equation for basic creep is

$$\varepsilon_{bc} = \sigma\beta\ [\alpha_1(1-e^{-t_\ell/\tau_1}) + \alpha_2(1-e^{-t_\ell/\tau_2}) + \phi_f t_\ell] \qquad (38)$$

where:

$\varepsilon_{bc}$ = basic creep strain at any time, $t_\ell$, for a sustained stress level $\sigma$

$\sigma$ = normal stress due to sustained load

$\beta$ = gel compliance factor

$$\beta = \frac{[1-V_a - (1-h)\ V_c]^2}{2.2\ h\ V_c}$$

where $V_a$, $V_c$ and h are as previously defined for Eq. 14

$\alpha_1, \alpha_2$ = compliance of Kelvin Springes

$\tau_1, \tau_2$ = retardation times of Kelvin dash pots

$\phi_f$ = effective fluidity of free dash pot

$t_\ell$ = time in days after initial loading

The rheological constants may be determined by curve fitting techniques. Wallo and Kesler suggest the following values as appropriate for a temperature environment of 70°F and a relative humidity of 100 percent:

$$\alpha_1 = 225 \times 10^{-9}$$

$$\alpha_2 = 115 \times 10^{-9}$$

$$\tau_1 = 35$$

$$\tau_2 = 2$$

$$\phi_f = 0.30 \times 10^{-9}$$

Eq. (38) is based on the assumption that no significant additional hydration occurs after loading and that stress levels are sufficiently low to insure linearity of the basic creep strain.

Ali and Kesler (26) observed that drying creep is a function of moisture migration from the specimen and is therefore, related to shrinkage. They recommend the use of the relationship

$$\varepsilon_{dc} = \sigma\beta \frac{\varepsilon_s}{V_{ch}} (a+\frac{b}{t}) \tag{39}$$

where:

$\varepsilon_{dc}$ = drying creep at time t

$\varepsilon_s$ = free drying shrinkage at time t, (Eq. 17)

a,b = constants independent of mix proportions

$V_{ch}$ = volume concentration of hydrated cement (Eq. 16).

For 70°F and 50 percent relative humidity they found that a = 2.99 x $10^{-4}$ and b = 7.33 x $10^{-4}$ gave reasonable agreement with experimental values.

Using Wallo and Kesler's prediction method, total creep is then obtained by

$$\varepsilon_c = \varepsilon_{bc} + \varepsilon_{dc} \tag{40}$$

Rheological models have also been used by other investigators including Pauw and Hollrah at the University of Missouri. Hollrah's model (Appendix II- A) provides useful relationships for extrapolating creep and shrinkage properties for concretes on the basis of data obtained from specimens made with the same materials but different mix proportions.

## 3.9 Temperature Effects

The information available on temperature effects on creep and shrinkage is sparse and contradictory. Generally, an increase in temperature will result in increased strain and in an increased rate of development at early ages. A forty degree increase in temperature over the normal ambient range of 68 - 72°F will be reflected in about a 60 percent increase in shrinkage and creep (47,48). Additional research is needed before the effect of temperature on the rate and magnitude of creep and shrinkage can be defined analytically.

The coefficient of thermal expansion is primarily dependent on the type of aggregate. Values ranging from as low as $4 \times 10^{-6}$ in./in./°F for some lightweight concretes to as high as $7 \times 10^{-6}$ in./in./°F for some normal weight concretes have been observed.

# CHAPTER IV
# PREDICTION OF AXIAL DEFORMATION UNDER TIME-DEPENDENT COMPRESSIVE STRESS

## 4.1 Introduction

Creep of concrete under constant uniaxial stress can be predicted with a reasonable degree of accuracy by means of a standard creep curve suitably modified for environmental, geometric, consistency and other factors, as discussed in the previous chapter. For structural analysis, however, these predictions are of only limited direct use. In actual structures a state of constant stress occurs rarely, if ever.

Most structural elements are subjected to a combination of interacting time-dependent changes in strain and stress. These changes are the result of stress redistribution due to both internal and external constraints. Thus the stress history of the member depends not only on variations of the external applied load but also on the elastic and time-dependent deformations due to these loads combined with the effect of stresses and strains induced by internal and external geometric constraints and by temperature and other environmental factors.

Even in simple structural elements, such as reinforced concrete columns subjected to constant sustained concentric loads, the stress distribution between concrete and reinforcement is time-dependent because the creep and shrinkage deformations in the concrete are restrained by the reinforcement. An exact analysis of the stress distribution for even such a simple member can be quite complicated and time consuming and is, of course, no more reliable than the accuracy with which the elastic and time-dependent properties of the concrete can be predicted.

Complex methods of analysis based on the creep and shrinkage properties of plain concrete, therefore, are rarely justified for design. The primary value of such methods is that they serve as a guide for evaluating the order of magnitude of error that may be introduced by the use of simplified assumptions and analysis.

Several of the recognized methods of analysis of deformation behavior under time-dependent compressive stress are described below. The validity of these methods is evaluated by comparing analytical results with actual test data. The comparisons are limited to cases of plain concrete specimens subjected to time-dependent concentrically applied compressive stresses to avoid complication due to internal stress redistribution.

## 4.2 The Effective Modulus Method

In its basic form the effective modulus method of analysis is the simplest but least accurate of the methods considered. The method lacks accuracy because it does not take into account the stress history or age at time of first loading. The method is based on the use of a single strain-time curve for a specimen under constant stress, initially applied at age t=k, as shown in Fig. 16.

The effective modulus, $E_{ce}$, is defined by

$$E_{ce} = \frac{\sigma}{\varepsilon_i + \Sigma\varepsilon_c} = \frac{E_c}{1+\varepsilon_c' E_c} = \frac{E_c}{1+C_t} \tag{41}$$

where:

$\sigma$ = stress, psi

$\varepsilon_i$ = initial or nominal elastic strain

$\Sigma\varepsilon_c$ = total creep strain

$E_c$ = elastic modulus, psi

$\varepsilon_c'$ = specific creep (creep strain per psi)

$C_t$ = creep strain ratio ($\Sigma\varepsilon_c/\varepsilon_i$).

The ordinates in the specific strain curve in Fig. 16 are proportional to $1/E_{ce}$ and at time of initial load application, t=k, $E_{ce} = E_c$, the nominal elastic modulus. Thus for a constant load, the above definition is equivalent to the sustained load modulus as defined by McHenry (22).

In applying the effective modulus method it is normally assumed

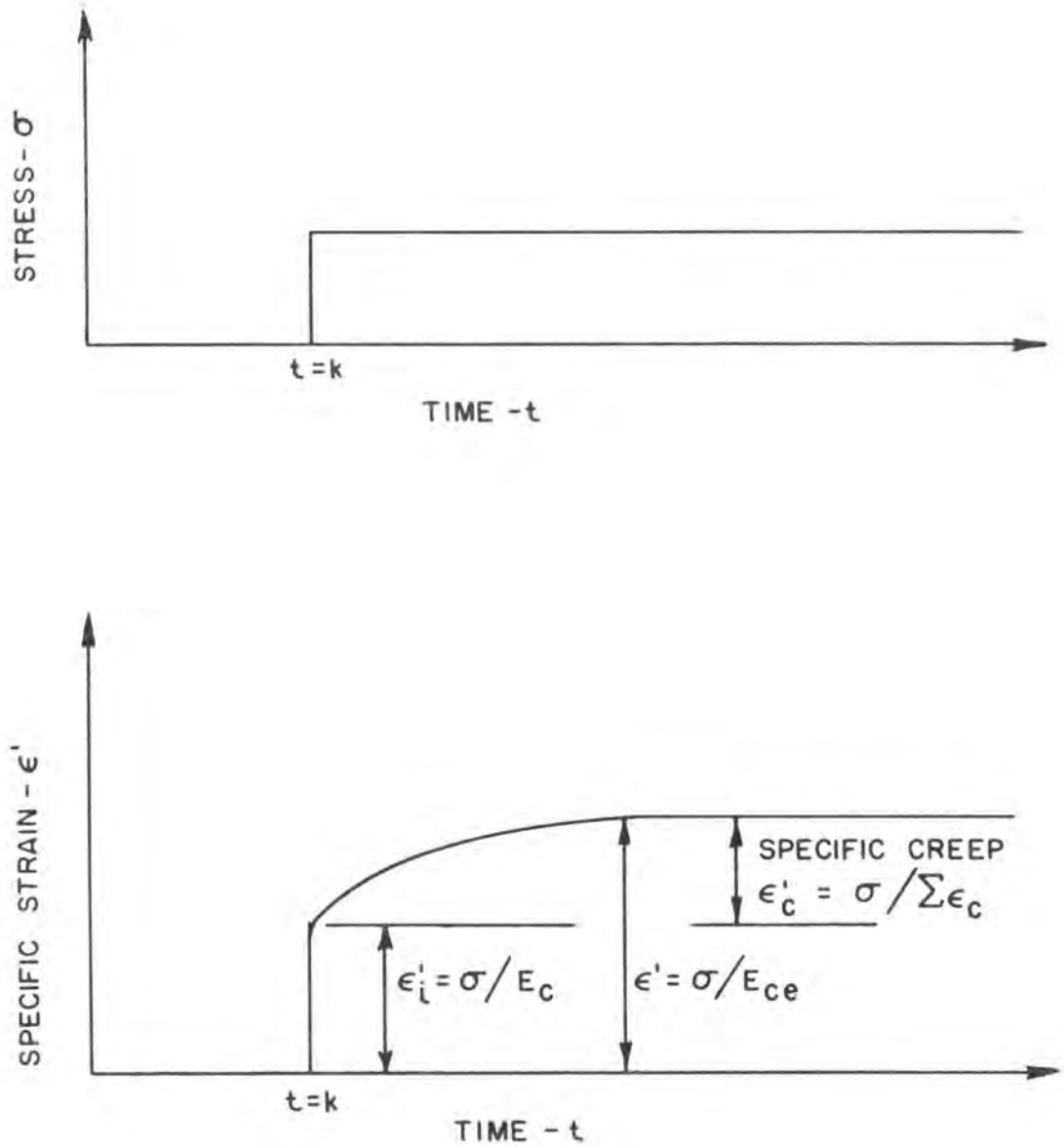


FIG.16 EFFECTIVE MODULUS $E_{ce}$

that the sum of the elastic and creep strains at any time is equal to the stress at that time divided by the appropriate value of the effective modulus. If the sustained load modulus is used as the value for the effective modulus, the method will overestimate the sum of the elastic and creep strain for stress due to loads which increase with time, and underestimate these strains, for stresses which decrease with time. In fact, since these strains are assumed to be proportional to stress, the effective modulus method tacitly assumes that both elastic and creep strain are fully recoverable. It is also clear that since the computed strain at any time is assumed to be only a function of the stress at that time, the method ignores the effect of stress history. Nevertheless, the simplicity of the effective modulus concept is so great that it makes it the most convenient method of analysis available. In most practical design applications concrete stresses tend to decrease gradually with time due to stress redistribution resulting from the stiffening effect of the reinforcement. The effect of this decrease is usually compensated by the effect of the time delay before the full design loads are applied. For such cases the method predicts the ultimate elastic and creep strains with acceptable accuracy.

## 4.3 The Method of Superposition

About 1938 McHenry (22) noted from measurements on concrete dams that creep occurred about equally for positive and negative load increments, that is creep and creep recovery were about equal for equal, but opposite, load changes. This observation led McHenry to the postulation of the principle of superposition for concrete:

> "The strains produced in concrete at any time t by a stress increment applied at any time k are independent of the effects of any stress applied earlier or later than k. The stress increment may be either positive or negative, but stresses which approach the ultimate strength are excluded."

McHenry's hypothesis implies that the principle of superposition can be applied both to the elastic strain and to the creep strain by assuming that creep is equivalent to delayed elasticity. The appli-

cation of this principle requires that specific creep/time curves be available for every stress increment or that the specific creep surface as shown in Fig. 5 be defined. Thus in the example shown in Fig. 17 the specific creep curves for initial loading at age $k_a$, $k_b$, and $k_c$ are required before the strain history can be predicted for the stress history shown.

For sufficiently large values of k, the concrete is mature and all specific creep/time curves are essentially identical. This implies that all strains due to loads applied after the concrete has matured are completely recoverable upon unloading as shown in Fig. 18.

The superposition method can be applied to compute the strain for any stress history by approximating the stress curve by a sufficiently large number of stress increments as shown by the example in Fig. 19. Where the stress history is dependent on redistribution of stress due to internal or external constraints, (e.g. the effect of stiffening due to reinforcement) the stress level at each time increment must be adjusted to satisfy both equilibrium and strain compatibility. An example of such a problem will be given in the next chapter.

It is generally not practical to determine specific creep/time curves by test for more than a few ages at time of loading. A mathematical model must be developed from such data to define the specific creep/time surface to permit interpolation for all load increments. While the method is the most accurate analysis available, for most loading cases it is quite laborious. The numerical calculations, however, can readily be programmed for computer analysis. The method is accurate only for load increments applied at early ages. Negative load increments applied at ages greater than about three months may overestimate computed strain increments by as much as fifty percent or more (30). Thus one should not be deluded by the complexity of the method into expecting a high degree of accuracy in all cases.

## 4.4 The Rate-of-Creep Method

The rate-of-creep method is based on the use of only a single specific-creep/time curve for the concrete. The method is most convenient if the curve can be expressed in mathematical form as a funct-

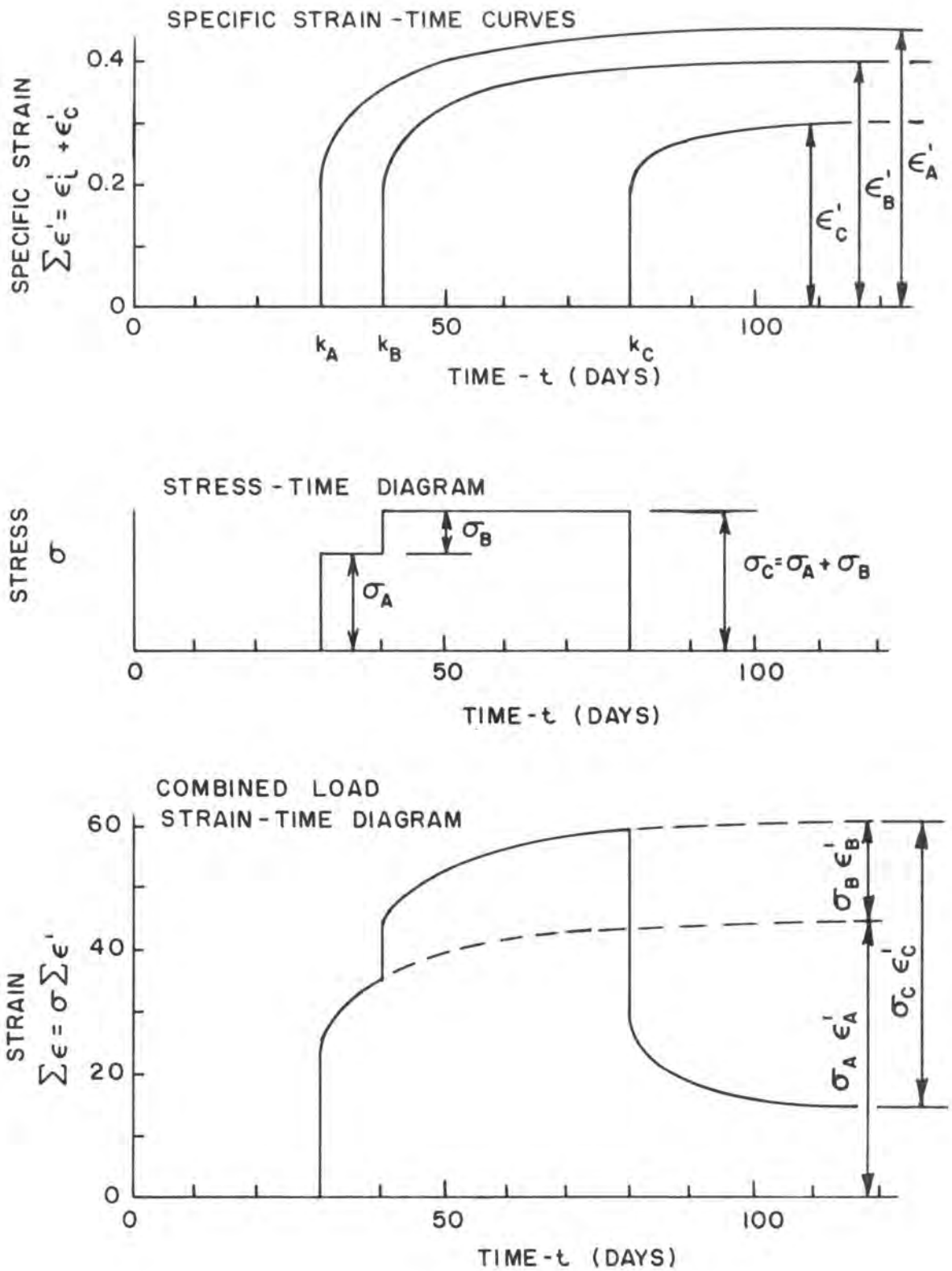


FIG. 17 SUPERPOSITION PRINCIPLE
SUM OF ELASTIC AND CREEP STRAIN

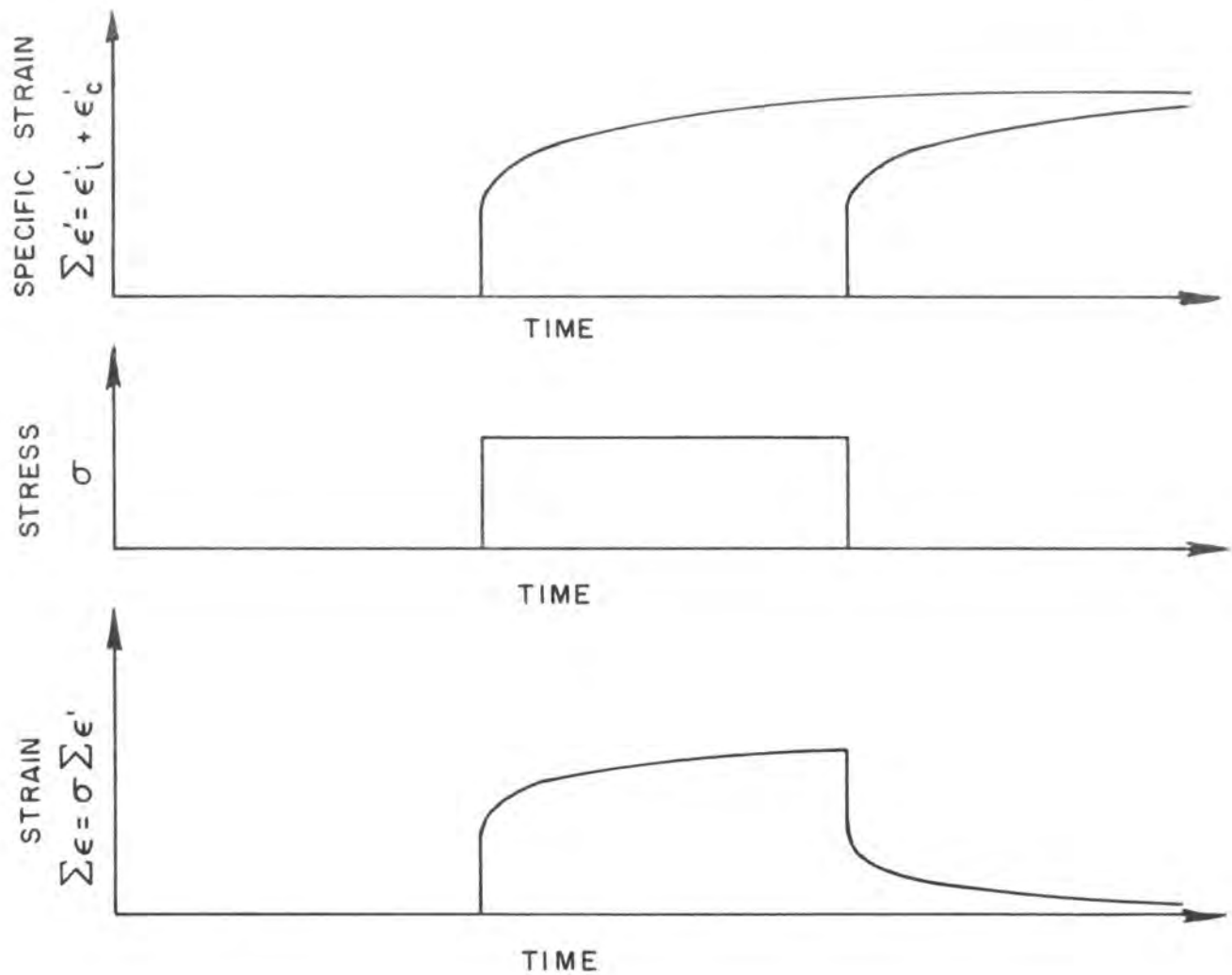


FIG. 18 CREEP RECOVERY FOR MATURE CONCRETE

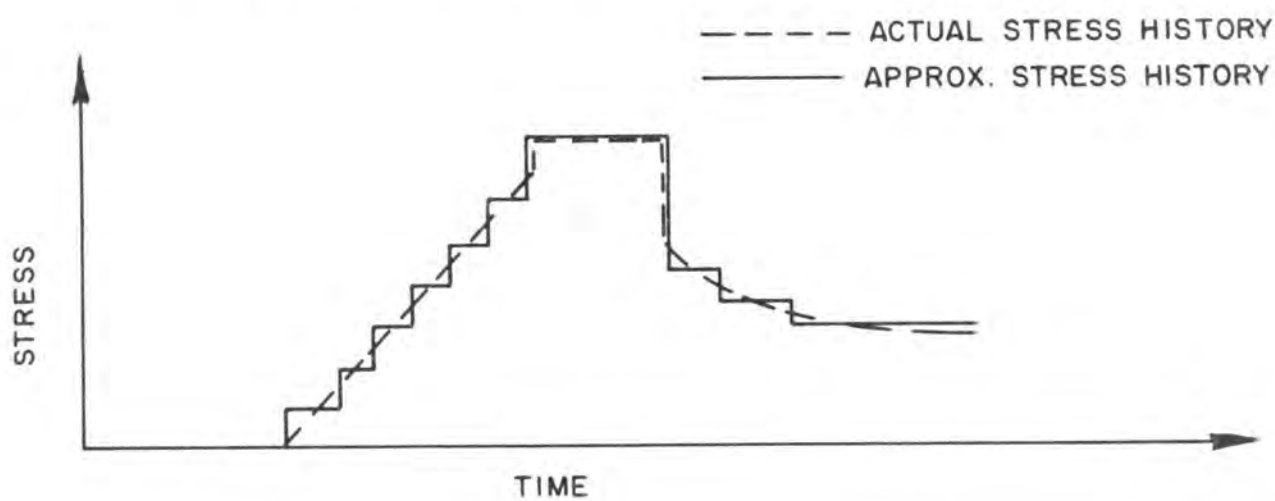


FIG. 19 APPROXIMATION OF STRESS HISTORY

ion of the time after first loading, thus

$$\varepsilon'_{ct} = A\ F(t-k) \tag{42}$$

where:

$\varepsilon'_{ct}$ = specific creep strain (strain/psi) at age t

A = constant

F() = function of ( )

t = age of concrete

k = age of concrete at first loading

The method assumes that the rate of creep at any age is equal to the stress multiplied by the slope of the specific-creep/time curve. The creep strain at age t is then

$$\varepsilon_{ct} = A \int_k^t \sigma \frac{dF(t-k)}{dt}\, dt \tag{43}$$

and the elastic strain is

$$\varepsilon_i = \frac{\sigma}{E_c}$$

An example of the application of this method is given in Fig. 20. The method does not make an allowance for creep recovery. In fact, it is equivalent to the superposition method if it is assumed that the specific creep/time curves can be generated by a parallel shift of the curve. Hence, the method overestimates creep under falling stress and underestimates, under rising stress.

## 4.5 Comparison of Analytical Results with Experimental Data

The testing program conducted at the University of Missouri included a study to determine the effect of age at time of loading as well as a study to determine the magnitude of creep recovery upon unloading (7). Fig. 21 shows the comparisons of predicted strain response compared to the observed strains for the normal weight concrete studied in this phase. From these results the following conclusions can be drawn:

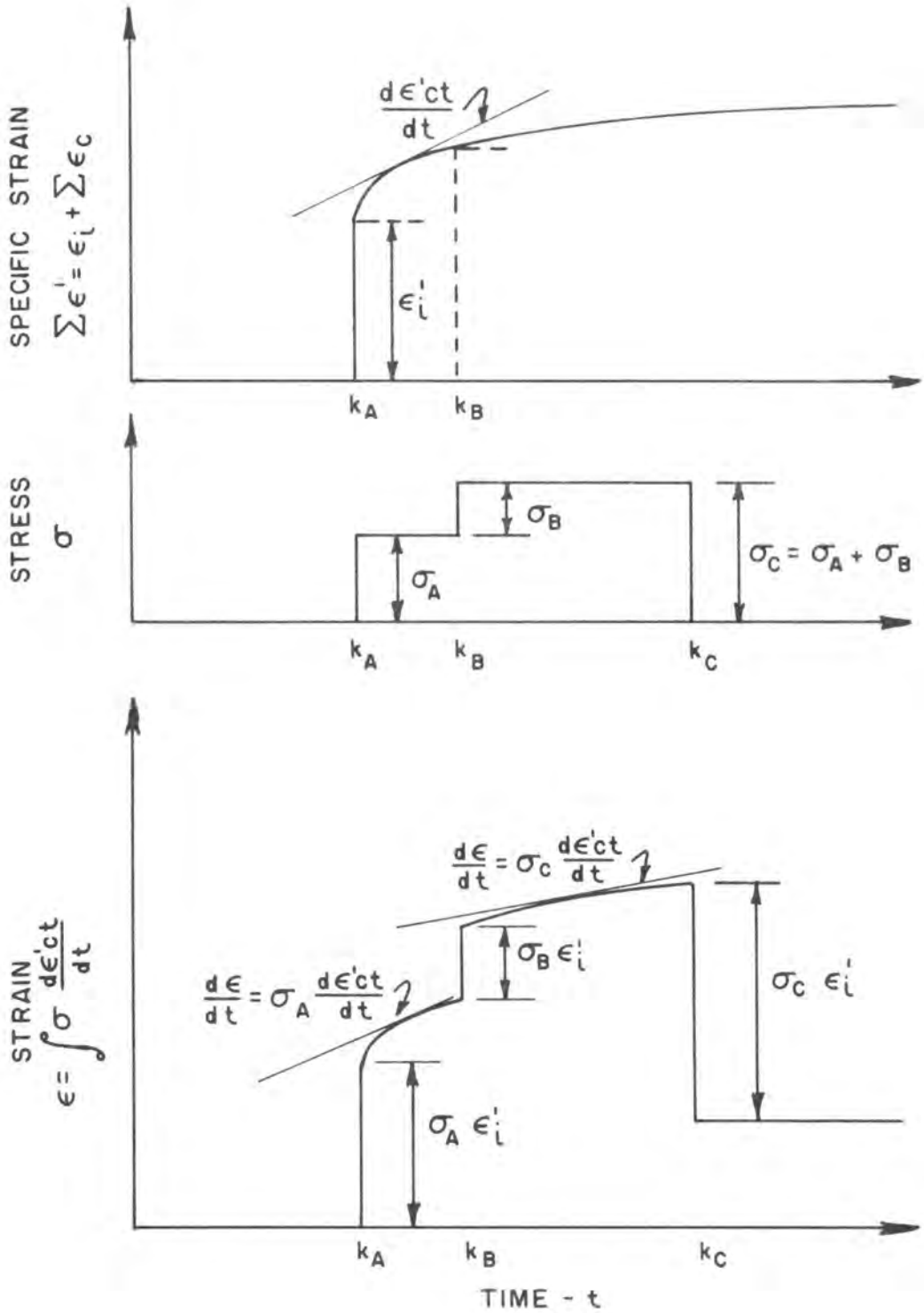


FIG.20 RATE-OF-CREEP METHOD

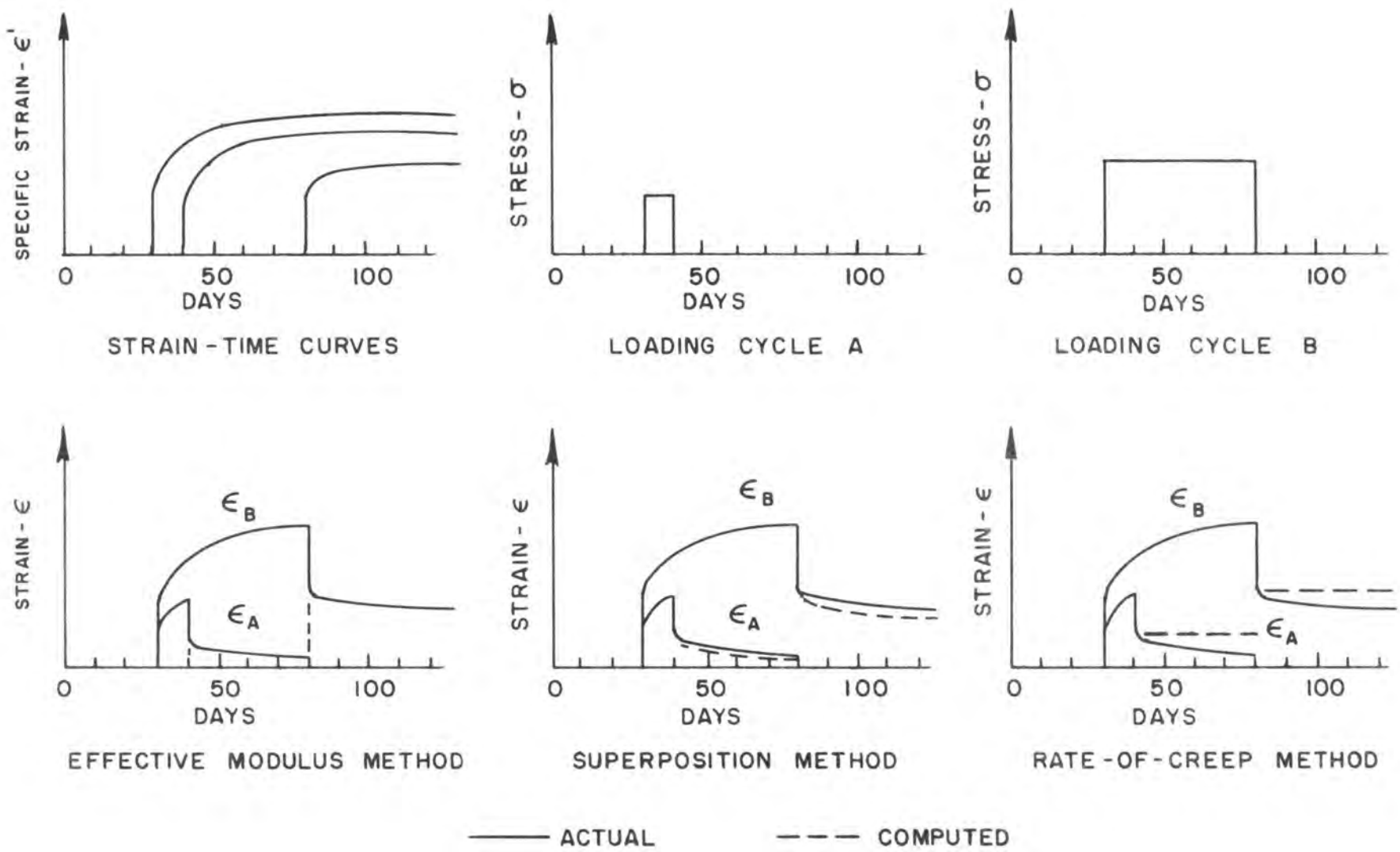


FIG. 21 COMPARISON OF CREEP ANALYSIS METHODS

a. For the effective modulus method, the computed strain can be matched only when the assumed modulus matches the sustained load modulus and provided that the applied load has been held constant from the time of initial loading up to the time corresponding to the value of the sustained modulus. Furthermore, upon unloading, both the elastic and creep strain are assumed to be fully recovered.

b. The superposition method overestimates creep recovery. Hence, for falling stress levels this method tends to underestimate strains. This conclusion has been confirmed by tests conducted by Kimishima and Kitahara (30) and may also be inferred from a consideration of the effect of loading and unloading fully matured concrete specimens. The superposition principle infers that the creep in such concretes would eventually be fully recoverable (22).

c. The rate-of-creep method overpredicts the strains for falling stress levels since upon unloading the strain rate is zero and only the elastic strain is recovered. Similarly the rate-of-creep method will tend to underpredict strains for a rising stress level.

Hollrah (6) measured the creep recovery of cylinders that had been under sustained load for two to three years. His measurements indicated that the maximum recovery occurred about thirty days after unloading and that the strains thereafter, again gradually increased. Maximum creep recovery, in general, was smaller than the creep observed when the previously unloaded companion shrinkage specimens were placed under load. These results again support the conclusion that the superposition principle is not valid for negative loads applied after full maturation of the concrete. Neville's studies (4) and Roll's tests (23) also confirm, that only about 10 to 30 percent of the creep strain is recoverable. Neville found that the recovery is quite sensitive to environmental humidity but that only a portion of the drying creep is reversible. Hollrah's tests (6) further revealed that specimens, unloaded, after having been subjected to a sustained

load for two to three years, exhibited an additional creep increment upon reloading.

Chai's work (7) led to the development of several modified methods of analysis to take into account incomplete recovery of creep strains under falling load. A modification of the superposition method was also developed to reduce the amount of test data required and to simplify the numerical analysis. These methods have certain basic features which are similar to the rate-of-flow method proposed by England and Illston (50).

## 4.6 The Rate-of-Flow Method (50)

In the rate-of-flow method, as developed by England and Illston, it is assumed that the stress-dependent strains of concrete under sustained load can be separated into three major components:

a. elastic
b. delayed elastic (recoverable creep)
c. flow (irrecoverable creep, drying creep and plastic deformation).

The main properties of these components as determined experimentally are depicted in Fig. 22. This figure shows the relative magnitude and variation with time of the three strain components for a concrete subjected to a constant stress between the times $k_a$ and $k_b$. The total stress dependent strain response is also shown.

As for the other methods of analysis, the stress/strength ratio is assumed to remain sufficiently small (0.4 to 0.5) so as not to result in a breakdown and failure of the structure of the concrete. The properties of the three strain components are:

a. Elastic. The initial elastic strain is the instantaneous strain and is assumed to be proportional to the applied stress. The ratio, stress/strain, is the modulus of elasticity, which varies with the age of the concrete and normally increases with time. Hence, as shown in Fig. 22, the elastic strain recovered upon removal of a sustained stress is less than the instantaneous strain which occurs when the stress is applied.

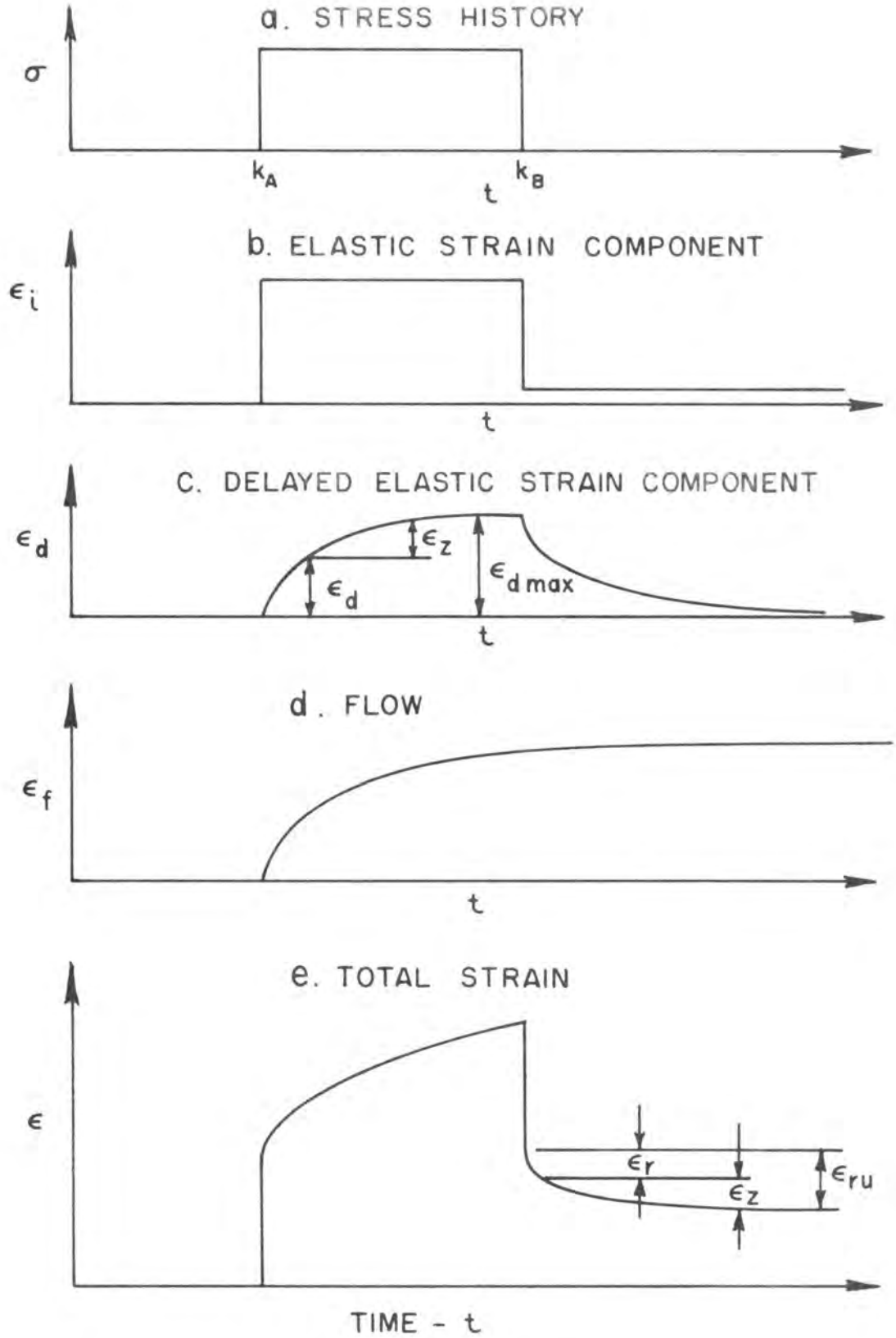


FIG. 22 STRAIN COMPONENTS FOR RATE-OF-FLOW METHOD

b. Delayed Elastic. The delayed elastic strain is a time-dependent strain which is fully recoverable upon removal of the applied stress. Its properties are assumed to be the same for either increasing or decreasing load increments. The limiting value is assumed to be proportional to the applied stress and not vary with maturity of the concrete. The time rate of strain is assumed to follow the law of mass action (i.e., to be proportional to the delayed strain, $\varepsilon_z$, yet to be developed). The time of development is a function of the maturity of the concrete, hence, the time of recovery is greater than the time of development in Fig. 22c.

c. Flow. The time-dependent irrecoverable strain, termed flow by England and Illston, is considered as viscous movement. Its rate of occurrence at a particular time is assumed to be independent of the previous stress history. The rate is proportional to the applied stress, and under constant stress, diminishes as the concrete matures. The decrease in rate is shown in Fig. 22d and the total flow remains unrecovered when the stress is removed at $t = k_b$.

The properties of the delayed elastic strain are approximated by two expressions of the form:

$$\varepsilon_d = \varepsilon_z \ (1-e^{-\Delta\varepsilon_f'/Q}) \quad , \qquad (45)$$

representing rapid and slow delayed elastic strains. In Eq. 45:

$\varepsilon_d$ = delayed elastic strain under constant stress applied during a time interval $\Delta t$

$\varepsilon_z$ = delayed elastic strain yet to come at the start of the interval

$\Delta\varepsilon_f'$ = flow per unit stress (specific flow) during the interval

$Q$ = constant to be determined from test data

$e$ = Naperian base.

Application of the method presumes that the following data are available or can be assumed:

1. Elastic modulus as a function of age
2. Specific flow as a function of age throughout the period of computation
3. Limiting values of the rapid and slow delayed elastic strains and the corresponding constants $Q_r$ and $Q_s$.

Modulus values may be determined from control specimens. The remaining data may be developed from two experimental curves such as shown in Fig. 23. Curve (a) gives the stress-dependent strains for a constant uniaxial compressive load maintained for the full period of computation. Curve (b) gives the strains resulting from a similar stress applied for a period just long enough for the delayed elastic strain to be fully developed and the test is then continued just long enough to obtain full recovery. Both tests are commenced at the beginning of the period covered by the computation and in each case the strains due to unit stress are plotted.

The recovery in curve (b) includes both the elastic and delayed elastic components. The elastic component can be determined from the appropriate value of the modulus and the remainder thus represents the delayed elasticity. Subtracting the initial elastic and limiting delayed elastic strain from curve (a) yields the required distribution of flow for the period of computation. The origin of flow is assumed to be at point A, the intersection of the limiting elastic plus delayed elastic strain with the time ordinate $k_a$ at the beginning of the period of computation. The curve between points A and B may be interpolated by a tangent line to the total strain curve because the interval is relatively short.

The two delayed elastic terms may be determined from the time-dependent recovery by plotting log $\varepsilon_z$ for the recovery curve in (b) vs. time as shown in Fig. 24. This curve may be approximated by two straight lines. The limiting values of the rapid and slow delayed elastic strains are then determined from the ordinate of the intersection of the two straight lines and the constants Q from the slopes

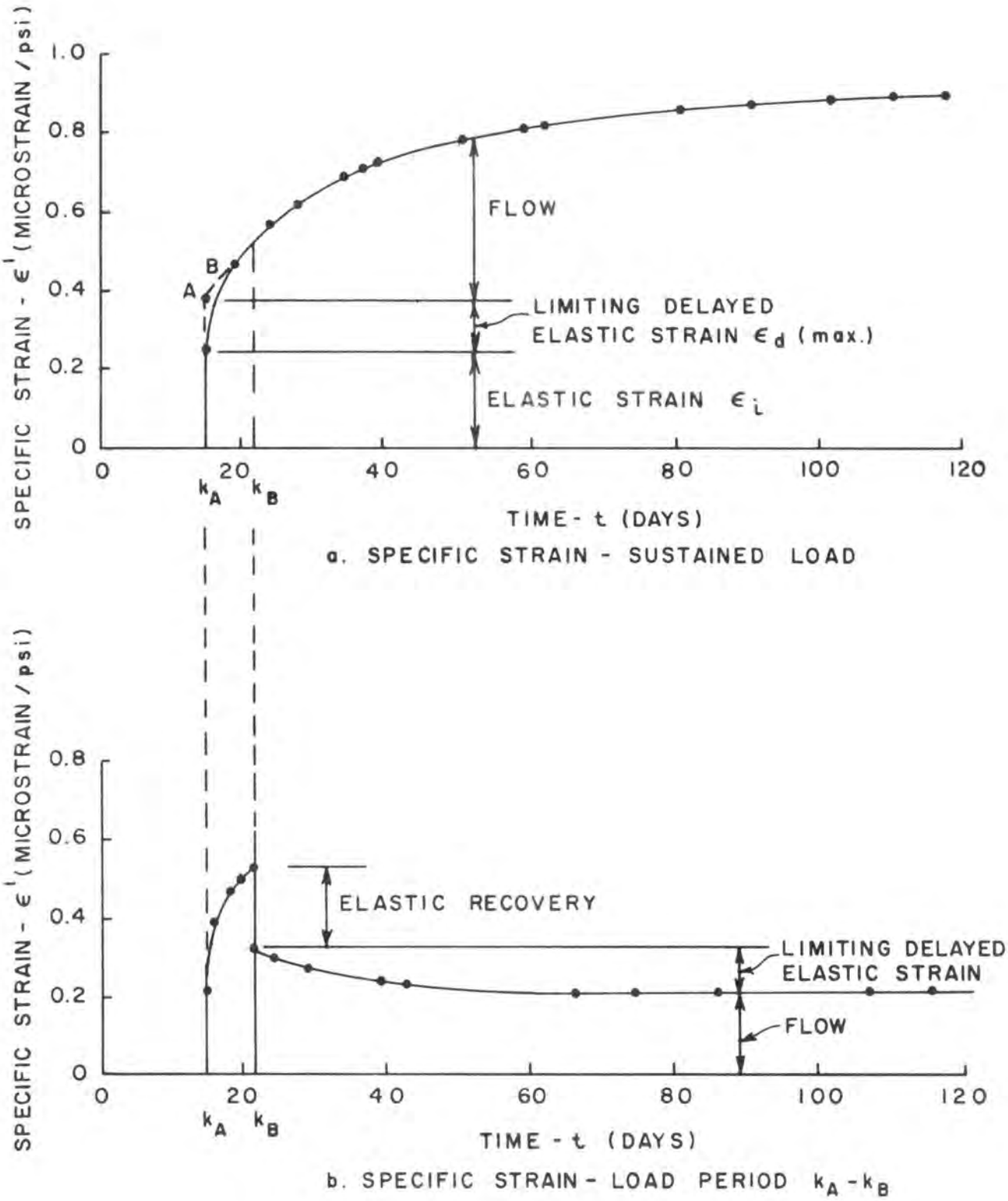


FIG. 23. BASIC CREEP DATA FOR RATE-OF-FLOW METHOD

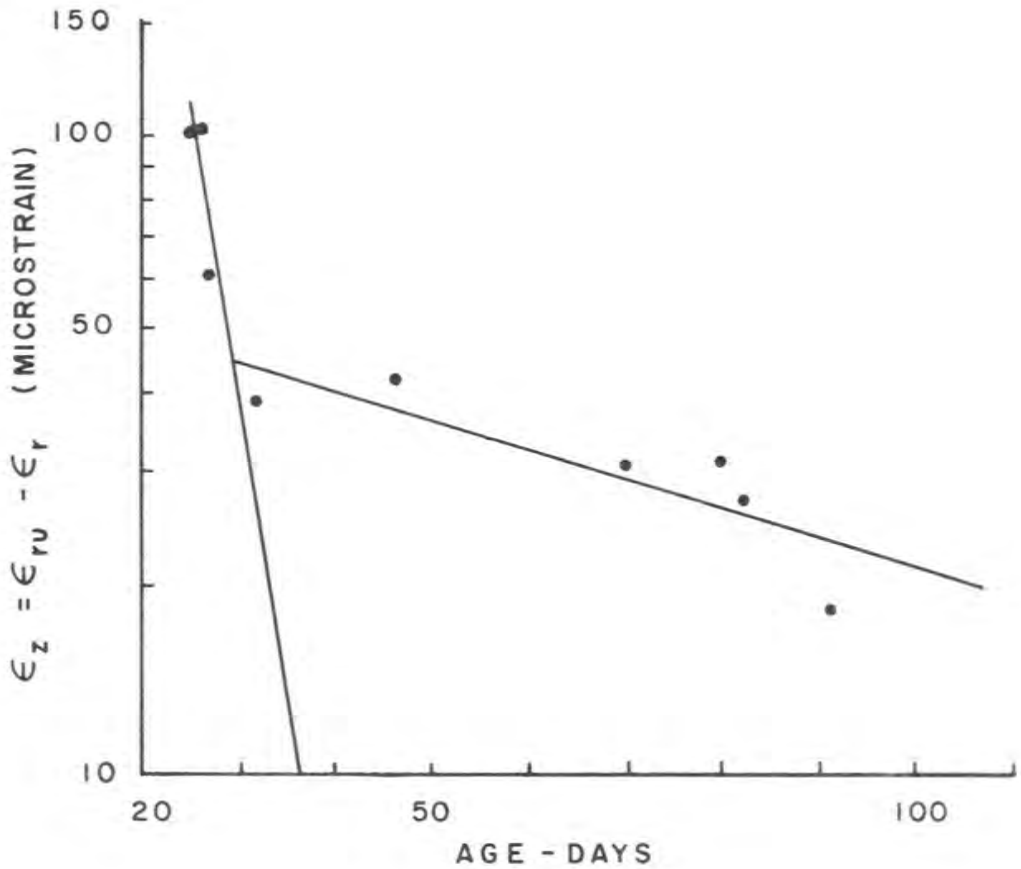


FIG. 24. PLOT FOR DETERMINING Q-VALUES

of the lines.

Solving Eq. 45 for Q:

$$Q = -\frac{\Delta\varepsilon_f'}{\ln(\frac{\varepsilon_z-\varepsilon_d}{\varepsilon_z})} \tag{46}$$

Thus, for example, for the slow delayed elastic strain

$$Q_s = \frac{\Delta\varepsilon_f'}{\Delta t}\ \frac{1}{2.3}\ \left(\frac{\Delta t}{\log_{10}\left[(\varepsilon_{dsu}-\varepsilon_{ds})/\varepsilon_{dsu}\right]}\right) \tag{47}$$

where:

$\Delta\varepsilon_f'/\Delta t$= average rate of specific flow during the period of recovery of the slow delayed elastic strain

$\varepsilon_{dsu}$ = limiting value of the slow delayed strain, $t=\infty$

$\varepsilon_{ds}$ = value of the delayed elasticity at the beginning of time interval

$\Delta t$ = time interval considered.

Hence, the third term in Eq. 47 is the slope of the slow delayed elastic strain line in Fig. 24.

## 4.7 The Residual Creep Limit Method

Based on Chai's experimental studies, Pauw and Chai proposed the residual creep limit principle. Residual creep limit curves may be generated for any specimen initially loaded at age k subjected to a constant sustained load until age t and then unloaded, by plotting the limiting or minimum value of the residual creep as ordinate at time t, the age of the specimen at time of unloading. The difference between the creep and the residual-creep-limit curve therefore, represents the limiting value of delayed elasticity or recoverable creep, as shown in Fig. 6 and also in Fig. 25. The residual-creep-limit curve is essentially the same as the flow curve defined by England and Illston. Based on Lorman type approximations,

$$\varepsilon_c = \frac{(t-k)}{t_{ck} + (t-k)}\ \varepsilon_{cu} \tag{48}$$

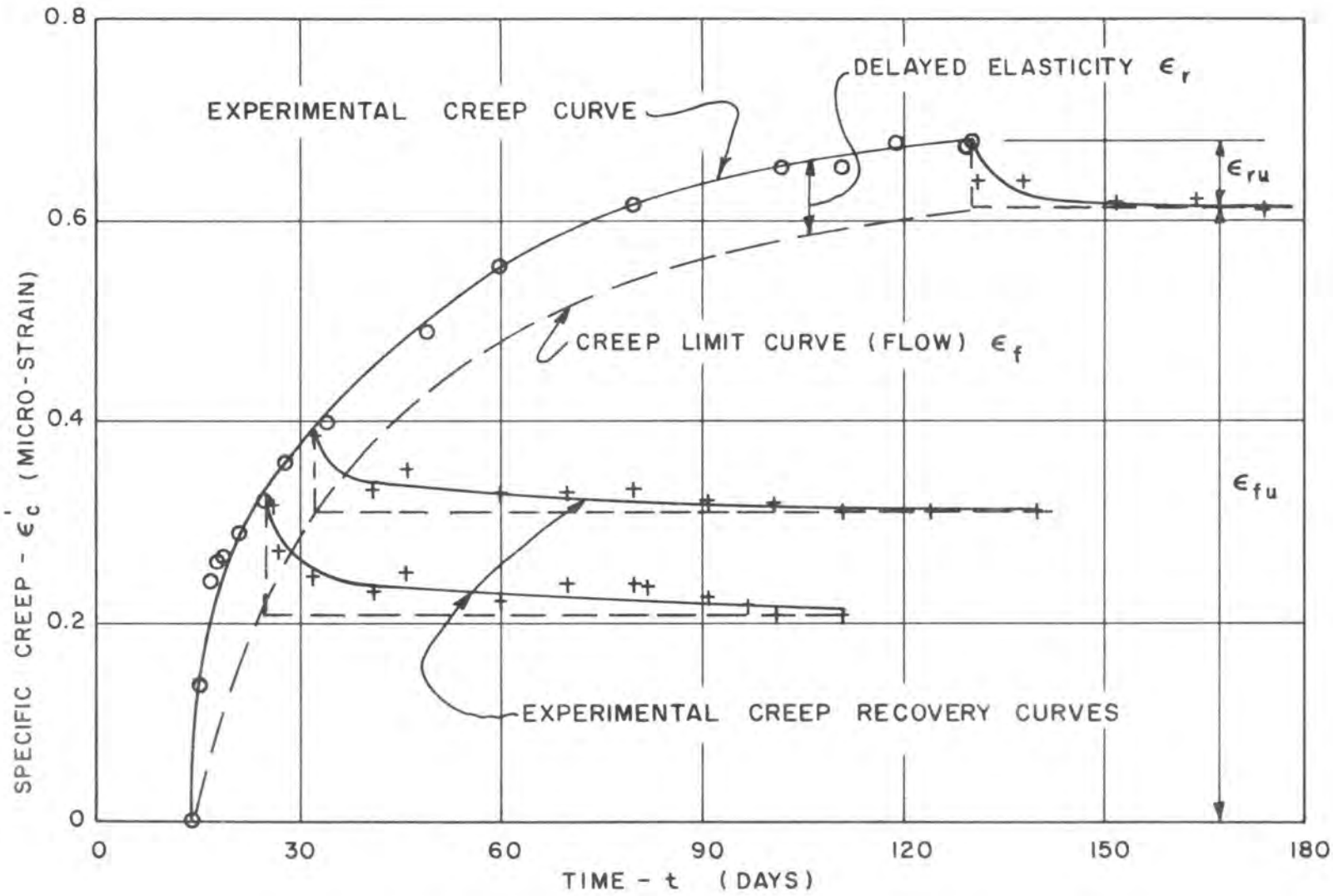


FIG. 25. TOTAL CREEP AND CREEP LIMIT CURVES

where:

$\varepsilon_c$ = strain

$\varepsilon_{cu}$ = limiting strain

t-k = time after initial loading

$t_{ck}$ = characteristic time, i.e., the time increment after loading to produce one-half the limiting strain.

The values of the characteristic time $t_{ck}$ for both the total creep and the residual creep limit were found to increase with age k at time of initial loading as shown in Fig. 26. It may be noted that $t_{ck}$ is approximately the same for both the total creep, and the residual creep curve, but is greater for normal weight concrete than for lightweight concrete. Based on the limited amount of data available it was found that $t_{ck}$ can be estimated by an equation of the form:

$$t_{ck} = A \left(\frac{k}{14}\right)^B \tag{49}$$

where:

A = value of $t_{ck}$ for k=14 days

B = constant which is a function of the type of concrete, size of specimen, and environment.

For specimens with a mass factor (area/perimeter ratio) of one inch, stored in a relative humidity of 50 percent at a temperature of 72°F, A was found to have a value of about 20 days for both the normal weight, and the lightweight concrete tested. B was found to have values of 0.4 and 0.2 for normal weight and for lightweight concrete, respectively. The rate of development of the delayed elasticity was found to be much more difficult to analyze. The limiting value is a relatively small fraction of the total creep, and must be determined by subtracting the flow from the total creep. The determination of this value is further complicated by the change in modulus of the concrete with age. Nevertheless, based on an analysis of creep recovery, it is apparent that the rate of development of the delayed elasticity is much more rapid than that of the flow. A characteristic time of 3

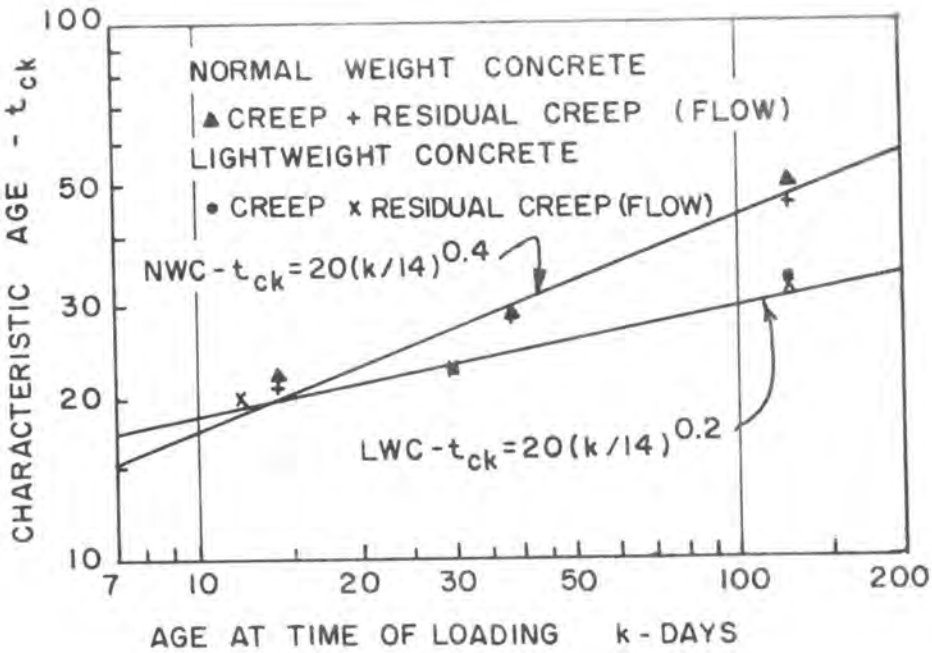


FIG. 26 CHARACTERISTIC AGE

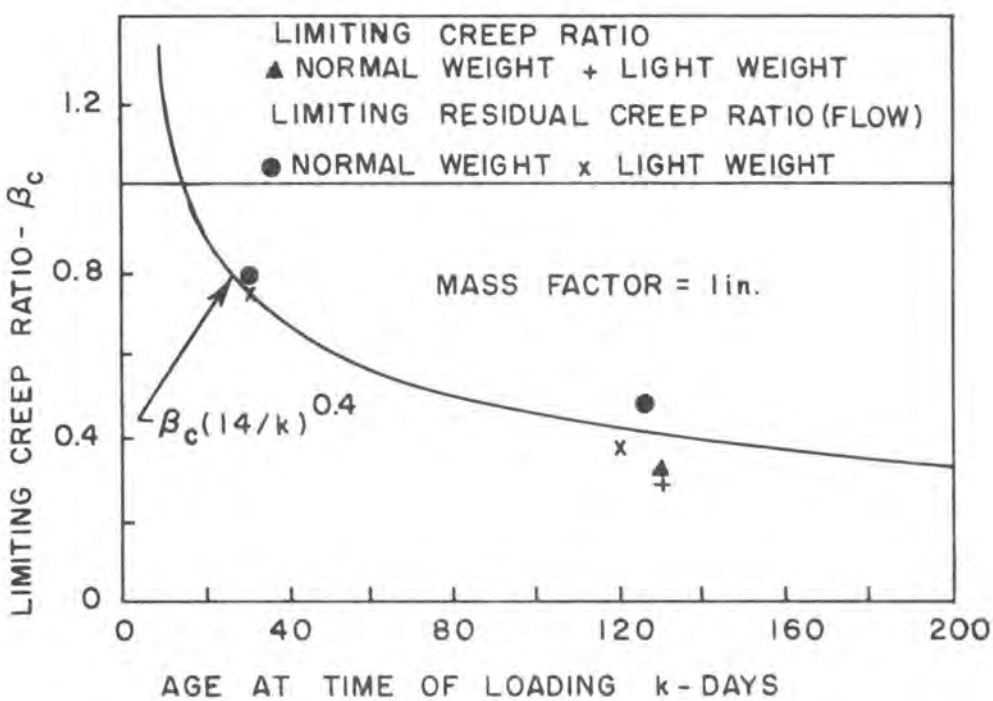


FIG. 27 LIMITING TOTAL CREEP AND FLOW RATIOS

to 4 days appears to give the best fit. This result is also consistent with the observation that a Lorman approximation tends to underestimate the total creep at early ages after initial loading. Hollrah (6) found that the limiting value of the delayed elastic recovery was reached in about thirty days, even for specimens unloaded after several years. Thus the total stress dependent strain may be estimated by

$$\varepsilon_c = \sigma \left(\frac{1}{E_c} + \frac{(t-k)}{t_{ck} + (t-k)} \varepsilon'_{fu} + \frac{(t-k)}{4 + (t-k)} \varepsilon'_{du}\right) \tag{50}$$

and the strain recovery, upon unloading, by:

$$\varepsilon_{rt} = \sigma \left(\frac{1}{E_c} + \frac{(t-k_r)}{4 + (t-k_r)} \varepsilon'_{du}\right. \tag{51}$$

where:

$\varepsilon_c$ = total stress dependent strain at age t days for sustained stress $\sigma$, initially applied at age k days

$\varepsilon_{rt}$ = total strain recovery at age t days when the stress $\sigma$ was removed at age $k_r$ days

$\sigma$ = stress level, psi

$\varepsilon'_{fu}$ = limiting specific flow (flow/psi) when initially loaded at age k days

$\varepsilon'_{du}$ = limiting delayed elastic strain recovery per psi when unloaded at age $k_r$ days

$t_{ck}$ = characteristic time, defined by Eq. 49.

The value of $\varepsilon'_{ru}$ appears to range from about 10 to 30 percent of $\varepsilon'_{fu}$, and about 20 to 40 percent of the instantaneous specific elastic strain, $\varepsilon'_i$. The value of $\varepsilon'_{ru}$ also tends to decrease with increased maturity of the concrete.

The limiting creep, $\varepsilon_{cu}$, and the limiting flow, $\varepsilon_{fu}$, decrease with increased age at time of loading. Fig. 27 shows typical observed values of the limiting creep and flow ratio

$$\beta_c = \frac{[\varepsilon_{cu}]_k}{[\varepsilon_{cu}]_{k'}} = \frac{[\varepsilon_{fu}]_k}{[\varepsilon_{fu}]_{k'}} \tag{52a}$$

plotted as a function of the age, k, at time loading and with the reference age, k', taken as fourteen days. While relatively little data is available, in the absence of specific data this ratio may be estimated by

$$\beta_c = \left(\frac{k'}{k}\right)^{\alpha_c} \tag{52b}$$

where $\alpha_c$ is a coefficient which must be determined experimentally. This coefficient appears to be also a function of the mass factor. For the data shown in Fig. 27 $\alpha_c$ was found to have a value of 0.40. Hence the creep characteristics of a given concrete can be estimated from a single strain/time curve for a loading-unloading cycle as shown in Fig. 25. Meyer's analysis of the Missouri University creep test data (4) has shown that the test load should be sustained for a minimum of about 90 days to obtain a reasonably accurate estimate of the ultimate creep strain based on the linearized Lorman plot. A corresponding point for the flow curve can be found at the time of unloading by measuring the residual creep about thirty days after unloading. The curves in Fig. 25 have been adjusted for elastic and shrinkage strains. It is convenient to assume a constant nominal modulus equal to the instantaneous modulus of time of initial loading and absorb the change in elastic strains in the value of the limiting delayed elastic strain. The latter is determined by subtracting the ordinance of the flow curve from the total creep strain at time of unloading. The flow curve may then be plotted by assuming the same value of $t_{ck}$ as was determined for the total creep curve by the linearized Lorman plot. Flow curves can then be generated for any other time of initial loading by estimating the limiting flow value by Eq. 52 and the characteristic time by Eq. 49. Similarly, the limiting total creep value can also be estimated by Eq. 52 and the limiting value of the delayed elasticity deduced by subtracting the limiting flow. Strains can then be computed for any applied stress increment by the use of Eq. 50 or Eq. 51. Although the computational procedure is somewhat involved and tedious, computations could readily be programmed for a computer.

## 4.8 Modified Effective Modulus Method

As noted before, the primary limitation of the elastic modulus method is the fact that it does not take into account the effect of stress history. Since all of the elastic and most of the delayed elastic strain is accounted for, the principal error introduced is due to the reduction in the limiting value of the specific flow as the concrete matures. If the stress history can be determined or approximated, the flow strain can be computed by a step by step procedure and added to the terminal elastic and delayed elastic strains. A modified effective modulus may then be computed by dividing the terminal stress by the total strain. In most cases, for nominally reinforced concrete members, the modified effective modulus will result in only minor changes in stress distribution provided the loading period is several times greater than the characteristic time. The application of the "Modified Effective Modulus" method will be considered in the next chapter in the analysis of columns subjected to a rising stress characteristic.

# CHAPTER V

# ELASTIC AND TIME-DEPENDENT DEFORMATIONS OF CONCENTRICALLY LOADED COLUMNS

## 5.1 Introduction

In the previous chapters, the time-dependent deformation properties of plain concrete, both under constant and variable load, have been considered. While these properties are of considerable interest in themselves, the designer's interest in them is in how these properties affect structural behavior. It has already been noted that these properties are dependent on a number of factors, many of which, such as environment and age at initial loading, are not completely under the control of the designer. Hence, the designer must assume some reasonable range of properties and analyze their effect on the behavior of his structure. Since this range of properties may be quite wide, an elaborate analysis for a single specific set of assumed properties is normally not warranted. An approximate analysis of the behavior of the structure for reasonable limiting values of the range of expected properties gives the designer information as to the sensitivity of the structure to time-dependent deformation. Based on this information potential trouble spots can be identified and the design modified if necessary.

## 5.2 Basic Analysis Assumptions

For the approximate analysis of reinforced concrete columns, two basic methods are considered: the effective-section-rigidity method and the rate-of-creep method. It may be demonstrated that for a given set of concrete properties and reinforcement ratio the first method slightly underestimates and the second method slightly overestimates the final strain and steel stress under constant sustained load. These approximate methods are, therefore, both very useful since they give

the designer an estimate of the error due to simplifications in the analysis.

The effective section rigidity is determined on the basis of an effective elastic modulus, suitably adjusted to take into account the stress history. The analysis is then based on the assumption that time-dependent strains can be computed as equivalent delayed elastic strains. Temperature and shrinkage effects may be analyzed by estimating internal stresses for full constraint and computing the deformations and stress relaxation due to balancing external force systems.

The rate-of-creep method is based on the assumption that creep strains are irrecoverable. The derivation of the governing equations for this method is somewhat more involved and is therefore given in Appendix III-A.

## 5.3 Section Rigidity Profile

Since the section rigidity analysis is based on the assumption that time-dependent strains can be treated as equivalent delayed elasticity, the section rigidity must be treated as a variable function of both time and stress history. It is convenient to express the section rigidity as a function of either the creep ratio as defined in Eq. 41:

$$C_t = \frac{\Sigma\varepsilon_c}{\varepsilon_i}$$

or of the equivalent modular ratio:

$$\eta_e = \frac{E_s}{E_{ce}} = \frac{E_s(1+C_t)}{E_c} \tag{53}$$

$$= \eta(1+C_t)$$

where:

$$\eta = \frac{E_s}{E_c}$$

is the instantaneous or elastic modular ratio.

## 5.4 Shrinkage Strains by the Section-Rigidity Method

The analysis of elastic and time-dependent strains in a column subjected to a constant stress level is a relatively simple matter by the effective section rigidity method provided the elastic and time-dependent properties of the concrete are known or may be assumed with a reasonable degree of accuracy. The shrinkage of the concrete may be assumed to develop at a rate equivalent to the creep, hence, the shrinkage stress history is effectively incorporated. The shrinkage is assumed to be equivalent to the strain due to a constant force equal to the sustained load modulus

$$E_{cu} = \frac{E_c}{(1+C_u)} = \frac{E_s}{\eta_u} \tag{54}$$

divided by the ultimate shrinkage strain.

This force must be applied to the transformed area to compute the reduced shrinkage strain due to the stiffening effect of the reinforcement. This procedure is equivalent to assuming that the concrete is first subjected to a tensile stress to prevent shrinkage and that equilibrium is then restored by applying, to the reinforced member, a sustained load equal to the net area of the concrete times the shrinkage stress. This method is most convenient when only the strain in the member and the stress in the reinforcement need be computed. Once the stress in the reinforcement is known, the stress in the concrete can be determined by considering internal equilibrium.

Alternately, it may be assumed that free shrinkage takes place by subjecting the compressive reinforcement to a unit stress equal to the product of the shrinkage strain and the modulus of the reinforcement. The shrinkage strain is then reduced by the elastic and creep strain produced by an equilibrating tensile load (equal to the area of the reinforcement times the shrinkage stress) applied to the composite reinforced section. The two methods give identical results.

Example. Method 1 - Shrinkage Initially Restrained

Assume:

$\eta = E_s/E_c = 10.$ ; $C_u = \varepsilon_{cu}/\varepsilon_i = 3.00$; $\varepsilon_{su} = 0.0006$

$\rho = A_s/A_g = 0.04$; $\eta_u = (1.0 + 3.00)\ \eta = 40.$

The net concrete area is:

$$A_c = (1-\rho)\ A_g = 0.96\ A_g$$

The total tensile force required to restrain shrinkage of the concrete is therefore:

$$F_t = (0.96)\ A_g\ \varepsilon_{su}\ E_{cu} = 0.000576\ A_g\ E_{cu}$$

The gross area transformed to equivalent concrete after creep is:

$$A_{gcu} = (1. + (\eta_u - 1)\rho)\ A_g = (1. + (39)(0.04))\ A_g = 2.56\ A_g$$

Since the tensile shrinkage restraining force $F_t$ must be in equilibrium with a compressive force $F_c$ ($F_c = F_t$), the restrained shrinkage of the column is

$$\varepsilon_{rs} = F_c/(A_{gcu}E_{cu}) = (0.000576\ A_g\ E_{cu})/(2.56\ A_g\ E_{cu}) = 0.000225$$

The stress in the reinforcement due to shrinkage is therefore

$$\sigma_{ss} = \varepsilon_{rs}\ E_s = (0.000225)(30000000) = 6750 \text{ psi (compression)}$$

and the stress in the concrete due to restrained shrinkage is

$$\sigma_{cs} = \rho\ \sigma_{ss}/(1-\rho) = (0.04)(6750)/0.96 = 282 \text{ psi (tension)}$$

Example. Method 2 - Initial Free Shrinkage of Concrete

Assume:

$\eta$, $C_u$, $\varepsilon_{su}$, $\rho$, and $\eta_u$ as for Method 1

The total compressive force which would have to be applied to develop a total strain equal to the free shrinkage of the concrete is:

$$F_c = \rho A_g E_s \varepsilon_{su}$$

The restrained shrinkage strain is equal to the free shrinkage less the strain due to the balancing tensile force ($F_t = F_c$). Thus

$$\varepsilon_{rs} = \varepsilon_{su} - F_t/(E_{cu} A_{gcu}) = \varepsilon_{su} (1 - \rho \eta_u/2.56)$$

$$= 0.0006 (1 - (0.04)(40)/2.56) = 0.000225$$

The tensile stress in the concrete is therefore

$$\sigma_{cs} = F_t/A_{gcu} = (\rho A_g E_s \varepsilon_{su})/(2.56 A_g)$$

$$= (0.04)(30000000)(0.0006)/2.56 = 282 \text{ psi (tension)}$$

and the compressive stress in the steel is

$$\sigma_{ss} = (\varepsilon_{su})(E_s) - \eta_u \sigma_{cs} = 18000 - 11250 = 6750 \text{ (compression)}$$

As may be seen by the above calculations the two methods do yield identical results. Thus the restrained shrinkage, $\varepsilon_{rs}$, of a reinforced column (symmetrically reinforced) may be computed by the simple relationship

$$\varepsilon_{rs} = \delta_{rs} \varepsilon_{su} = (1-\rho) \varepsilon_{su} / \alpha_{gcu} \tag{55}$$

where the effective transformed area ratio after creep is defined by

$$\alpha_{gcu} = A_{gcu}/A_g = 1 + (\eta_u - 1)\rho \tag{56}$$

and the restrained shrinkage is computed by multiplying the free shrinkage by

$$\delta_{rs} = (1-\rho) / (1 + (\eta_u - 1)\rho) = (1-\rho) / \alpha_{gcu}$$

In the above

$\rho$ = reinforcement ratio, $(A_s/A_g)$

$\eta_u$ = sustained load modular ratio, $(1 + C_u)\eta$

$\varepsilon_{su}$ = limiting value of free shrinkage of the concrete

Graphical solutions for Eq. 53 and 55 are given in Fig. 28. The change in stress in the reinforcement due to shrinkage is computed from the restrained shrinkage strain:

$$\sigma_{ss} = \delta_{rs} \, \varepsilon_{su} \, E_s \tag{57}$$

From equilibrium, the tensile stress in the concrete may be seen to be:

$$\sigma_{cs} = \rho \, \sigma_{ss} \, / \, (1-\rho) \tag{58}$$

## 5.5 Comparison of Computed Shrinkage Values with Test Data

An extensive study of reinforced concrete columns, both loaded and unloaded, has been made by Pfeifer (51). Fig. 8 in this reference is reproduced in Fig. 29a together with the computed shrinkage of the unloaded columns based on measured concrete and steel properties reported in the paper. It may be noted that, while there was some experimental scatter of the data, the computed results are in good agreement with observed values except for large reinforcement ratios, $\rho$. This discrepancy may be attributed, in part, to the development of shrinkage cracks in the unloaded specimen due to the high tensile stress induced in the concrete by the restraining effect of the reinforcement.

## 5.6 Elastic and Creep Strains by the Section-Rigidity Method

By the effective section-rigidity method both the elastic and the elastic plus creep strain can be computed from the average stress on the section:

$$\sigma_{ave} = P \, / \, A_g \tag{59}$$

where:

$P$ = total load applied to the column

$A_g$ = gross area of the reinforced section.

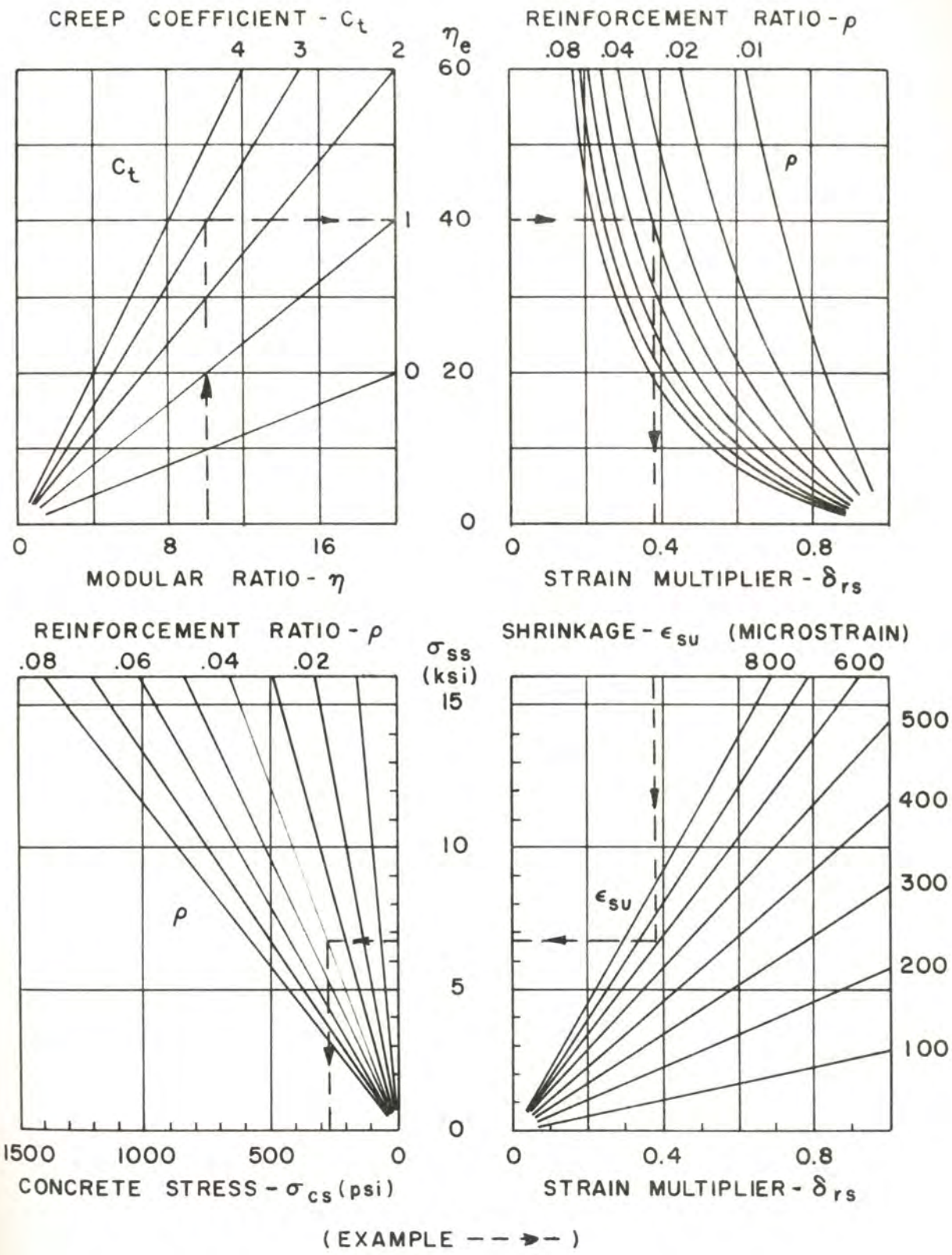


FIG. 28. COLUMN SHRINKAGE
SECTION RIGIDITY METHOD

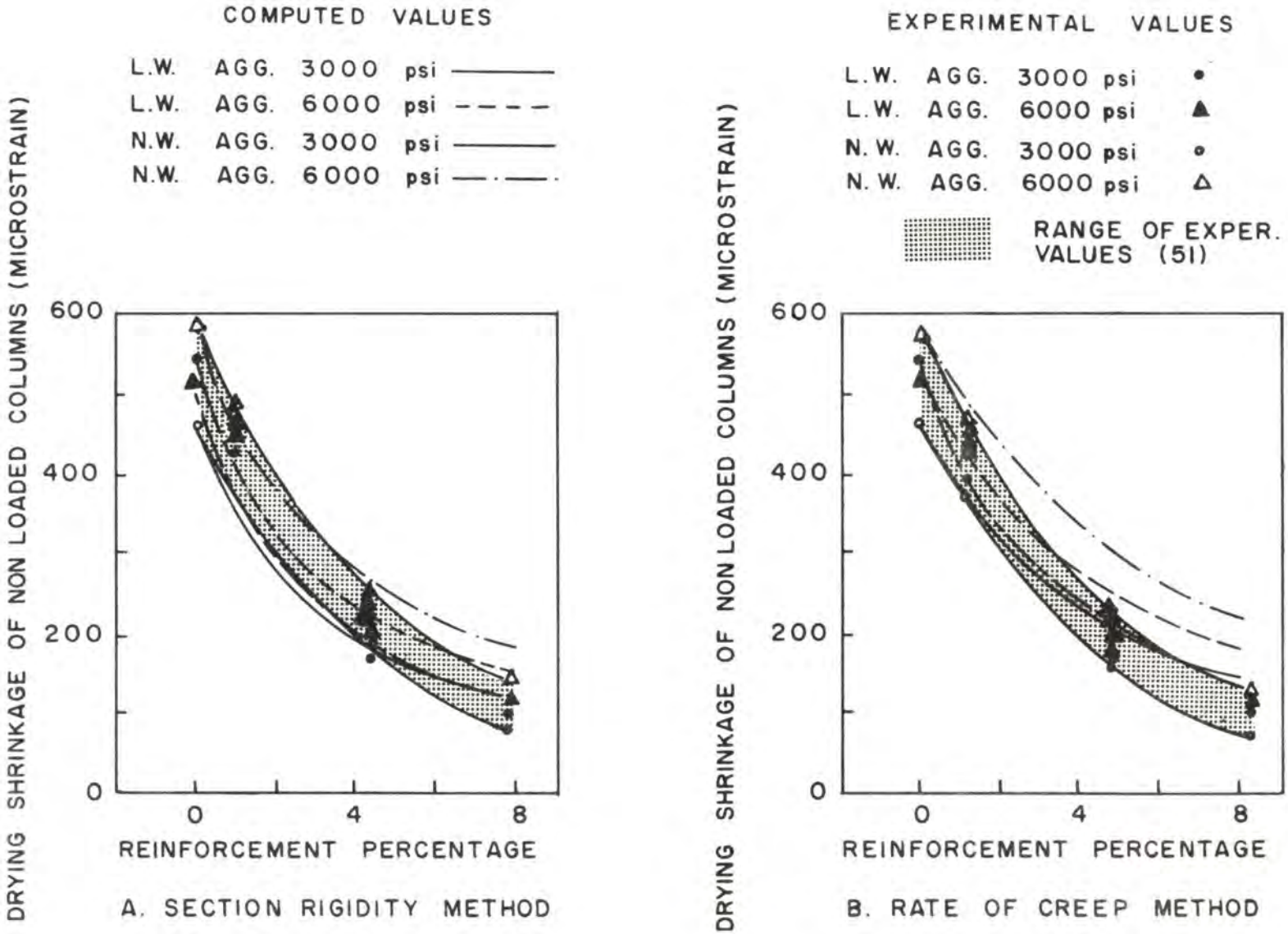


FIG. 29. PREDICTION OF COLUMN SHRINKAGE

Strain is computed by dividing this stress by the effective section rigidity. The effective rigidity ratio is defined as the product of the transformed area ratio and the effective modulus of the concrete. Since it is usually desirable to calculate both the concrete and steel stress as well as the total strain it is convenient to first compute these stresses and then compute the strain by dividing the steel stress by the modulus of the steel.

The transformed area ratio is given by

$$\alpha_{gc} = (1 + (\eta - 1)\ \rho) \tag{56a}$$

or after creep, by,

$$\alpha_{gcu} = (1 + (\eta_u - 1)\ \rho) \tag{56b}$$

where:

$\alpha_{gc}$ = instantaneous transformed area ratio

$\alpha_{gcu}$ = effective transformed area ratio after creep.

The steel stress may be computed by multiplying the average unit stress by the ratio:

$$\delta_r = \eta\ /\ \alpha_{gc} \tag{60}$$

or

$$\delta_{rc} = \eta_u\ /\ \alpha_{gcu}$$

The equations for initial or elastic, and for initial plus creep values for the concrete stress, steel stress and elastic plus creep strain are listed below:

| Initial | | Initial + Creep | |
|---|---|---|---|
| $\sigma_c = \sigma_{ave}\ /\ \alpha_{gc}$ | (61a) | $\sigma_{cr} = \sigma_{ave}\ /\ \alpha_{gcu}$ | (61b) |
| $\sigma_s = \eta\ \sigma_c = \delta_r\ \sigma_{ave}$ | (62a) | $\sigma_{sr} = \eta_u\ \sigma_{cr} = \delta_{rc}\ \sigma_{ave}$ | (62b) |
| $\varepsilon_r = \sigma_s\ /\ E_s$ | (63a) | $\varepsilon_{rc} = \sigma_{sr}\ /\ E_s$ | (63b) |

Graphical solutions for the above equations are given in Fig. 30. Adding the effect of shrinkage, the ultimate values are:

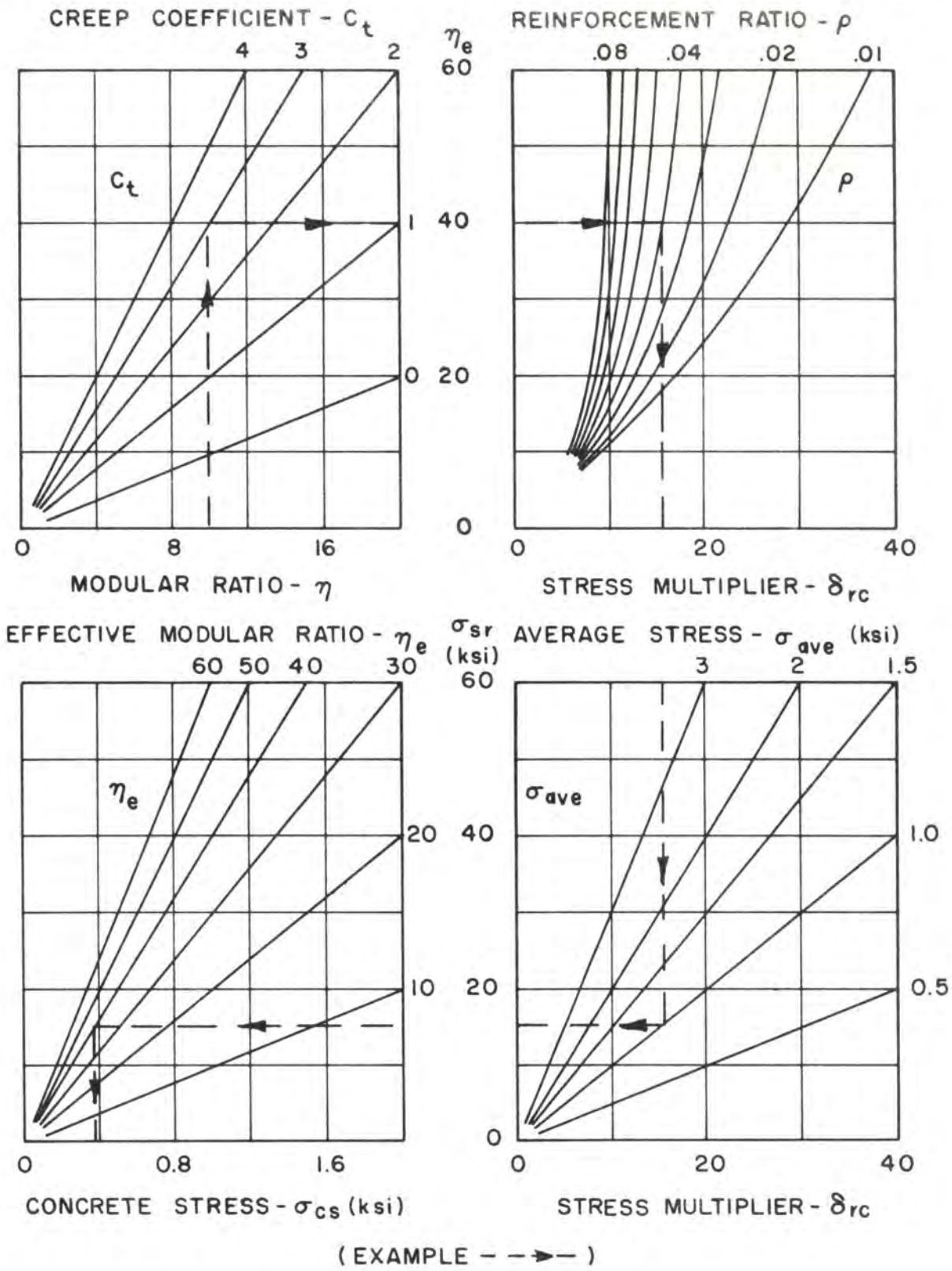


FIG. 30. ELASTIC AND CREEP COLUMN STRESS
SECTION RIGIDITY METHOD

$$\sigma_{cu} = \sigma_{cr} + \sigma_{cs} = (\sigma_{ave} - \rho\, \varepsilon_{su}\, E_s) \,/\, \alpha_{gcu} \tag{64}$$

$$\sigma_{su} = \sigma_{sr} + \sigma_{ss} = (\eta_u\, \sigma_{ave} + (1-\rho)\varepsilon_{su}\, E_s) \,/\, \alpha_{gcu} \tag{65}$$

and

$$\varepsilon_{ru} = \varepsilon_{rc} + \varepsilon_{rs} = \sigma_s \,/\, E_s \tag{66}$$

Example:

Assume $\sigma_{ave}$ = 1000 psi; $\rho$ = 0.04, $C_u$ = 3.00, $\eta$ = 10, as in previous examples, and $E_s$ = 30,000 ksi.

| Initial | Initial + Creep |
|---|---|
| $\eta = 10$ | $\eta_u = (1 + C_u)\eta = (1 + 3.0)10 = 40$ |
| $\alpha_{gc} = 1 + (\eta - 1)\rho$ | $\alpha_{gcu} = 1 + (\eta_u - 1)\rho$ |
| $= 1 + 9(0.04) = 1.36$ | $= 1 + 39\ (0.04) = 2.56$ |
| $\delta_r = \eta \,/\, \alpha_{gc} = 10/1.36 = 7.35$ | $\delta_{rc} = \eta_u/\alpha_{gcu} = 40/2.56 = 15.62$ |
| $\sigma_c = \sigma_{ave} \,/\, \alpha_{gc}$ | $\sigma_{cr} = \sigma_{ave} \,/\, \alpha_{gcu}$ |
| $= 1000/1.36 = 735$ psi | $= 1000/2.56 = 391$ psi |
| $\sigma_s = \eta\, \sigma_c = \delta_r\, \sigma_{ave}$ | $\sigma_{sr} = \eta_u\, \sigma_{cr} = \delta_{rc}\, \sigma_{ave}$ |
| $= (10)\ (735) = 7350$ psi | $= (40)\ (391) = 15620$ psi |
| $\varepsilon_r = \sigma_s \,/\, E_s$ | $\varepsilon_{rc} = \sigma_{sr} \,/\, E_s$ |
| $= 7350/30000000 = 0.000245$ | $= 15620/30000000 = 0.000521$ |

To obtain the final stresses and strains, the effect of shrinkage must be added to the initial plus creep values. Thus

$$\sigma_{cu} = \sigma_{cr} + \sigma_{cs} = 391 - 282 = 109 \text{ psi}$$

$$\sigma_{su} = \sigma_{sr} + \sigma_{ss} = 15620 + 6750 = 22370 \text{ psi}$$

$$\varepsilon_{ru} = \varepsilon_{rc} + \varepsilon_{rs} = 0.000521 + 0.000225 = 0.000746$$

Table IV shows a comparison of computed strains and stresses with observed values as reported by Pfeifer (51). Computed strains and corresponding steel stresses may be seen to be generally smaller than observed values. This result is attributed to the fact that in the section-rigidity-method a reduction in concrete stress due to stress redistribution is reflected by both creep and elastic strain recovery.

## 5.7 Creep and Shrinkage Strains by the Rate-of-Creep Method

In the rate-of-creep method the initial "elastic" stresses and column strain may be obtained by the transformed area method in the same manner as for the section rigidity method. Thus,

$$\sigma_c = \sigma_{ave}/\alpha_{gc} \tag{61a}$$

where:

$$\sigma_{ave} = P/A_g \tag{59}$$

$$\alpha_{gc} = (1 + (\eta-1)\ \rho) \tag{56a}$$

and

$$\sigma_s = \eta\ \sigma_c \tag{62a}$$

$$\varepsilon_r = \sigma_s\ /\ E_s \tag{63a}$$

The method is based on determining the creep strain by the rate-of-creep method and satisfying the compatibility and equilibrium conditions. Only the elastic strain component is assumed to be recovered. A detailed derivation of the equations required for analysis is given in Appendix III-A and only the resulting equations are summarized below. In this method, shrinkage and creep are considered to be proportional at all times. Thus, the shrinkage may be computed by considering the creep due to an effective stress (assumed to be constant):

$$\sigma_{se} = \frac{\varepsilon_{su}}{C_u} E_c \tag{67}$$

where:

$\varepsilon_{cu}$ = limiting free shrinkage, $t=\infty$

$C_u$ = corresponding creep ratio, $\varepsilon_{cu}/\varepsilon_i$

TABLE IV

COMPARISON OF COMPUTED AND OBSERVED RESULTS (51)
SECTION-RIGIDITY METHOD

CONCRETE PROPERTIES

| Test Specimens | Concrete Type | $f'_c$ psi | $E_c$ ksi | $\eta$ | $C_u$ | $n_u$ | $\varepsilon_{su}$ x $10^{-6}$ |
|---|---|---|---|---|---|---|---|
| 14 A-C | LW | 3260 | 2240 | 13.26 | 2.163 | 41.94 | 550 |
| 14 E-K | LW | 6040 | 2770 | 10.72 | 1.766 | 29.65 | 525 |
| 8 A-D | NW | 3020 | 3590 | 8.27 | 3.126 | 34.13 | 475 |
| 8 E-K | NW | 5080 | 4040 | 7.35 | 2.633 | 26.71 | 590 |

STRESSES AND STRAINS

| Test Specimen | $\rho$ | $\sigma_{ave}$ psi | COMPUTED $\varepsilon_r$ ($\times 10^6$) | COMPUTED $\sigma_{su}$ ksi | COMPUTED $\varepsilon_{ru}$ ($\times 10^6$) | OBSERVED $\varepsilon_r$ ($\times 10^6$) | OBSERVED $\sigma_{su}$ ksi | OBSERVED $\varepsilon_{ru}$ ($\times 10^6$) |
|---|---|---|---|---|---|---|---|---|
| 14 B | 0.0117 | 775 | 303 | 32.89 | 1107 | 300 | 36.23 | 1220 |
| 14 C | 0.0467 | 1330 | 378 | 24.50 | 825 | 385 | 27.03 | 910 |
| 14 D | 0.0838 | 1910 | 421 | 21.46 | 722 | 422 | 22.93 | 772 |
| 14 F | 0.0117 | 1370 | 444 | 41.96 | 1413 | 440 | 43.96 | 1480 |
| 14 G | 0.0467 | 1925 | 478 | 30.77 | 1036 | 487 | 32.14 | 1082 |
| 14 H | 0.0838 | 2500 | 497 | 26.00 | 875 | 485 | 27.18 | 915 |
| 14 J | 0.0117 | 1460 | 473 | 43.96 | 1480 | 463 | 44.05 | 1483 |
| 14 K | 0.0467 | 2300 | 571 | 35.52 | 1196 | 549 | 35.91 | 1209 |
| 8 B | 0.0117 | 775 | 199 | 29.11 | 980 | 208 | 32.02 | 1078 |
| 8 C | 0.0467 | 1330 | 277 | 23.10 | 778 | 293 | 25.63 | 863 |
| 8 D | 0.0838 | 1910 | 331 | 20.68 | 696 | 355 | 23.02 | 775 |
| 8 F | 0.0117 | 1370 | 316 | 41.44 | 1395 | 320 | 41.28 | 1390 |
| 8 G | 0.0467 | 1925 | 367 | 30.95 | 1042 | 370 | 32.52 | 1095 |
| 8 H | 0.0838 | 2500 | 404 | 26.26 | 884 | 407 | 28.13 | 947 |
| 8 J | 0.0117 | 1460 | 336 | 43.28 | 1457 | 348 | 44.19 | 1488 |
| 8 K | 0.0467 | 2300 | 439 | 35.50 | 1195 | 426 | 37.90 | 1276 |

$E_s$ = 29,700 ksi

The effective transformed-area reinforcement ratio is defined by:

$$\rho_e = \frac{\eta\rho}{\alpha_{gc}} = \frac{\eta\rho}{1+(\eta-1)\rho} \tag{68}$$

The changes in the concrete and steel stresses and the strain due to shrinkage are given by the relationships:

$$\sigma_{cs} = -\sigma_{se}\,(1-e^{-\rho_e C_u}) \tag{69}$$

$$\sigma_{ss} = -\,\frac{1-\rho}{\rho}\;\sigma_{cs} \tag{70}$$

$$\varepsilon_{rs} = \sigma_{ss}/E_s \tag{71}$$

The initial plus creep stresses in the concrete and reinforcement and the column strain may be computed by:

$$\sigma_{cr} = \sigma_c\; e^{-\rho_e C_u} \tag{72}$$

$$\sigma_{sr} = \frac{\sigma_s}{\rho_e} - \frac{1-\rho}{\rho}\;\sigma_{cr} = \frac{(\sigma_{ave}-(1-\rho)\sigma_{cr})}{\rho} \tag{73}$$

$$\varepsilon_{rc} = \sigma_{sr}/E_s \tag{74}$$

Fig. 31 provides a graphical design aid for the above equations. The final stresses and strains are obtained by superimposing the changes due to shrinkage. Thus,

$$\sigma_{cu} = \sigma_{cr} + \sigma_{cs} \tag{75}$$

$$\sigma_{su} = \sigma_{sr} + \sigma_{ss} \tag{76}$$

$$\varepsilon_{ru} = \sigma_{su}/E_s \tag{77}$$

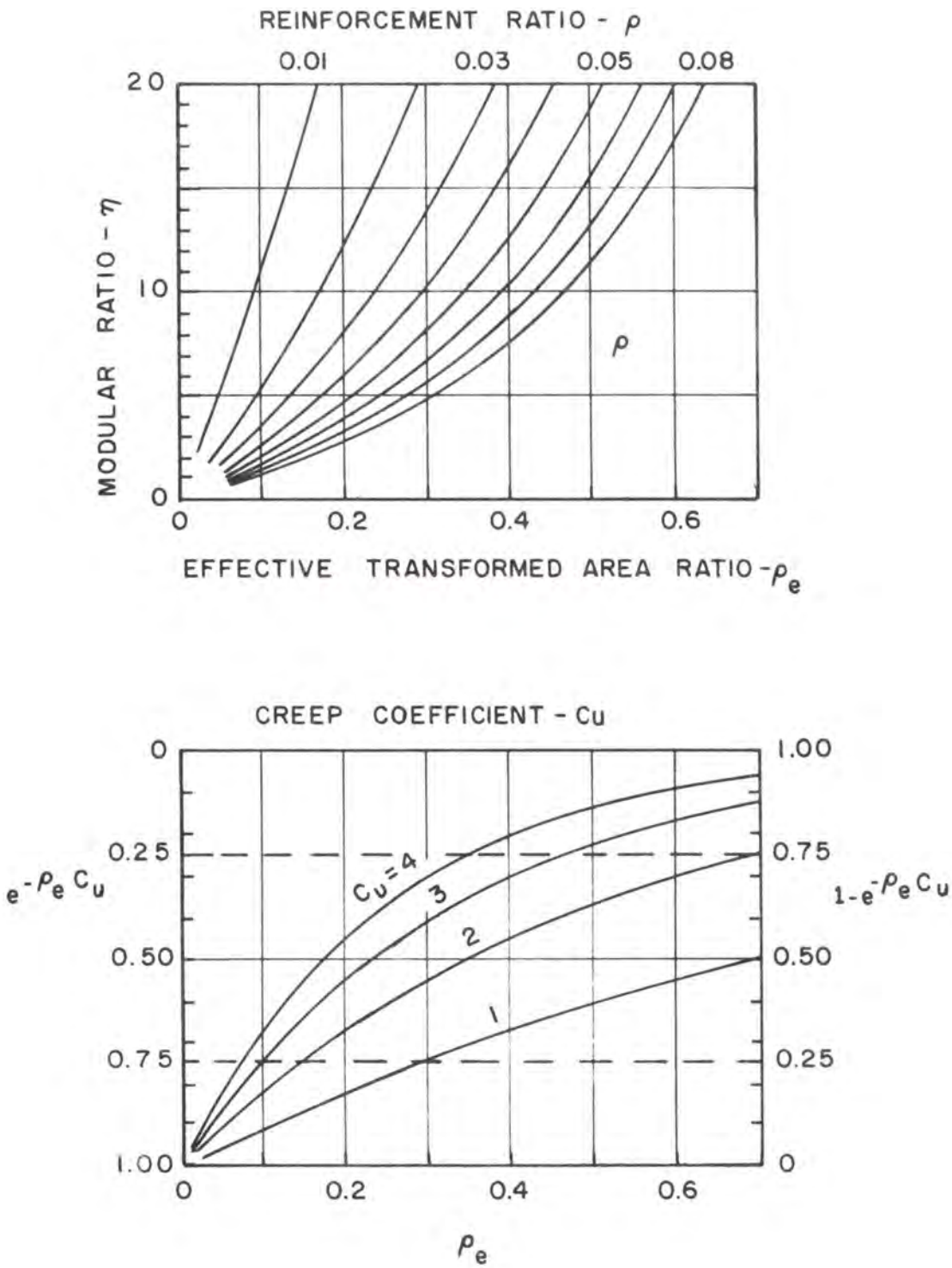


FIG. 31. DESIGN AID FOR RATE-OF-CREEP METHOD

Example:

Assume the same data as in the previous example for the section-rigidity method.

$$\alpha_{gc} = (1 + (\eta - 1)\rho) = 1 + 9(0.04) = 1.36$$

$$\sigma_c = \sigma_{ave}/\alpha_{gc} = 1000/1.36 = 735 \text{ psi}$$

$$\sigma_s = \eta\, \sigma_c = 10(735) = 7350 \text{ psi}$$

$$\rho_e = \eta\, \rho/\alpha_{gc} = 10(0.04)/1.36 = 0.294$$

$$\rho_e\, C_u = (0.294)(3.0) = 0.882$$

$$e^{-\rho_e C_u} = e^{-0.882} = 0.414; \quad 1 - e^{-\rho_e C_u} = 0.586$$

$$\sigma_{se} = \varepsilon_{su}\, E_c/C_u = (0.0006)(3000000)/3.0 = 600 \text{ psi}$$

Due to shrinkage:

$$\sigma_{cs} = -\, \sigma_{se}(1 - e^{-\rho_e C_u}) = -\, 600(0.586) = -\, 352 \text{ psi (tension)}$$

$$\sigma_{ss} = -\, (1-\rho)\sigma_{cs}/\rho = -\, (1-0.04)(-352)/0.04 = 8448 \text{ psi (compression)}$$

$$\varepsilon_{rs} = 8448/30000000 = 0.000282$$

Creep plus elastic:

$$\sigma_{cr} = \sigma_c\, e^{-\rho_e C_u} = 735\ (0.414) = 304 \text{ psi}$$

$$\sigma_{sr} = (\sigma_{ave} - (1-\rho)\sigma_{cr})/\rho = (1000 - (0.96)\ 304)/0.04 = 17704 \text{ psi}$$

$$\varepsilon_{rc} = \sigma_{sr}/E_s = 17704/30000000 = 0.000590$$

The total stresses are:

$$\sigma_{cu} = \sigma_{cr} + \sigma_{cs} = 304 - 352 = -48 \text{ psi (tension)}$$

$$\sigma_{su} = \sigma_{sr} + \sigma_{ss} = 17704 + 8448 = 26152 \text{ psi}$$

The total strain is:

$$\varepsilon_{ru} = \varepsilon_{rc} + \varepsilon_{rs} = 0.000590 + 0.000282 = 0.000872$$

$$= \sigma_{su}/E_s = 26152/30000000 = 0.000872$$

Table V shows a comparison of the computed stresses and strains by the rate-of-creep method with the observed values reported by Pfeifer (51). It should be noted that for this method of analysis the computed column strains and steel stresses are greater than the observed values. The maximum computed shrinkage strains using Eq.'s 67-71 may be shown to reduce to

$$\varepsilon_{rs} = \frac{1-\rho}{\eta\rho} \frac{\varepsilon_{su}}{C_u} (1-e^{-\rho}e^{C_u}) \tag{78}$$

Computed values are compared with observed values in Fig. 29b.

## 5.8 The Modified Rate-Of-Creep Method

It was noted in Chapter IV that creep may be separated into two components. The residual-creep limit or flow can be considered as irrecoverable whereas the recoverable creep can be treated as delayed elasticity. It was noted that the recoverable creep strain ranges from about ten to thirty percent of the creep strain and about twenty to forty percent of the elastic strain. With the delayed elastic strain ratio defined by

$$\beta_d = \frac{\varepsilon_d}{\varepsilon_i}$$

where:

$\varepsilon_d$ = delayed elastic strain,

the effective elastic modulus (for elastic plus delayed elastic strain) is:

$$E_{cd} = \frac{E_c}{1+\beta_d} \tag{79}$$

TABLE V

COMPARISON OF COMPUTED AND OBSERVED RESULTS (51)
RATE-OF-CREEP METHOD

CONCRETE PROPERTIES

| Test Specimens | Concrete Type | $f'_c$ psi | $E_c$ ksi | $\eta$ | $C_u$ | $\varepsilon_{su}$ ($\times 10^6$) | $\sigma_{se}$ psi |
|---|---|---|---|---|---|---|---|
| 14 A-D | LW | 3260 | 2240 | 13.26 | 2.163 | 550 | 570 |
| 14 E-K | LW | 6040 | 2770 | 10.72 | 1.766 | 525 | 824 |
| 8 A-D | NW | 3020 | 3590 | 8.27 | 3.126 | 475 | 546 |
| 8 E-K | NW | 5080 | 4040 | 7.35 | 2.633 | 590 | 905 |

STRESSES AND STRAINS

| Test Specimen | $\rho$ | $\sigma_{ave}$ psi | $\rho_e$ | $e^{-\rho_e C_u}$ | COMPUTED $\sigma_{su}$ psi | COMPUTED $\varepsilon_{ru}$ $\times 10^6$ | OBSERVED $\sigma_{su}$ ksi | OBSERVED $\varepsilon_{ru}$ $\times 10^6$ |
|---|---|---|---|---|---|---|---|---|
| 14 B | 0.0117 | 775 | 0.136 | 0.746 | 35.78 | 1205 | 36.23 | 1220 |
| 14 C | 0.0467 | 1330 | 0.394 | 0.427 | 27.78 | 935 | 27.03 | 910 |
| 14 D | 0.0838 | 1910 | 0.548 | 0.306 | 23.97 | 807 | 22.93 | 772 |
| 14 F | 0.0117 | 1370 | 0.113 | 0.820 | 44.47 | 1497 | 43.96 | 1480 |
| 14 G | 0.0467 | 1925 | 0.344 | 0.544 | 34.16 | 1150 | 32.14 | 1082 |
| 14 H | 0.0838 | 2500 | 0.495 | 0.417 | 28.80 | 970 | 27.18 | 915 |
| 14 J | 0.0117 | 1460 | 0.113 | 0.820 | 46.56 | 1568 | 44.05 | 1483 |
| 14 K | 0.0467 | 2300 | 0.344 | 0.544 | 39.33 | 1324 | 35.91 | 1209 |
| 8 B | 0.0117 | 775 | 0.089 | 0.757 | 31.80 | 1071 | 32.02 | 1078 |
| 8 C | 0.0467 | 1330 | 0.288 | 0.406 | 26.86 | 905 | 25.63 | 863 |
| 8 D | 0.0838 | 1910 | 0.431 | 0.260 | 23.83 | 802 | 23.02 | 775 |
| 8 F | 0.0117 | 1370 | 0.080 | 0.810 | 44.38 | 1494 | 41.28 | 1390 |
| 8 G | 0.0467 | 1925 | 0.265 | 0.498 | 35.40 | 1192 | 32.52 | 1095 |
| 8 H | 0.0838 | 2500 | 0.402 | 0.347 | 30.11 | 1014 | 28.13 | 947 |
| 8 J | 0.0117 | 1460 | 0.080 | 0.810 | 46.34 | 1560 | 44.19 | 1488 |
| 8 K | 0.0467 | 2300 | 0.265 | 0.498 | 40.49 | 1363 | 37.90 | 1276 |

$E_s$ = 29,700 ksi

and the modular ratio:

$$\eta_d = (1+\beta_d)\eta \tag{80}$$

To compensate for the reduced elastic modulus due to delayed elasticity a modified creep coefficient $C_{ud}$ would then have to be defined so that

$$(C_{ud} + 1)\eta_d = (C_u + 1)\eta$$

Thus

$$C_{ud} = \frac{C_u - \beta_d}{(1+\beta_d)} \tag{81}$$

The equations of section 5.7 may then be applied with $E_{cd}$, $\eta_d$ and $C_{ud}$ replacing $E_c$, $\eta$ and $C_u$, respectively.

Example:

The same data is assumed as for the example in the previous section. The delayed elastic strain is assumed to be 30 percent of the elastic strain or 10 percent of the creep strain. Thus,

$E_{cd} = E_c/(1+\beta_d) = 3000000/(1+0.3) = 2300000$ psi

$\eta_d = (1+\beta_d)\eta = (1+0.3)(10) = 13$

$C_{ud} = (C_u-\beta_d)/(1+\beta_d) = (3.0-0.3)/(1+0.3) = 2.08$

$\alpha_{gc} = (1+(\eta_d-1)\rho) = 1 + 12(0.04) = 1.48$

$\sigma_c = \sigma_{ave}/\alpha_{gc} = 1000/1.48 = 676$ psi

$\sigma_s = \eta_d\ \sigma_c = 13(676) = 8780$ psi

$\rho_e = \eta_d\ \rho/\alpha_{gc} = 13(0.04)/1.48 = 0.351$

$\rho_e\ C_{ud} = (0.351)(2.08) = 0.731$

$e^{-\rho_e\ C_{ud}} = e^{-0.731} = 0.482;\quad 1-e^{-\rho_e\ C_{ud}} = 0.518$

$\sigma_{se} = \varepsilon_{su}\ E_{cd}/C_{ud} = (0.0006)(2300000)/2.08 = 667$ psi

The shrinkage stresses are:

$$\sigma_{cs} = - \sigma_{se}(1-e^{-\rho_e C_{ud}}) = - 667\ (0.518) = - 346 \text{ psi}$$

$$\sigma_{ss} = - (1-\rho)\sigma_{cs}/\rho = - (0.96)(-346)/0.04 = 8300 \text{ psi}$$

The shrinkage strain is,

$$\varepsilon_{rs} = \sigma_{ss}/E_s = 8300/30000000 = 0.000277$$

The creep plus elastic stresses are:

$$\sigma_{cr} = \sigma_c\ e^{-\rho_e C_{ud}} = 676\ (0.482) = 326 \text{ psi}$$

$$\sigma_{sr} = (\sigma_{ave}-(1-\rho)\sigma_{cr})/\rho = (1000-0.96(326))/0.04 = 17180 \text{ psi}$$

The creep and elastic strain is:

$$\varepsilon_{rc} = \sigma_{sr}/E_s = 17180/30000000 = 0.000573$$

The combined stresses are:

$$\sigma_{cu} = \sigma_{cr} + \sigma_{cs} = 326 - 346 = - 20 \text{ psi (tension)}$$

$$\sigma_{su} = \sigma_{sr} + \sigma_{ss} = 17180 + 8300 = 25480 \text{ psi}$$

The total strain is:

$$\varepsilon_{ru} = \varepsilon_{rc} + \varepsilon_{rs} = 0.000573 + 0.000277 = 0.000850$$

It may be noted that the above computed values are intermediate between those obtained by the section-rigidity and the rate-of-creep method. Table VI shows a comparison of the steel stresses and column strains computed by the modified rate-of-creep method with the observed values reported by Pfeifer (51). The computed values may be seen to fall in a range of plus or minus five percent of the observed values.

## 5.9 Comparison of Analysis Methods

Table VII shows a comparison of the results obtained by the three methods of analysis for the above example.

TABLE VI

COMPARISON OF COMPUTED AND OBSERVED RESULTS (51)
MODIFIED RATE-OF-CREEP METHOD

CONCRETE PROPERTIES

| Test Specimens | Concrete Type | $f'_c$ psi | $E_{cd}$ ksi | $\eta_d$ | $C_{ud}$ | $\varepsilon_{su}$ $\times 10^6$ | $\sigma_{se}$ psi |
|---|---|---|---|---|---|---|---|
| 14 A-D | LW | 3260 | 1600 | 18.56 | 1.259 | 550 | 699 |
| 14 E-K | LW | 6040 | 1979 | 15.01 | 0.975 | 525 | 1065 |
| 8 A-D | NW | 3020 | 2564 | 11.58 | 1.947 | 475 | 626 |
| 8 E-K | NW | 5080 | 2886 | 10.29 | 1.595 | 590 | 1067 |

STRESSES AND STRAINS

| Test Specimen | $\rho$ | $\sigma_{ave}$ psi | $\rho_e$ | $e^{-\rho_e C_{ud}}$ | COMPUTED $\sigma_{su}$ ksi | COMPUTED $\varepsilon_{ru}$ $\times 10^6$ | OBSERVED $\sigma_{su}$ ksi | OBSERVED $\varepsilon_{ru}$ $\times 10^6$ |
|---|---|---|---|---|---|---|---|---|
| 14 B | 0.0117 | 775 | 0.180 | 0.797 | 34.94 | 1176 | 36.23 | 1220 |
| 14 C | 0.0467 | 1330 | 0.476 | 0.549 | 26.72 | 900 | 27.03 | 910 |
| 14 D | 0.0838 | 1910 | 0.629 | 0.453 | 23.15 | 779 | 22.93 | 772 |
| 14 F | 0.0117 | 1370 | 0.151 | 0.863 | 43.58 | 1467 | 43.96 | 1480 |
| 14 G | 0.0467 | 1925 | 0.424 | 0.661 | 32.87 | 1107 | 32.14 | 1082 |
| 14 H | 0.0838 | 2500 | 0.579 | 0.569 | 27.70 | 933 | 27.18 | 915 |
| 14 J | 0.0117 | 1460 | 0.151 | 0.863 | 45.63 | 1537 | 44.05 | 1483 |
| 14 K | 0.0467 | 2300 | 0.424 | 0.661 | 37.83 | 1274 | 35.91 | 1209 |
| 8 B | 0.0117 | 775 | 0.121 | 0.791 | 31.23 | 1052 | 32.02 | 1078 |
| 8 C | 0.0467 | 1330 | 0.362 | 0.494 | 25.96 | 874 | 25.63 | 863 |
| 8 D | 0.0838 | 1910 | 0.514 | 0.367 | 23.05 | 776 | 23.02 | 775 |
| 8 F | 0.0117 | 1370 | 0.109 | 0.841 | 43.66 | 1470 | 41.28 | 1390 |
| 8 G | 0.0467 | 1925 | 0.335 | 0.586 | 34.18 | 1151 | 32.52 | 1095 |
| 8 H | 0.0838 | 2500 | 0.485 | 0.461 | 29.03 | 977 | 28.13 | 947 |
| 8 J | 0.0117 | 1460 | 0.109 | 0.841 | 45.58 | 1535 | 44.19 | 1488 |
| 8 K | 0.0467 | 2300 | 0.335 | 0.586 | 39.09 | 1316 | 37.90 | 1276 |

$E_s$ = 29,700 ksi

TABLE VII

COMPARISON OF RESULTS FROM THREE METHODS OF ANALYSIS

| | Section Rigidity | Rate of Creep | Modified Rate of Creep |
|---|---|---|---|
| Strain | | | |
| Shrinkage | 0.000225 | 0.000282 | 0.000277 |
| Final | 0.000746 | 0.000872 | 0.000850 |
| Final Stress | | | |
| Concrete | 109 psi | -48 psi | -20 psi |
| Steel | 22.37 ksi | 26.15 ksi | 25.48 ksi |

Similarly Table VIII shows a comparison of the ratios of the computed steel stresses for the specimens tested by Pfeifer to the observed values. The ratios for the modified rate-of-creep method are based on an arbitrary assumption of a delayed elastic strain to elastic strain ratio, $\beta_d$, of 0.40.

From Table VIII it may be seen that the section-rigidity method underestimates and the rate-of-creep method overestimates the final stress in the reinforcement by about ten percent. Considering the difficulty in estimating the probable creep and shrinkage properties of the concrete, the more refined modified rate-of-creep analysis is probably seldom justified except to verify experimental data. When stress in the reinforcement is the critical design parameter, the rate-of-creep analysis is recommended, because it is more conservative. The primary appeal of the section-rigidity method is its relative simplicity. If the shrinkage and the creep ratio are conservatively estimated this method is normally adequate for analysis and design purposes.

## 5.10 Analysis for Variable Loading

As has been noted in the previous chapter, the limiting creep ratio and the limiting flow ratio decrease with increased age at time of initial loading and may be estimated by Eq. 52:

TABLE VIII

COMPARISON OF METHODS OF ANALYSIS

$$\text{Ratio } \frac{\sigma_{su}(\text{Test})}{\sigma_{su}(\text{calculated})} = \frac{\varepsilon_{ru}(\text{Test})}{\varepsilon_{ru}(\text{calculated})}$$

| Test Specimen | $\rho$ | $f'_c$ psi | Section Rigidity Method | Rate of Creep Method | Modified Rate of Creep Method |
|---|---|---|---|---|---|
| 14 B | 0.0117 | 3260 | 1.10 | 1.01 | 1.04 |
| 14 C | 0.0467 | 3260 | 1.10 | 0.97 | 1.01 |
| 14 D | 0.0838 | 3260 | 1.07 | 0.96 | 0.99 |
| 14 F | 0.0117 | 6040 | 1.05 | 0.99 | 1.01 |
| 14 G | 0.0467 | 6040 | 1.04 | 0.94 | 0.98 |
| 14 H | 0.0838 | 6040 | 1.05 | 0.94 | 0.98 |
| 14 J | 0.0117 | 6040 | 1.00 | 0.95 | 0.97 |
| 14 K | 0.0467 | 6040 | 1.01 | 0.91 | 0.95 |
| 8 B | 0.0117 | 3020 | 1.10 | 1.01 | 1.03 |
| 8 C | 0.0467 | 3020 | 1.11 | 0.95 | 0.99 |
| 8 D | 0.0838 | 3020 | 1.11 | 0.97 | 1.00 |
| 8 F | 0.0117 | 5080 | 1.00 | 0.93 | 0.95 |
| 8 G | 0.0467 | 5080 | 1.05 | 0.92 | 0.95 |
| 8 H | 0.0838 | 5080 | 1.07 | 0.93 | 0.97 |
| 8 J | 0.0117 | 5080 | 1.02 | 0.95 | 0.97 |
| 8 K | 0.0467 | 5080 | 1.07 | 0.94 | 0.97 |

AVERAGE RATIOS

| | | | |
|---|---|---|---|
| $f'_c$ = 3000 psi (Nominal) | 1.099 | .978 | 1.008 |
| $f'_c$ = 6000 psi (Nominal) | 1.036 | .940 | .969 |
| $\rho$ = 0.0117 | 1.045 | .973 | .992 |
| $\rho$ = 0.0467 | 1.064 | .939 | .974 |
| $\rho$ = 0.0838 | 1.074 | .950 | .985 |

$$(\varepsilon_{cu})_k \doteq \left(\frac{14}{k}\right)^{0.4} (\varepsilon_{cu})_{14} \tag{52}$$

where:

$(\varepsilon_{cu})_k$ = limiting creep strain for specimen loaded at age k days,

$(\varepsilon_{cu})_{14}$ = limiting creep strain for specimen loaded at age 14 days,

k = age of specimen at time of initial load application.

Thus, the limiting creep strains for specimens initially loaded at ages 28 days and 90 days are, respectively, about 76 percent and 48 percent of the limiting creep for initial loading at age 14 days. The delayed elastic strain appears to be affected in only a minor way by an increase in age at time of loading. This change is further overshadowed by the decrease in elastic strain due to the normal increase in elastic modulus with increased maturity of the concrete.

Most structural members such as columns are not initially subjected to their full sustained loading. This delay can have a significant effect on the time-dependent behavior as demonstrated in the example below.

Example:

A column with a reinforcement ratio of 0.04 is subject to a total stress $\sigma_{ave} = P/A_g$ of 2000 psi in four equal increments applied at two week intervals. Assume $E_c$ = 3,000,000 psi, $E_s$ = 30,000,000 psi, $(C_u)_{14} = 3.0$, and $\varepsilon_{su} = 0.000,500$. Compute the limiting stress in the reinforcement and the limiting strain in the column and compare with the values obtained for a column subjected to a constant sustained stress $\sigma_{ave}$ = 2000 psi. The analysis is to be based on the section-rigidity method.

a. Shrinkage

$$\eta = 10, \quad C_u = 3.0 \quad \varepsilon_{su} = 0.0005$$

$$\eta_u = (1+C_u)\eta = (4.)(10) = 40$$

$$\alpha_{gcu} = (1 + (\eta_u - 1)\rho) = 1 + 39\ (0.04) = 2.56$$

$\varepsilon_{rs} = (1-\rho)\varepsilon_{su}/\alpha_{gcu} = (0.96)(0.0005)/2.56 = 0.000188$

$\sigma_{ss} = \varepsilon_{rs}\ E_s = (0.000188)(30000) = 5.63$ ksi

b. Creep plus elastic

First load increment - load applied at k = 14 days

$(C_u)_{14} = 3.0 \quad \eta_u = (1+C_u)\eta = (4.)10 = 40 \quad \alpha_{gcu} = 2.56$

$\sigma_{sr1} = \eta_u\ \sigma_{ave}/\alpha_{gcu} = (40)(0.50)/2.56 = 7.81$ ksi

Second load increment - load applied at k = 28 days

$(C_u)_{28} = (\frac{14}{28})^{0.4}\ (3.0) = (0.758)(3.0) = 2.274$

$(\eta_u)_{28} = (1+C_u)\eta = (3.274)\ 10 = 32.74$

$\alpha_{gcu} = 1+(\eta_u-1)\rho = 1+(31.74)(0.04) = 2.27$

$\sigma_{sr2} = \eta_u\ \sigma_{ave}/\alpha_{gcu} = (32.74)(0.50)/2.27 = 7.21$ ksi

Third load increment - load applied at k = 42 days

$(C_u)_{42} = (\frac{14}{42})^{0.4}\ (3.0) = (0.644)(3.0) = 1.932$

$(\eta_u)_{42} = (1+C_u)\eta = (2.932)10 = 29.32$

$\alpha_{gcu} = 1+(\eta_u-1)\rho = 1+(28.32)(0.04) = 2.13$

$\sigma_{sr3} = \eta_u\ \sigma_{ave}/\alpha_{gcu} = (29.32)(0.50)/2.13 = 6.88$ ksi

Fourth load increment - load applied at k = 56 days

$(C_u)_{56} = (\frac{14}{56})^{0.4}\ (3.0) = (0.574)(3.0) = 1.722$

$(\eta_u)_{56} = (1+C_u)\ \eta = (2.722)10 = 27.22$

$\alpha_{gcu} = 1+(\eta_u-1)\rho = 1+(26.22)(0.04) = 2.05$

$\sigma_{sr4} = \eta_u\ \sigma_{ave}/\alpha_{gcu} = (27.22)(0.50)/2.05 = 6.64$ ksi

Thus $\sigma_{sr} = 7.81 + 7.21 + 6.88 + 6.64 = 28.54$ ksi

$$\sigma_{su} = \sigma_{sr} + \sigma_{ss} = 28.54 + 5.63 = 34.17 \text{ ksi}$$

and $\varepsilon_{ru} = \sigma_s/E_s = 34.17/30000 = 0.001139$

c. Constant sustained stress

$$\sigma_{sr} = \eta_u \, \sigma_{ave}/\alpha_{gcu} = 40(2.0)/2.56 = 31.24 \text{ ksi}$$

Thus, $\sigma_{su} = \sigma_{sr} + \sigma_{ss} = 31.24 + 5.63 = 36.87$ ksi

and $\varepsilon_{ru} = 36.87/30000 = 0.001229$

It may be concluded that the incremented load regime decreases the limiting steel stress and column strain by about 7.5 percent. An analysis could also be made using the rate-of-creep method. Such an analysis would be more complex but would also result in an apparent reduced steel stress and a correspondingly reduced column strain. It should be noted however, that since the rate-of-creep method does not correct for delayed elasticity, the accuracy is dependent on the loading history. For very slowly applied loading regimes, this method could in fact, underestimate the steel stress. Hence, if improved accuracy is needed, the modified rate-of-creep method should be employed.

## 5.11 Stress-Time and Strain-Time Relationships

The methods discussed above have assumed that the limiting values of stress and strain due to creep and shrinkage are of primary interest. Stress distribution at intermediate times may be estimated based on effective values of creep and shrinkage. These may be estimated, in turn, by Lorman type approximations with limiting values and time factors suitably modified to reflect member size and environment and age at time of loading. It should be noted that change in steel stress due to creep is not linearly proportional to the effective modulus. Thus, in the previous example it may be noted that a decrease in the average

sustained-load modular ratio of twenty percent resulted in only a ten percent decrease in the steel stress. Hence, the stress redistribution in a reinforced member tends to stabilize more rapidly than the rate of creep and shrinkage in a plain concrete specimen.

## 5.12 Prestress Losses in Uniformly Prestressed Elements

The methods discussed in this chapter are also applicable to uniformly prestressed elements, provided suitable adjustments are made to take into account the stress relaxation in the prestressing tendons. Since the rate-of-creep method predicts somewhat greater terminal strains, this method would be recommended to obtain a conservative estimate of prestress losses. For most prestressed members, the reinforcement percentage is relatively small, hence, stress redistribution due to reinforcement constraint is a minor factor in determining prestress losses and strain behavior.

# CHAPTER VI

# ELASTIC AND TIME DEPENDENT DEFORMATIONS OF FLEXURAL MEMBERS

## 6.1 Introduction

The discussion in this chapter is limited to methods for predicting the initial and time-dependent deflections of beams and one-way slabs. While application of the basic principles to two-way slabs and to grids is feasible, for such members, the problem is further complicated by a redistribution of the stress when the relative rigidity in each direction is changed due to creep.

In the previous chapter it was noted, that for columns, the use of an "effective" modulus tends to underestimate creep strains, because the method tacitly assumes full creep recovery for the reduction in compressive stress in the concrete due to stress redistribution. Conversely, the rate-of-creep analysis overestimates creep strain, because no creep recovery is assumed.

In the case of beams, and in flexural members in general, a further complication arises. Concrete being weak in tension, will tend to crack in the tension zone. Thus, as shown in Fig. 32, the moment due to the dead and applied loads is usually assumed to be resisted by a couple consisting of a tension force, at the centroid of the tension steel, and an equal and opposite compression force applied at the center of force in the compression zone. The effect of uncracked concrete in the tension zone is usually neglected.

As the concrete creeps under stress, two conditions must be satisfied at all times, namely strain compatibility and force equilibrium. The first condition implies that plane sections remain plane, hence, the strains in the tension steel and the strains in the compression zone are proportional to the distance from the neutral axis. As the strains in the compression zone increase due to creep, the neutral axis is depressed. As a result, the compression zone

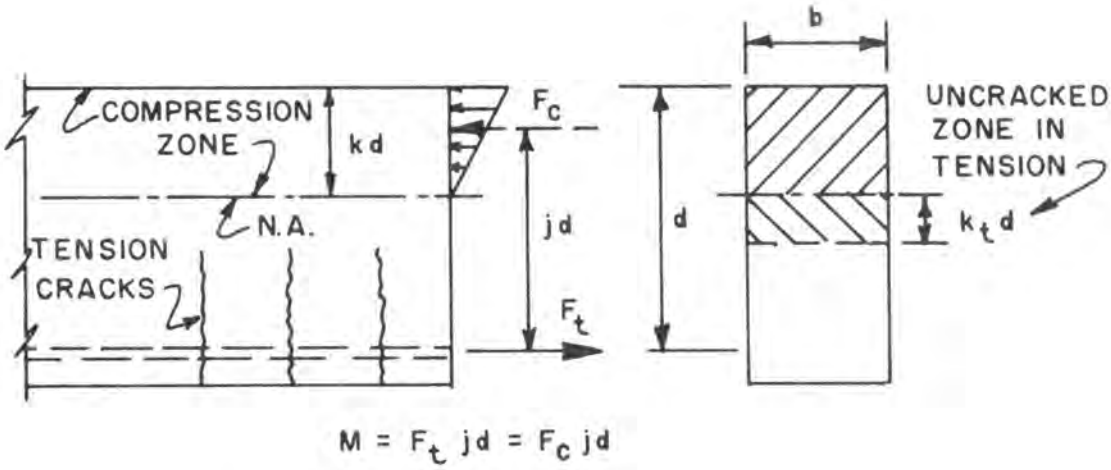


FIG. 32. MOMENT-COUPLE IN REINFORCED CONCRETE BEAM

increases and hence, the concrete stress at the extreme fiber decreases. But this depression of the neutral axis also decreases the internal moment arm jd, hence, for constant applied moment, both the tensile force $F_t$ and the compressive force $F_c$ will increase, thereby, in part, offsetting the decrease in the maximum compressive stress at the extreme fiber.

The pattern of stress redistribution in flexural members is quite different than in axially loaded reinforced concrete columns. The problem is complicated further by the fact that the development of the tension cracks in the tension zone is both time dependent and a function of the loading history. Hence, not only the effective modulus, but also the moment of inertia of the section is time dependent.

Several so-called rigorous methods have been developed to analyze time-dependent behavior due to creep [55,56]. These methods require that the time-dependent creep relationship be mathematically defined and they normally require a complex numerical integration procedure. It has already been noted that the creep relationship is quite sensitive to such factors as age at time of loading, shape and size of member, stress distribution in the member, etc. Furthermore, it has been demonstrated that for equivalent assumptions, a pseudo-elastic

analysis based on an effective modulus gives essentially the same predicted deflections as a more rigorous analysis [57]. The more rigorous methods of analysis, therefore, do not appear to be warranted for design, for no degree of mathematical complexity can be expected to compensate for lack of information on the time-dependent behavior of the concrete under indeterminate stress and environmental conditions. The relatively simple analysis discussed below can be expected, however, to give reasonably reliable predictions for the effects of creep and shrinkage.

## 6.2 Basic Assumptions - Moment Curvature and Deflection Calculations

Time-dependent deflections should be computed on the basis that only the normal service loads produce creep. Superimposed live-load deflection response is essentially elastic although repeated live loads may affect the rate of creep development [58]. Under service-load conditions, and for the usual permissible deflection limits, the strain distribution at any section is assumed to be linear for both instantaneous and sustained loads on the member. The concrete stress in the compression zone is assumed to be proportional to the appropriate effective modulus $E_{ce}$ as defined by Eq. 41. It should be noted however, that the creep coefficient selected should reflect not only the properties of the concrete, but also the loading history and the probable environmental conditions. The stress in the reinforcement is proportional to the strain; the constant of proportionality being $E_s$, the modulus of elasticity of the steel. Compression steel is assumed to be perfectly bonded to the concrete, i.e., the compression steel strains are assumed to be equal to those in adjacent concrete fibers. The member curvature at a given section at any time is given by the relationship

$$\frac{1}{r} = \frac{M}{EI} = \frac{M}{K_b} \tag{82}$$

where,

$r$ = radius of curvature

$M$ = moment at the section

$K_b$ = beam section rigidity, $K_b = EI$

For sustained loads, the moment is constant. The section rigidity, however, is a time-dependent variable. Not only does the effective modulus of the concrete vary with time, but this change in modulus also has an indirect effect on the section properties because the modulus of the reinforcement is constant. For purposes of calculation, it is convenient to use the "transformed" section method wherein the reinforcement is replaced by an equivalent area of concrete. This equivalent area of concrete is equal to $\eta_e$ times the area of the reinforcement, where $\eta_e$ is defined by Eq. 53. Since $\eta_e$ is time dependent, I is also time dependent. Furthermore, the effective moment of inertia of the section is sensitive to the degree of cracking developed in the tension zone. Where a high degree of accuracy is required, the depth of the tensile cracks can be estimated on the basis of the modulus of rupture which in turn may be estimated by the relationship given in Eq. 6. Alternately, the effective moment of inertia may be estimated by an empirical formula proposed by Branson [31]. For structural members subjected to intermittent live loads, a fully cracked section may be assumed when the modulus of rupture is exceeded at the extreme tensile fiber. For sections in the neighborhood of the point of contraflexure, where the modulus of rupture is not exceeded, the gross transformed section may be assumed. These assumptions will normally result in conservative deflection estimates, especially at early ages when the effect of shrinkage has not yet contributed to the development of cracks in the tension zone.

Eq. 82 is completely general. Member deflections may be computed by double integration subject to suitable boundary conditions. Alternately, of course, deflections may be calculated by applying such techniques as the moment-area theorem or the conjugate-beam method. For members having constant geometric proportions and when the change in moment of inertia can be assumed to be independent of the loading (i.e., where a fully cracked section can be assumed for the full length of the member) the maximum deflection is given by

$$a_{max} = \delta_a M_{max} \ell^2 / K_b \tag{83}$$

where:

$a_{max}$ = maximum deflection

$M_{max}$ = maximum moment

$\ell$ = length of the span

$K_b$ = section rigidity (time-dependent), $K_b = EI$

and,

$\delta_a$ = constant which is a function of the load distribution and the boundary or support conditions.

Typical values for $\delta_a$ for simple beams range from 1/12 for a concentrated load at the center to 5/48 for a uniformly distributed load. For continuous beams, values of $\delta_a$ are readily obtained by the conjugate beam method. For such members, however, the assumption of constant geometric properties is usually invalid since the moment of inertia for negative moment is not usually the same as that for positive moment. In that case, $\delta_a$, becomes a time dependent function since the ratio of the section rigidities in the positive and negative moment regions does not necessarily remain constant as creep strains develop.

When the $\delta_a$ does remain constant, the ratio of the ultimate to initial deflection is inversely proportional to the ratio of the effective section rigidities before and after creep, thus

$$\phi_a = \frac{a_u}{a_i} = \frac{K_{bi}}{K_{bu}} \tag{84}$$

where:

$\phi_a = a_u/a_i$ = ratio of ultimate to initial deflection

$K_{bi}/K_{bu}$ = ratio of initial to ultimate section rigidity.

The center line deflection of a uniformly loaded span of a continuous beam with constant moment of inertia may be shown to be [59]:

$$a = \frac{\ell^2}{48\ K_b}\left[5M_o + 3(M_{e1} + M_{e2})\right] \tag{85}$$

where:

$M_o$ = simply supported beam centerline moment, ($M_o = w\ell^2/8$ for a uniform load w),

$M_{e1}$, $M_{e2}$ = left and right support moments respectively (usually negative).

For continuous beams and for haunched beams the assumption of constant moment of inertia is usually invalid. This assumption may lead to serious discrepancies in estimating both instantaneous and time dependent deflections. No easy rational solution of this problem appears to be available. An improved estimate can be obtained by assuming piecewise constant moment of inertia as shown in Fig. 33.

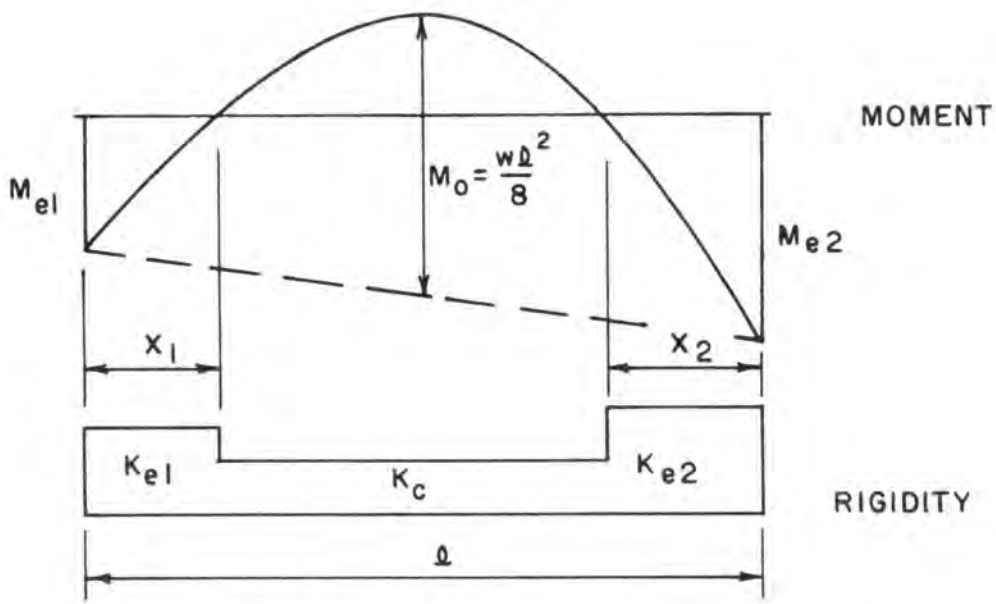


FIG. 33. MOMENTS AND SECTION RIGIDITIES FOR HAUNCHED BEAM

The effective rigidities $K_{e1}$ and $K_{e2}$ may be due either to beam haunches or a difference in section properties (as for example in a T-beam) in the negative moment region. The analysis is simplified by the introduction of the following dimensionless parameters:

$m_i$ = support moment ratio, $M_{ei}/M_o$

$\alpha_i$ = haunch flexibility ratio, $K_c/K_{ei}$

$\chi_i$ = haunch length ratio, $x_i/\ell$

The subscripts, i, are used to denote ends 1 and 2. Three additional dimensionless parameters may be defined in terms of parameters $\alpha_i$ and $\chi_i$:

$$A_i = 8(1-\alpha_i)(\chi_i^3)\ (4-3\chi_i) \qquad i = 1,2$$

$$B_i = 4(1-\alpha_i)(\chi_i^2)\ (3-2\chi_i) \qquad i = 1,2$$

$$C_i = 8(1-\alpha_i)(\chi_i^3) \qquad i = 1,2$$

The deflection may then be shown to be given by

$$a = \frac{M_o \ell^2}{48K_c}\left[(5-A_1-A_2) + (3-B_1-C_2)\ m_1 + (3-B_2-C_1)m_2\right] \tag{86}$$

In applying Eq. 86, the support moments should be computed on a basis consistent with the assumed section rigidities. This requires the use of modified member stiffness factors and carry-over factors. Formulas for computing these factors are given in Appendix IV - A. Curves for computing the necessary parameters are also shown. It should be noted that creep and shrinkage will result in a redistribution of support moments. Hence deflections after creep must take into account both changes in moment and section rigidities.

A more rigorous analysis can be made by dividing the beam into a suitable number of segments and assuming that the section rigidity is constant for any section in the segment. Such an analysis was made for a box girder bridge by the double integration method using the singularity function (MacAulay's notation) and has been previously reported [19, 60]. One conclusion drawn from this study was that for large values of the modular ratio, the section-rigidity of the uncracked section approaches the rigidity of the cracked section, as may be seen in Fig. 34. It may further be noted that for this example the section

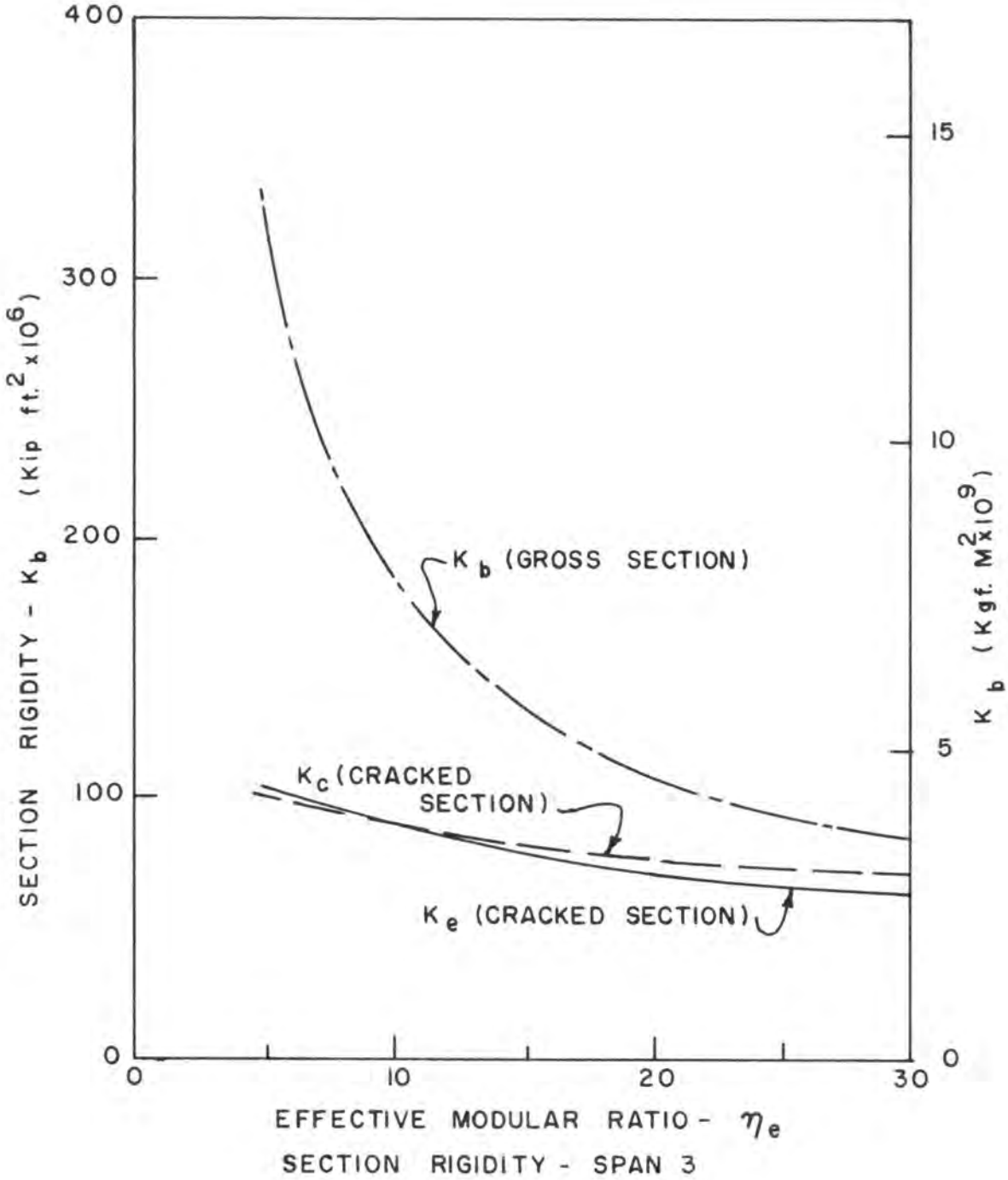


FIG. 34. FLEXURAL RIGIDITY AS FUNCTION OF MODULAR RATIO INTERIOR SPAN OF A BOX GIRDER BRIDGE [19]

rigidities at the centerline and supports were not significantly different. Since this is normally the case for box girders, except when members are haunched, an analysis based on Eq. 85 or Eq. 86 should be adequate for design purposes. While these equations do not take into account the increased moment of inertia in the uncracked zones, this simplification does not significantly affect the deflection regardless of the value of the section rigidity since the moments are low.

## 6.3 Calculation of Section Rigidity - Section Moulding

As previously noted, the flexural rigidity for a given section is computed by the use of the "transformed" area. To determine this area the following information is required:

The geometry of the section
The modulus of elasticity of the reinforcement, $E_s$
The modulus of elasticity of the concrete, $E_c$
The appropriate creep coefficient, $C_t$

The transformed steel area is computed by multiplying the steel area by the effective modular ratio

$$\eta_e = \frac{E_s\ (1 + C_t)}{E_c} = \eta(1 + C_t) \tag{53}$$

The effective uncracked concrete area is indeterminate but can be calculated by a trial and error process. The depth of penetration of the tension cracks is a function of the maximum moment at the section and of the modulus of rupture. As previously noted, the latter may be estimated by

$$f_{cr} = \alpha_r \sqrt{Wf_c'} \doteq 50\sqrt{W} \tag{6}$$

where:

$f_{cr}$ = modulus of rupture, psi

$W$ = unit weight of the concrete, pcf

$f_c'$ = 28-day strength, psi

and,

$$\alpha_r = \text{constant ranging from } 0.6 - 0.95$$

When a fully cracked section can be assumed, (i.e., concrete in the tension zone neglected), the depth of the compression zone is determined by the neutral axis. The position of the neutral axis can then be computed by equating the static moment of the compression area to the static moment of the transformed area for the tension reinforcement. This condition leads to a quadratic equation. For cases where the geometry of the section is complex and where the effective area of the reinforcement is variable, an iterative solution based on the "Section Moulding" method is recommended, both for determining the location of the neutral axis and for computing the effective moment of inertia [19].

Derivation of the necessary equations are based on the nomenclature defined as shown below. Let $I_j$ be the moment of inertia of an area $A_j$ about a centroidal axis parallel to, and at a distance $\bar{y}_j$ from, a given reference axis. Let $\Delta I_j$ be the moment of inertia of an area increment, $\Delta A_j$, about its centroidal axis located at a distance $s_j$ from the centroidal axis of area $A_j$. To satisfy the condition of equilibrium,

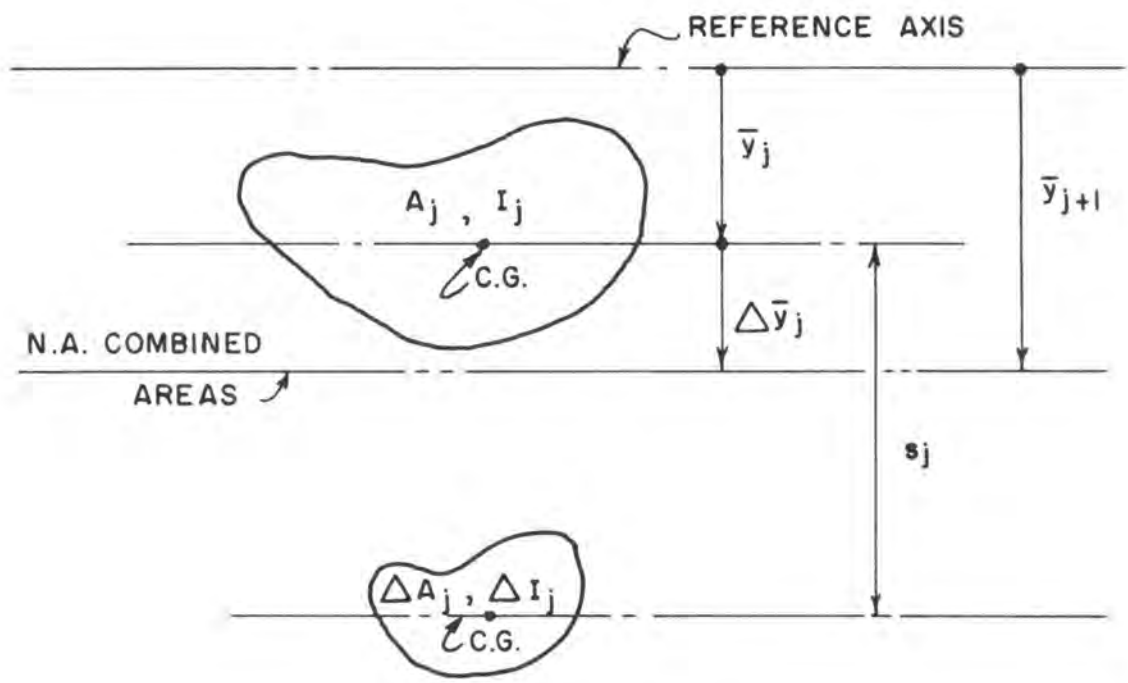


FIG. 35. SECTION MOULDING

the neutral axis of the combined areas

$$A_{j+1} = A_j + \Delta A_j \tag{87}$$

is located so that

$$(A_j)(\Delta\bar{y}_j) = (\Delta A_j)(s_j - \Delta\bar{y}_j)$$

The addition of the incremental area $\Delta A_j$ therefore causes a shift of the centroidal axis by a distance

$$\Delta\bar{y}_j = (\Delta A_j)(s_j) \;/\; (A_j + \Delta A_j) = (\Delta A_j)(s_j) \;/\; A_{j+1} \tag{88}$$

The location of the centroidal axis for the combined areas is therefore given by

$$\bar{y}_{j+1} = \bar{y}_j + \Delta\bar{y}_j \tag{89}$$

The moment of inertia for the combined areas may be calculated by the well-known parallel axis transfer formula:

$$I_{j+1} = I_j + \Delta I_j + (A_j)(\Delta\bar{y}_j)^2 + (\Delta A_j)(s_j - \Delta\bar{y}_j)^2$$

Substituting $(A_j)(\Delta\bar{y}_j)$ for $(\Delta A_j)(s_j - \Delta\bar{y}_j)$ in the third term and combining terms,

$$I_{j+1} = I_j + \Delta I_j + I_{\Delta\bar{y}_j} \tag{90}$$

where

$$I_{\Delta\bar{y}_j} = (A_j)(\Delta\bar{y}_j)\, s_j$$

Substituting Eq. (88) in Eq. (90) the moment of inertia of the combined areas may also be computed by:

$$I_{j+1} = I_j + \Delta I_j + (A_j)(\Delta A_j)(s_j)^2 \;/\; A_{j+1} \tag{91}$$

Example - Section Moulding

To illustrate the application of the section moulding method consider the T-beam section shown in Fig. 36 [15].

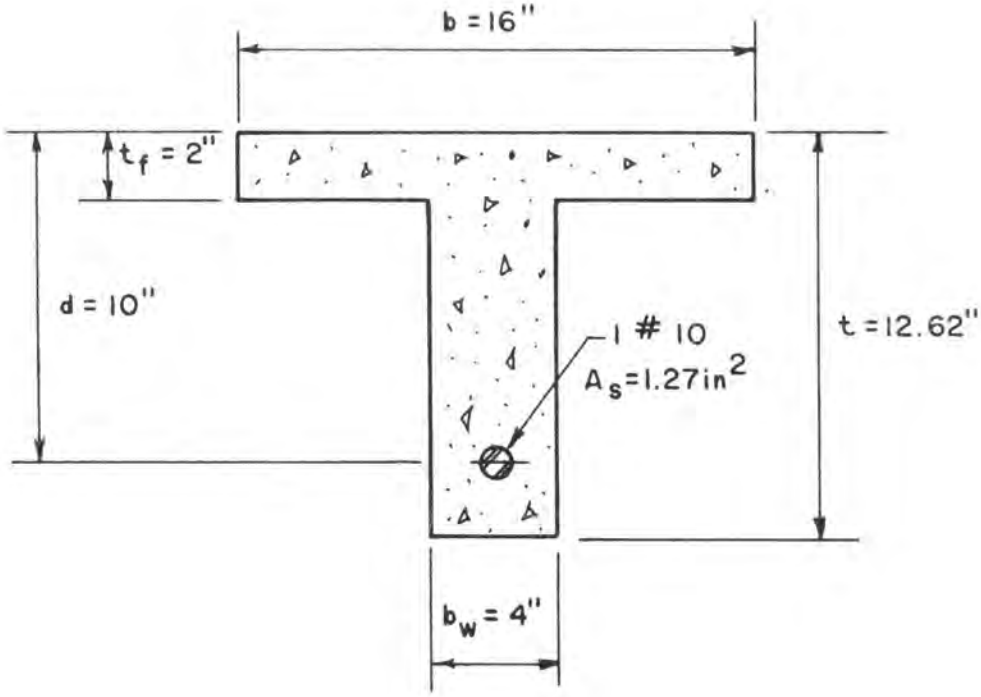


FIG. 36. T-BEAM

The following additional information is assumed

$$E_s = 29.80 \times 10^6 \text{ psi}$$

$$E_c = 4.07 \times 10^6 \text{ psi}$$

$$C_u = 2.06$$

$$M_{max} = 210000 \text{ in lbs}$$

$$f_{cr} = \alpha_r\sqrt{Wf'_c} = 600 \text{ psi}$$

The elastic modular ratio is therefore

$$\eta = E_s/E_c = 29.8/4.07 = 7.32$$

and the effective modular ratio after creep is

$$\eta_u = (C_u+1)\eta = (3.06)(7.32) = 22.40$$

The required calculations are readily made in tabular form as shown in Table IX. It is desired to calculate the effective moment of inertia and the position of the neutral axis for the following cases:

1. Fully cracked section, elastic modulus
2. Partially cracked section, elastic modulus, $f_{cr}$ = 600 psi
3. Fully cracked section, effective modulus after creep.

The computation is started by first neglecting the area of the web between the bottom of the flange and the neutral axis. To obtain the first estimate of the position of the neutral axis the flange area is taken as $A_1$ and, for case 1, the transformed area of the reinforcement, $\eta\ A_s$, is taken as $\Delta A_1$. Hence:

$$A_1 = (b)(t_f) = (16)(2) = 32.00 \text{ in}^2$$

$$\bar{y}_1 = (t_f)\ /\ 2 = (2)/(2) = 1.00 \text{ in}$$

$$I = (b)(t_f)^3/12 = (32)(4)/12 = 10.67 \text{ in}^4$$

$$\Delta A_1 = \eta\ A_s = (7.32)(1.27) = 9.30 \text{ in}^2$$

$$s_1 = d-\bar{y}_1 = 10.0-1.0 = 9.00 \text{ in}$$

$$\Delta I_1 = 0 \text{ in}^4$$

The results of these calculations are shown in tabular form in Table IX, line 1, columns 2-7, inclusive. The combined area $A_2$, $\Delta\bar{y}_1$, and $I_{\Delta\bar{y}_1}$ are computed next using Eq's 87, 88, and 90, respectively. Thus

$$A_2 = A_1+\Delta A_1 = (32.00 + 9.30) = 41.30 \text{ in}^2$$

$$\Delta\bar{y}_1 = (\Delta A_1)(s_1)/A_2 = (9.30)(9.0)/41.30 = 2.026 \text{ in}$$

$$I_{\Delta\bar{y}_1} = (A_1)(\Delta\bar{y}_1)(s_1) = (32.0)(2.026)(9.0) = 583.61 \text{ in}^4$$

These values are also shown in Table IX. In addition to $A_2$ the starting values for the second iteration are

$$\bar{y}_2 = \bar{y}_1 + \Delta\bar{y}_1 = 1.0 + 2.026 = 3.026 \text{ in}$$

$$I_2 = I_1 + \Delta I_1 + I_{\Delta\bar{y}_1} = 10.67 + 0 + 583.61 = 594.28 \text{ in}^4$$

The incremental area $\Delta A_2$ for the second iteration is that portion of the web between $\bar{y}_2$ and the bottom of the flange. Hence:

$$\Delta A_2 = (\bar{y}_2 - t_f)(b_w) = (3.026 - 2)\ 4 = 4.106 \text{ in}^2$$

$$s_2 = -\ (\bar{y}_2 - t_f)/2 = -\ 1.026/2 = -\ 0.513 \text{ in}$$

$$\Delta I_2 = (\Delta A_2)(s_2)^2/3 = 4.106\ (-0.513)^2/3 = 0.360 \text{ in}^4$$

These values, in turn, are recorded on line 2 of Table IX. It should be noted that since the incremental area lies above the centroidal axis, $s_2$ is negative. As before, $A_3$, $\Delta\bar{y}_2$, and $I_{\Delta\bar{y}_2}$ are calculated by applying Eq's 87, 88, and 90, thus

$$A_3 = A_2 + \Delta A_2 = 41.299 + 4.106 = 45.404 \text{ in}^2$$

$$\Delta\bar{y}_2 = (\Delta A_2)(s_2)/A_3 = (4.106)(-0.513)/45.404 = -0.046 \text{ in}$$

$$I_{\Delta\bar{y}_2} = (A_2)(\Delta\bar{y}_2)(s_2) = (41.299)(-0.046)(-0.513) = 0.984 \text{ in}^4$$

Hence:

$$\bar{y}_3 = \bar{y}_2 + \Delta\bar{y}_2 = 3.026 - 0.046 = 2.980 \text{ in}$$

$$I_3 = I_2 + \Delta I_2 + I_{\Delta\bar{y}_2} = 594.28 + 0.36 + 0.98 = 595.62 \text{ in}^4$$

Since the incremental shift of the neutral axis is negative, the next incremental area is negative. The results of these computations are shown on line 3 of Table IX. It may be seen that the iteration is strongly convergent and the next step results in only very small changes.

The computations for case 2, the partially cracked section, may be carried out in a similar manner. The case of the fully cracked

TABLE IX

T-BEAM SECTION PROPERTIES BY SECTION MOULDING

| 1 | 2 | 3 | 4 | 5 | 6 | 7 | 8 | 9 | 10 | 11 |
|---|---|---|---|---|---|---|---|---|---|---|
| | $A_2$ in | $\bar{y}$ in | I $in^4$ | $\Delta A$ $in^2$ | s in | $\Delta I$ $in^4$ | $\Delta\bar{y}$ in | $I_{\Delta\bar{y}}$ $in^4$ | $k_t d$ in | $\Delta k_t d$ in |
| | | | Case 1. Elastic - Fully Cracked Section | | | | | | | |
| 1 | 32.000 | 1.000 | 10.667 | 9.299 | 9.000 | 0.000 | 2.026 | 583.611 | | |
| 2 | 41.299 | 3.026 | 594.277 | 4.106 | -0.513 | 0.360 | -0.046 | 0.984 | | |
| 3 | 45.404 | 2.980 | 595.621 | -0.186 | 0.023 | -0.000 | -0.000 | -0.000 | | |
| 4 | 45.219 | 2.980 | 595.621 | -0.000 | 0.000 | -0.000 | -0.000 | -0.000 | | |
| | | | Case 2. Elastic - Partially Cracked Section | | | | | | | |
| 5 | 45.219 | 2.980 | 595.621 | 6.807 | 0.851 | 1.643 | 0.111 | 4.284 | 1.702 | 0.128 |
| 6 | 52.026 | 3.091 | 601.547 | 0.513 | 1.655 | 0.001 | 0.016 | 1.391 | 1.830 | 0.020 |
| 7 | 52.539 | 3.107 | 602.938 | 0.081 | 1.713 | 0.000 | 0.003 | 0.236 | 1.850 | 0.003 |
| 8 | 52.619 | 3.110 | 603.174 | | | | | | | |
| | | | Alternate Solution | | | | | | | |
| 9 | 45.219 | 2.980 | 595.621 | 7.414 | 0.927 | 2.122 | 0.131 | 5.470 | 1.853 | 0.152 |
| 10 | 52.633 | 3.110 | 603.213 | | | | | | | |
| | | | Case 3. Elastic Plus Creep - Fully Cracked Section | | | | | | | |
| 11 | 32.000 | 1.000 | 10.667 | 28.454 | 9.000 | 0.000 | 4.236 | 1219.987 | | |
| 12 | 60.454 | 5.236 | 1230.653 | 12.944 | -1.618 | 11.296 | -0.285 | 27.912 | | |
| 13 | 73.398 | 4.951 | 1269.861 | -1.141 | 0.143 | -0.008 | -0.002 | -0.024 | | |
| 14 | 72.257 | 4.948 | 1269.830 | -0.009 | 0.001 | -0.000 | -0.000 | -0.000 | | |
| 15 | 72.248 | 4.948 | 1269.830 | -0.000 | 0.000 | -0.000 | -0.000 | -0.000 | | |

section may be used as the starting point. The results of these calculations are shown on lines 5-8 of Table IX. The initial incremental area is determined from the effective depth, $k_t d$, of the uncracked concrete area in the tension zone computed from the modulus of rupture.

$$k_t d = (f_{cr})(I)/M_{max}$$

Thus:

$$A_5 = A_4 = 45.219 \text{ in}^2$$

$$\bar{y}_5 = \bar{y}_4 = 2.980 \text{ in}$$

$$I_5 = 595.621 \text{ in}^4$$

$$(k_t d)_5 = (f_{cr})(I_5)/M_{max} = (600)(595.62)/210000 = 1.702 \text{ in}$$

$$\Delta A_5 = (k_t d)_5 \, b_w = (1.702)(4.0) = 6.807 \text{ in}^2$$

$$s_5 = (k_t d)_5/2 = 1.702/2.0 = 0.851 \text{ in}$$

$$\Delta I_5 = (\Delta A_5)(s_5)^2/3 = (6.807)(0.851)^2/3 = 1.643 \text{ in}^4$$

$$A_6 = A_5 + \Delta A_5 = (45.219 + 6.807) = 52.026 \text{ in}^2$$

$$\Delta\bar{y}_5 = (\Delta A_5)(s_5)/A_6 = (6.807)(0.851)/52.026 = 0.111 \text{ in}$$

$$I_{\Delta\bar{y}_5} = (A_5)(\Delta\bar{y}_5)(s_5) = (45.219)(0.111)(0.851) = 4.284 \text{ in}^4$$

Hence:

$$\bar{y}_6 = \bar{y}_5 + \Delta\bar{y}_5 = 2.980 + 0.111 = 3.091 \text{ in}$$

$$I_6 = I_5 + \Delta I_5 + I_{\Delta\bar{y}_5} = 595.621 + 1.643 + 4.284 = 601.547 \text{ in}^4$$

An additional correction may be made for the shift in the neutral axis and the effect of the incremental moment of inertia. Thus

$$\Delta(k_t d)_5 = \Delta\bar{y}_5 + (\Delta I_5 + I_{\Delta\bar{y}_5}) \, f_{cr}/M_{max}$$

$$= 0.111 + (1.643 + 4.284)(600)/210000$$

$$= 0.111 + 0.018 = 0.128 \text{ in}$$

hence,

$$(k_t d)_6 = (k_t d)_5 + \Delta(k_t d)_5 = 1.702 + 0.128 = 1.830 \text{ in}$$

and

$$\Delta A_6 = \Delta(k_t d)_5 \, b_w = (0.128)(4.0) = 0.513 \text{ in}^2$$

$$s_6 = (k_t d)_6 - \Delta\bar{y}_5 - \Delta(k_t d)_5/2$$

$$= 1.830 - 0.111 - 0.064 = 1.655 \text{ in}$$

$I_6$, $\Delta\bar{y}_6$, $I_{\Delta\bar{y}_6}$, $A_7$ and $I_7$ may next be computed in the same manner. The results of continued iterations are shown on lines 6-8 of Table IX. Alternately the corrected values of $k_t d$ can be used with the initial values for the cracked section. The results of this alternative method of calculation are shown on lines 9 and 10.

The computations for case 3, fully cracked section, effective modulus after creep, are essentially the same as for case 1. The only significant change is the calculation of the tensile steel area transformed to equivalent concrete. For this case

$$\Delta A_{11} = (\eta_u)(A_s) = (22.40)(1.27) = 28.454 \text{ in}^2$$

The calculations are summarized on lines 11 to 15 of Table IX. It should be noted that for this case the drop in the neutral axis is approximately equal to the depth of the uncracked concrete in case 2. Hence, the location of the neutral axis

$$\bar{y}_{15} = 4.948 \doteq \bar{y}_9 + (k_t d)_9 = 2.980 + 1.853 = 4.833 \text{ in.}$$

Since concrete, once cracked, is not likely to regain tensile strength, the assumption of a partially cracked section after creep does not appear to be warranted.

With the moments of inertia determined, the section rigidities may be computed by multiplying by the effective modulus of elasticity of the concrete. The elastic or initial section rigidity of the fully cracked section (Case 1) is:

$$K_{bi} = (E_c)\,(I_4) = (4.07 \times 10^6)\,(595.621)$$
$$= 2.424 \times 10^9 \text{ lb in}^2$$

For the partially cracked section, (Case 2), the initial section rigidity is:

$$K_{bi} = (E_c)\ (I_{10}) = (4.07 \times 10^6)\ (603.213)$$
$$= 2.455 \times 10^9 \text{ lb in}^2$$

After creep, the effective section rigidity of the cracked section (Case 3) is:

$$K_{bu} = (E_{cu})(I_{15}) = [(4.07 \times 10^6)/3.06]\ (1269.83)$$
$$= 1.689 \times 10^9 \text{ lb in}^2$$

Provided creep does not result in a moment redistribution in the member, the ratio of the creep plus elastic deflection to the elastic deflection would be

$$K_{bi}/K_{bu} = 2.455/1.689 = 1.45$$

It should be noted that while the creep coefficient had a value of 2.06, for this example, the deflection due to creep is only forty-five percent of the calculated instantaneous deflection.

As has already been noted, the neutral axis drops due to creep. In this example, the final depth of the compression zone was slightly greater than the initial depth of the uncracked concrete (Case 2). While the concrete between flexural cracks in the tension zone may make a small contribution to the total rigidity of the section, the magnitude of this contribution is difficult to assess. For normal reinforcement ratios and stress levels the assumption of a fully cracked section after creep gives a reasonable and conservative estimate of the section rigidity.

## 6.4 Section Properties - Rectangular Beams with Tension Reinforcement Only

Formulas for fully cracked rectangular beams, and for tee, channel or box teams where the neutral axis lies inside the compression flange, can readily be developed to compute the section properties when only tension reinforcement must be considered.

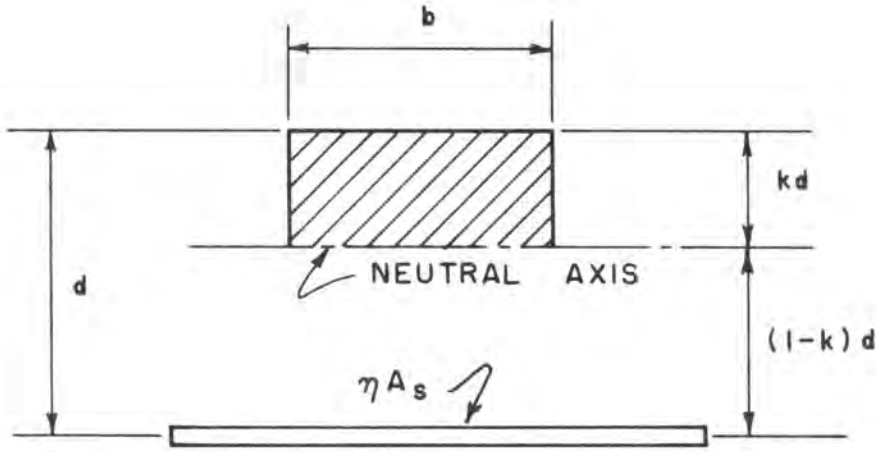


FIG. 37. TRANSFORMED AREA, RECTANGULAR BEAM WITH TENSION REINFORCEMENT ONLY

From statics:

$$b(kd)\ (kd)/2 = (1-k)d\ \eta\ A_s = (1-k)\eta\rho\ bd^2$$

$$k^2/2 = (1-k)\ \rho\eta$$

where,

$\rho$ = the reinforcement ratio, $A_s/(bd)$

Solving for k:

$$k = \sqrt{(\rho\eta)^2 + 2\rho\eta} - \rho\eta$$

$$= \rho\eta\ \left(\sqrt{1 + \frac{2}{\rho\eta}} - 1\right) \qquad (92)$$

The second form of Eq. 92 is especially convenient for slide rule solution. A graphical solution, as given in Fig. 38 can readily be obtained by noting that

$$\rho\eta = \frac{k^2}{2(1-k)}$$

The moment of inertia of the transformed section is given by

$$I = \frac{b}{3}(kd)^3 + \rho\eta\ db^3(1-k)^2$$

$$= bd^3\ (\frac{k^3}{3} + \frac{k^2}{2}\ (1-k))$$

$$= \frac{bd^3}{6}\ (3-k)k^2 \qquad (93)$$

By substituting the value of $k^2$ the equation for I may also be written in the form

$$I = \rho\eta(1-k)(3-k)\frac{bd^3}{3}$$

A graphical solution for the coefficient $(3-k)k^2/6$ is given in Fig. 39. The maximum fiber stress is given by:

$$\sigma_c = \frac{M\ kd}{I} = \frac{6\ kd\ M}{(3-k)k^2\ bd^3}$$

$$= \frac{6}{(3-k)k}\ \frac{M}{bd^2} \qquad (94)$$

The stress in the tensile reinforcement is

$$\sigma_s = \eta\ \frac{M(1-k)d}{I} = \frac{3\eta\ (1-k)d\ M}{\rho\eta(1-k)(3-k)\ bd^3}$$

$$= \frac{3}{(3-k)}\ \frac{M}{\rho\ bd^2} \qquad (95)$$

Graphical solutions of the coefficients for computing $\sigma_c$ and $\sigma_s$ are given in Figs. 40 and 41, respectively.

The effect of creep is to change the effective value of the modular ratio $\eta$ to

$$\eta_u = (C_u + 1)\ \eta \qquad (53)$$

Thus, the location of the neutral axis is obtained by substituting $\rho\eta_u$, for $\rho\eta$ in Eq. 92 or in Fig. 38. Designating the initial

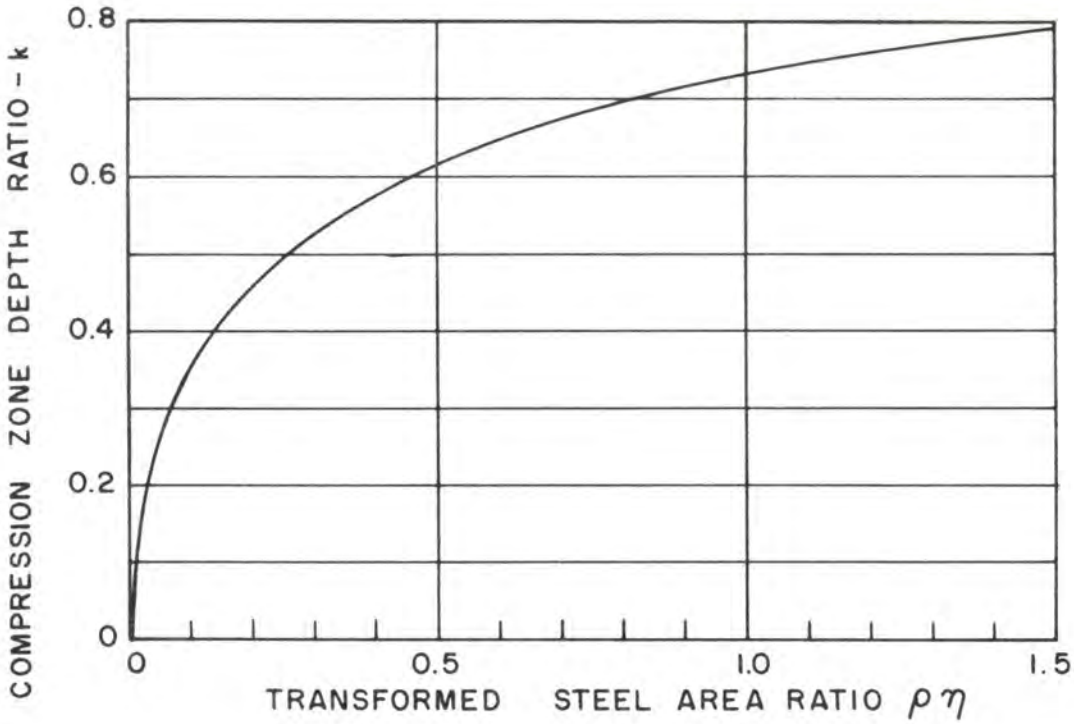


FIG. 38. DEPTH OF COMPRESSION ZONE AS FUNCTION OF TRANSFORMED STEEL AREA

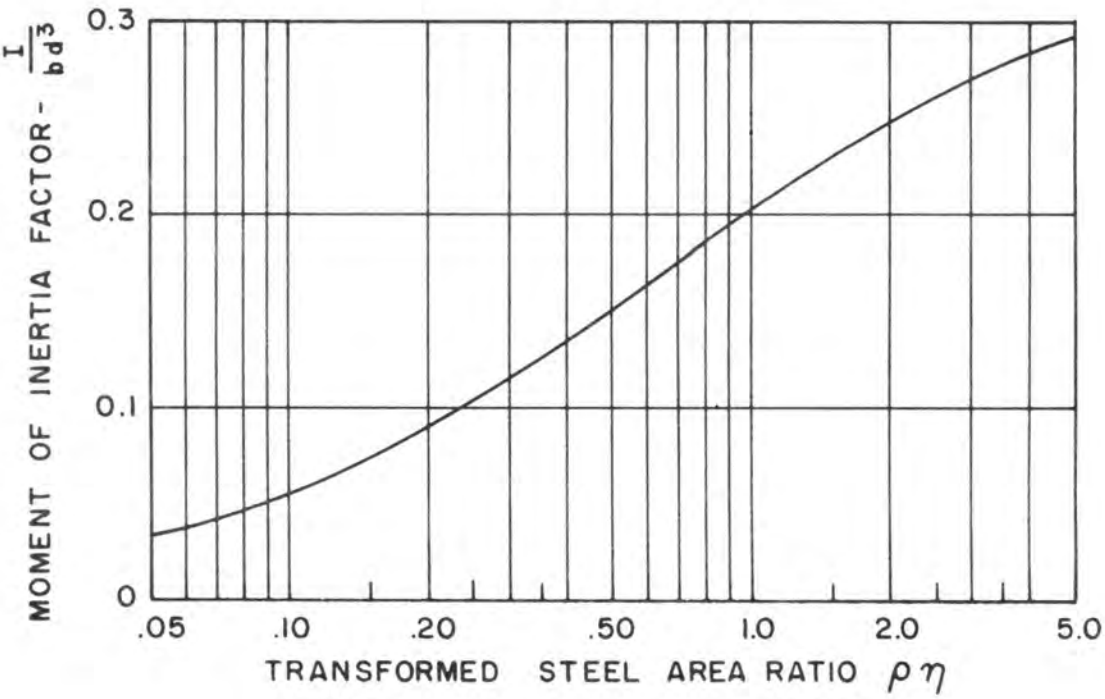


FIG. 39. MOMENT OF INERTIA COEFFICIENT

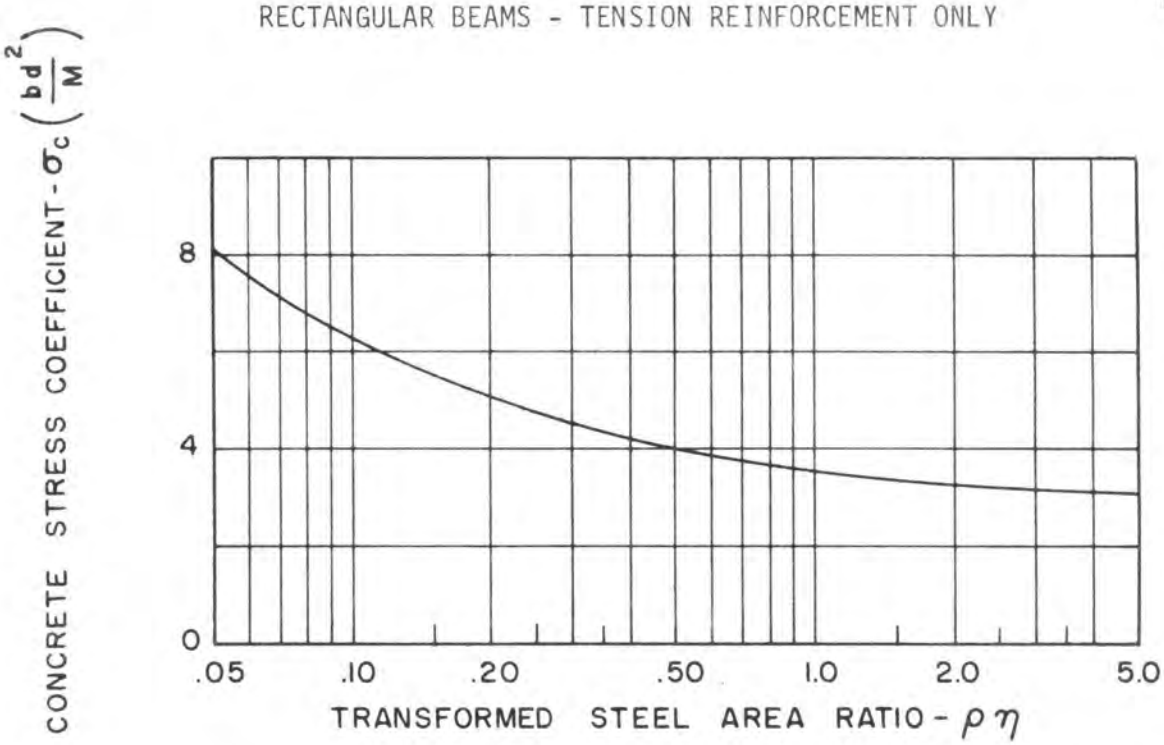


FIG. 40. CONCRETE STRESS COEFFICIENT

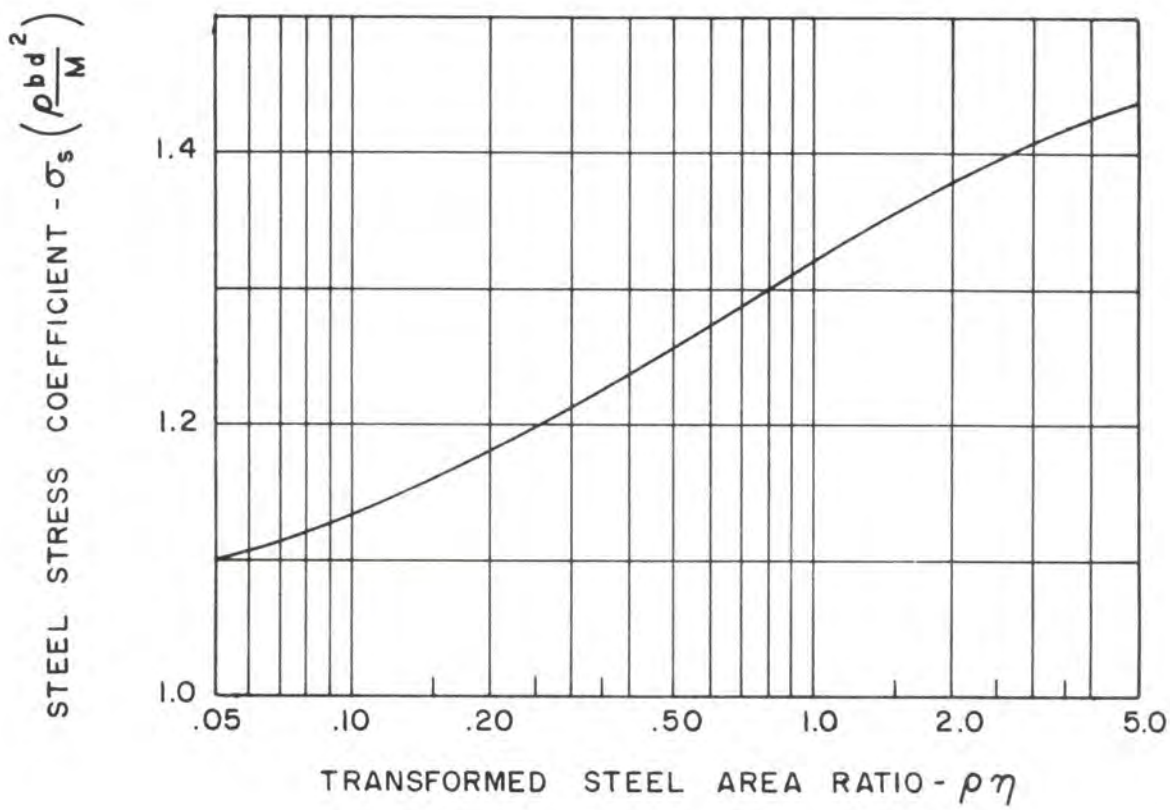


FIG. 41. STEEL STRESS COEFFICIENT

value of k, as $k_i$, and the value after creep as $k_u$, the ratio of the stress in the reinforcement after creep to the initial stress may be seen to be:

$$\phi_t = \frac{\sigma_{su}}{\sigma_{si}} = \frac{3-k_i}{3-k_u} \tag{96}$$

Similarly the ratio for the concrete stress is given by

$$\phi_c = \frac{\sigma_{cu}}{\sigma_{ci}} = \frac{(3-k_i)k_i}{(3-k_u)k_u} = \frac{k_i}{k_u}\phi_t \tag{97}$$

The section rigidity is initially

$$K_{bi} = E_c I(0) = \rho\eta(1-k_i)(3-k_i)\frac{bd^3}{3}E_c \tag{98}$$

After creep the section rigidity is

$$K_{bu} = \left(\frac{E_c}{1+C_u}\right)I(t) = \rho(1+C_u)\eta(1-k_u)(3-k_u)\frac{bd^3}{3}\left(\frac{E_c}{(1+C_u)}\right)$$

$$= \rho\eta\,(1-k_u)(3-k_u)\frac{bd^3}{3}E_c \tag{99}$$

Hence, if creep does not produce moment redistribution (i.e., $\delta_a$ in Eq. 83 is constant) the creep-deflection ratio is given by

$$\phi_a = \frac{a_u}{a_i} = \frac{(1-k_i)(3-k_i)}{(1-k_u)(3-k_u)} = \frac{1-k_i}{1-k_u}\phi_t \tag{100}$$

The coefficients $\phi_t$, $\phi_c$, and $\phi_a$ may be determined from Fig's 42, 43, and 44, respectively.

Example - Graphical Solution

To illustrate the application of these design aids, the section properties and stresses for a typical beam will be determined. The

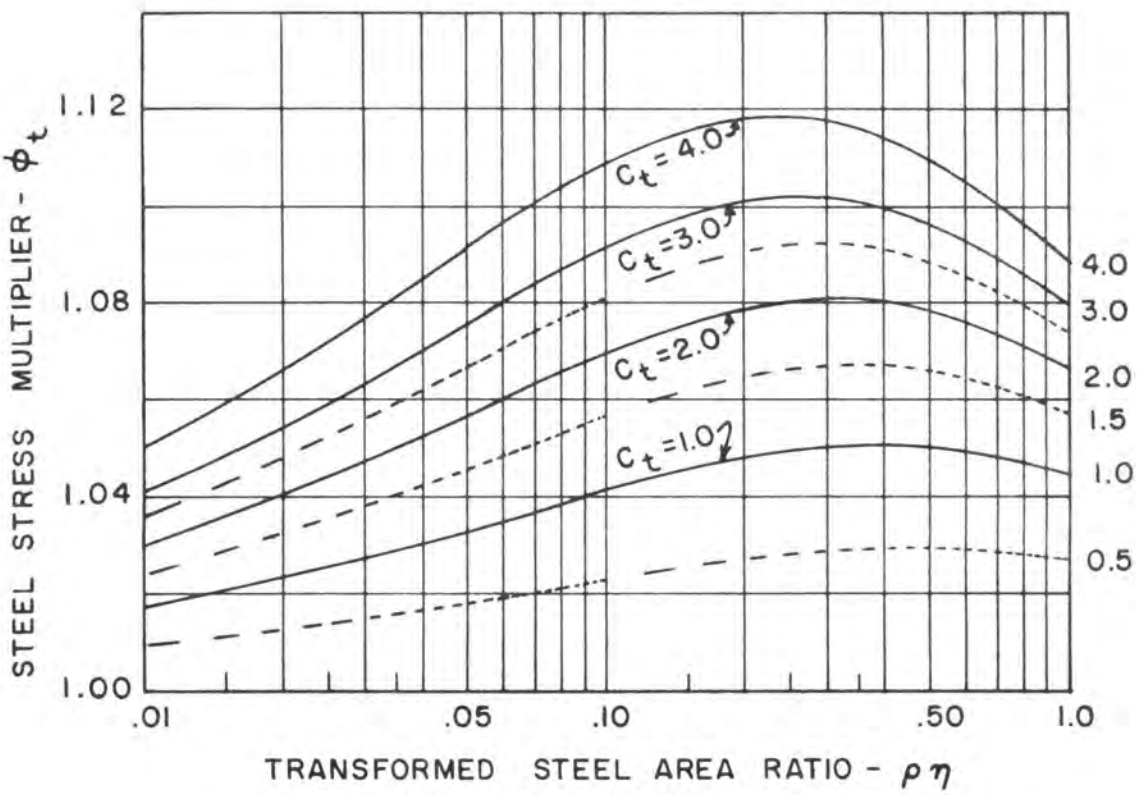


FIG. 42. STEEL STRESS MULTIPLIER

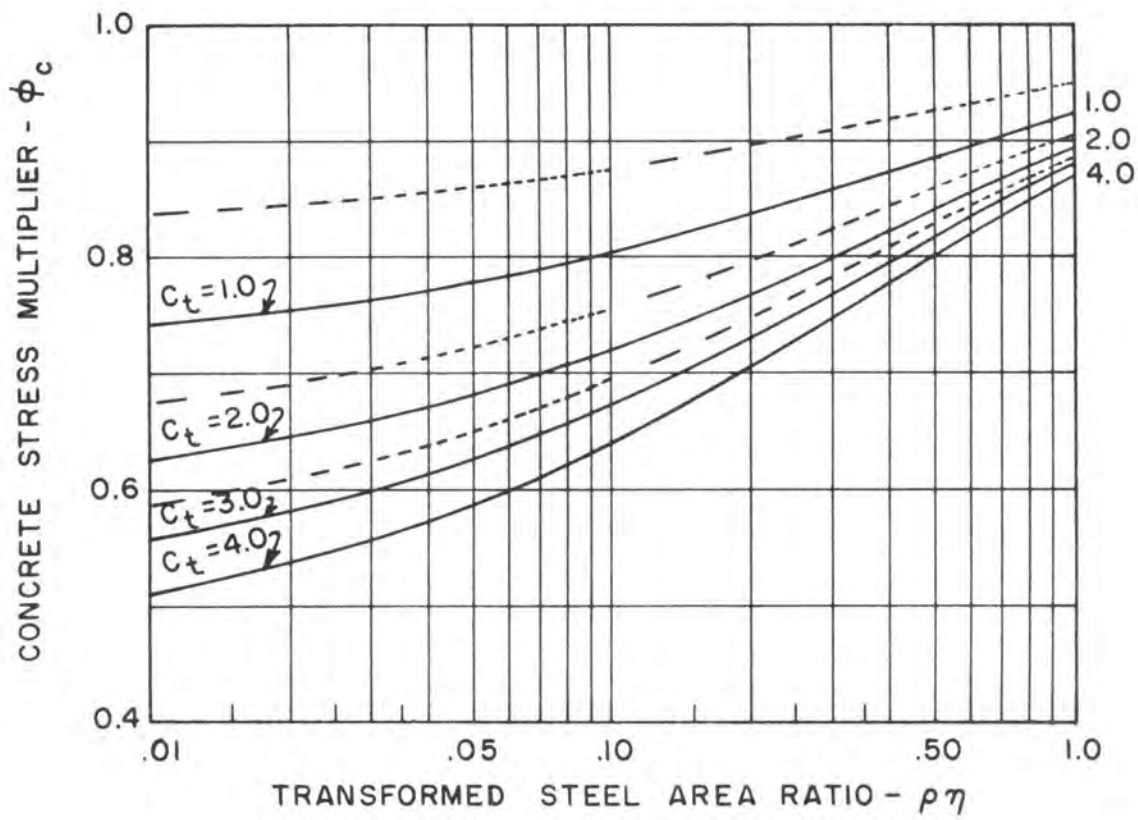


FIG. 43. CONCRETE STRESS MULTIPLIER

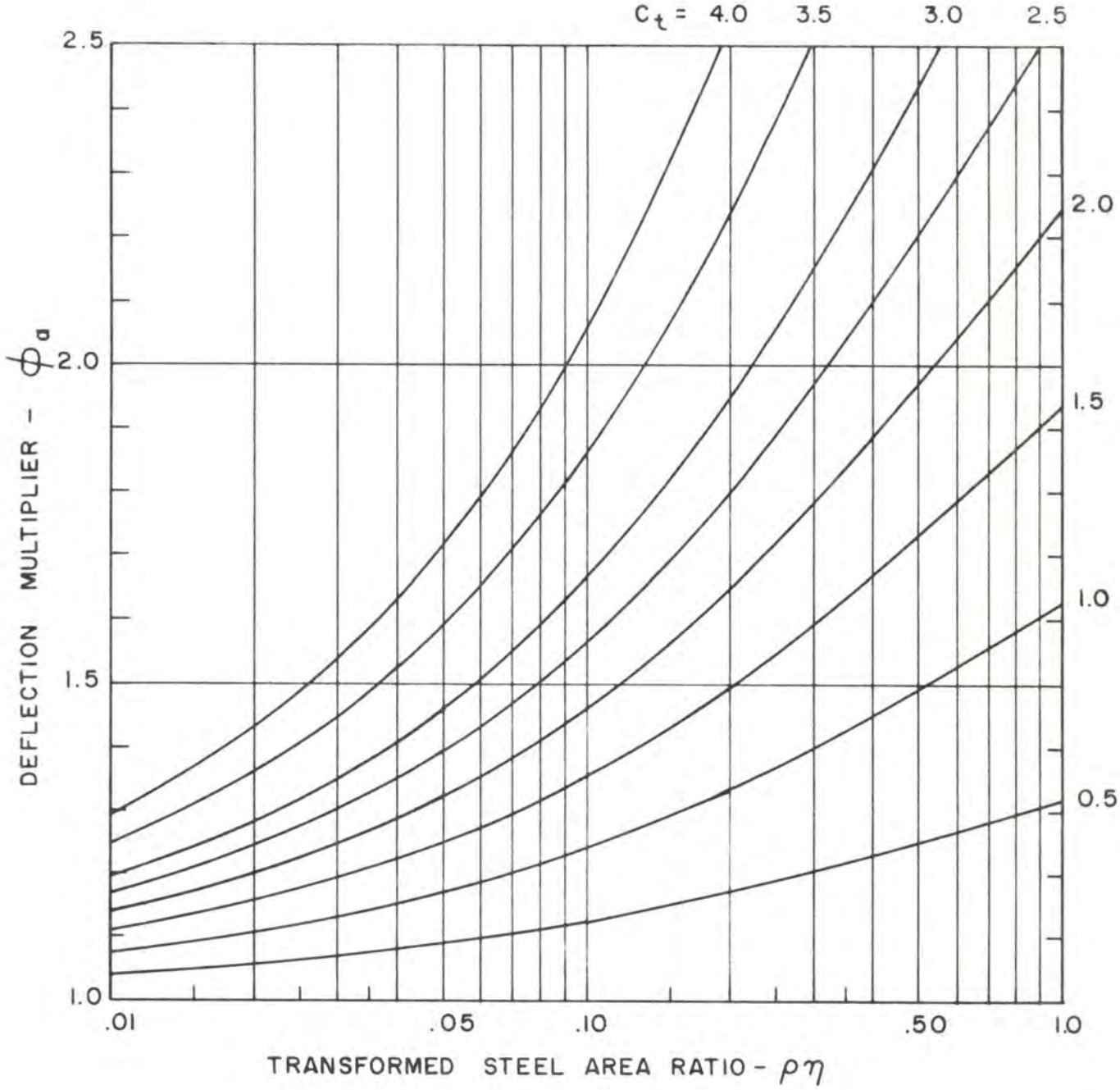


FIG. 44. DEFLECTION MULTIPLIER

beam section is shown in Fig. 45 [15].

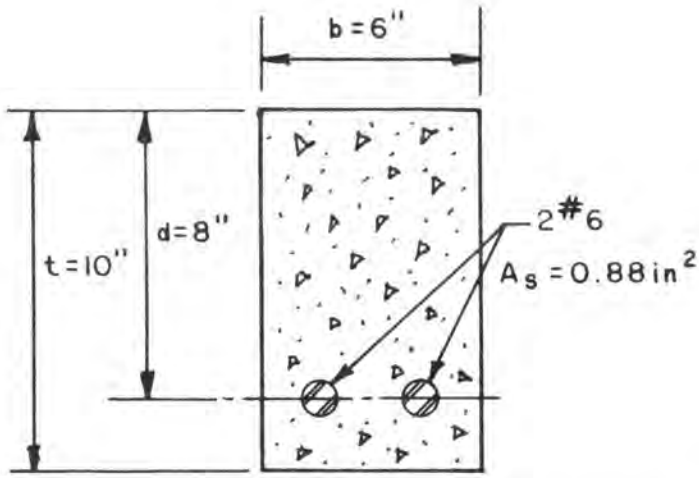


FIG. 45. RECTANGULAR BEAM-TENSION REINFORCEMENT ONLY

The following additional data is assumed:

$$E_s = 29.80 \times 10^6 \text{ psi}$$

$$E_c = 2.31 \times 10^6 \text{ psi}$$

$$C_u = 2.86$$

$$M_{max} = 95000 \text{ in lbs}$$

$$f_{cr} = \alpha_r \sqrt{Wf'_c} = 510 \text{ psi}$$

The elastic modular ratio is therefore

$$\eta = E_s/E_c = 29.8/2.31 = 12.9$$

and the effective modular ratio after creep is

$$\eta_u = (C_u+1)\eta = (3.86)(12.9) = 49.8$$

The reinforcement ratio is

$$\rho = A_s/bd = 0.88/48 = 0.0183$$

and the initial transformed tensile reinforcement area ratio is

$$\rho\eta = (0.0183)(12.9) = 0.2365$$

For a fully cracked section, from Eq. 92 or Fig. 38:

$$k_i = \rho\eta\ (\sqrt{1+2/\rho\eta}-1) = 0.2365\ (\sqrt{1+2/0.2365}-1) = 0.49$$

Also since,

$$bd^3 = 6(8)^3 = 3072\ in^4$$

from Eq. 93 or from Fig. 39:

$$I = \rho\eta\ (1-k)(3-k)\frac{bd^3}{3} = 0.2365(0.51)(2.51)(3072)/3$$

$$= (0.101)\ (3072) = 310\ in$$

$$K_{bi} = E_c I = (2.31 \times 10^6)(310) = 0.716 \times 10^9\ psi$$

From Eq. 94 (Fig. 40):

$$\sigma_c = \frac{6}{(3-k)k}\ \frac{M}{bd^2} = \frac{6}{(2.51)(0.49)}\ \frac{M}{bd^2} = 4.88\ \frac{M}{bd^2}$$

$$\frac{M}{bd^2} = 95000\ /\ [(6)(8)^2] = 248\ psi$$

Hence:

$$\sigma_c = (4.88)(248) = 1210\ psi$$

From Eq. 95 (Fig. 41):

$$\sigma_s = 3/(3-k)(M/(\rho bd^2)) = (3/2.51)(248/0.0183)$$

$$= (1.195)(13550) = 16200\ psi$$

After creep, the transformed tensile reinforcement area ratio is:

$$\rho\eta_u = (0.0183)(49.8) = 0.913$$

For a fully cracked section the compressive depth ratio after creep is (Eq. 92 or Fig. 38):

$$k_u = \rho\eta_u\ (\sqrt{1+2/\rho\eta_u} - 1) = 0.913\ (\sqrt{1+2/0.913} - 1) = 0.719$$

From Eq. 96 or Fig. 42:

$$\phi_t = (3-k_i)/(3-k_u) = 2.51/2.281 = 1.10$$

hence

$$\sigma_{su} = \phi_t \, \sigma_s = (1.10)(16200) = 17800 \text{ psi}$$

The compressive stress in the concrete decreases. From Eq. 97 (Fig. 43)

$$\phi_c = \frac{k_i}{k_u} \phi_t = (0.49/0.719)(1.10) = 0.75$$

Hence the compressive stress after creep is

$$\sigma_{cu} = \phi_c \sigma_c = (0.75)(1210) = 906 \text{ psi}$$

Further, from Eq. 99 or Fig. 44:

$$\phi_a = ((1-k_i)/(1-k_u))\phi_t = (0.51/0.281)(1.10) = 2.00$$

Hence:

$$K_{bu} = K_{bi}/\phi_a = (0.716/2) \times 10^6 = 0.358 \times 10^6 \text{ psi}$$

The above data may also be used to estimate the initial rigidity of a partially cracked section. For the cracked section the total effective area transformed to equivalent concrete is:

$$A = (k_i + \rho n)bd = (0.49 + 0.2365)bd = 0.7265 \text{ bd}$$

By proportion:

$$\frac{k_i}{k_t} = \frac{\sigma_c}{f_{cr}}$$

Hence:

$$k_t = (f_{cr})(k_i)/\sigma_c = (510)(0.49)/1210 = 0.2065$$

and

$$\Delta A = 0.2065 \text{ bd}$$

$$s = k_t/2 = 0.1032 \text{ d}$$

$$\Delta I = (\Delta A)s^2/3 = 0.000734 \text{ bd}^3$$

$$I_{\Delta\bar{y}} = (A)(\Delta A)s^2 \;/\; (A+\Delta A)$$

$$= [(0.7265)(0.2065)(0.1032)^2 \;/\; 0.933]\; bd^3$$

$$= 0.001713\; bd^3$$

Hence the total change in moment of inertia is

$$\Delta I + I_{\Delta\bar{y}} = (0.000734 + 0.001713)\; bd^3$$

$$= 0.002447\; bd^3 = (0.002447)(3072) = 7.5\; in^4$$

The increase in section rigidity is therefore slightly less than 2.5 percent. The total depth of the uncracked concrete zone is:

$$(k_i + k_t)d = (0.49 + 0.21)d = 0.70\; d$$

Since this depth is smaller than $k_u d$, the assumption of a fully cracked section after creep is reasonable.

It should be noted that while creep increased the steel stress about 10 percent, the concrete stress decreased by 25 percent.

## 6.5 Section Properties - Flanged Beams and Beams With Compression Reinforcement

Formulas for computing the section properties of flanged beams and beams with compression reinforcement can be developed by defining some additional dimensionless parameters. The nomenclature used is shown in Fig. 46. The concrete flange area ratio is defined as

$$\alpha_{fa} = \frac{b_f t_f}{b_w d} \tag{101}$$

The tensile reinforcement ratio is

$$\rho = \frac{A_s}{b_w d} \tag{102}$$

and the compression reinforcement ratio is

$$\rho' = \frac{A_s'}{b_w d} \tag{103}$$

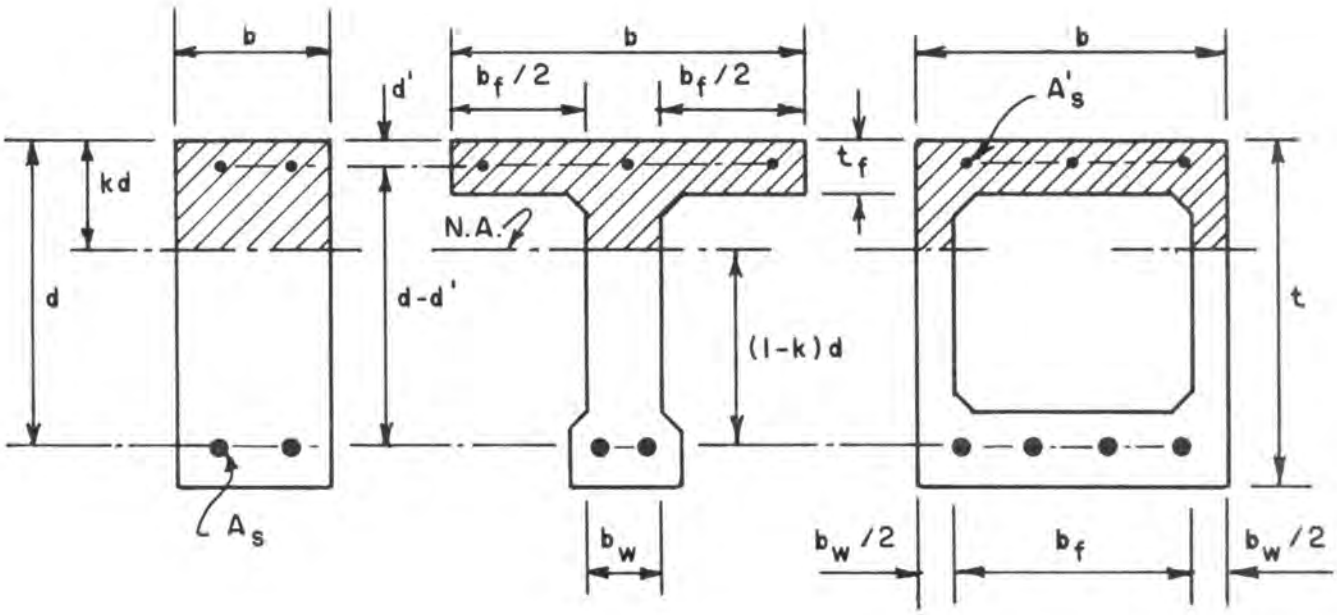


b = width of rectangular beam or total width of flanged or box beams

$b_w$ = total width of web in T, TT or box beams

$b_f$ = net width of compression flange, $(b-b_w)$

$A_s$ = area of tension reinforcement

d = depth of tension reinforcement

$A'_s$ = area of compression reinforcement

d' = depth to compression reinforcement

t = total depth of section

$t_f$ = thickness of compression flange

FIG. 46. FLANGED BEAMS AND BEAMS WITH COMPRESSION REINFORCEMENT

The equivalent transformed flange area ratio is defined to be

$$\alpha_{ef} = (\eta-1)\rho' + \alpha_{fa} \tag{104}$$

Eq. 104 takes into account both the area of the flange and the excess of the compression reinforcement transformed into equivalent concrete. The distance from the top fiber to the centroid of this area is given by $k_{ef}d$, where:

$$k_{ef} = \frac{(\eta-1)\rho'd' + (\alpha_{fa}t_f)/2}{\alpha_{ef}d}$$

$$= \frac{2(\eta-1)\rho'd' + \alpha_{fa}t_f}{2\,\alpha_{ef}d} \tag{105}$$

It is now convenient to consider that the reinforcement ratio $\rho$ may be split into two components, $\rho_w$ and $\rho_f$, respectively, in equilibrium with the compression zone of the web and with the equivalent flange area, as shown in Fig. 47.

For static equilibrium of the web,

$$\eta\rho_w(1-k) = k^2/2,$$

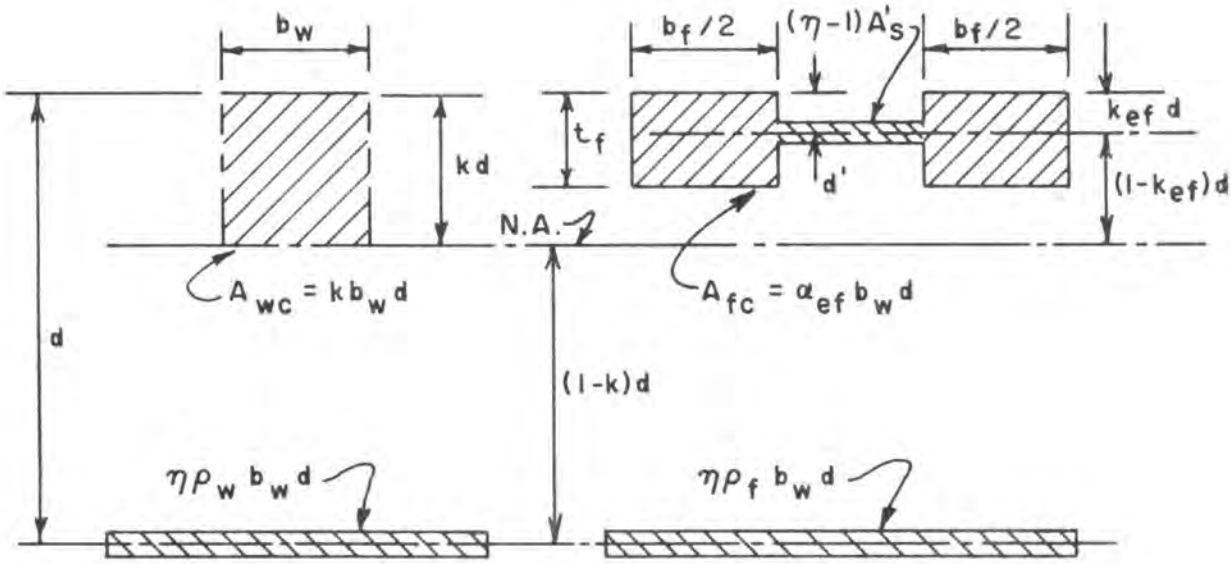


FIG. 47. EQUILIBRIUM CONDITIONS FOR FLANGED BEAMS

hence:

$$\eta\ \rho_w = k^2/[2(1-k)] \tag{106}$$

For static equilibrium of the flange

$$\eta\ \rho_f(1-k) = \alpha_{ef}(k-k_{ef})$$

hence:

$$\eta\ \rho_f = \alpha_{ef}(k-k_{ef})/(1-k) \tag{107}$$

Adding Eq's 106 and 107:

$$\eta\ \rho = \eta(\rho_w+\rho_f) = (k^2+2\ \alpha_{ef}(k-k_{ef}))\ /\ 2(1-k)$$

Thus

$$k^2+2(\eta\rho + \alpha_{ef})k = 2(\eta\rho + \alpha_{ef}k_{ef}) \tag{108}$$

Introducing two more dimensionless parameters:

$$\beta_e = \eta\ \rho + \alpha_{ef} \tag{109}$$

and

$$\gamma_e = [\eta\rho + (\alpha_{ef})(k_{ef})]\ /\ \beta_e \tag{110}$$

Eq. 108 may be written in the form:

$$k^2 + 2\ \beta_e\ k = 2\ \gamma_e\beta_e \tag{111}$$

Eq. 111 is a linear quadratic equation and its solution may be written in the form:

$$k = \beta_e\ [\sqrt{1 + 2\gamma_e/\beta_e} - 1] \tag{112}$$

A graphical solution of Eq. 112 as given in Fig. 48 can readily be obtained by noting that

$$\beta_e = k^2\ /\ [2(\gamma_e-k)] \tag{113}$$

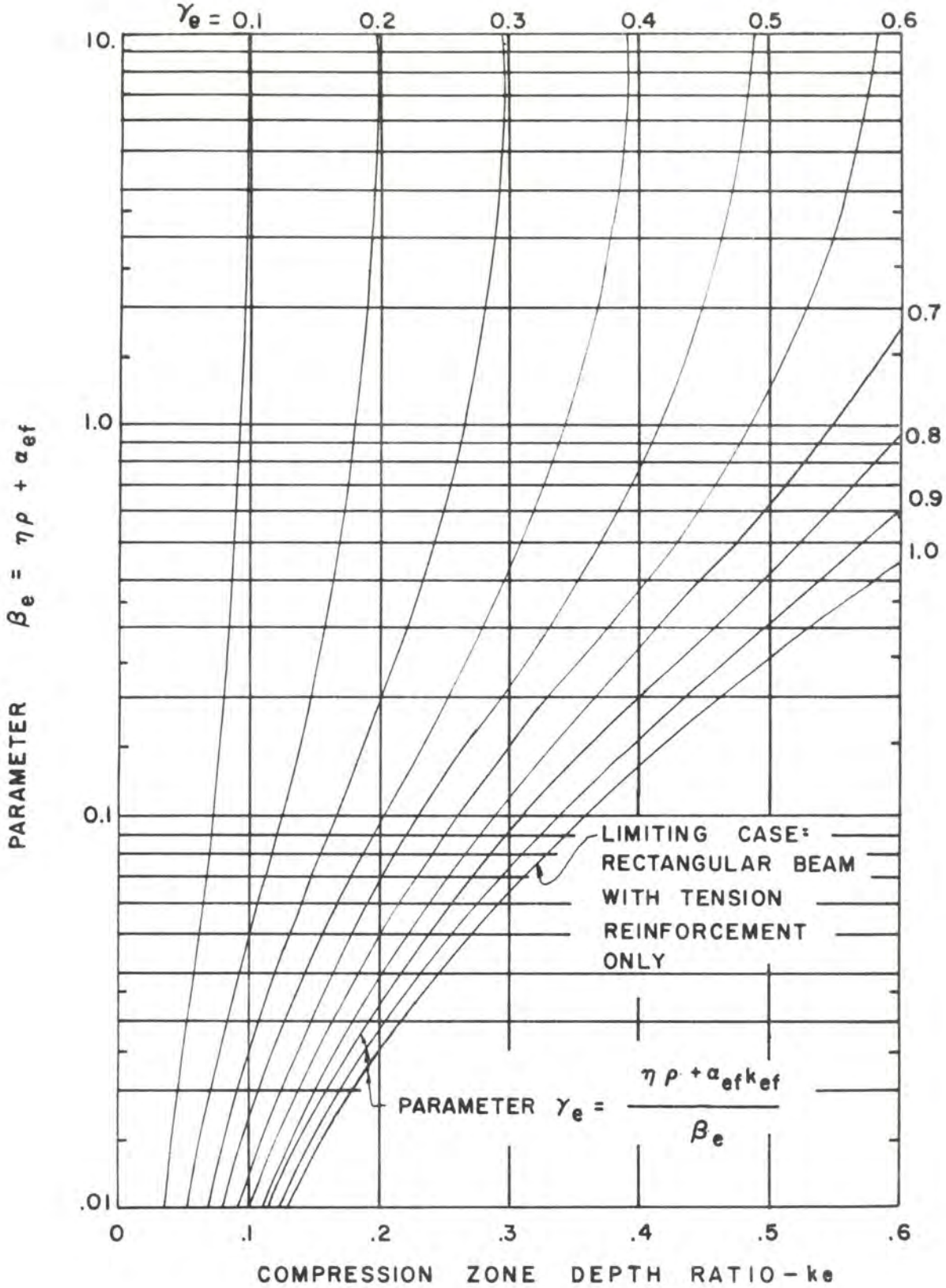


FIG. 48. COMPRESSION ZONE DEPTH RATIO
FLANGED BEAMS

Example: The example in Fig. 36 will be used to demonstrate the use of these relationships. Noting that for this example

$$b = 16 \text{ in.}$$

$$b_w = 4 \text{ in.}$$

$$d = 10 \text{ in.}$$

$$t_f = 2 \text{ in.}$$

$$A_s = 1.27 \text{ in.}^2$$

Hence:

$$\rho = A_s/(b_w d) = 1.27/40 = 0.03175$$

The flange area ratio is

$$\alpha_{fa} = b_f t_f \,/\, (b_w d) = (16-4)(2) \,/\, [(4)(10)] = 0.60$$

For this example, since there is no compression reinforcement, $\rho' = 0$, hence

$$\alpha_{ef} = \alpha_{fa} = 0.60$$

Also,

$$k_{ef} = t_f/(2d) = 2/20 = 0.10$$

For case 1, the elastic modular ratio is

$$\eta = E_s/E_c = 7.32$$

hence:

$$\beta_{ei} = \eta\rho + \alpha_{ef} = (7.32)(0.03175) + 0.60 = 0.832$$

$$\gamma_{ei} = (\eta\rho + \alpha_{ef}\, k_{ef})/\beta_{ei} = (0.232 + 0.06)/0.832 = 0.351$$

Thus from Eq. 112 (Fig. 48)

$$k_i = \beta_{ei}\, [\sqrt{1 + 2\gamma_{ei}/\beta_{ei}} - 1]$$

$$= 0.832\, [\sqrt{1 + 0.844} - 1] = 0.298$$

For case 3, the effective modular ratio is

$$\eta_u = 22.40$$

hence:

$$\beta_{eu} = \eta_u \rho + \alpha_{ef} = (22.4)(0.03175) + 0.60 = 1.311$$

$$\gamma_{eu} = (\eta_u \rho + \alpha_{ef} k_{ef})/\beta_{eu} = (0.711 + 0.06)/1.311 = 0.588$$

and

$$k_u = \beta_{eu} [\sqrt{1 + 2\gamma_{eu} / \beta_{eu}} - 1]$$

$$= 1.311 [\sqrt{1 + 0.898} - 1] = 0.495$$

These values are in agreement with the results of the iterative solution. Once the position of the neutral axis is determined the moment of inertia can readily be computed by the transfer formula. All coefficients may be expressed in dimensionless form by defining the ratio of the flange thickness to the depth by

$$\tau_f = t_f/d \tag{114}$$

The equation for the moment of inertia will then be found to be

$$I = \phi\, b_w d^3/12$$

where

$$\phi = 2k^2(3-k) + 12\alpha_{ef}(k-k_{ef})(1-k_{ef}) + \alpha_{fa}\, \tau_f^{\,2} \tag{115}$$

The first term of $\phi$ represents the contribution of the web and corresponds to Eq. 93. The last term represents the moment of inertia of the concrete flange about its own centroidal axis and is usually quite small compared to the total value. For this case, the moment of inertia is a function of three variables and it is not feasible to develop simple relationships for stress and deflection multipliers as was done for the rectangular beams with tension reinforcement only. Eq. 115 however, can be readily programmed for computer solution and

the stresses and deflections after creep can therefore be solved with little difficulty. If it is desired to determine the partially cracked-section moment of inertia, the Section Moulding method described in Section 6.3 is recommended since a direct solution involves a cubic equation.

Example:

To demonstrate the application of Eq. 115, the moments of inertia of the fully cracked sections of the previous example are calculated below, both before and after creep.

$$b_w d^3/12 = 4000/12 = 333.33 \text{ in}^4$$

$$\alpha_{ef} = 0.60 \qquad 12\alpha_{ef} = 7.2$$

$$k_{ef} = 0.10 \qquad 1-k_{ef} = 0.9$$

$$\alpha_{fa} = 0.60$$

$$\tau_f = t_f/d = 0.2$$

$$\alpha_{fa}\,\tau_f^2 = (0.6)(0.04) = 0.024$$

$$12\alpha_{ef}(1-k_{ef}) = 6.48$$

Case 1

$k_i = 0.298$

$k_i^2 = 0.089$

$2k_i^2(3-k_i) = 2(0.089)(2.702) = 0.479$

$6.48(k_i-k_{ef}) = (6.48)(0.198) = 1.283$

$\alpha_{fa}\,\tau_f^2 = \underline{0.024}$

$\phi_i = 1.786$

$I_i = \phi_i\, b_w d^3/12 = 595.6 \text{ in}^4$

Case 3

$k_u = 0.495$

$k_u^2 = 0.245$

$2k_u^2(3-k_u) = 2(0.245)(2.505) = 1.230$

$6.48(k_u-k_{ef}) = (6.48)(0.395) = 2.560$

$\alpha_{fa}\,\tau_f^2 = \underline{0.024}$

$\phi_u = 3.814$

$I_u = \phi_u\, b_w d^3/12 = 1269.8 \text{ in}^4$

The maximum compressive concrete stress can be computed by the standard formula

$$\sigma_c = \frac{(M)kd}{I} \tag{116}$$

and the tensile reinforcement stress by

$$\sigma_s = \frac{n(M)\ (1-k)d}{I} \tag{117}$$

both before and after creep by using the appropriate values of k, I and n.

## 6.6 Analysis of Shrinkage and Temperature Effects

Shrinkage and temperature strains can produce serious deflections or warping with accompanying induced stresses. The method of analysis for both is similar but presumes that the shrinkage distribution or temperature gradient is known. The analysis is based on the superposition principle. Fictitious internal stresses are applied to the section so that the resulting elastic strains are equal and opposite to the shrinkage or temperature strains. Under these conditions, the member, of course, does not deflect although internal stresses are introduced. To restore force and moment equilibrium, an equal and opposite eccentric force is applied to the section. This eccentric force will of course apply a moment to the section with a resulting curvature given by M/EI. The deflection is then computed as in the case of the deflections due to external load, by integrating the curvature subject to the appropriate boundary or support conditions. The stresses due to the eccentric force can also be computed and must be added algebraically to the initial stresses applied to restrain the shrinkage or temperature strains.

In one important respect does temperature warping differ markedly from shrinkage warping. Temperature gradients are usually temporary. Furthermore, a member may be subjected to many temperature cycles during its service life. Shrinkage on the other hand is a sustained loading type of effect; it starts when curing stops, and continues, although at a diminishing rate, until the member is completely dried out. Thus, shrinkage warping is accompanied by creep whereas the member may normally be assumed to respond elastically due to temperature gradients.

Shrinkage analysis is usually made on the basis that each element of the concrete in the cross section is subjected to a uniform potential shrinkage strain, $\varepsilon_{su}$, which develops gradually. This assumption is not strictly correct, especially for such members as T-sections which have a relative thin flange and thick web. While the total ultimate potential shrinkage strain may not be too much different in different parts of such members, the initial shrinkage rate is greater in the flange than in the web. Nevertheless, since both the ultimate shrinkage potential and the environmental conditions governing the rate of development can at best only be estimated, the simplifying assumption of a uniform shrinkage potential is a reasonable approximation. For this assumption, it is somewhat more convenient to analyze the section on the basis that free shrinkage first takes place and that the equilibrium restoring force is due to a fictitious force which must be applied to the reinforcement so that the elastic strains are equal to the shrinkage strains as shown in Fig. 49. Under this stress condition the section is subjected to axial deformation only.

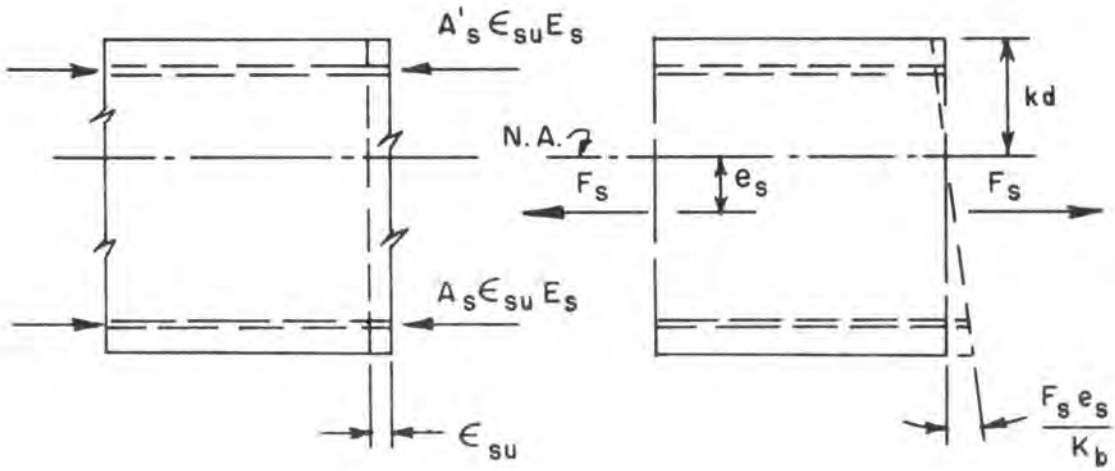


Stress system producing axial deformation only

Restoring force system producing warping

FIG. 49. WARPING ANALYSIS FOR UNIFORM SHRINKAGE

The warping force is therefore:

$$F_s = (A_s + A_s')\,\varepsilon_{su}E_s$$

$$= \varepsilon_{su}E_s(\rho + \rho')b_w d \qquad (118)$$

applied at an eccentricity

$$e_s = [\frac{(\rho + \rho' d'/d)}{\rho + \rho'} - k_u]\, d \tag{119}$$

The warping moment is therefore,

$$M_s = F_s e_s = \varepsilon_{su} E_s\, [\rho(1-k_u) - \rho'\, (k_u - d'/d)] b_w d^2 \tag{120}$$

Since warping due to shrinkage develops at about the same rate as the concrete creeps under stress the limiting value of the section rigidity after creep is employed. Thus from Eq. 115

$$K_{bu} = [E_c/(C_u+1)]\, I_u = \frac{E_s}{\eta_u}\, \phi_u\, \frac{b_w d^3}{12}$$

and the limiting warping curvature is

$$\frac{1}{r_{su}} = \frac{M_s}{K_{bu}} = \frac{12\, \varepsilon_{su}\, \eta_u\, [\rho(1-k_u) - \rho'(k_u - d'/d)]}{[2k_u^2(3-k_u) + 12\alpha_{efu}(k_u - k_{efu})(1-k_{efu}) + \alpha_{fa}\, \tau_f^2]d} \tag{121}$$

The warping deflection may then be obtained by double integration of the section curvature subject to the support boundary conditions. For a simply supported beam of constant section rigidity, the shrinkage deflection may be shown to be:

$$a_s = \frac{M_s\, \ell^2}{8K_{bu}} = \frac{\ell^2}{8r_{su}} \tag{122}$$

For a rectangular beam with tension reinforcement only, Eq. 121 reduces to:

$$\frac{1}{r_{su}} = \frac{6\, \varepsilon_{su}\, \eta_u \rho(1-k_u)}{k_u^2(3-k_u)d}$$

From Eq. 91,

$$\eta_u\, \rho = \frac{k_u^2}{2(1-k_u)}$$

hence,

$$\frac{1}{r_{su}} = \frac{3\, \varepsilon_{su}}{(3-k_u)d} \tag{123}$$

If the beam is simply supported, the deflection due to shrinkage warping is

$$a_s = \frac{3}{8} \frac{\varepsilon_{su}}{3-k_u} \frac{\ell^2}{d}$$

$$= \phi_{as} \, \varepsilon_{su} \frac{\ell^2}{d} \qquad (124)$$

where:

$$\phi_{as} = \text{shrinkage coefficient, } \frac{3}{8(3-k_u)}$$

Fig. 50 is a graphical representation of this shrinkage coefficient as a function of $\rho\eta$ and the creep coefficient.

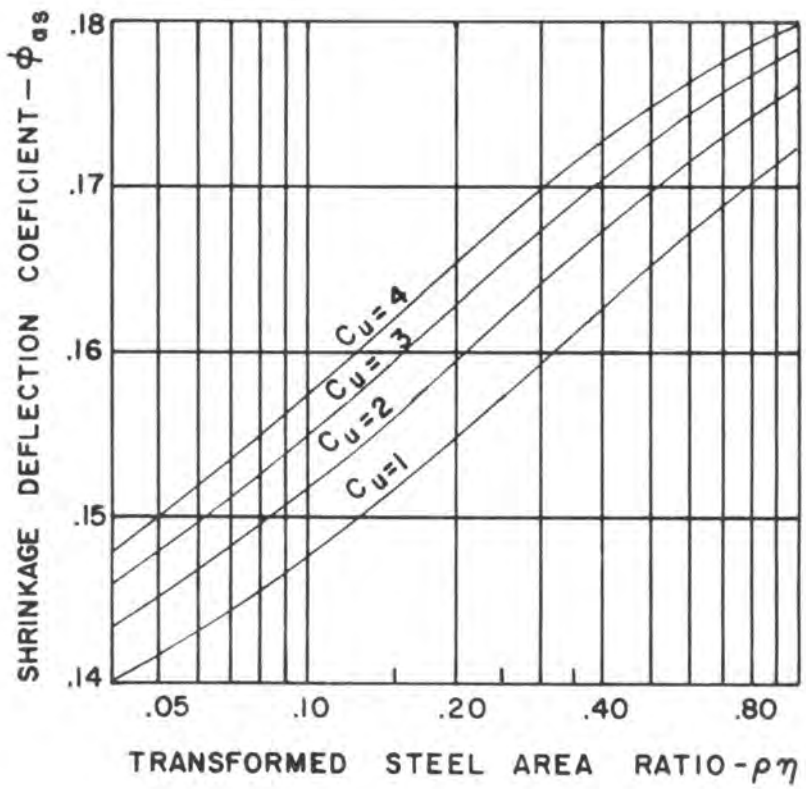


FIG. 50. SHRINKAGE COEFFICIENT - RECTANGULAR BEAMS, TENSION REINFORCEMENT ONLY

Examples. To illustrate the application of these relationships, the shrinkage curvature and deflections for the two previously used examples are computed below:

Rectangular beam, tension reinforcement only, 18-ft span,

$$\ell = 18 \text{ ft} = 216 \text{ in}; \quad d = 8 \text{ in}; \quad k_u = 0.719$$

Therefore,

$$\phi_s = \frac{3}{8(3-k_u)} = 0.375/2.281 = 0.1645$$

and the deflection is

$$a_s = \phi_s \, \varepsilon_{su} \, \ell^2/d$$

$$= 0.1645 \, \varepsilon_{su} \, \frac{(216)^2}{8} = 960 \, \varepsilon_{su} \text{ in}$$

T-beam, 18 ft span

$$\ell = 18 \text{ ft} = 216 \text{ in}; \quad b_w = 4 \text{ in}; \quad d = 10 \text{ in}; \quad \rho = 0.03175;$$

$$k_u = 0.495, \quad \eta_u = 22.4, \quad I_u = 1270 \text{ in}^4$$

From Eq. 120 the warping moment is seen to be

$$M_s = E_s[\rho(1-k_u)] \, b_w d^2 \varepsilon_{su}$$

$$= (0.03175)(0.505)(400) \, E_s \, \varepsilon_{su}$$

$$= 6.42 \, E_s \, \varepsilon_{su}$$

The section rigidity is $1270 \, E_s/\eta_u$, hence, the warping curvature is

$$\frac{1}{r_{su}} = \frac{6.42 \, \eta_u}{1270} \, \varepsilon_{su} = 0.113 \, \varepsilon_{su}$$

and the deflection due to shrinkage is

$$a_s = \frac{1}{r_{su}} \, \frac{\ell^2}{8} = 0.113 \, \varepsilon_s \, \frac{(216)^2}{8} = 661 \, \varepsilon_{su} \text{ in}$$

It has been noted that the analysis can also be made by determining the stresses required to restrain shrinkage of the concrete. These stresses

are of course effective only in the uncracked compression zone. Thus, for example, for a rectangular beam with tension reinforcement only, tensile forces would be induced equal to $\varepsilon_{su}E_{cu}$. To restore equilibrium, a compressive force would have to be applied at the centroid of the compression zone inducing a warping moment

$$M_s = \varepsilon_{su}E_{cu}\ k_u bd(\frac{k_u d}{2}) = \frac{k_u^2}{2}\ bd^2\ E_{cu}\ \varepsilon_{su} \tag{125}$$

With the moment of inertia given by Eq. 93

$$\frac{1}{r_{su}} = \frac{M_s}{K_{bu}} = \frac{M_s}{E_{cu}\ I_u}$$

$$= \frac{k_u^2\ bd^2\ E_{cu}\ \varepsilon_{su}}{2}\ \frac{6}{E_{cu}bd^3\ (3-k_u)k_u^{\ 2}} = \frac{3}{3-k_u}\ \frac{\varepsilon_{su}}{d}$$

which is identical with the result shown in Eq. 123.

## 6.7 Typical Computations

To demonstrate the application of the equations derived in this chapter the elastic and time-dependent deflections will be calculated for two beams tested in the laboratory [15]. The sections for these beams were analyzed in the previous examples. Both beams were simply supported beams with an effective span length of 18 feet and with equal liveloads applied at the third points. To compute the deflections, the $\delta_a$ coefficients (Eq. 83) must first be calculated.

For third point loading:

$$M_{max} = \frac{P\ell}{3}$$

and

$$a_{max} = \frac{P}{24EI}\ \frac{\ell}{3}\ \ [3\ell^2 - 4\ \frac{\ell^2}{9}] = \frac{P}{24EI}\ \frac{\ell}{3}\ [\frac{23}{9}\ \ell^2]$$

Substituting the value for $M_{max}$

$$a_{max} = \delta_a\ \frac{M_{max}}{EI}\ \ell^2 = \frac{23}{216}\ \frac{M_{max}}{EI}\ \ell^2$$

Thus for third point loading, $\delta_a = \frac{23}{216}$

For uniformly distributed loading:

$$M_{max} = \frac{w\ell^2}{8}$$

and

$$a_{max} = \frac{5}{384} \frac{w\ell^4}{EI} = \delta_a \frac{M_{max}}{EI} \ell^2$$

Hence, for this loading

$$\delta_a = \frac{(5)(8)}{384} = \frac{5}{48}$$

<u>Rectangular Beam</u>, tension reinforcement only, $\ell$ = 18 ft.

The beam was made with lightweight aggregate concrete weighing about 109 pcf. The weight per lineal foot of beam was therefore,

$$w = \frac{(6)(10)}{144} (109) = 45.5 \text{ lb/ft}$$

$$M_{d\ell} = \frac{w\ell^2}{8} = \frac{45.4}{12} \frac{(216)^2}{8} = 22000 \text{ in lb} = 22 \text{ kip in}$$

The total applied live load was 2030 lbs, therefore,

$$P = 1015 \qquad M_{\ell\ell} = \frac{P\ell}{3} = (1015)(72) = 73000 \text{ in lb} = 73 \text{ kip in}$$

and the total maximum moment was therefore, 95 in kips. The elastic rigidity, $K_{bi}$, has been calculated to be $0.716 \times 10^6$ ksi. The computed elastic deflection is therefore,

$$(a_i)_{max} = \delta \frac{M\ell^2}{K_{bi}}$$

$$= \frac{[(5/48)\ 22 + (23/216)\ 73]\ (216)^2}{716000}$$

$$= (2.29 + 7.77)(0.0651) = 0.655 \text{ in}$$

Assumption of a partially cracked section would reduce this estimate about three percent or to about 0.635 in. The observed instantaneous deflection for this beam was about 0.46 in., although this deflection had increased to 0.63 in. by the end of the week.

Since the limiting value of the section rigidity after creep, $K_{bu}$ was $0.358 \times 10^6$ ksi, the computed creep plus elastic deflection at the end of 300 days is

$$(a_u)_{max} = \frac{(10.06)(216)^2}{358000} = 1.31 \text{ in}$$

This value could also be obtained by multiplying the instantaneous computed deflection by $\phi_a = 2.00$. The 300-day shrinkage strain as measured on companion 6"x12" cylinders was $682 \times 10^{-6}$. The shrinkage measured on a vertical gage length directly on the beam was only about 250 microinches per inch. This large discrepancy may have been due to the difference in the mass factor but may also have been due to a measurement error.

From the shrinkage analysis, the computed shrinkage deflection for this beam was found to be given by

$$a_s = 960\ \varepsilon_s \text{ in}$$

Thus, the shrinkage deflection could be expected to fall between the values

$$(960)(0.000682) = 0.655 \text{ in}$$

and

$$(960)(0.000250) = 0.240 \text{ in}$$

The total computed deflection is the sum of the shrinkage and the elastic plus creep deflection. Hence,

$$a_{max} = 1.55 \text{ to } 1.965 \text{ in}$$

The measured 300-day deflection was 1.47 in

<u>T-Beam</u>, $\ell = 18$ ft., $K_{bi} = 2.455 \times 10^6$ ksi, $K_{bu} = 1.689 \times 10^6$ ksi

The weight per lineal foot of this beam was

$$\frac{74.48}{144} \times 146 = 75.5 \text{ lb/ft}$$

The dead load moment was therefore,

$$M_{d\ell} = \frac{75.5}{12}\,\frac{(216)^2}{8} = 36600 \text{ in lb} = 36.6 \text{ kip in}$$

The live-load applied at each third point was 2415 lb, and the live-load moment was therefore,

$$M_{\ell\ell} = (2415)(72) = 173900 \text{ in lb} = 173.9 \text{ kip in}$$

The computed instantaneous deflection is therefore,

$$(a_i)_{max} = \frac{[(\frac{5}{48})(36.6) + (\frac{23}{216})(173.9)]\,(216)^2}{2455000}$$

$$= [3.82 + 18.51](0.019) = 0.42 \text{ in}$$

This value compares very favorably with the observed instantaneous deflection of 0.40 in. The computed creep plus elastic deflection after 300 days is

$$(a_u)_{max} = \frac{(22.33)(216)^2}{1689000} = 0.616 \text{ in.}$$

The measured 300-day shrinkage strain was 0.00032 for the 6" x 12" companion cylinders and 0.00034 from a measurement on a transverse gage length on top of the beam flange. These values are reasonably consistent since the beam had a somewhat smaller mass ratio than the companion cylinders. The computed shrinkage deflection therefore, is

$$a_s = 661\ \varepsilon_{su} = 661\ (0.00034) = 0.224 \text{ in}$$

The total 300-day computed deflection therefore, is

$$a_u = 0.616 + 0.224 = 0.84 \text{ in}$$

This value is also in excellent agreement with the observed value of 0.85 inches.

It may be concluded that the accuracy of predicted values is quite sensitive both to the validity of the assumption of a fully cracked section and the accuracy with which the shrinkage can be predicted. The deflection prediction for T-beams and beams with compressive reinforcement can be expected to be more reliable because the assumption of a fully cracked section is more likely to be valid. Deflection predictions for rectangular beams with only tensile reinforcement will generally be conservative, especially at early ages.

## 6.8 Summary and Conclusions

Design trends, in recent years, such as longer spans, the use of high strength reinforcement and the use of ultimate-strength design have increased the flexibility of structures to the point where deflections have become a serious design problem. Ultimate-strength design has gained widespread acceptance because engineers have realized that creep, shrinkage and temperature affect the eventual stresses in reinforced concrete members to such an extent that the designer's stress calculations based on traditional working stress analysis do not adequately represent actual stress conditions.

The conclusion that elastic stress analysis should therefore, be abandoned in favor of ultimate strength analysis, however, is not valid. Rather, elastic analysis should be suitably modified to take into account the effects of creep, shrinkage and temperature. The procedures outlined above are relatively simple and can readily be applied using the design aids furnished or with standardized computer programs. The advantage of the proposed analysis is that both stresses and deflections can be predicted with reasonable accuracy.

The question whether the assumption of a fully cracked section is valid is often raised. As shown in the examples, the assumption of a partially cracked section based on a reasonable modulus of rupture can readily be incorporated. However, the apparent increase in rigidity seldom warrants the increase in complexity of the calculations. The error introduced is only serious in lightly reinforced slabs and in deep beams.

It is also recognized that the uncracked concrete between tension cracks does contribute to the rigidity of the section. But at the present time no simple method is available to estimate the magnitude of this increase. On the other hand it has been noted that the assumption of an effective reduced modulus implies complete elastic and creep recovery. These factors tend to compensate each other.

The applicability of section rigidity analysis to prestressed concrete flexural members requires further study. Such members are subject to large changes in concrete stress level when superimposed loads are applied. As in the case of axially loaded columns this method may underestimate actual strains because the method tacitly assumes both elastic and creep strain recovery under decreasing stress levels.

# CHAPTER VII

# SUMMARY AND RECOMMENDATIONS

## 7.1 Summary

While the phenomena of creep and shrinkage are subject to a multitude of variables it is not valid to conclude that the problem of their effect on the behavior of reinforced concrete is hopeless. As demonstrated in the previous two chapters the presence of reinforcement has a considerable ameliorating influence. Hence, even when creep factors and shrinkage can only be estimated, the designer can make reasonably accurate predictions of probable behavior. This then opens up two avenues to the solution of his problem. He can control behavior, if necessary, by providing additional reinforcement, such as compression reinforcement, or by specifying performance requirements of the concrete with respect to creep and shrinkage. If behavior can not be satisfactorily controlled, he must modify his design so as to avoid the problem.

A better understanding of these phenomenon and their effect on structural behavior can be expected to influence the development of concrete specifications to include limitations on creep and shrinkage behavior. On the other hand, excessively restrictive material specifications will raise construction costs and should, therefore, be avoided if not required by the design.

## 7.2 Design Recommendations - Material Properties

Accurate predictions of structural behavior require an accurate evaluation of material properties and of their dependence on environmental conditions. Design details which are sensitive to small variations in material properties should be avoided wherever possible. Where this is not possible such details should be analyzed to determine the effect of extreme values established by the most accurate information available. Most of the material properties with which the designer will be concerned can best be determined by test, but even when test values are available, adjustments will be required to compensate for the

effect of such factors as member size, age, conditions of curing and environmental conditions. Where test data is not available, properties may be estimated from empirical equations developed on the basis of past experience. In most design situations where strains and deflections are not particularily critical, such estimates will result in adequate design. Some of the more important stress and strain relationships are summarized below.

### 7.2.1 Strength of Concrete

Specified compressive strength, $f'_c$, is usually defined as the 28-day compressive strength. This property is of special importance since many other properties are given in relation to this value. Since concrete changes in strength with age this change must be taken into consideration, especially when concrete is loaded prior to full maturity.

The compressive strength at any age t days of a concrete of a given specified strength may be estimated by the empirical hyperbolic relationship suggested by Branson:

$$f'_c(t) = \frac{t}{a+bt} f'_c(28) \qquad (5)$$

where:

$f'_c(t)$ = compressive strength at age t days

t = age of concrete in days

$f'_c(28)$ = 28-day compressive strength

a,b = experimentally determined constants

The constants a and b are functions both of the type of cement used and type of curing employed. Typical values recommended by Branson are listed in the table below (Table I)

| Cement Type | Type of Curing | a | b | t days | $\frac{f'_c(t)}{f'_c(28)}$ | $\frac{f'_c(\infty)}{f'_c(28)}$ |
|---|---|---|---|---|---|---|
| I | Moist | 4.00 | 0.85 | 7 | .70 | 1.18 |
| III | Moist | 2.30 | 0.92 | 7 | .80 | 1.09 |
| I | Steam | 1.00 | 0.95 | 2.5 | .74 | 1.05 |
| III | Steam | 0.70 | 0.98 | 2.5 | .80 | 1.02 |

The modulus of rupture is usually determined from a flexure test and may be related to the compressive strength by the approximate equation:

$$f_{cr} = \alpha_r \sqrt{W f_c'} \tag{6}$$

where:

$f_{cr}$ = modulus of rupture, psi

$W$ = density of the concrete, pcf

$f_c'$ = specified compressive strength, psi

$\alpha_r$ = constant determined by test

The parameter $\alpha_r$ ranges from 0.60 to 0.95. The lower values tend to apply to higher strengths and lower concrete densities and the higher values to lower strength and higher concrete densities.

The tensile strength of concrete is usually determined by the tensile splitting test and is related to the compressive strength by the approximate equation

$$f_{ct} = \alpha_t \sqrt{W f_c'} \tag{7}$$

where

$W$ and $f_c'$ are as previously defined and

$f_{ct}$ = tensile strength, psi

$\alpha_t$ = constant determined by test, ($\alpha_t \doteq 1/3$)

7.2.2 Elastic Modulus

Experimentally the elastic modulus of concrete is normally obtained by plotting stress vs. strains for data obtained from a standard compression test. The elastic modulus is usually assumed to be the numerical value of the average slope of the stress-strain curve for stress levels up to about 0.45 $f_c'$. When approximate values suffice, the modulus may be estimated from the specified compressive strength and the density of the concrete by the equation:

$$E_c = 33\sqrt{W^3 f_c'} \tag{3}$$

Somewhat more accurate estimates may be made if the volumetric proportions of the mix are known as well as the physical properties of the constituents. Typical of equations used by researchers to extrapolate test information are Eq. 8 and Eq's III-A 9 and 10.

### 7.2.3 Shrinkage

Shrinkage and drying creep are closely related phenomena in that they are both functions of the hygral-thermal environment of concrete. With respect to design analysis two approaches may be used. The first is based on the shrinkage potential, i.e., the terminal unrestrained shrinkage strain. The second approach is based on the assumption of a constant potential shrinkage force derived from this strain. As in the case of strength and modulus, shrinkage should normally be determined by test. Shrinkage however is a time dependent strain and furthermore is affected by the hygral-thermal environment as well as by member size. Hence, even when test data is available, design values must normally be adjusted to take into account actual service conditions.

The most convenient and commonly used method for predicting the shrinkage at any age is the use of Lorman's hyperbolic equation

$$\varepsilon_s = \frac{\varepsilon_{su}\, t_d}{t_{sk} + t_d} \tag{9}$$

where:

$\varepsilon_s$ = the unrestrained shrinkage strain after $t_d$ days

$t_d$ = the number of days after drying is initiated

$\varepsilon_{su}$ = the terminal value of shrinkage at $t_d \to \infty$

$t_{sk}$ = a characteristic time in days for which $\varepsilon_s = \varepsilon_{su}/2$

The values of $\varepsilon_{su}$ and $t_{sk}$ may be determined experimentally as discussed in Chapter 3. Normally, shrinkage characteristics are measured at a

relative humidity of 50 percent and a constant temperature of 70°F. Dutron's equation may be used to estimate free shrinkage at other values of relative humidity.

$$\varepsilon_s = \varepsilon_{sh} \left(0.96 \log \frac{105-H}{5}\right) \tag{17}$$

where:

$\varepsilon_{sh}$ = the unrestrained shrinkage in a 50 percent relative humidity environment

H = ambient relative humidity in percent

The effect of member size is primarily one of the time rate at which shrinkage is developed. This effect can most readily be taken into account by adjustment of the value of the characteristic time $t_{sk}$ in Eq. 9. Hansen and Mattock's equation is recommended (45):

$$t_{sk} = \alpha_{sk}\, e^{0.36\, \gamma_{vs}} \tag{27}$$

where

$\alpha_{sk}$ = appropriate coefficient to fit test data

e = base of naperian logarithm

$\gamma_{vs}$ = mass factor, i.e. volume to surface ratio, inches

For the test data used by Hansen and Mattock $\alpha_{sk}$ had a value of 26. Very little data is available for the effect of ambient temperature variations hence no specific recommendations can be made for adjusting experimental values.

Shrinkage is primarily a function of the shrinkage characteristics of the paste and of the aggregate volume concentration. Hence, if the shrinkage of a given mix has been determined, the shrinkage of a mix with different proportions but with equivalent paste quality can be estimated by the approximate relationship:

$$\frac{\varepsilon_{su}}{\varepsilon_{sp}} = 1.5 \left(1 - \sqrt[3]{V_a}\right) \tag{23}$$

where:

$V_a$ = the aggregate volume concentration

$\varepsilon_{sp}$ = the free shrinkage strain of the paste.

Thus the ratio of the shrinkage of two mixes with different paste contents is given by

$$\frac{(\varepsilon_{su})_1}{(\varepsilon_{su})_2} = \frac{(1 - \sqrt[3]{(V_a)_1})}{(1 - \sqrt[3]{(V_a)_2})}$$

Lacking applicable test data the following relationship is recommended for concrete moist cured at least 7 days (31):

$$\varepsilon_s = (1.4-0.01H) \frac{t_d}{35 + t_d} \varepsilon_{su}, \quad 40\%<H<80\% \qquad (28)$$

where $\varepsilon_{su}$ may be assumed to have a value of 0.000800 based on a relative humidity of 40 percent.

7.2.4 Creep

It has been noted that creep and shrinkage are not independent phenomena. Since creep is stress dependent, for the purpose of analysis, it becomes convenient to consider shrinkage and creep as additive strains. Depending on the nature of the problem, creep may be expressed in terms of either the total creep strain, $\varepsilon_c$, the specific creep $\varepsilon_c'$ (creep strain per unit stress) or the creep coefficient $C_t$ (ratio of the creep strain to elastic strain for equivalent stress). As in the case of shrinkage, the most practical and reliable method for predicting the creep characteristics of a particular concrete is by extrapolation of short-time experimental data. The most convenient formulation is the modified hyperbolic form proposed by Branson (31).

$$C_t = \frac{t_\ell^{0.60}}{t_c + t_\ell^{0.60}} C_u \qquad (33)$$

where:

$C_t$ = the ratio of creep to elastic strain at age $t_\ell$

$t_c$ = a characteristic time constant, ($t_c \doteq 10$)

$t_\ell$ = age in days after loading

$C_u$ = ultimate or limiting creep ratio

When experimental data is not available the creep may be estimated from the paste volume ratio by the Troxell and Davis relationship (4).

The limiting creep ratio can then be expressed as a function of the paste volume ratio, the unit weight of the concrete and the specified strength.

$$C_u = \alpha_{cu} V_p \sqrt{W^3/f'_c} \qquad (36)$$

where:

$\alpha_{cu}$ = a constant ranging from 0.30 to 0.50, when

$V_p$ = the paste volume ratio

$W$ = the unit weight of the concrete in pcf

$f'_c$ = the specified compressive strength in psi

As in the case for shrinkage, the limiting creep ratio is reduced somewhat for large mass factors and $C_u$ may therefore be decreased by about fifteen percent if the minimum thickness of the member exceeds fifteen inches. For creep, however, member size has a relatively minor effect on the time rate of strain development and the value of $t_c$. In the absence of specific data, Branson recommends an average value of $C_u = 2.35$ based on a relative humidity of 40 percent. Creep also is quite sensitive to relative humidity and the creep coefficient should be corrected by the ratio

$$(C.F.)_{cp} = 1.27 - 0.0067\,H \qquad H>40\%$$

where H = the relative humidity in percent. Lacking more specific data,

the creep coefficient may thus be assumed to be

$$C_t = (3 - 0.016\ H)\ \frac{t^{0.60}}{10 + t^{0.60}}, \qquad H>40\% \tag{34}$$

The age at time of loading has an influence at least as great as that of the environmental conditions. Both the ultimate creep magnitude and the characteristic time constant are affected. When the limiting creep (specific creep, or creep coefficient) has been determined for a specific age at time of loading, k' (normally, 28 days), the limiting creep at any other age, k, at time of loading may be estimated by multiplying by the coefficient

$$\beta_c = \left(\frac{k'}{k}\right)^{\alpha_c} \tag{52b}$$

where:

$\alpha_c$ = is a coefficient which should be determined experimentally.

The coefficient $\alpha_c$ appears to be primarily a function of the mass factor but may also be somewhat influenced by mix proportions and type of aggregate. Based on rather sparse data this constant may be assumed to have a value of approximately

$$\alpha_c = \frac{0.40}{\sqrt{\gamma_{vs}}} \tag{126}$$

where:

$\gamma_{vs}$ = mass factor (volume/surface area, in inches)

At the same time that the limiting creep decreases with increasing age at time of loading, the characteristic time constant increases. The characteristic time constant $t_c$ in Eq. 33 may be modified by multiplying the value for a specific age at loading, k' (normally 28 days), by the coefficient

$$\beta_t = \left(\frac{k}{k'}\right)^{\alpha_{ct}} \tag{127}$$

where:

$k$ = age at time of loading in days

$\alpha_{ct}$ = experimentally determined coefficient

The coefficient $\alpha_{ct}$ is known to be dependent on the mix proportions and type of aggregate. It may also be presumed to be dependent on the mass factor of the member since larger members tend to dry out more slowly. For a mass factor of one inch $\alpha_{ct}$ was found to have values of 0.24 and 0.12 for normal and lightweight concrete, respectively. These values are recommended until more extensive data becomes available and are based on the use of the characteristic time constant, $t_c$, of Eq. 33 rather than the characteristic time, $t_{ck}$, used in Eq. 49.

## 7.3 Design Recommendations - Concentrically Loaded Columns

Two basic methods of analysis, the effective section-rigidity method and the rate-of-creeep method may be employed. The first method is based on an effective or sustained load modulus of elasticity and tends to slightly under-estimate final strains and reinforcement stress levels. The second method tends to overestimate these values slightly because the effect of creep recovery due to stress redistribution is neglected. The second method is therefore somewhat more conservative. The two methods may be combined by assuming part of the creep to be effective delayed elasticity. An example of the use of this modified rate-of-creep method is given in Chapter V.

Since columns are generally designed by ultimate strength methods, the designer is usually not too concerned with the actual stress in the reinforcement or in the concrete. In both methods, however, it is more convenient to calculate the stress in the reinforcement first and then determine the column strain from this stress. Equations for both stress and strain are therefore given in the method summaries below.

### 7.3.1 Section Rigidity Method

To calculate initial and ultimate stresses and strains in an axially

loaded column, the following parameters must first be calculated:

The reinforcement ratio $\rho$:

$$\rho = A_s/A_g$$

where:

$A_s$ = total area of the column compression reinforcement

$A_g$ = gross cross-sectional area of the column

The initial and ultimate values of the modular ratio:

$$\eta = E_s/E_c \tag{53}$$

where:

$\eta$ = initial or elastic modular ratio

$E_s$ = modulus of elasticity of the reinforcement

$E_c$ = modulus of elasticity of the concrete

and, $$\eta_u = (1 + C_u)\eta \tag{54}$$

where:

$\eta_u$ = limiting value of the effective modular ratio, $t \to \infty$

$C_u$ = limiting value of the creep coefficient $C_t$, $t \to \infty$

The initial and ultimate values of the transformed area ratios:

$$\alpha_{gc} = 1 + (\eta - 1)\rho \tag{56}$$

and $$\alpha_{gcu} = 1 + (\eta_u - 1)\rho$$

The average stress, $\sigma_{ave}$:

$$\sigma_{ave} = P/A_g \tag{59}$$

where:

P = total axial force

The initial stresses and strain may then be calculated by the following formulas:

$$\sigma_c = \sigma_{ave}/\alpha_{gc} \tag{61}$$

$$\sigma_s = \eta\ \sigma_c \tag{62}$$

$$\varepsilon_r = \sigma_s/E_s \tag{63}$$

where:

$\sigma_c$ = initial stress in the concrete

$\sigma_s$ = initial stress in the reinforcement

$\varepsilon_r$ = initial strain in the column

After creep and shrinkage the column stresses and strain are given by:

$$\sigma_{cu} = \frac{1}{\alpha_{gcu}} (\sigma_{ave} - \rho\ \varepsilon_{su}\ E_s) \tag{64}$$

$$\sigma_{su} = \frac{1}{\alpha_{gcu}} (\eta_u\ \sigma_{ave} + (1-\rho)\varepsilon_{su}\ E_s) \tag{65}$$

$$\varepsilon_{ru} = \frac{1}{\alpha_{gcu}} (\frac{\eta_u\ \sigma_{ave}}{E_s} + (1-\rho)\varepsilon_{su}) \tag{66}$$

where:

$\sigma_{cu}$ = stress in the concrete after creep and shrinkage

$\sigma_{su}$ = stress in the reinforcement after creep and shrinkage

$\varepsilon_{ru}$ = strain in the column after creep and shrinkage

$\varepsilon_{su}$ = limiting value of unrestrained concrete shrinkage

Graphical design aids for this method are given in Fig's 28 and 30.

### 7.3.2 Rate-of-Creep Method

The initial stresses and strain are calculated as for the section rigidity method using Eq's 61 to 63. The following additional parameters are defined:

The free shrinkage effective stress, $\sigma_{se}$, is:

$$\sigma_{se} = \varepsilon_{su} E_c/C_u \tag{67}$$

where, $\varepsilon_{su}$, $E_c$ and $C_u$ are as defined in the previous section. The effective reinforcement, transformed to equivalent concrete, area ratio, $\rho_e$, is:

$$\rho_e = \eta\rho/\alpha_{gc} = \frac{\eta\rho}{1+(\eta-1)\rho} \tag{68}$$

where, $\eta$, $\rho$, and $\alpha_{gc}$ are as previously defined. The ultimate column stresses and strains may then be calculated by the following formulas:

$$\sigma_{cu} = \frac{\sigma_{ave}}{\alpha_{gc}}(e^{-\rho_e C_u}) - \sigma_{se}(1-e^{-\rho_e C_u}) \tag{75}$$

$$\sigma_{su} = \frac{1}{\rho}\,[\sigma_{ave} - (1-\rho)\,\sigma_{cu}] \tag{76}$$

$$\varepsilon_{ru} = \sigma_{su}/E_s \tag{77}$$

Graphical design aids for the rate-of-creep method are given in Fig. 31.

## 7.4 Design Recommendations - Flexural Members

As in the case of columns, actual stresses in the concrete and reinforcement in flexural members are of less concern to the designer than are the resulting deflections. This is especially true when such members are designed by the ultimate strength method. The deflections, however, both before and after creep and shrinkage, are intimately related to these stresses, especially to the stress distribution in the

tensile reinforcement under normal working load conditions. Equations have therefore been developed whereby these stresses as well as the resulting deflections can be estimated.

The deflection equations summarized below were developed on the basis of an effective modulus of elasticity of concrete. This assumption introduces some inaccuracies because the method tacitly assumes full creep recovery of the reduced compressive stress in the concrete due to stress redistribution and therefore the method tends to underestimate the strain in the compression zone. This effect however is, in part, offset by the partial stiffening effect of the concrete in the tension zone even when the concrete is cracked. In spite of its limitations, the effective section rigidity method appears to be the simplest and most rational approach to the problem of estimating time dependent deflections of flexural members under normal working load conditions.

In estimating deflections the designer should recognize that not only is the effective section rigidity dependent on stress levels and the effect of time-dependent deformations of the concrete but the stress levels themselves are in turn dependent on the deformation of the member. This problem is especially complex in continuous members where the end restraint conditions may change due to creep and shrinkage effects. For routine design only gross approximations of these effects are feasible and great refinement in calculating section properties is therefore not warranted.

Shrinkage stresses and resulting warping deflections are estimated on the assumption that the superposition principle is valid. Stress levels in the concrete and reinforcement are determined by considering both internal equilibrium and strain compatibility based on the assumption of linear rotation of the section.

### 7.4.1 Flexural Stresses Due to Load

As in the case of columns, the designer may not be particularly interested in the calculated stress distribution at working load levels. These stresses usually do not control the design from the point of view

of strength of the member. Furthermore, the stresses change with time due to stress redistribution resulting from the effects of creep and shrinkage. Nevertheless, these stresses are of interest since they are directly related to the deflection behavior of the member. They may be calculated by the standard formulas of strength of materials. Thus:

$$\sigma_c = \frac{M\ k_e d}{I_e} \tag{128}$$

and

$$\sigma_s = \eta_e \frac{M(1-k_e)d}{I_e} \tag{129}$$

where:

$\sigma_c$ = calculated maximum concrete stress in the extreme compressive fiber

$\sigma_s$ = calculated stress in the tensile reinforcement

$M$ = moment due to dead and live load

$k_e$ = depth ratio of the compression zone

$d$ = effective depth of member, distance from extreme compressive fiber to centroid of tension reinforcement

$I_e$ = effective moment of inertia of the section with the reinforcement transformed to equivalent concrete

$\eta_e$ = effective modular ratio, $E_s/E_{ce}$

It should be noted that $\eta_e$, $I_e$ and $k_e$ are non-constant parameters, since they change with time due to the effects of creep. The relationship between these stresses and the corresponding deflections may be established as follows:

The elastic strain in the reinforcement is

$$\varepsilon_s = \sigma_s/E_s = \frac{\eta_e}{E_s}\frac{M(1-k_e)d}{I_e} = \frac{M(1-k_e)d}{E_{ce}I_e}$$

The curvature of the member is the rotation of a section of unit length, thus

$$\frac{1}{r} = \frac{\varepsilon_s}{(1-k)d} = \frac{M}{E_{ce}I_e} = \frac{M}{K_{be}} \tag{82}$$

where:

$r$ = radius of curvature

$K_{be}$ = effective beam section rigidity, $K_{be} = E_{ce}I_e$

### 7.4.2 Effect of Member Geometry and Support Constraints

Deflections can be calculated by integrating the curvature obtained by Eq. (82). For statically determinate members this is a relatively simple matter provided the section rigidity can be assumed to be constant over the full length of the span of the member. In that case the maximum deflection can be expressed as a function of the maximum moment:

$$a_{max} = \delta_a \, M_{max} \, \ell^2 / K_{be} \tag{83}$$

where:

$a_{max}$ = maximum deflection

$M_{max}$ = maximum moment

$\ell$ = span length

$K_{be}$ = section rigidity

$\delta_a$ = constant, function of load distribution and the boundary or support conditions

Typical values for $\delta_a$ for simply supported beams range from 1/12 for a concentrated load at the center to 5/48 for a uniformly distributed load.

For uniformly loaded spans of continuous beams where a constant section rigidity may be assumed, the centerline deflection is given by:

$$a = \frac{\ell^2}{48\ K_{be}}\ [5\ M_o + 3(M_{e1} + M_{e2})] \tag{85}$$

where:

$M_o$ = simple beam centerline moment, $M_o = w\ell^2/8$

$M_{e1}$, $M_{e2}$ = left and right support moments (usually negative)

For unusual loading or constraint conditions such as haunched beams, more refined methods may be required based on direct integration of the curvature or the assumption of piecewise constant section rigidity. For such cases generally both the direct effect of variable section rigidity and the indirect effect on the support moments must be evaluated. A suggested procedure is outlined in Appendix IV-A.

7.4.3 Section Properties

To apply the above stress and deflection equations the effective transformed section properties must be computed, both before and after creep. If the sections may be assumed to be cracked in the tension zone, (tension in the concrete neglected) the following equations may be used:

7.4.3a Rectangular beams, tension reinforcement only.

The position of the neutral axis is defined by

$$k_e = \rho\ \eta_e\ [\sqrt{1+2/(\rho\ \eta_e)}-1] \tag{92}$$

The effective moment of inertia of the section is

$$I_e = (3-k_e)k_e^{\ 2}\ \frac{bd^3}{6} \tag{93}$$

where:

$b$ = width of beam

$d$ = depth to centroid of reinforcement

$\rho$ = reinforcement ratio, $A_s/bd$

$\eta_e$ = effective modular ratio, $(1+C_t)\eta$

Graphical solutions for k and I are given in Fig's 38 and 39.

7.4.3b Flanged beams, (T-beams, box beams) and rectangular beams with compressive reinforcement.

The position of the neutral axis is defined by

$$k_e = \beta_e \left[ \sqrt{1 + 2\,\gamma_e/\beta_e} - 1 \right] \tag{112}$$

The effective moment of inertia of the section is

$$I_e = \left[2k_e^{\,2}(3-k_e) + 12\alpha_{ef}(k_e-k_{ef})(1-k_{ef}) + \alpha_{fa}\,\tau_f^{\,2}\right] \frac{b_w d^3}{12} \tag{115}$$

where:

$\alpha_{fa}$ = the concrete flange area ratio

$$\alpha_{fa} = b_f t_f/(b_w d) \tag{101}$$

$b_w$ = total width of web (Fig. 46)

$b_f$ = net width of compression flange, $(b-b_w)$

$t_f$ = thickness of the compression flange

and where:

$\alpha_{ef}$ = the equivalent transformed flange area ratio

$$\alpha_{ef} = (\eta_e-1)\rho' + \alpha_{fa} \tag{104}$$

$\rho'$ = the compression reinforcement ratio

$$\rho' = A_s'/(b_w d) \tag{103}$$

$A_s'$ = area of compression reinforcement

$k_{ef}d$ = distance from extreme compression fiber centroid of equivalent transformed flange area

where:

$$k_{ef} = \frac{2(\eta_e-1)\rho' d' + (\alpha_{fa}\,t_f)}{2\,\alpha_{ef} d} \tag{105}$$

$d'$ = depth to center of compression reinforcement

and where the parameter $\beta_e$ and $\gamma_e$ are defined by

$$\beta_e = \eta_e\rho + \alpha_{ef} \tag{109}$$

$$\gamma_e = [\eta_e\rho + (\alpha_{ef})(k_{ef})]/\beta_e \tag{110}$$

In Eq's 109 and 110, the tensile reinforcement ratio, $\rho$, is defined as

$$\rho = A_s/b_w d \tag{102}$$

Eq. 112 may be solved by the use of the plots in Fig. 48.

7.4.3c Irregular sections; partially cracked sections.

For irregular sections the use of the "Section Moulding" technique is recommended for computing the section properties. By the use of this method the section may be cut into simple geometric segments. The effect on the composite section properties of adding segments in sequence is calculated by a simple algorithm. This method therefore lends itself to tabular arrangement of the required computations and is particularly useful when a section is modified by the addition of an area segment or a change in reinforcement area. As shown in Fig. 35, let:

$A_j$ = area of a given section for which the section properties have been computed

$I_j$ = moment of inertia of $A_j$ about its centroidal axis

$\bar{y}_j$ = location of centroidal axis of $A_j$

$\Delta A_j$ = incremental area

$s_j$ = distance between centroidal axis of $A_j$ and $\Delta A_j$

$\Delta I_j$ = moment of inertia of $\Delta A_j$ about its centroidal axis

then:

$A_{j+1}$ = combined area of composite section

$$A_{j+1} = A_j + \Delta A_j \tag{87}$$

$\Delta\bar{y}_j$ = shift of the centroidal axis of composite section with respect to centroidal axis of $A_j$

$$\Delta\bar{y}_j = (\Delta A_j)(s_j)/A_{j+1} \tag{88}$$

and hence the location of the centroidal axis of the composite section is

$$\bar{y}_{j+1} = \bar{y}_i + \Delta\bar{y}_j \tag{89}$$

The moment of inertia of the composite section is given by

$$I_{j+1} = I_j + \Delta I_j + I_{\Delta\bar{y}_j} \tag{90}$$

where, the incremental change in the moment of inertia, $I_{\Delta\bar{y}_j}$, due to the shift of the centroidal axis may be computed by either

$$I_{\Delta\bar{y}_j} = (A_j)(\Delta\bar{y}_j)\ s_j$$

or by

$$I_{\Delta\bar{y}_j} = (A_j)(\Delta A_j)(s_j)^2/A_{j+1} \tag{91}$$

This procedure is especially useful if it is desired to correct the moment of inertia calculated on the basis of a fully cracked section to include the effect of the uncracked area in the tension zone. The depth of the uncracked area of the tension zone, $k_t d$, may be estimated by the relationship

$$k_t d \doteq (f_{cr})(I)/M_{max} \tag{130}$$

where:

$k_t d$ = depth of uncracked section of concrete in tension zone

$f_{cr}$ = modulus of rupture of the concrete (Eq. 6)

$I$ = moment of inertia of the cracked section

$M_{max}$ = maximum moment in the section

This correction will in turn result in a shift in the neutral axis and a small increase in the moment of inertia which would be reflected in

a further increase in the depth of the uncracked section. This secondary correction, however, is normally insignificant and may safely be ignored. Because the neutral axis is depressed as creep takes place due to a redistribution of stress, the assumption of a partially cracked section after creep is normally not justified.

### 7.4.4 Stress and Deflection Augmentation Factors

In rectangular beams with tension reinforcement only the stresses in, and the curvature of, a member at a given section may be computed by Eq's 128, 129 and 82. For the case of rectangular beams with tension reinforcement only, the stress in the reinforcement is given by

$$\sigma_s = \frac{3}{(3-k)} \frac{M}{\rho b d^2} \tag{95}$$

With the proper adjustment of the value of k, Eq. 95 is equally valid for the initial stress and the stress after creep. Hence the stress after creep may be computed from the initial stress by the use of a multiplier or augmentation factor, $\phi_t$, thus

$$\sigma_{su} = \phi_t \, \sigma_{si}$$

where:

$$\phi_t = \frac{3-k_i}{3-k_u} \tag{96}$$

Since $k_i$ and $k_u$ may be computed by Eq. (92) in terms of $\rho$ and $\eta_e$, the augmentation factor may be shown to be a function of $\rho$, $\eta$, and $C_u$. A graphical solution of this relationship is given in Fig. 42.

Since creep causes a redistribution of stress and depresses the neutral axis, the maximum compressive stress in the concrete decreases. The ratio of this stress after creep to the initial stress is

$$\phi_c = \frac{k_i}{k_u} \phi_t \tag{97}$$

A graphical solution for $\phi_c$ is given in Fig. 43.

It has been noted that for some simply supported beams the section rigidity can be assumed to be constant. For that case the beam deflection after creep may be calculated by multiplying the elastic deflection by the augmentation factor, $\phi_a$. Thus

$$a_u = \phi_a \, a_i$$

where:

$$\phi_a = \frac{1-k_i}{1-k_u} \phi_t \tag{100}$$

A graphical solution for $\phi_a$ is given in Fig. 44.

The use of multipliers or augmentation factors for more complex sections than rectangular beams with tension reinforcement only is generally not practical because of the number of parameters involved.

### 7.4.5 Shrinkage Stresses and Deflections

Both shrinkage and temperature effects may be analyzed on the assumption that the principle of superposition is valid. Two approaches are possible leading to identical results.

1. Unrestrained concrete strains are first assumed to develop and the effect of the stresses induced in the reinforcement is analyzed.
2. Shrinkage or temperature effects are initially fully restrained and the effect of the restraining forces is analyzed.

For uniform shrinkage, the first approach is slightly more convenient. The warping force, $F_s$, is then

$$F_s = (A_s + A_s') \, \varepsilon_{su} \, E_s$$

$$= \varepsilon_{su} \, E_s \, (\rho + \rho') b_w d \tag{118}$$

This force is applied at an eccentricity

$$e_s = [\frac{\rho + \rho' d'/d}{\rho + \rho'} - k_u] \, d \tag{119}$$

The resulting warping moment is therefore

$$M_s = F_s e_s = \varepsilon_{su} E_s [\rho(1-k_u) - \rho'(k_u - d'/d)]bd^2 \qquad (120)$$

where:

$\varepsilon_{su}$ = limiting shrinkage strain, $t=\infty$

$k_u$ = limiting value of depth ratio of the compression zone

The resulting curvature is given by

$$\frac{1}{r_{su}} = \frac{M_s}{K_{bu}} \qquad (82)$$

where:

$$K_{bu} = \frac{E_c}{1+C_u} I_u = E_s I_u / \eta_u$$

and the effective moment of inertia of the section after creep, $I_u$, is calculated by either Eq. 93, Eq. 115, or the section moulding method.

For a simply supported rectangular beam of constant section rigidity the shrinkage deflection is given by

$$a_s = \frac{M_s \ell^2}{8K_{bu}} = \frac{\ell^2}{8r_{su}} \qquad (122)$$

$$= \phi_{as} \frac{\ell^2}{d} \varepsilon_{su} \qquad (124)$$

where:

$$M_s = \frac{k_u^2}{2} bd^2 \frac{E_s}{\eta_u} \varepsilon_{su} \qquad (125)$$

and

$$\phi_{as} = \frac{3}{8(3-k_u)}$$

The value of the coefficient $\phi_{as}$ may be obtained directly from Fig. 50.

## 7.5 Analysis for Delayed Load Application

Where columns or flexural elements are loaded in such a sequence that a major portion of the sustained load is not applied until after the concrete has fully matured, some adjustment of the creep coefficient may be justified. This reduction is more usual in columns for multistory buildings where the full column load on the lower story column is applied in a sequence of steps as each story is constructed. The creep coefficient may then be multiplied by the coefficient

$$\beta_c = (k_t/k)^{0.4} \tag{52}$$

where

$k_t$ = age at time of loading for coefficient $C_u$

$k$ = age at time of actual loading

Analysis of both columns and flexural members by the section-rigidity method is both relatively simple and reasonably accurate, provided the effective modulus coefficients are suitably modified to take into account the load history, environmental conditions and member geometry. This method should be especially useful in preliminary design since, even where it lacks in accuracy, it gives reliable qualitative results with respect to the effect of minor design adjustments such as changes in the amount or location of reinforcement.

## 7.6 Recommendations for Further Research

While the analysis methods discussed in this report provide adequate tools for the design and analysis of axially loaded columns and for reinforced concrete members loaded in flexure, their applicability to other structural members needs to be explored. Further work should be undertaken to develop simple and reliable analysis of members subjected to both axial load and bending and to structural systems such as grids and plates wherein the effects of creep and shrinkage results in an internal load redistribution between component members or elements. Very little if anything is known as to the effect of creep and shrinkage on shear and torsion strains in structural members.

Finally, more reliable information needs to be developed to estimate the effects of loading history, environmental conditions and member geometry on both the magnitude and the rate of development of creep and shrinkage strains.

# BIBLIOGRAPHY


1. Missouri State Highway Dept., Div. of Bridges Preliminary Report - Camber Study, June 8, 1961.

2. Meyers, Bernard L., "A Review of Literature Pertaining to Creep and Shrinkage of Concrete," University of Missouri - Eng. Exp. Station, Bul. No. 56, Feb. 26, 1963.

3. ACI Committee 209, "ACI Bibliography, Shrinkage and Creep in Concrete, 1905-1964," ACI Bibliography.

4. Neville, Adam M., and Meyers, Bernard L., "Creep of Concrete: Influencing Factors and Prediction," Paper No. 1 Symposium on Creep of Concrete, ACI Publication SP-9, 1964.

5. Pauw, A., and Meyers, Bernard L., "Apparatus and Instrumentation for Creep and Shrinkage Studies," Highway Research Record No. 34, Publication 1154, 1963.

6. Buettner, Donald R., and Hollrah, Ronald L., "Creep Recovery and Creep of Preshrunk Concrete," Report prepared for Missouri State Highway Department, 1965.

7. Pauw, Adrian, and Chai, James Wen-Yu, "Creep and Creep Recovery for Plain Concrete," Missouri Cooperative Highway Research Program, Report 67-8, 1967.

8. Bayazid, Hakam, and Pauw, Adrian, "Creep and Shrinkage of Eccentrically Loaded Prisms," Missouri Cooperative Highway Research Program, Report 68-15, 1968.

9. Vaishnev, Ramesh N., and Kesler, Clyde E., "Correlation of Creep of Concrete with its Dynamic Properties," University of Illinois, T & AM Report No. 603, 1961.

10. Buettner, Donald R., and Bhavsar, Pravin D., "Creep and Damping Characteristics of Concrete," MCHRP Report, University of Missouri, 1966.

11. Ali, Iqbal, and Kesler, Clyde E., "Creep in Concrete with and Without Exchange of Moisture with the Environment," University of Illinois, T & AM Report No. 641, 1963.

12. Alcock, Donald C., and Pauw, Adrian, "Controlled - Deflection Design Method for Reinforced Concrete Beams and Slabs," Proceedings, Am. Conc. Inst. Title 59-22, Vol. 59, No. 5, 1962.

13. McCafferty, Robert M., "Sustained - Load Deflections of Concrete Beams," M.S. Thesis, University of Missouri, August, 1963.

14. Pauw, Adrian, and Meyers, Bernard L., "Effect of Creep and Shrinkage on the Behavior of Reinforced Concrete Members," Paper No. 6, Symposium on Creep of Concrete, ACI Publication SP 9, 1964.

15. Jones, Myron L., "Deflection of Concrete Beams due to Sustained Load," M.S. Thesis, University of Missouri, January, 1966.

16. Branson, Dan E., Scordelis, A.C., and Sozen, A. Mete, "Deflections of Prestressed Concrete Members," ACI Journal, Proceedings V. 60, 1963, pp. 1697-1726.

17. Long, Jack R., and Buettner, Donald R., "Deflections of Prestressed Concrete Beams," MCHRP Report, University of Missouri, August, 1966.

18. Brautigam, Paul A., "Deflections and Strains in Reinforced Concrete Bridges," M.S. Thesis, University of Missouri, 1965.

19. Pauw, Adrian, and Sherkat, A. Akbar, "Time-Dependent Deflection of a Box Girder Bridge," Missouri Cooperative Highway Research Program, Report 67-9, 1967.

20. Bresler, Boris, and Selna, Lawrence, "Analysis of Time-Dependent Behavior of Reinforced Concrete Structures," Symposium on Creep of Concrete, Paper 5, ACI Publication SP 9, 1964.

21. ACI Committee 318, "ACI Standard Building Code Requirements for Reinforced Concrete (ACI 318-63)," Am. Conc. Inst., 1963.

22. McHenry, Douglas, "A New Aspect of Creep in Concrete and its Application to Design," ASTM, Proceedings V. 43, 1943, pp. 1069-1084.

23. Roll, Frederic, "Long-Time Creep-Recovery of Highly Stressed Concrete Cylinders," Paper No. 4, Symposium on Creep of Concrete, ACI Publication SP 9, 1964.

24. C.E.B., "Recommendations Internationales pour le Calcul et l'Execution des Ouvrages en Beton," 1. Principles et Recommendations, 2. Manuel d'Application, XIII-e Session Pleniere Delft, June 30, 1969.

25. Ross, A.D., "Creep of Concrete Under Variable Stress," ACI, Proceedings, V. 54, Title 54-41, March, 1958, pp. 739-757.

26. Ali, I., and Kesler, C.E., "Rheology of Concrete: A Review of Research," Bulletin 476, University of Illinois Eng. Exp. Sta., March, 1965.

27. Sackman, Jerome L., "Creep in Concrete and Concrete Structures," Proceedings, Princeton University Conference on Solid Mechanics, 1963, pp. 15-48.

28. Lewis, M., "Kruip en Krimp van Beton (Creep and Shrinkage of Concrete)," Delft Technical University-Stevin Lab., Report 9-65-3, August, 1965.

29. Desayi, Prakash, and Sen, B.R., "Brief Review on Shrinkage, Creep and Effect of Rate of Loading on Concrete," Indian Engineer, April - Sept., 1966.

30. Johnson, R. Paul, "Structural Concrete," McGraw-Hill, London, 1967.

31. Branson, Dan E., "Creep Shrinkage, and Temperature Effects in the Design of Concrete Structures - State of the Art," Preliminary Draft for 1970 ACI Symposium on Creep and Shrinkage, 1969.

32. Hirsch, Teddy J., "Modulus of Elasticity of Concrete Affected by Elastic Moduli of Cement Paste Matrix and Aggregate," Proceedings V. 59, ACI, 1962, p. 427.

33. Dougill, John W., "Discussion of Reference 32," Proceedings V. 59, ACI, 1962, p. 1363.

34. Hansen, T.C., "Strength, Elasticity and Creep as Related to the Internal Structure of Concrete," Proceedings V. 2, Fourth Int. Symp. on Chemistry of Cement, 1960, pp. 709-723.

35. Neville, A.M., "Creep of Concrete as a Function of its Cement Paste Content," Magazine of Concrete Research, V. 16, No. 46, March, 1964, pp. 21-30.

36. Hickey, Ken B., "Creep of Concrete Predicted from Elastic Modulus Tests," Report No. C-1242, U.S. Dept. of the Interior, Bureau of Reclamation, Jan., 1968.

37. Lerch, William, "Plastic Shrinkage," ACI, Proceedings V. 53, Title 53-44, Feb. 1957, p. 797.

38. Hansen, Torben C., and Nielsen, Knud E., "Influence of Aggregate Properties on Concrete Shrinkage," ACI, Proceedings V. 62, Title 62-48, July 1965, pp. 783-794.

39. Hveem, F.N., and Tremper, Bailey, "Some Factors Influencing Shrinkage of Concrete Pavements," ACI, Proceedings V. 53, Title 53-42, Feb. 1957.

40. Wallo, Edward M., and Kesler, Clyde E., "Prediction of Creep in Structural Concrete," University of Illinois Eng. Exp. Sta., Bul. 498, Nov. 1968.

41. Lyse, Inge, "The Shrinkage and Creep of Concrete," Magazine of Concrete Research, V. 11, No. 33, Nov. 1960, pp. 143-150.

42. Verbeck, G., "Energetics of the Hydration of Portland Cement," Proceedings, Fourth Int. Symp. on the Chemistry of Cement, Washington D.C., 1960, pp. 453-465.

43. Pickett, Gerald, "Effect of Aggregate on Shrinkage of Concrete and a Hypothesis Concerning Shrinkage," ACI, Proceedings V. 52, Title 52-36, Jan. 1956, pp. 581-590.

44. England, George L., "Method of Estimating Creep and Shrinkage Strains in Concrete from Properties of Constituent Materials," ACI, Proceedings, V. 62, Title 62-78, Nov. 1965, pp. 1411-1420.

45. Hansen, T.C., and Mattock, Allan H., "Influence of Size and Shape of Member on the Shrinkage and Creep of Concrete," ACI, Proceedings, V. 63, Title 63-10, Feb. 1966, pp. 267-290.

46. Keeton, J.R., "Study of Creep", U.S. Naval Civil Engineering Laboratory, Tech. Reports R333 I, II, and III, Jan., Feb. and May 1965.

47. Nasser, Karim W., and Neville, Adam M., "Creep of Concrete at Elevated Temperatures," ACI, Proceedings V. 62, Title 62-87, Dec. 1965, pp. 1567-1577.

48. Hickey, Ken B., "Creep, Strength and Elasticity of Concrete at Elevated Temperatures," U.S. Dept. of Interior, Bureau of Reclamation, Report No. C-1257, Dec. 1967.

49. Troxell, G.E., Raphael, J.M. and Davis, R.E., "Long-Time Creep and Shrinkage Tests of Plain and Reinforced Concrete," ASTM, Proceedings V. 58, 1958, pp. 1101-1120.

50. England, G.L., Illston, J.M., "Methods of Computing Stress in Concrete from a History of Measured Strain," Civil Engineering and Public Works Review, April, May, June, 1965.

51. Pfeifer, Donald W., "Reinforced Lightweight Concrete Columns," ASCE, Journal of the Structural Division V. 95, N. ST1, Jan. 1969, pp. 57-82.

52. Holm, Thomas, and Pistrang, Joseph, "Time-Dependent Load Transfer in Reinforced Lightweight Concrete Columns", Journal ACI Title 63-56, Nov. 1966, pp. 1231-1246.

Discussion by Illston, J.M., and Leonhard, Fritz - Journal ACI, June 1967, pp. 1587-1589.

53. Peabody, D., Jr., "Reinforced Concrete Structures", John Wiley and Sons, Inc., New York, 1946, pp. 186-188, 196-198.

54. Mörsh, E., "Statik der Gewölbe and Rahmen," K. Witter, Stuttgart, 1947.

55. Miller, C.A., Guralnick, S.A., "Reinforced Concrete Beams Subjected to Repeated Loads", Proc. ASCE, Journal of the Structural Division, J93 ST 5, pp. 67-84.

56. Selna, L.G., "Time-Dependent Behavior of Reinforced Concrete Structures", Interim Technical Report, U.S. Army Research Office, Durham, North Carolina, Proj. No. 4547E, Report No. 67-19, University of California, Berkely, California.

57. Miller, C.A., Guralnick, S.A., Private Communication, Review of proposed paper, "Creep Deflection of Reinforced Concrete Beams".

58. Bazant, Z.P., "Effects of Concrete Under Repeated Stresses Superposed on Sustained Stresses", Final Report, Eighth Congress, International Association for Bridge and Structural Engineers, New York, September 9-14, 1968, pp. 741-747.

59. Wang, C.K., Salmon, C.G., "Reinforced Concrete Design", International Textbook Company, Scranton, Pennsylvania, 1965.

60. Pauw, Adrian, "Time Dependent Deflections of a Box Girder Bridge", Creep, Shrinkage and Temperature Effects Symposium, American Concrete Institute, New York, April, 1970.

61. Meyers, B.L., Branson, D.E., Schuman, C.G., Christiason, M.L., "The Prediction of Creep and Shrinkage Properties of Concrete", Report 70-5, Iowa State Highway Commission, Univ. of Iowa, August, 1970.

62. Hollrah, Ronald, "Rheological Models for the Deformation of Concrete", PhD Thesis, Univ. of Missouri - Columbia, May 1971.

# APPENDIX I-A

# PHENOMENOLOGICAL STUDIES

# APPENDIX I-A

## PHENOMENOLOGICAL STUDIES

### Introduction

The test program described below was initiated following the compilation of an extensive bibliography and an evaluation of previous research on creep and shrinkage. The primary objective of this phase was to verify observations and conclusions of research by others as well as to study the effect of some variables that had not been considered in previous studies. The test program was designed using the phenomenological approach to evaluate the effect of changes in mix constituents. This approach proved to be more complex than at first anticipated. Since it is not possible to alter one constituent of concrete without altering at least one other, it became very difficult to accurately interpret some of the observed behavior because of the large number of variables involved. The problem was further complicated by the fact that the effect of some of the variables was so subtle that they were completely overshadowed by instrumentation and environment control limitations. Nevertheless, while for some of the variables, the results of this test program only yielded only qualitative results rather than reliable quantitative formulas or curves, the test program was an important phase in that it led to a much clearer understanding of the complex mechanisms involved.

### Objectives and Scope of Test Program

The objectives of this study were as follows:

1. To obtain quantitative information on the normal variation of creep and shrinkage strains for concrete made and tested under controlled conditions.
2. To obtain quantitative information regarding the effect on creep and shrinkage of mix constituents and other variables, specifically:

a. Mix proportions
b. Type of aggregate used in mix
c. Addmixtures, including air entrainment
d. Environment during loading and curing
e. Age at time of loading
f. Size of specimen
g. Amount of reinforcement

3. To establish the feasibility of predicting ultimate creep and shrinkage from short duration test data.
4. To evaluate the suitability of available mathematical models (equations) for predicting time-dependent creep and shrinkage behavior.
5. To investigate the possibility of developing a method for predicting creep and shrinkage strains based only on a knowledge of concrete constituents and environment.

The program designed to achieve these objectives was conducted over a period of two years following over one year of work required to develop the instrumentation system, to select suitable materials and to design the concrete mixes used in the tests. Two-hundred specimens comprising twenty-five separate series were tested. The data obtained from these tests furnished a comprehensive picture of the effect of most of the important variables on creep and shrinkage.

## Analysis of Test Data

To permit analysis of the test data it was necessary to make two basic assumptions:

1. That elastic, creep and shrinkage strains may be treated as independent phenomena;
2. That for normal working stress levels, creep is proportional to stress.

These assumptions have been accepted by most researchers as being reasonably valid and are also necessary in order to apply creep and shrinkage data to design problems. It has been recognized, however, that creep and shrinkage are not completely independent phenomena. In fact it is known that creep is increased when accompanied by shrinkage.

This interdependence was one of the primary factors making quantitative interpretations of the data extremely difficult. The second assumption is reasonably accurate but the stress range for which it is valid may vary considerably. This assumption is necessary only when test data for specimens loaded to different stress levels must be compared.

Test Specimens

The large number of specimens required to study all the variables listed above dictated the selection of the specimen geometry. Specimens were required which could be cast quickly and which would be adaptable to available instrumentation. Other important considerations were concerned with the placement of reinforcement. It was felt that the effect of reinforcment should be studied using the same type of specimen as was to be used for studying the other variables.

Rectangular prism specimens, 16 inches long, and either four inches by three inches, or four inches by four inches in cross-section, were selected for this study. The principal reasons for using prisms rather than cylinders was the ease with which strain measurement points could be attached to the flat surfaces of prisms and the simplicity of using a casting bed for prisms as compared to using individual cylinder molds. In view of the large number of specimens to be loaded, speed in casting was of considerable importance.

In order to have a reference to which creep and shrinkage of all concrete mixes could be compared, it was necessary to decide on a standard specimen. The mix selected, for this standard specimen of normal-weight concrete, conformed to the requirements for class B concrete as defined by the Missouri State Highway Commission, "Standard Specifications".

A Kaw River sand was used for the fine aggregate and a Wisconsin trap rock for the standard coarse aggregate. The mix was designed to yield a minimum 28-day compressive strength of 4500 psi. The gradation used for the coarse aggregate conforms to the Missouri Highway Commission "Standard Specification" requirements, for Gradation "D" of coarse aggregate for Class B concrete, and was at the middle of the permissible specification range. The mix proportions used for all test series are shown in Table I. The standard specimen is designated by Series 5.3 and had a

resulting 28-day compressive strength of 5460 psi and a 2 inch slump.

Table I identifies the principal variable investigated, for each of the twenty-five series of tests made in this program, and summarizes the material properties, stress level, strength, slump and other significant factors. In general, a series consisted of four prisms; a compressive strength specimen, a shrinkage specimen, and two creep specimens. In Series 24 and 25, more than four prisms were made to provide considerable replication of both creep and shrinkage specimens. Except as otherwise noted in the table, the coarse aggregate in all specimens was Wisconsin trap rock. Series 1 and 11 were used to calibrate the instrumentation and are not reported. Series 3, 14, and 24 are not reported due to instrumentation difficulties which could not be resolved. Series 25 was used only to evaluate variation in test data under constant load and environment.

## Fabrication and Curing of Test Specimens

All concrete for the specimens of this program was mixed in a 4.5 cubic foot rotary-drum mixer. All prism specimens were cast in a flat multiple-prism steel-form casting bed. Concrete was transferred in a wheelbarrow from the mixer to the casting bed, deposited in the forms with shovels and finished with a vibrating screed. Use of metal end forms eliminated the necessity for capping the prisms prior to loading.

In Series 10.4 a small number of four-inch-diameter cylindrical specimens were cast in metal forms for the purpose of comparison with creep in prisms. Standard ASTM procedures were used for casting these cylinder specimens.

All concrete was allowed to cure in air for twenty-four hours and then for the remainder of the twenty-eight day period in the moist room, except in cases where the effect of the length of curing time was being studied.

## Loading Procedure and Instrumentation

All loaded specimens were placed in specially constructed loading frames. Both a hydraulic loading system and a spring loading system were used. Each frame accommodated three prisms or cylinders. The

TABLE I. A-I

CONCRETE MIX DATA

| Series | Specimen Section in. | Variable Studied | Mix Proportions for 1 cubic yard: Agg. lb | Sand lb | Cement lb | Water lb | Slump in. | Stress $\sigma$ psi | Strength $f'_c$ psi |
|---|---|---|---|---|---|---|---|---|---|
| 2.1 | 3 x 4 | Slump-1 inch | 1725 | 1660 | 497 | 307 | 1 | 1200 | 4650 |
| 2.2 | 3 x 4 | Slump-5 inches | 1645 | 1578 | 559 | 347 | 5 | 1200 | 4460 |
| 2.3 | 3 x 4 | Slump-7 inches | 1670 | 1603 | 397 | 380 | 7 | 1200 | 4690 |
| 4.1 | 3 x 4 | Type Aggregate-Missouri Limestone | 1622 | 1562 | 506 | 317 | 3 | 1200 | 5560 |
| 4.2 | 3 x 4 | Type Aggregate-Missouri Limestone | 1622 | 1562 | 506 | 317 | 3 | 1200 | 5630 |
| 5.1 | 3 x 4 | Curing Time-14 days | 1687 | 1625 | 527 | 328 | 2.25 | 1200 | 5380 |
| 5.2 | 3 x 4 | Curing Time-21 days | 1687 | 1625 | 527 | 328 | 2.25 | 1200 | 5920 |
| 5.3 | 3 x 4 | Standard Specimen Wisconsin Trap Rock | 1687 | 1625 | 527 | 328 | 2 | 1200 | 5460 |
| 6.1 | 3 x 4 | Type Aggregate-Missouri Limestone #1 | 1622 | 1562 | 506 | 317 | 2 | 1200 | 5230 |
| 6.2 | 3 x 4 | Type Aggregate-Missouri Limestone #2 | 1622 | 1562 | 506 | 317 | 2 | 1200 | 5540 |
| 6.3 | 3 x 4 | Type Aggregate-Missouri Limestone #3 | 1622 | 1562 | 506 | 317 | 2.25 | 1200 | 8420 |
| 7.1 | 3 x 4 | Age at Loading-3 days | 1687 | 1625 | 527 | 328 | 2.25 | 1200 | 3890 |
| 7.2 | 3 x 4 | Age at Loading-7 days | 1687 | 1625 | 527 | 328 | 2.75 | 1200 | 2790 |

TABLE I. A-I

CONCRETE MIX DATA

| Series | Specimen Section in. | Variable Studied | Mix Proportions for 1 Cubic Yard Agg. lb | Sand lb | Cement lb | Water lb | Slump in. | Stress $\sigma$ psi | Strength $f'_c$ psi |
|---|---|---|---|---|---|---|---|---|---|
| 8.1 | 3 x 4 | Age at Loading-2 days | 1687 | 1625 | 527 | 328 | 3 | 1200 | 2154 |
| 8.2 | 3 x 4 | Age at Loading-3 days | 1687 | 1625 | 527 | 328 | 3 | 1200 | 2390 |
| 8.3 | 3 x 4 | Age at Loading-7 days | 1687 | 1625 | 527 | 328 | 3 | 1200 | 2154 |
| 9.1 | 3 x 4 | Water Cement Ratio | 1723 | 1412 | 741 | 329 | 3 | 1200 | 8880 |
| 9.2 | 3 x 4 | Water Cement Ratio | 1618 | 1753 | 438 | 329 | 3 | 1200 | 3430 |
| 9.3 | 3 x 4 | Age at Loading-14 days | 1687 | 1625 | 527 | 328 | 3 | 1200 | 3460 |
| 10.1 | 3 x 4 | Type Aggregate-L.W. #1 | F=785 M=410 C=541 | | 470 | 335 | 2 | 1200 | 4972 |
| 10.2 | 3 x 4 | Type Aggregate-L.W. #2 | F=1050 M=450 | | 705 | 540 | 2.75 | 1200 | 4330 |
| 10.3 | 3 x 4 | Type Aggregate-L.W. #3 | F=900 M=1984 | | 658 | 540 | 3 | 1200 | 4580 |
| 10.4 | 4-Diam | Shape of Specimen-Cylinder | 1687 | 1625 | 527 | 328 | 3.5 | 1150 | 5400 |
| 12.1 | 3 x 4 | Admixture-Placewell, 2-3/4 oz/sack | 1687 | 1625 | 527 | 328 | 3.5 | 1200 | 5420 |
| 12.2 | 3 x 4 | Admixture-Retardwell, 3 fl. oz/sack | 1687 | 1625 | 527 | 328 | 2.75 | 1200 | 4580 |

TABLE I. A-1

CONCRETE MIX DATA

| Series | Specimen Section in. | Variable Studied | Mix Proportions for 1 Cubic Yard Agg. lb | Sand lb | Cement lb | Water lb | Slump in. | Stress $\sigma$ psi | Strength $f'_c$ psi |
|---|---|---|---|---|---|---|---|---|---|
| 13.1 | 3 x 4 | Admixture-Sicacrete, 1-1/2 gallon/cubic yard | 1687 | 1625 | 527 | 328 | 3 | 1200 | 4410 |
| 13.2 | 3 x 4 | Admixture-Calcium Chloride, 1.88 lb/sack | 1687 | 1625 | 527 | 328 | 3 | 1200 | 5380 |
| 13.3 | 3 x 4 | Admixture-Possolith, 4 oz/sack | 1687 | 1625 | 527 | 328 | 3 | 1200 | 4640 |
| 15.1 | 4 x 4 | Type Aggregate-L.W. #1 | F=785 M=410 C=541 | | 470 | 358 | 3 | 900 | 4734 |
| 15.2 | 4 x 4 | Type Aggregate-L.W. #2 | F=1090 M= 450 | | 705 | 625 | 2.75 | 900 | 4198 |
| 15.3 | 4 x 4 | Type Aggregate-L.W. #3 | F=1090 M= 450 | | 705 | 541 | 3.5 | 900 | 4854 |
| 16.1 | 4 x 4 | Reinforcement ($\rho$=1.25%) | 1687 | 1625 | 527 | 328 | 3 | 900 | 4125 |
| 16.2 | 4 x 4 | Reinforcement ($\rho$=2.75%) | 1687 | 1625 | 527 | 328 | 3 | 900 | 4125 |
| 16.3 | 4 x 4 | Reinforcement ($\rho$=4.94%) | 1687 | 1625 | 527 | 328 | 3 | 900 | 4125 |

TABLE I. A-I

CONCRETE MIX DATA

| Series | Specimen Section in. | Variable Studied | Mix Proportions for 1 Cubic Yard Agg. lb | Sand lb | Cement lb | Water lb | Slump in. | Stress $\sigma$ psi | Strength $f'_c$ psi |
|---|---|---|---|---|---|---|---|---|---|
| 17.1 | 4 x 4 | Type Aggregate-Missouri Limestone No environmental control. | 1622 | 1562 | 506 | 317 | 3 | 900 | 4365 |
| 17.2 | 4 x 4 | Type Aggregate-Missouri Limestone No environmental control. | 1622 | 1562 | 506 | 317 | 3 | 900 | 4552 |
| 17.3 | 4 x 4 | Type Aggregate-Missouri Limestone No environmental control. | 1622 | 1562 | 506 | 317 | 3 | 900 | 4672 |
| 18.1 | 4 x 4 | Type Aggregate-Missouri Limestone No environmental control. Air cured | 1622 | 1562 | 506 | 317 | 3 | 900 | 3116 |
| 18.2 | 4 x 4 | Type Aggregate-Missouri Limestone No environmental control. Air cured | 1622 | 1562 | 506 | 317 | 3 | 900 | 3985 |
| 18.3 | 4 x 4 | Type Aggregate-Missouri Limestone No environmental control. Air cured | 1622 | 1562 | 506 | 317 | 3 | 900 | 4481 |
| 19.1 | 4 x 4 | Readymix, N.W. Preshrunk with 6% Air. | 2110 | 1192 | 585 | 229 | 3 | 900 | 6000 |

TABLE I. A-I

CONCRETE MIX DATE

| Series | Specimen Section in. | Variable Studied | Mix Proportions for 1 Cubic Yard Agg. lb | Sand lb | Cement lb | Water lb | Slump in. | Stress $\sigma$ psi | Strength $f'_c$ psi |
|---|---|---|---|---|---|---|---|---|---|
| 20.1 | 4 x 4 | Readymix, L.W. Preshrunk with 6% Air. | 1740 | | 658 | -- | 3 | 900 | 5290 |
| 21.1 | 4 x 4 | Air Content-2.6% Add Air- 1/2 /oz sack | 1642 | 1583 | 513 | 320 | 3 | 900 | 3250 |
| 21.2 | 4 x 4 | Air Content-5.2% Add air 3/4 oz/sack | 1597 | 1539 | 498 | 311 | 3 | 900 | 2667 |
| 21.3 | 4 x 4 | Air Content-7.4% Add air 1-1/4 oz/sack | 1562 | 1504 | 488 | 304 | 3 | 900 | 2292 |
| 22.1 | 4 x 4 | Type Aggregate-Missouri Limestone, High Stress Level | 1622 | 1562 | 506 | 317 | 3 | 2500 | 4208 |
| 22.2 | 4 x 4 | Type Aggregate-Missouri Limestone, High Stress Level | 1622 | 1562 | 506 | 317 | 3 | 2500 | 3718 |
| 22.3 | 4 x 4 | Type Aggregate-Missouri Limestone, High Stress Level | 1622 | 1562 | 506 | 317 | 3 | 2500 | 4198 |
| 23.1 | 4 x 4 | High Stress Level | 1687 | 1625 | 527 | 328 | 3 | 2500 | 4235 |
| 25.1 | 3 x 4 | Standard Specimen-Wisconsin Trap Rock | 1687 | 1625 | 527 | 328 | 6 | 1200 | 3990 |

apparatus used has been described previously (5) and will not be described in detail here. A few important details of these systems are discussed below.

In the hydraulic system, a constant load was maintained using a fuel injection pump and a regulator. Pressure was maintained to within ten psi of the desired level. Several different levels of stress were used in the program. The lowest of these levels was 900 psi and the highest stress level was 2500 psi. Most specimens were loaded to 1200 psi. Nested railroad car springs were used in the spring loading system. These springs were selected because of their low creep characteristics.

The procedure for applying load to the specimens was as follows. Specimens were accurately centered in the loading frames. Load cells were provided to check on the accuracy of the magnitude of applied load. Instrumentation points were attached to all sides of the prisms one day before loading. After load was applied, strain readings for the four sides were taken. By examining the four readings it was possible to determine if the prisms were carrying the applied load concentrically or with a small eccentricity. If the strains indicated an excessive eccentricity had been introduced, the prism was unloaded and recentered in the loading frame to eliminate the eccentricity.

The apparatus used for strain measurement has also been described previously (5). Both longitudinal and lateral creep strains were measured. Longitudinal strains were measured with a portable longitudinal compressometer, clip-on strain meters and a mechanical compressometer. Lateral strains were measured with a specially designed lateral extensometer.

Specimens, once centered, were pre-loaded twice before the final load was applied. Load was applied in 50 psi increments so that the elastic properties of the concrete could be measured utilizing both the clip-on strain meters and the mechanical compressometer. Use of the portable longitudinal compressometer was made while clip-on strain meters were in place. The clip-on meters were removed after specimens had been under load for some time and the reliability of the portable compressometer had been established.

All of the strain measuring devices were subjected to a calibration check at bi-monthly intervals throughout the testing period. The mechanical compressometer utilized a .0001 dial gage with a multiplication ratio of 3.75. All other units with SR-4 strain gages as sensing elements provided for strain measurement to ± 20 micro-inches per inch. Load cells were accurate to ± 100 pounds.

Strain measurements were taken at regular time intervals for all specimens for a minimum of 600 days. Except during the first month, immediately after application of the sustained load, when shorter intervals were used, the normal interval between measurements was one month.

## Shrinkage Measurements

Companion unloaded specimens were used to measure the shrinkage. For the series tested in the controlled environment (72°F, 50% R.H.) room these specimens were stored on racks in the same room used for the loaded specimens. The same strain instrumentation was used. As previously noted, the creep in the loaded specimens was determined on the assumption that creep and shrinkage strains may be considered independent phenomena. Thus the creep in loaded specimens was obtained from the total strain by subtracting the shrinkage strain of the corresponding companion specimen.

## Test Results

Test data was reduced and plotted. Creep curves were obtained by subtracting shrinkage strains on companion specimens from total time dependent strains on loaded specimens. Typical creep and shrinkage curves are shown in Fig. 1. Various known creep prediction methods were used to test their validity. The various variables studied were analyzed to determine if any correlation could be found with creep and shrinkage behavior.

## Variation in Measured Data

The first objective of this program was to obtain quantitative information on the normal variation of creep and shrinkage strains for concrete made and tested under controlled conditions. The prisms of Series

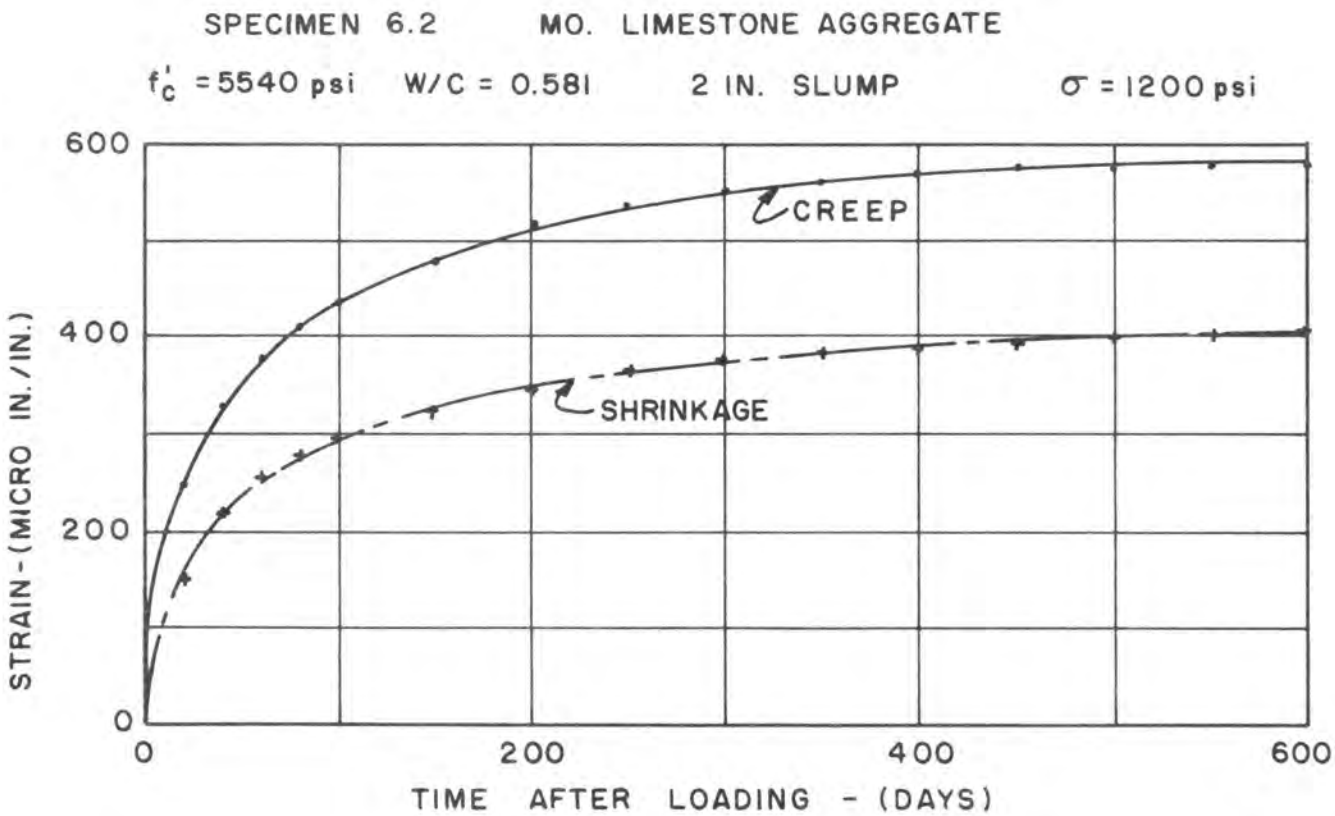


Fig. I. A-1 Typical Creep and Shrinkage Strains

24 and 25 were made in order to establish a frame of reference by which the accuracy of this test program could be judged. All specimens of these two series had the same mix proportions and materials as the standard trap rock specimens of Series 5.3, although the gradation for Series 24 and 25 was slightly different. The spectrum of specific creep time curves for the 25 series (all 3" x 4" specimens) is shown in Fig. 2.

This spectrum shows that at 100 days, the creep for the Series 25 specimens varied in the range from 565 micro-in/in to 700 micro-in/in. The 100 day creep for the standard specimens (Series 5.3) was 545 micro-in/in. This lower creep may be explained by the lower slump and the higher strength of that mix.

Fig. 3 shows the spectrum of shrinkage strain versus time for the specimens of Series 24 and 25. The early shrinkage for the specimens of Series 24 was less than that for Series 25 since the prisms of Series 24 were 4" x 4" and those of the Series 25 were 3" x 4". Thus, while the hyperbolic approximation show that both series had about the same ultimate shrinkage potential, the characteristic time (age at which the shrinkage of the concrete is one half the ultimate) of the 3 x 4 in. specimens was less than half that of the 4 x 4 in. specimens. It has been shown that both creep and shrinkage are sensitive to specimen size and that these properties for a specimen of one size may be related to a similar specimen of another size by a comparison of their surface area to volume ratios (mass factor). Specimens with higher surface-to-volume ratios will tend to exhibit larger creep and shrinkage strains. The surface-to-volume ratio is 1.17 for the prisms of Series 25 and 1.00 for the prisms of Series 24. The importance of Fig. 3, however, lies in that it illustrates the observed variation in shrinkage strains for "identical" specimens. For Series 25, 100-day shrinkage ranged from 240 micro-in/in to 300 micro-in/in, or a $\pm$ ten percent variation from the mean. This indicates that much of the variation found in creep strains may be attributed to variations in shrinkage strains. Creep itself appears to be a fairly uniform process.

Thus Fig.'s 2 and 3 show that even under controlled laboratory conditions, a $\pm$ 10 percent variation from mean values in creep and shrinkage strains can be expected for a given concrete mix. Variables which had only minor effect on creep and shrinkage therefore, could not be

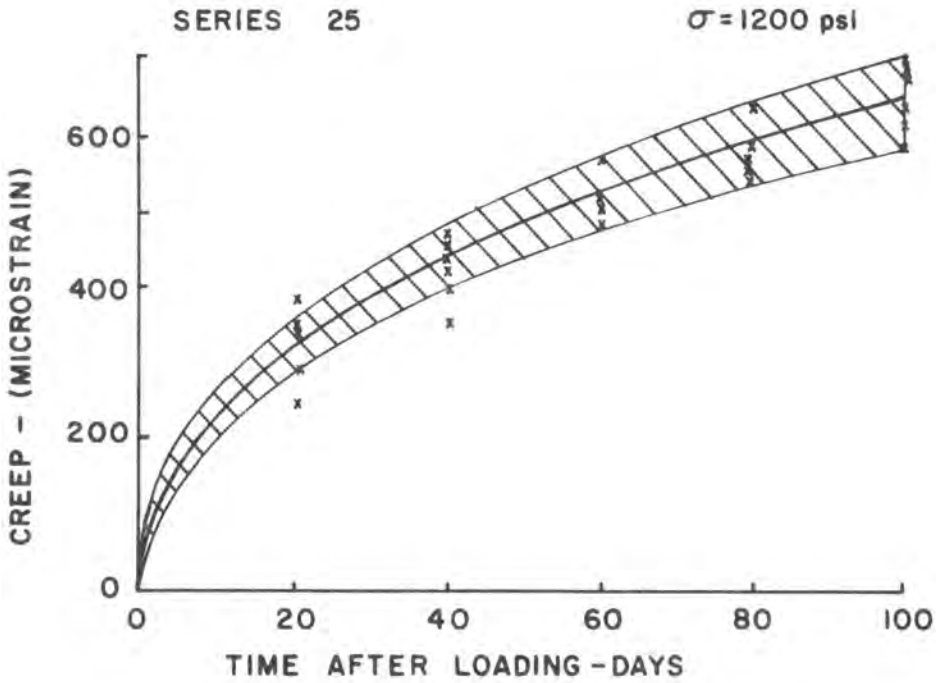


Fig. I. A-2 Spectrum of Specific Creep vs. Age
Series 25

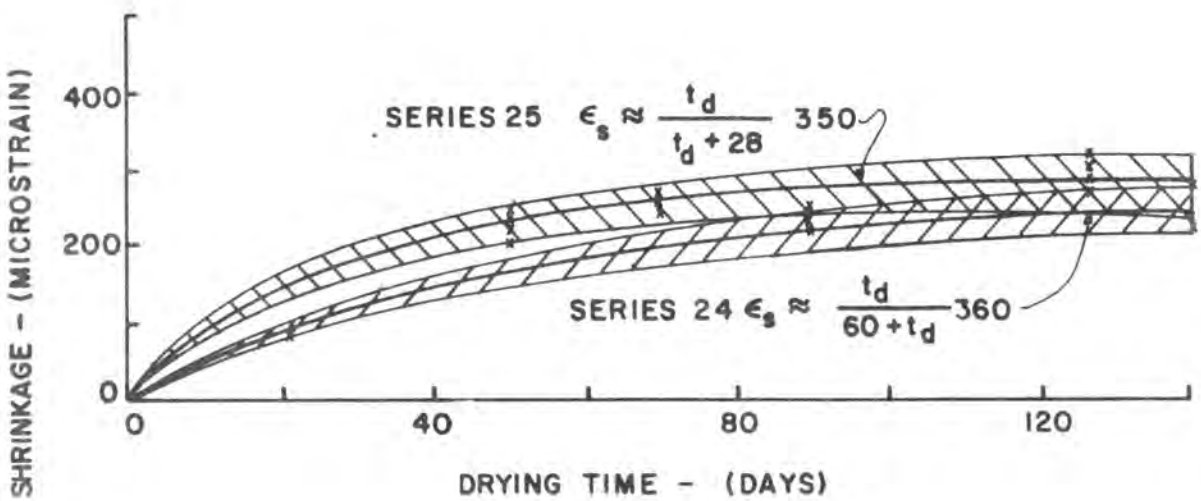


Fig. I. A-3 Spectrum of Shrinkage vs. Age
Series 24 and 25

clearly identified.

All prisms had gage points on all four sides. The strain values used in the computations and comparisons which follow, are the average of four strain readings on the four sides. If the prism had been perfectly centered in the loading frame and the exact same tension been applied through each of the loading rods, the strain on the four sides would have been exactly the same. The strains on the four sides were generaly the same for most prisms. There were several prisms, however, where the measured strain on one side was obviously incorrect. In such cases, the obviously erroneous value was disregarded and not included in the averaging process to obtain the average strain for the prism.

Influence of Mix Constituents

The mix constituents are the main variables in concrete as a structural material. The effect of these constituents on the creep of concrete was therefore first studied. These studies confirmed the conclusion found by others that, within the working range, creep is proportional to the stress-strength ratio and the paste volume ratio (cf. Eq. 35 and Fig. 15). Table II shows the 100-day and one-year creep, the paste volume ratio, the adjusted one-year creep and the stress-strength ratio. Fig. 4 shows the relationship between one year creep, adjusted for a paste volume ratio of 0.294 and the stress-strength ratio. While there is considerable scatter, there does appear to be a general trend and the majority of the points fall within a $\pm$ 20 percent band predicted by a modified Troxell-Davis relationship (Eq. 35). On the average, the Troxell-Davis relationship appears to over-predict creep somewhat. Fig. 5 shows the one-year creep adjusted for a stress-strain ratio of fifty percent plotted as a function of the paste volume ratio. Tabular values of $\varepsilon_{c1}$ as well as the values predicted by the Troxell-Davis relationship also are shown in Table II. Unfortunately the test program did not provide a wide range of paste volume ratios, most of the values being clustered in a stress-strength range of 0.27 to 0.30. Nevertheless the data is reasonably consistent with the Troxell-Davis relationship. Fig.'s 4 and 5 do not include the data for specimens loaded at an early age or for the Series 12 and 13 prisms which were included to determine the effect of admixtures. For the remaining 3 in. x 4 in. specimens, the

TABLE I-A-II CREEP

| Series | $f'_c$ psi | $\sigma$ psi | $\sigma/f'_c$ | Elastic Strain $\varepsilon_i \times 10^6$ | Observed Creep $\varepsilon_c(t) \times 10^6$ t=100 | t=365 | Paste Vol. Ratio $V_p$ | Adjusted Creep $\sigma/f'_c$=0.5 $V_p$=.294 $\varepsilon_{cl}(\sigma/f'_c)$ | $\varepsilon_{cl}(V_p)$ | Computed Creep $\varepsilon_{cl}$(comp) | $\frac{\varepsilon_{cl}(\text{comp})}{\varepsilon_{cl}(V_p)}$ | Spec. Creep ($V_p$ = .294) $\varepsilon'_{cl} \times 10^6$ |
|---|---|---|---|---|---|---|---|---|---|---|---|---|
| 2.1 | 4560 | 1200 | .263 | 279 | 385 | 510 | .275 | 970 | 546 | 694 | 1.27 | .45 |
| 2.2 | 4460 | 1200 | .269 | 286 | 495 | 665 | .311 | 1235 | 628 | 710 | 1.13 | .52 |
| 2.3 | 4690 | 1200 | .256 | 290 | 450 | 595 | .300 | 1152 | 584 | 675 | 1.15 | .49 |
| 4.1 | 5560 | 1200 | .216 | 270 | 440 | 570 | .284 | 1320 | 590 | 570 | .97 | .49 |
| 4.2 | 5630 | 1200 | .213 | 266 | 435 | 540 | .284 | 1268 | 559 | 562 | 1.00 | .47 |
| 5.1 | 5380 | 1200 | .223 | 261 | 475 | 635 | .294 | 1425 | 635 | 588 | .93 | .53 |
| 5.2 | 5920 | 1200 | .203 | 247 | 473 | 600 | .294 | 1480 | 600 | 535 | .89 | .50 |
| 5.3 | 5460 | 1200 | .220 | 258 | 545 | 696 | .294 | 1582 | 696 | 580 | .83 | .58 |
| 6.1 | 5230 | 1200 | .229 | 279 | 424 | 566 | .284 | 1238 | 586 | 605 | 1.03 | .49 |
| 6.2 | 5540 | 1200 | .217 | 270 | 436 | 562 | .284 | 1295 | 581 | 572 | .98 | .48 |
| 6.3 | 8420 | 1200 | .142 | 218 | 210 | 290 | .284 | 1020 | 300 | 374 | 1.24 | .25 |
| 7.1 | 3890 | 1200 | .308 | 304 | 500 | 655 | .294 | (1065) | 655 | ( 812) | (1.24) | .55 |
| 7.2 | 2790 | 1200 | .430 | 364 | 775 | 965 | .294 | (1120) | 965 | (1135) | (1.18) | .80 |
| 8.1 | 2154 | 1200 | .557 | 407 | 870 | 1010 | .294 | ( 905) | 1010 | (1470) | (1.46) | .81 |
| 8.2 | 2390 | 1200 | .502 | 387 | 932 | 1132 | .294 | (1128) | 1132 | (1325) | (1.17) | .94 |
| 8.3 | 2154 | 1200 | .557 | 406 | 736 | 976 | .294 | ( 876) | 976 | (1470) | (1.51) | .82 |

( ) Predicted value not applicable. Loading at an early age.

TABLE I-A-II CREEP

| ries | $f'_c$ psi | $\sigma$ psi | $\sigma/f'_c$ | Elastic Strain $\varepsilon_i \times 10^6$ | Observed Creep $\varepsilon_c(t) \times 10^6$ t=100 | t=365 | Paste Vol. Ratio $V_p$ | Adjusted Creep $\sigma/f'_c$=0.5 $V_p$=.294 $\varepsilon_{cl}(\sigma/f'_c)$ | $\varepsilon_{cl}(V_p)$ | Computed Creep $\varepsilon_{cl}$(comp) | $\frac{\varepsilon_{cl}(\text{comp})}{\varepsilon_{cl}(V_p)}$ | Spec. Creep ($V_p$ = .294) $\varepsilon'_{cl} \times 10^6$ |
|---|---|---|---|---|---|---|---|---|---|---|---|---|
| 9.1 | 8880 | 1200 | .135 | 198 | 165 | 290 | .334 | 1075 | 254 | 356 | 1.40 | .21 |
| 9.2 | 3430 | 1200 | .350 | 328 | 760 | 1010 | .278 | 1445 | 1068 | 924 | .87 | .89 |
| 9.3 | 3460 | 1200 | .347 | 324 | 775 | 1055 | .294 | 1520 | 1055 | 915 | .87 | .88 |
| 10.1 | 4972 | 1200 | .242 | 571 | 690 | 925 | .288 | 1912 | 943 | 638 | .68 | .79 |
| 10.2 | 4330 | 1200 | .277 | 545 | 1100 | 1405 | .453 | 2535 | 913 | 730 | .80 | .76 |
| 10.3 | 4580 | 1200 | .262 | 421 | 602 | 1030 | .444 | 1960 | 682 | 691 | 1.01 | .57 |
| 10.4 | 5400 | 1150 | .212 | 246 | 336 | 613 | .294 | 1450 | 613 | 559 | .91 | .53 |
| 12.1 | 5420 | 1200 | .222 | 258 | 560 | 808 | .294 | 1820 | 808 | 586 | .73 | .67 |
| 12.2 | 4580 | 1200 | .262 | 278 | 392 | 618 | .294 | 1180 | 618 | 691 | 1.12 | .51 |
| 13.1 | 4410 | 1200 | .272 | 286 | 427 | 672 | .294 | 1235 | 672 | 718 | 1.07 | .56 |
| 13.2 | 5380 | 1200 | .223 | 258 | 404 | 646 | .294 | 1450 | 646 | 588 | .91 | .54 |
| 13.3 | 4640 | 1200 | .258 | 278 | 383 | 585 | .294 | 1135 | 585 | 680 | 1.16 | .49 |
| 15.1 | 4734 | 900 | .190 | 430 | 248 | 404 | .301 | 1065 | 394 | 500 | 1.27 | .45 |
| 15.2 | 4198 | 900 | .214 | 384 | 550 | 730 | .504 | 1705 | 426 | 563 | 1.32 | .47 |
| 15.3 | 4854 | 900 | .185 | 375 | 319 | 510 | .454 | 1380 | 330 | 487 | 1.48 | .37 |
| 16.1 | 4125 | 900 | .218 | 222 | 158 | 275 | .294 | -- | 275 | -- | -- | -- |
| 16.2 | 4125 | 900 | .218 | 222 | 185 | 268 | .294 | -- | 268 | -- | -- | -- |
| 16.3 | 4125 | 900 | .218 | 222 | 117 | 186 | .294 | -- | 186 | -- | -- | -- |

TABLE I-A-II CREEP

| eries | $f'_c$ psi | $\sigma$ psi | $\sigma/f'_c$ | Elastic Strain $\varepsilon_i \times 10^6$ | Observed Creep $\varepsilon_c(t) \times 10^6$ t=100 | t=365 | Paste Vol. Ratio $V_p$ | Adjusted Creep $\sigma/f'_c=0.5$ $V_p=.294$ $\varepsilon_{cl}(\sigma/f'_c)$ | $\varepsilon_{cl}(V_p)$ | Computed Creep $\varepsilon_{cl}(comp)$ | $\frac{\varepsilon_{cl}(comp)}{\varepsilon_{cl}(V_p)}$ | Spec. Creep ($V_p$ = .294) $\varepsilon'_{cl} \times 10^6$ |
|---|---|---|---|---|---|---|---|---|---|---|---|---|
| 17.1 | 4365 | 900 | .206 | 228 | 348 | 405 | .284 | 984 | 419 | 544 | 1.30 | .47 |
| 17.2 | 4552 | 900 | .198 | 225 | 304 | 422 | .284 | 1065 | 437 | 522 | 1.20 | .49 |
| 17.3 | 4672 | 900 | .193 | 220 | 262 | 367 | .284 | 950 | 380 | 509 | 1.34 | .42 |
| 18.1 | 3116 | 900 | .289 | 268 | 372 | 482 | .284 | 834 | 499 | 762 | 1.53 | .56 |
| 18.2 | 3985 | 900 | .226 | 240 | 506 | 649 | .284 | 1435 | 671 | 596 | .89 | .75 |
| 18.3 | 4481 | 900 | .201 | 225 | 585 | 720 | .284 | 1790 | 745 | 530 | .71 | .83 |
| 19.1 | 6000 | 900 | .150 | 188 | 146 | 175 | .247 | 583 | 208 | 396 | 1.91 | .23 |
| 21.1 | 3250 | 900 | .277 | 260 | 367 | 467 | .287 | 844 | 478 | 730 | 1.53 | .53 |
| 21.2 | 2667 | 900 | .337 | 300 | 284 | 333 | .279 | 494 | 351 | 888 | 2.53 | .39 |
| 21.3 | 2292 | 900 | .393 | 334 | 427 | 503 | .272 | 640 | 545 | 1035 | 1.90 | .61 |
| 22.1 | 4208 | 2500 | .595 | 641 | 1170 | 1380 | .284 | 1160 | 1430 | 1570 | 1.10 | .57 |
| 22.2 | 3718 | 2500 | .672 | 685 | 950 | 1170 | .284 | 872 | 1212 | 1770 | 1.46 | .49 |
| 22.3 | 4198 | 2500 | .594 | 650 | 910 | 1078 | .284 | 906 | 1115 | 1567 | 1.40 | .45 |
| 23.1 | 4235 | 2500 | .348 | 610 | 585 | 905 | .294 | 1300 | 905 | 920 | 1.02 | .36 |

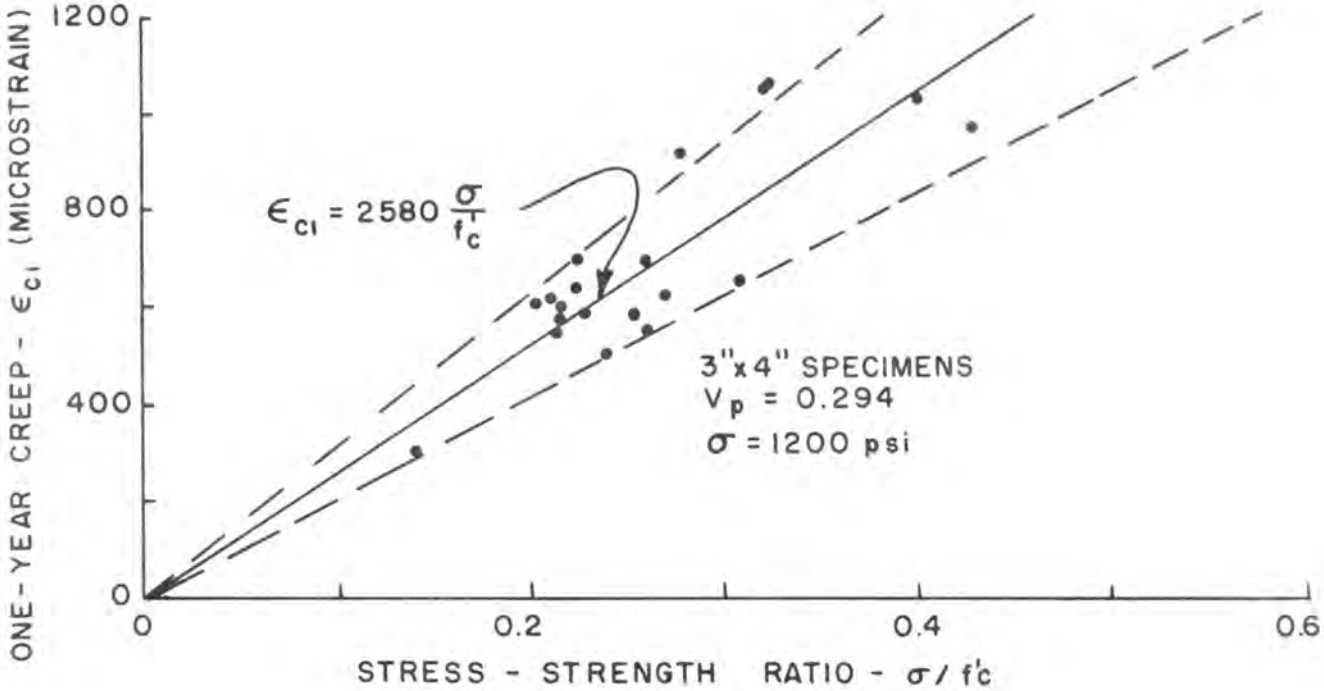


Fig. I. A-4 One-Year Creep as Function of Stress-Strength Ratio

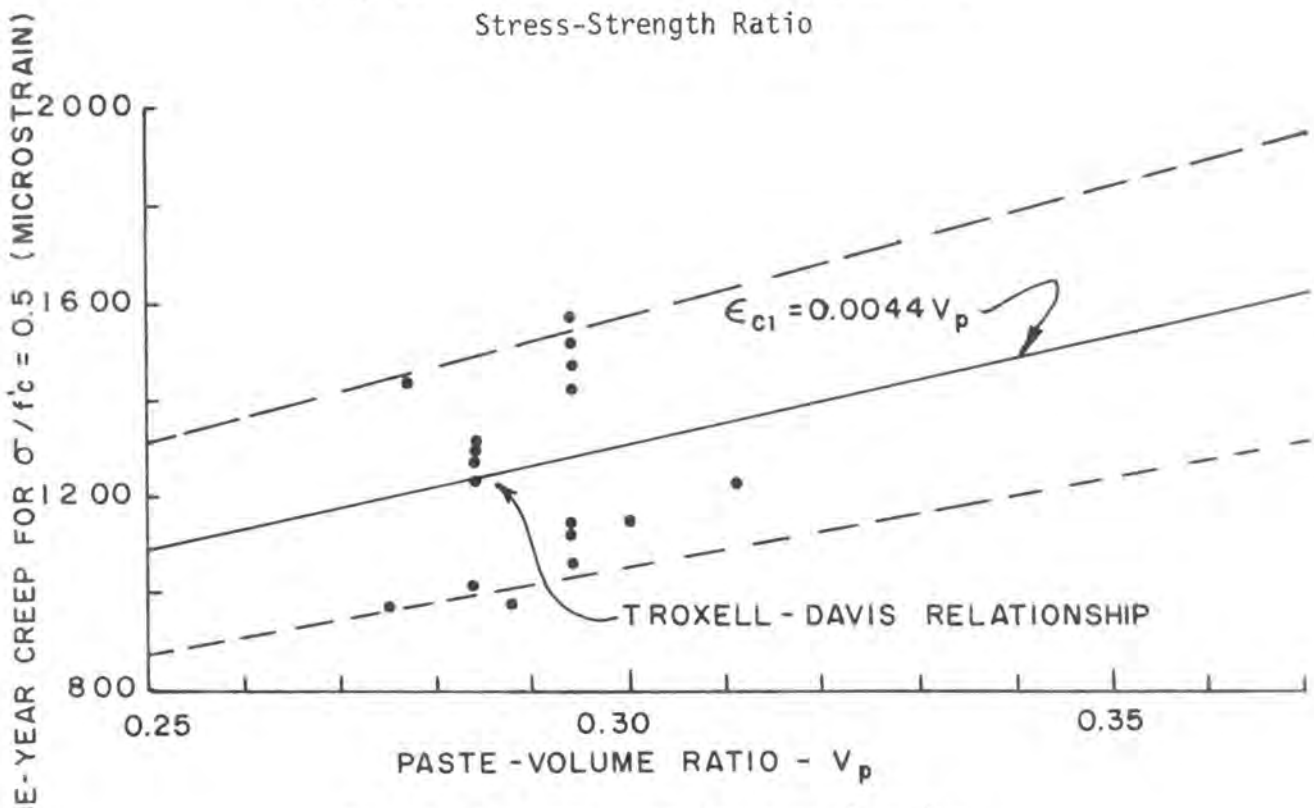


Fig. I. A-5 One-Year Creep as Function of Paste Volume Ratio

average observed creep was about 98 percent that predicted by the Troxell-Davis relationship and the coefficient of variation is about 15%.

Observed shrinkage values, computed elastic modulus, 100-day and one-year creep coefficients and computed restrained shrinkage stress potentials are shown in Table III. The shrinkage data exhibits somewhat more scatter than the creep data and appears to be more sensitive to mix constituents, especially to the type of aggregate. The observed variations may be explained, in part, by variations in elastic modulus of the aggregate and by variations in paste content. The Missouri limestone and the Wisconsin trap rock samples had about equivalent paste volume ratios and exhibited about the same shrinkage characteristics. For normal 28-day curing, both aggregates produced concrete with a 100-day shrinkage of about 200-280 micro-in/in. However, the average one year shrinkage values of 340 micro-in/in for the limestone concrete was considerably higher than the average value of 250 micro-in/in for the trap rock. This result may be due to the fact that the elastic modulus of the trap rock is considerably higher. Conversely, the type of aggregate appears to have little effect on the creep, with the possible exception for some lightweight aggregates. For normal curing and loading conditions the 365-day specific creep adjusted for a paste volume ratio of 0.294, ranged from 0.45 to 0.58 micro-in/in per psi for the standard trap rock concrete and was about 0.49 micro-in/in for the limestone concrete. Comparative values for the lightweight concretes ranged from 0.37 to 0.79 micro-in/in. but for the lower values the paste volume ratio was much greater.

Shrinkage for the lightweight aggregates was considerably higher than for the normal weight concretes. The observed 100-day shrinkage values ranged from a low of 259 to a high of 693 micro-in/in and the one-year values from 378 to 800 micro-in/in. The major portion of this increase may be explained by the effect of the lower modulus of the aggregate and by the higher paste volumes required (cf. Fig. 12). The lightweight aggregate concrete exhibiting the lowest shrinkage also had the lowest paste volume ratio.

Admixtures, whether retarders, accelerators, or plasticizers, all tend to increase shrinkage with the more pronounced effect tending to show up at the later ages. The increase of the 100-day shrinkage was

TABLE I-A-III SHRINKAGE

| Series | $f'_c$ | Paste Vol. Ratio $V_p$ | $E_c$* psix$10^{-6}$ | Creep Ratics, $C_t$ 100-day | 365-day | Shrinkage Strains $E_s$ micro-in/in 100-day | 365-day | Shrinkage Stress Potential $\sigma_{sh}$ psi 100-day | 365-day | Potential Stress Ratio |
|---|---|---|---|---|---|---|---|---|---|---|
| 2.1 | 4560 | .275 | 4.3 | 1.38 | 1.82 | 175 | 190 | 315 | 290 | .92 |
| 2.2 | 4460 | .311 | 4.2 | 1.73 | 2.33 | 228 | 249 | 351 | 315 | .90 |
| 2.3 | 4690 | .300 | 4.15 | 1.55 | 2.05 | 221 | 230 | 360 | 313 | .87 |
| 4.1 | 5560 | .284 | 4.45 | 1.63 | 2.11 | 201 | 223 | 340 | 320 | .94 |
| 4.2 | 5630 | .284 | 4.50 | 1.64 | 2.03 | 220 | - | 375 | - | - |
| 5.1 | 5380 | .294 | 4.60 | 1.82 | 2.43 | 177 | 206 | 289 | 276 | .96 |
| 5.2 | 5920 | .294 | 4.85 | 1.91 | 2.42 | 207 | 252 | 345 | 358 | 1.03 |
| 5.3 | 5460 | .294 | 4.65 | 2.11 | 2.70 | 263 | 321 | 393 | 403 | 1.03 |
| 6.1 | 5230 | .284 | 4.3 | 1.52 | 2.02 | 230 | 268 | 393 | 382 | .97 |
| 6.2 | 5540 | .284 | 4.45 | 1.61 | 2.08 | 293 | 381 | 500 | 550 | 1.10 |
| 6.3 | 8420 | .284 | 5.5 | .96 | 1.33 | 250 | 343 | 700 | 810 | 1.16 |
| 7.1 | 3890 | .294 | 3.95 | 1.64 | 2.13 | 258 | 298 | 387 | 376 | .97 |
| 7.2 | 2790 | .294 | 3.3 | 2.13 | 2.65 | 278 | 333 | 293 | 302 | 1.03 |
| 8.1 | 2154 | .294 | 2.95 | 2.14 | 2.48 | 332 | 395 | 312 | 334 | 1.07 |
| 8.2 | 2390 | .294 | 3.1 | 2.48 | 2.92 | 297 | 359 | 271 | 284 | 1.05 |
| 8.3 | 2154 | .294 | 2.95 | 1.81 | 2.40 | 273 | 317 | 286 | 275 | .96 |
| 9.1 | 8880 | .334 | 6.05 | .83 | 1.47 | 169 | 231 | 560 | 566 | 1.01 |
| 9.2 | 3430 | .278 | 3.65 | 2.32 | 3.08 | 210 | 281 | 230 | 252 | 1.09 |
| 9.3 | 3460 | .294 | 3.7 | 2.38 | 3.26 | 280 | 375 | 307 | 326 | 1.06 |

TABLE I-A-III SHRINKAGE

| Series | $f'_c$ | Paste Vol. Ratio $V_p$ | $E_c$* psix$10^{-6}$ | Creep Ratios, $C_t$ 100-day | Creep Ratios, $C_t$ 365-day | Shrinkage Strains $E_s$ micro-in/in 100-day | Shrinkage Strains $E_s$ micro-in/in 365-day | Shrinkage Stress Potential $\sigma_{sh}$ psi 100-day | Shrinkage Stress Potential $\sigma_{sh}$ psi 365-day | Potential Stress Ratio |
|---|---|---|---|---|---|---|---|---|---|---|
| 10.1 | 4972 | .288 | 2.1 | 1.21 | 1.62 | 270 | 472 | 256 | 378 | 1.48 |
| 10.2 | 4330 | .453 | 2.2 | 2.02 | 2.58 | 570 | 800 | 415 | 492 | 1.19 |
| 10.3 | 4580 | .444 | 2.85 | 1.43 | 2.44 | 343 | 470 | 402 | 390 | .97 |
| 10.4 | 5400 | .294 | 4.65 | 1.36 | 2.47 | 162 | 241 | 319 | 323 | 1.01 |
| 12.1 | 5420 | .294 | 4.65 | 2.17 | 3.12 | 298 | 393 | 438 | 444 | 1.01 |
| 12.2 | 4580 | .294 | 4.3 | 1.41 | 2.22 | 273 | 373 | 487 | 498 | 1.02 |
| 13.1 | 4410 | .294 | 4.2 | 1.49 | 2.35 | 244 | 329 | 412 | 412 | 1.00 |
| 13.2 | 5380 | .294 | 4.65 | 1.57 | 2.51 | 246 | 333 | 445 | 442 | .99 |
| 13.3 | 4640 | .294 | 4.3 | 1.38 | 2.10 | 270 | 382 | 487 | 530 | 1.09 |
| 15.1 | 4734 | .301 | 2.1 | .58 | .94 | 259 | 378 | 346 | 409 | 1.18 |
| 15.2 | 4198 | .504 | 2.35 | 1.43 | 1.90 | 693 | - | 670 | - | - |
| 15.3 | 4854 | .454 | 2.4 | .85 | 1.36 | 507 | 692 | 657 | 702 | 1.07 |
| 16.1 | 4125 | .294 | 4.05 | - | - | 207 | 288 | - | - | - |
| 16.2 | 4125 | .294 | 4.05 | - | - | 177 | 225 | - | - | - |
| 16.3 | 4125 | .294 | 4.05 | - | - | 140 | 160 | - | - | - |
| 17.1 | 4365 | .284 | 3.95 | 1.53 | 1.78 | 307 | 375 | 480 | 532 | 1.10 |
| 17.2 | 4552 | .284 | 4.0 | 1.35 | 1.88 | 359 | 437 | 611 | 607 | 1.00 |
| 17.3 | 4672 | .284 | 4.1 | 1.19 | 1.67 | 307 | 435 | 574 | 668 | 1.16 |

TABLE I-A-III SHRINKAGE

| Series | $f'_c$ | Paste Vol. Ratio $V_p$ | $E_c$* psix$10^{-6}$ | Creep Ratios, $C_t$ 100-day | 365-day | Shrinkage Strains $E_s$ micro-in/in 100-day | 365-day | Shrinkage Stress Potential $\sigma_{sh}$ psi 100-day | 365-day | Potential Stress Ratio |
|---|---|---|---|---|---|---|---|---|---|---|
| 18.1 | 3116 | .284 | 3.35 | 1.39 | 1.80 | 289 | 339 | 408 | 456 | 1.11 |
| 18.2 | 3985 | .284 | 3.75 | 2.10 | 2.70 | 292 | 382 | 354 | 377 | 1.06 |
| 18.3 | 4481 | .284 | 4.0 | 2.60 | 3.20 | 297 | 357 | 330 | 340 | 1.03 |
| 19.1 | 6000 | .247 | 4.8 | .75 | .93 | 205 | 257 | 562 | 640 | 1.14 |
| 21.1 | 3250 | .287 | 3.45 | 1.41 | 1.79 | 157 | 170 | 225 | 210 | .94 |
| 21.2 | 2667 | .279 | 3.0 | .95 | 1.11 | 162 | 189 | 249 | 268 | 1.08 |
| 21.3 | 2292 | .272 | 2.7 | 1.28 | 1.51 | 177 | 231 | 210 | 248 | 1.18 |
| 22.1 | 4208 | .284 | 3.9 | 1.83 | 2.16 | 233 | 340 | 321 | 419 | 1.30 |
| 22.2 | 3718 | .284 | 3.65 | 1.39 | 1.71 | 247 | 330 | 378 | 444 | 1.18 |
| 22.3 | 4198 | .284 | 3.85 | 1.40 | 1.66 | 245 | 347 | 392 | 500 | 1.28 |
| 23.1 | 4235 | .294 | 4.1 | .96 | 1.48 | 239 | 358 | 512 | 572 | 1.12 |

*Computed $E_c$ based on ACI code formula $E_c = 33\sqrt{W^3 f'_c}$

only about ten percent. The average 365-day shrinkage increase was about 40 percent. Air entrainment on the other hand reduced shrinkage by about twenty percent. This reduction may have been due to a decrease in water requirements for the same workability. The effect of admixtures on creep was similar, the average increase in specific creep being about eight percent. The data for the effect on creep of air entrainment was very scattered and no specific trend could be established. A wide variety of admixtures are available on the market and based on present information their effect on creep and shrinkage properties can not be readily predicted. The effect of any particular product, therefore, should be established by test under environmental and loading conditions corresponding to the application contemplated.

Curing appears to play a major role in the shrinkage behavior of concrete. The companion specimens for the specimens loaded at an early age (2-7 days) as well as the specimens cured in air exhibited about forty percent greater shrinkage. The effect on specific creep was even more dramatic. The adjusted specific creep increased to 0.88 micro-in/in per psi for the air cured specimens and to 0.94 micro-in/in per psi for the early loaded specimens. This increase, of course, reflects the lower strength for these concretes. The effect of age at time of loading for the latter as well as the effect of delay in loading until after shrinkage (preshrunk specimens) was quite consistent with the observed behavior in subsequent studies (cf. Fig. 27).

The ratio of the mass factor (volume to surface ratio) between the 4 in. x 4 in. specimens and the 3 in. x 4 in. specimens was only 1.17. While the mass factor is known to have some influence on both creep and shrinkage, this ratio was too small to detect any significant trends. Some small variations in observed creep and shrinkage undoubtedly are attributable to this effect.

Most of the specimens were loaded in a controlled environment of fifty percent relative humidity and a constant temperature of 72°F. The 17-series were loaded in the laboratory without any temperature or humidity control. These specimens exhibited about twenty-five percent more shrinkage. The specific creep, however, was about the same or slightly less.

Some researchers have attempted to correlate creep and shrinkage

characteristics with the water cement ratio and with the paste-aggregate ratio (weight of paste/weight of aggregate) or the cement paste content (weight of paste/total weight). No significant trends could be established in these studies. In fact, there seemed to be rather large variations in compressive strength for the same water-cement ratio. It appears therefore that the paste-volume ratio and the paste-strength characteristics as reflected in the compressive strength provide more significant reference parameters. Elastic modulus also appears to be a significant parameter. Unfortunately, measured values were not reported for all series and only computed values based on strength and weight could be used in analyzing the data.

The Series 16 specimens were used to study the restraining effect of reinforcement. As expected both shrinkage and creep were markedly reduced. The observed reduction in shrinkage was consistent with the percentage of reinforcement in the specimens, as may be seen in Table IV-a. Computed values in the table were obtained by the effective modulus method. Since no companion unreinforced specimens were included in this series, the elastic, creep and shrinkage properties of the standard mix (Series 5.3) were used for the calculated values in Table IV. The predicted shrinkage of the reinforced specimens was computed by multiplying the shrinkage of the reference mix by the ratio of the net concrete area to the effective transformed area after creep, thus:

$$\varepsilon_{rs} = \frac{1-\rho}{1+(\eta_e-1)\rho}\,\varepsilon_s$$

where:

$\varepsilon_{rs}$ = the shrinkage of the reinforced specimen

$\rho$ = the reinforcement ratio

$\eta_e$ = the effective modular ratio = $(C+1)\eta$

$\varepsilon_s$ = the shrinkage of the plain concrete specimen.

It may be noted that the agreement between predicted and observed shrinkage strains is well within the range of experimental error.

Predicted and observed creep strains are compared in Table IV-6. The creep values do not agree as well as the shrinkage values. There appears to have been an error in the observed value for the 100-day creep of the specimen with a reinforcement ratio of 1.25 percent since the value reported was less than that for the specimen with 2.75 percent reinforcement. Predicted creep strains were calculated using the

TABLE I-A-IV

Time-Dependent Strains in Reinforced Concrete

a. Shrinkage Strains

| | 100-day Shrinkage | | | 365-day Shrinkage | | |
|---|---|---|---|---|---|---|
| ρ% | $\varepsilon_{rs}$(comp) x $10^6$ | $\varepsilon_{rs}$(obs) x $10^6$ | $\frac{\varepsilon_{rs}(comp)}{\varepsilon_{rs}(obs)}$ | $\varepsilon_{rs}$(comp) x $10^6$ | $\varepsilon_{rs}$(obs) x $10^6$ | $\frac{\varepsilon_{rs}(comp)}{\varepsilon_{rs}(obs)}$ |
| 1.25 | 211 | 207 | 1.02 | 249 | 288 | .86 |
| 2.75 | 170 | 177 | .96 | 194 | 225 | .86 |
| 4.96 | 131 | 140 | .93 | 146 | 160 | .91 |

b. Creep Strains

| | 100-day Creep | | | 365-day Creep | | |
|---|---|---|---|---|---|---|
| ρ% | $\varepsilon_{cr}$(comp) x $10^6$ | $\varepsilon_{cr}$(obs) x $10^6$ | $\frac{\varepsilon_{cr}(comp)}{\varepsilon_{cr}(obs)}$ | $\varepsilon_{cr}$(comp) x $10^6$ | $\varepsilon_{cr}$(obs) x $10^6$ | $\frac{\varepsilon_{cr}(comp)}{\varepsilon_{cr}(obs)}$ |
| 1.25 | 308 | 158 | 1.95 | 380 | 275 | 1.38 |
| 2.75 | 231 | 185 | 1.25 | 276 | 268 | 1.03 |
| 4.96 | 161 | 117 | 1.37 | 187 | 186 | 1.00 |

c. Combined Creep and Shrirkage

| | 100-day Creep plus Shrinkage | | | 365-day Creep plus Shrinkage | | |
|---|---|---|---|---|---|---|
| ρ% | $\varepsilon_{rcs}$(comp) x $10^6$ | $\varepsilon_{rcs}$(obs) x $10^6$ | $\frac{\varepsilon_{rcs}(comp)}{\varepsilon_{rcs}(obs)}$ | $\varepsilon_{rcs}$(comp) x $10^6$ | $\varepsilon_{rcs}$(obs) x $10^6$ | $\frac{\varepsilon_{rcs}(comp)}{\varepsilon_{rcs}(obs)}$ |
| 1.25 | 519 | 365 | 1.42 | 629 | 563 | 1.12 |
| 2.75 | 401 | 362 | 1.11 | 470 | 493 | .95 |
| 4.96 | 292 | 257 | 1.14 | 333 | 346 | .96 |

effective transformed area method by subtracting the predicted initial or elastic strains from the predicted combined elastic and creep strains. Thus:

$$\varepsilon_{cr} = \varepsilon_{rc} + \varepsilon_i = \frac{\sigma}{E_c} \quad \frac{C_t+1}{1+(\eta_e-1)\rho} - \frac{1}{1+(\eta-1)\rho}$$

where:

$\varepsilon_{cr}$ = the creep of the reinforced specimen

$\varepsilon_i$ = the elastic strain

$\varepsilon_{rc}$ = the elastic plus creep strain

$C_t$ = the creep ratio

Predicted combined creep and shrinkage strains are compared with observed values in Table IV-c. As is to be expected, the agreement here is much better than for creep alone. Since the experimental values for creep were obtained by subtracting the shrinkage on a companion specimen from the total measured strain, the probability of experimental error was doubled. Except for the Series 16.1 specimen, the agreement between predicted and observed values is remarkably good and probably would have been better if exact properties of the concrete in the Series 16 mix had been determined by test.

The data from the Series 19 and 20 specimens demonstrated the interdependence between creep and shrinkage. The effect of maturity upon creep was therefore studied in a subsequent test program [7].

Creep and Shrinkage Prediction Formulas

Several of the standard prediction formulas were tested. Generally the hyperbolic forms suggested by Lorman and Ross (Eq.'s 9 and 11) were found to be most convenient. These equations tend to predict an excessive leveling off of creep strains after one year. Their main advantage is that they can be written in linear form (Eq. 10) thus permitting a ready evaluation of the terminal values. Since very little creep and shrinkage data was collected for periods in excess of two years these equations yielded reasonable predictions within that time period except for creep at early ages. Subsequent studies by Meyers and Branson (61) have shown that an improved prediction of creep can be obtained by modifying the time factor in the hyperbolic equation suggested by Lorman, thus:

$$\varepsilon_c = \frac{t^{0.60}}{t_c + t^{0.60}} \varepsilon_{cu} \tag{32}$$

This form seems to give a much better fit at early ages and also is in reasonable agreement with the continued increase after one year observed by Troxell, Raphael, and Davis (49). Meyers and Branson suggested a value of 10.5 for the coefficient $t_c$. For this value the predicted ultimate creep would be about 1.33 times the one-year creep. This is in reasonable agreement with the 36 percent increase after thirty years reported by Troxell, Raphael, and Davis. With this value for $t_c$, the predicted ratio between the 365-day and the 100-day creep would be 1.25. For most of the applicable data in this program, this ratio ranges from about 1.21 to 1.41 with an average value of 1.29 and a standard variation of 0.05. Thus based on this data alone, a value of 11.5 would be recommended for the coefficient $t_c$.

Meyer's studies [4] of the shrinkage data have indicated that Lorman's equation (Eq. 9) is most suitable and that it can be used to predict ultimate shrinkage from 60-day test data with a coefficient of variation of 15 percent.

These studies were by themselves not sufficiently extensive to permit the development of prediction formulas based solely on a knowledge of concrete constituents, member geometry and environment. They did lead to the subsequent studies by Chai (7), Bayazid (8) and Hollrah (6,62) which yielded further information of the influence of such factors as age at time of loading, effect of repeated loads, stress distribution and specimen geometry as well as the effect of varying mix proportions.

## Conclusions

This study demonstrated that empirical interpretation of phenomenological studies is very difficult due to the complex interaction of the variables affecting creep and shrinkage. Nevertheless such data is invaluable as a check on theoretically developed formulas. The assumption of superposition of creep and shrinkage introduces both theoretical and experimental problems. In spite of these limitations the data obtained proved to be adequate to confirm general trends and to demonstrate that, under controlled conditions, creep and shrinkage can be predicted with sufficient accuracy to satisfy normal design requirements.

# APPENDIX I-B

# RHEOLOGICAL MODELS

## RHEOLOGICAL MODELS*

Some of the rheological models which have been suggested by other researchers are briefly reviewed below. The purpose of this review is to present the reader with examples of the types of models which have been proposed. A critical analysis of the merits of each model is not included herein. For additional information regarding the composition or equations, the reader is referred to a more extensive analysis of some of the models by Desayi and Sen (20)*, and to the particular papers in which these models were introduced.

In 1933, Bingham and Reiner (1) presented a study of the rheological properties of cement and concrete. In 1948, Burgers (2) suggested a model which was named after him, consisting of a Maxwell and Kelvin body in series as shown in Fig. I. B.1. The Maxwell body was to represent the elastic deformation and the irrecoverable creep permanent set, and the Kelvin body represented the delayed recovery.

In 1949 and 1950, Freudenthal and Reiner (3, 4, 5) considered concrete to be a visco-elastic material in their studies, however they did not suggest any new models, but rather studied the visco-elastic properties of the material. In 1950, Flugge (6) took creep data from tests of Glanville, R. Davis, and H. Davis and derived coefficients of the elements of a mechanical model which were suggested for explaining the creep behavior of concrete. This model is shown in Fig. I. B.2.

Reiner, in his book on building materials, gives a model suggested by Torroja and Paez (7). The elementary and complete rheological models are shown in Fig's I. B.3, and I. B.4. In these models, a new element was introduced named after Paez, consisting of a spring sliding against the friction of the walls of a cylinder. This element was also used in a model recommended by Ross (8,9). In his model, Ross suggested that the failure mechanism of the member also be included. If the load on

---

*This study was made by Mr. Ronald L. Hollrah as a part of his research for a doctoral dissertation. The references cited are listed at the end of this appendix.

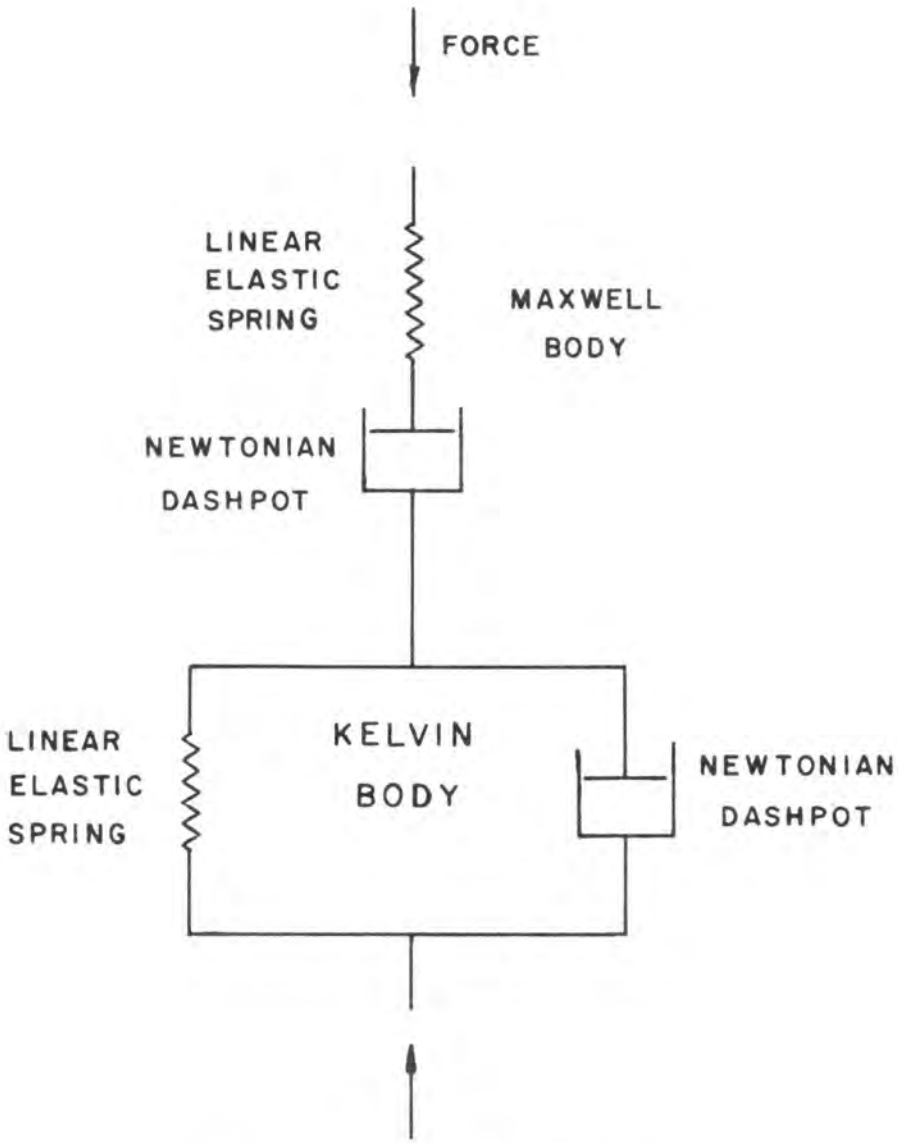


FIG. I. B.1 THE BURGERS BODY

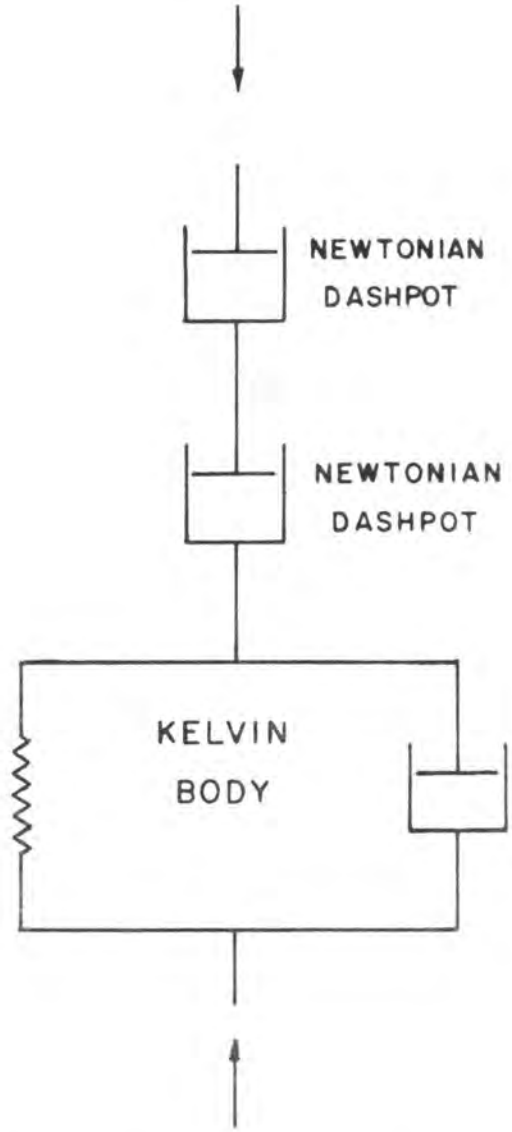


FIG. I. B.2 MODEL SUGGESTED BY FLUGGE

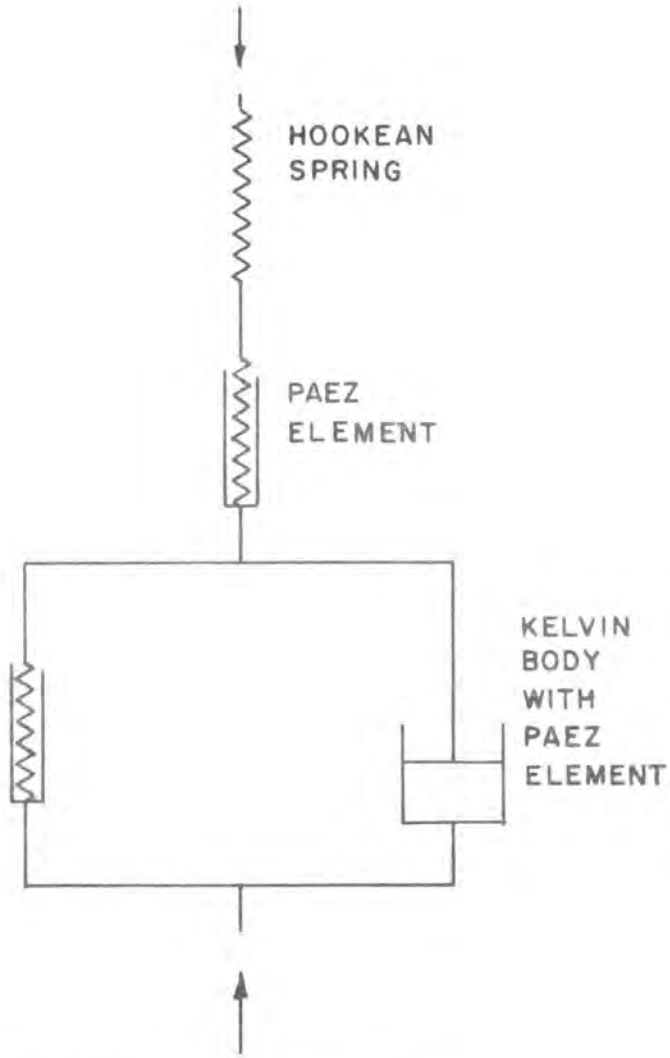


FIG. I. B.3 ELEMENTARY MODEL, TORROJA AND PAEZ (ALSO ROSS)

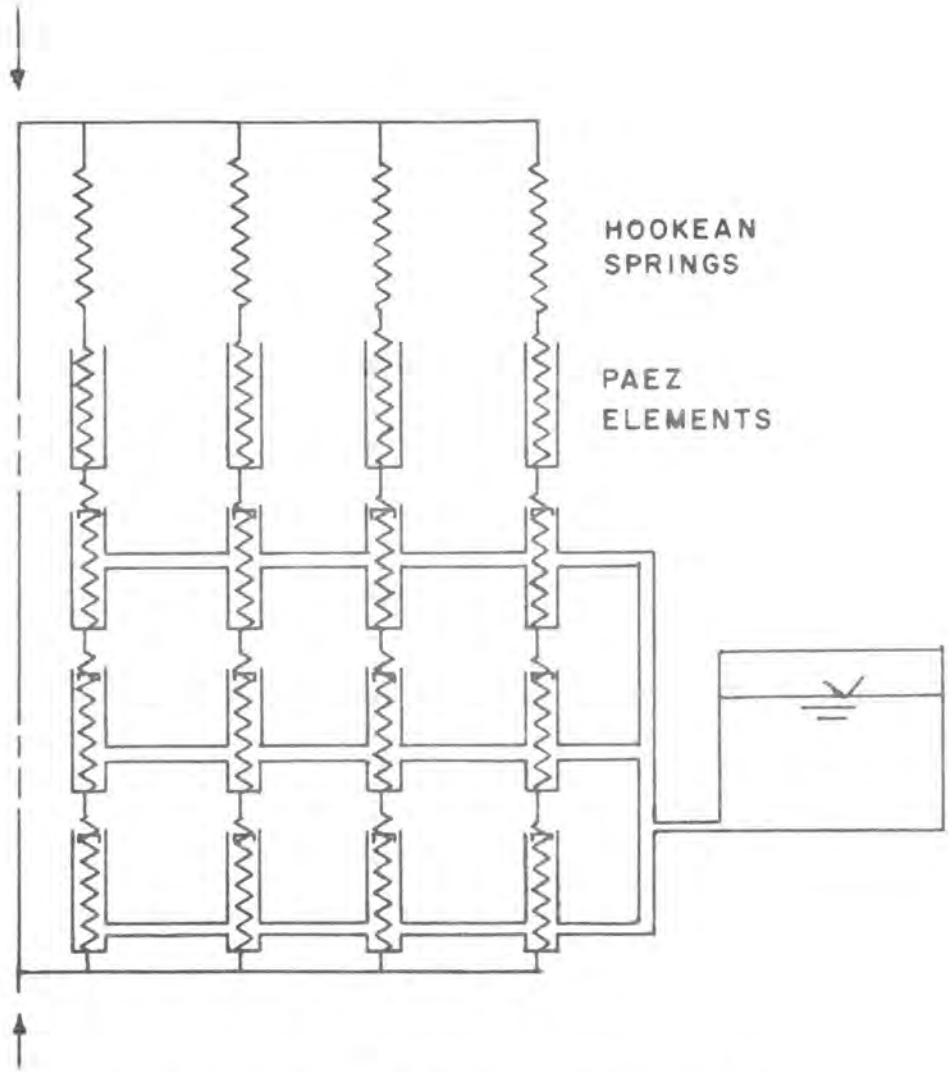


FIG. I. B.4 COMPLETE MODEL, TORROJA AND PAEZ

the member is increased sufficiently, the frictional resistance of the entire spring is overcome, so that the spring is pushed into the casing.

In 1955, Chang (10,11) used a non-linear Maxwell model for the prediction of the rheological behavior of concrete from its sonic properties. This model is shown in Fig. I. B.5. In this model, the spring is stress softening, and the dash pot is time thickening. Softening of spring is inversely proportional to the stress, and the dash pot fluid thickens as an exponential function of time.

In 1958, Freudenthal and Roll (12) suggested a mechanical model consisting of four elements, each representing a specific type of creep response which contributes to the total creep. From this model, equations were derived to predict creep at different stress levels. This model is shown in Fig. I. B.6. The parts of the model and the creep response which they represent are as follows:

1. Maxwell element coupled in series, to represent the long time visco-elastic response in shear resulting in irrecoverable creep.
2. A Kelvin element to represent the visco-elastic interaction in shear of the solid and fluid phases resulting in recoverable creep or delayed elasticity.
3. A Kelvin element, non-linear with respect to force to represent the short time "consolidation" effects of irrecoverable pore water motion (seepage).
4. A Kelvin element, non-linear with respect to force, to represent the irrecoverable deformation due to initial internal, partially destructive readjustments within the granular mass of the concrete.

Hansen (13), in 1958, suggested two models for concrete studies (Fig. I. B.7 and I. B.8). In Fig. I. B.7, the different elements of the model are supposed to represent the different components of concrete, viz. aggregate, solid component of cement paste, and voids. The simplified model of Fig. I. B.8 does not include an element for representing the instantaneous elastic deformation.

In a study of the rheological behavior of cement paste, Glucklich (4), in 1959, suggested three models based on two theories proposed by

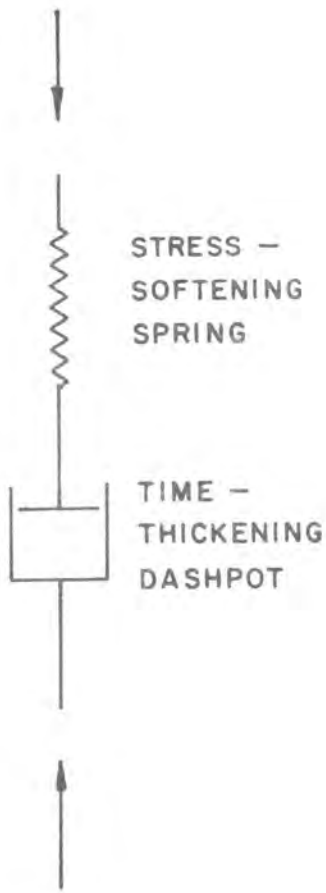


FIG. I. B.5. NON-LINEAR MAXWELL MODEL SUGGESTED BY CHANG

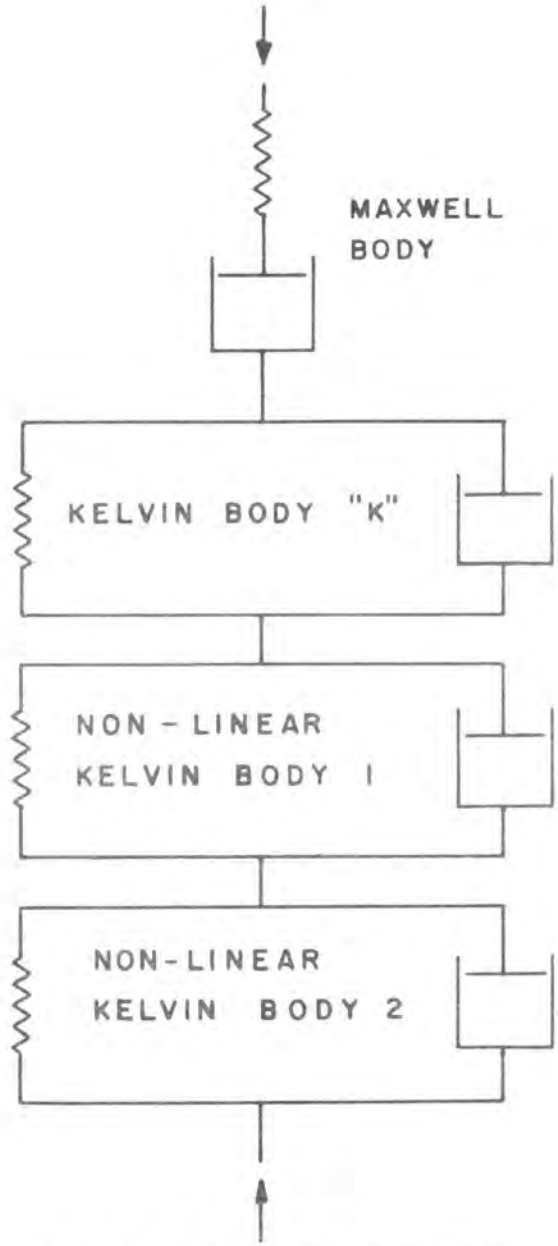


FIG. 1. B.6. MODEL SUGGESTED BY FREUDENTHAL AND ROLL

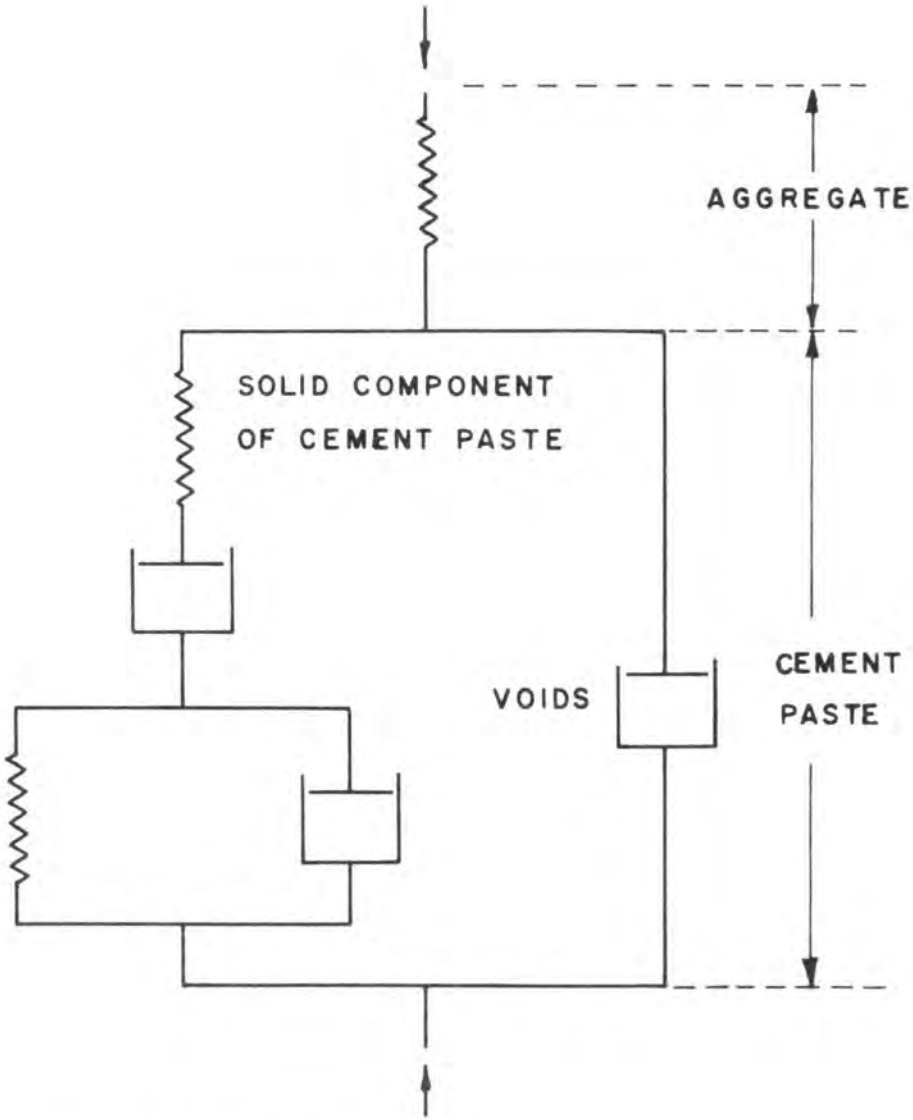


FIG. I. B.7 MODEL SUGGESTED BY HANSEN

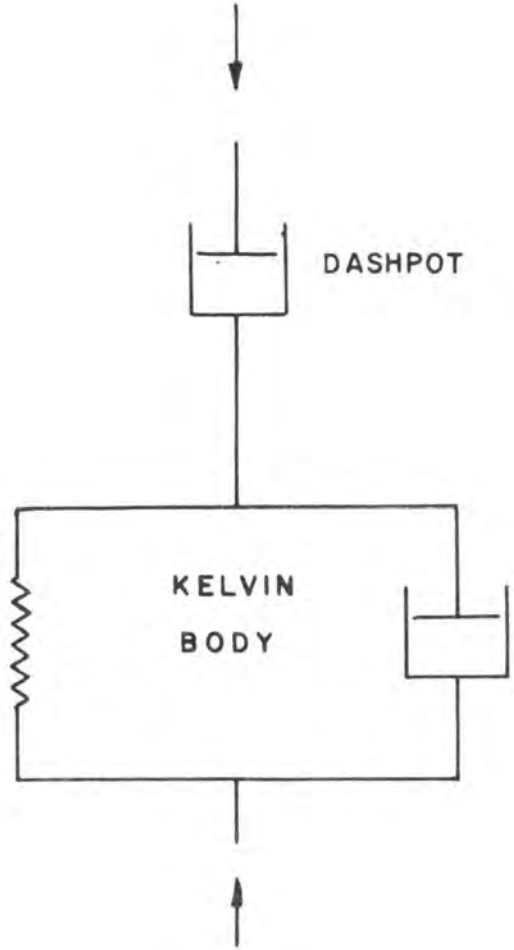


FIG. I. B.8 SIMPLIFIED MODEL
SUGGESTED BY HANSEN

him. These models are shown in Fig. I. B.9(a), I. B.9(b), and I. B.10. In his first theory, Glucklich assumed that creep was composed of two types of deformation, primary and secondary creep, such that total creep = primary creep + secondary creep as shown in Fig. I. B.11.

The primary creep can be represented by a Kelvin element. The retardation time of this element was found to be about 20 weeks. The complete model representation of the material according to this theory is illustrated in Fig. I. B.9(a). Glucklich stated that the theory can be reconciled with accepted theories of internal structure of the material by interpreting the reversible delayed deformation as linked with flow of water within completely saturated zones, and the non-reversible creep as a reflection of the flow of water into under-saturated zones which is made nonreversible by virtue of capillary forces and the surface tension of the water. If the model is visualized as in Fig. I. B.9(b) rather than I. B.9(a), the model explains the well-known dependence of secondary creep on submergence in water, and also the effect of shrinkage on creep.

Glucklich proposed his second theory because the experimental results of his studies indicated that the secondary creep depends also on deformation and not only on load. This would suggest that this creep is part of a deformation such as that of a Kelvin body. Thus, Glucklich suggested that secondary creep is the nonreversible part of a deformation of a nonperfect Kelvin body in the same sense that permanent set is the nonreversible part of the deformation of a nonperfect Hooke body. In fact he recommended that we could name the secondary creep "delayed permanent set", and could represent the behavior of the material by means of a model shown in Fig. I. B.10.

In Fig. I. B.9(b) and I. B.10, a new element is introduced by Glucklich. This element represents the permanent set of the material. The Hooke spring contains elements in series which transmit force by friction. These elements of the spring represent a spectrum of coefficients of friction. When a load is applied, the spring undergoes a deformation. Permanent deformation occurs through slippage of the elements whose frictional resistance are lower than the applied load. The proportionality between permanent set and load is a result of the number of elements which slip for any given load.

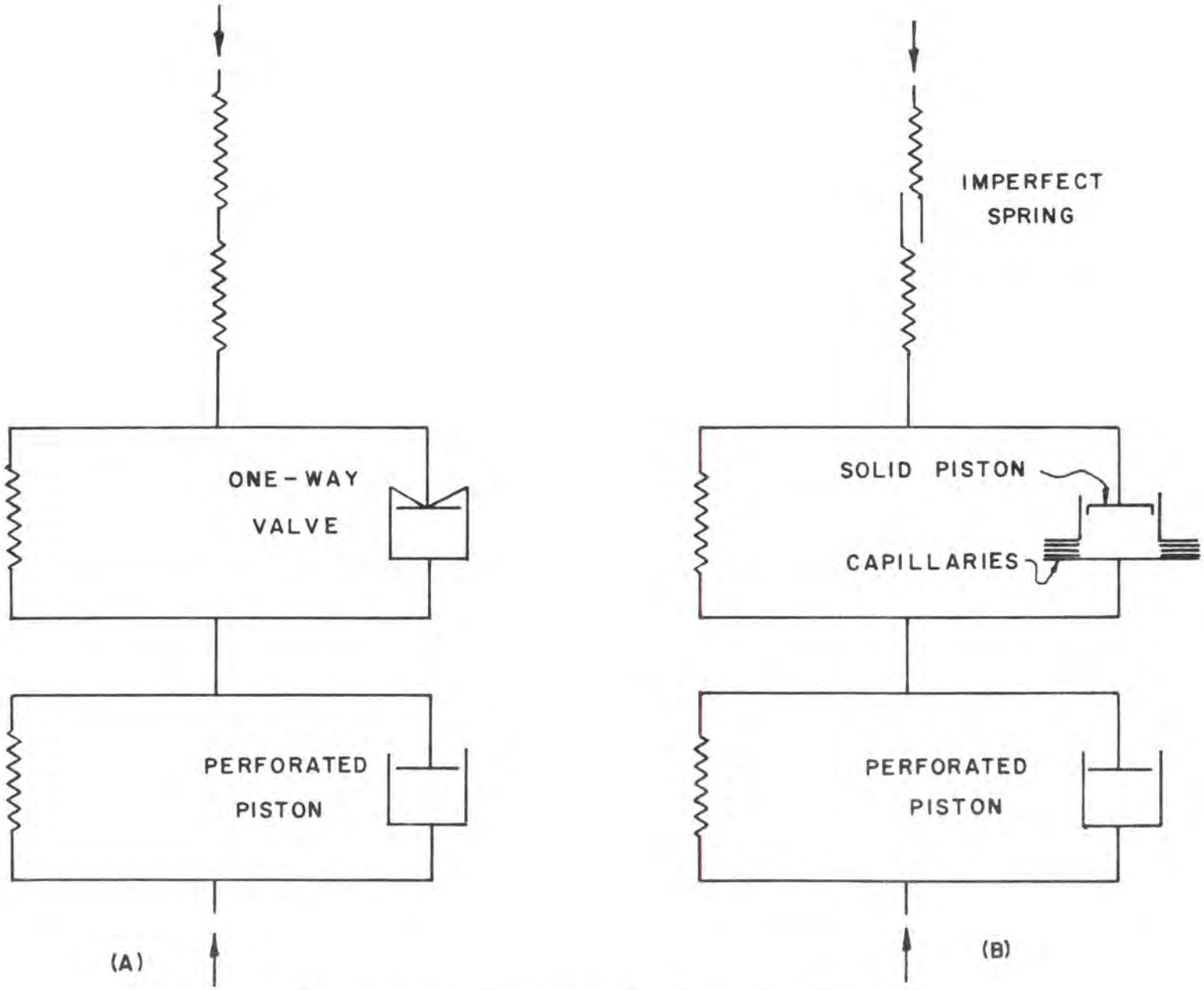


FIG. I. B.9 MODELS BY GLUCKLICH (FIRST THEORY)

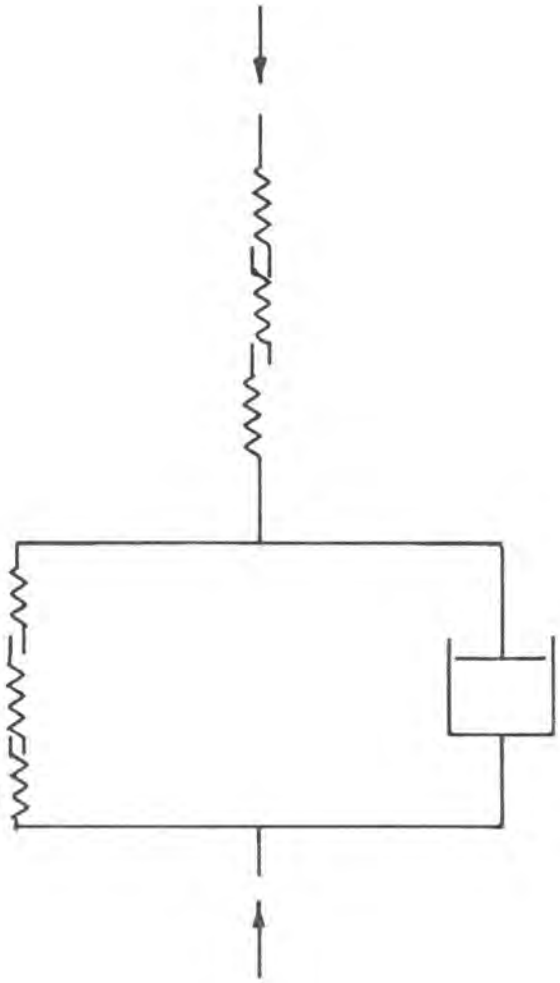

FIG. I. B.10 MODEL BY GLUCKLICH (SECOND THEORY)

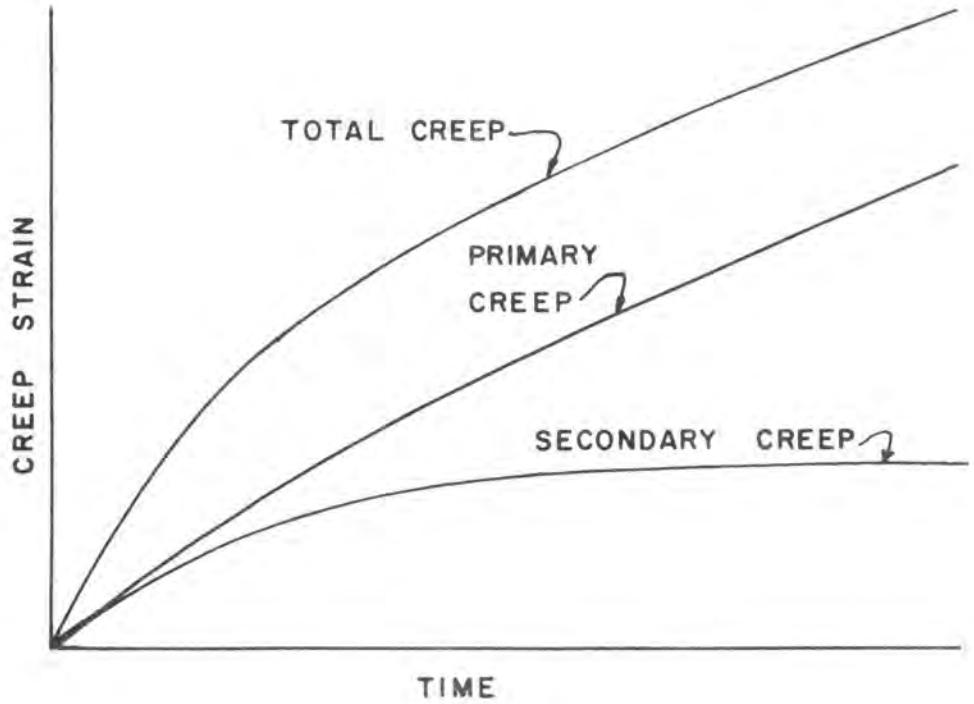


FIG. I. B.11 CREEP STRAIN-TIME CURVE (GLUCKLICH)

In 1960, Constantinescu-Catunesti (15) proposed a model for concrete studies shown in Fig. I. B.12. In this model a Paez-element was used in series with a Burgers body.

In 1961, Glucklich and Ishai (16) proposed a model consisting of five elements for the mechanism of creep in cement paste and determined experimentally the different parameters involved. This model is shown in Fig. I. B.13. In this model, "H" represent the entire instantaneous linear elastic response. The other four elements represent time deformation. $K_1$ and $K_2$ are Kelvin elements which represent the reversible creep (actually delayed elasticity). It was found that the two Kelvin elements were needed due to the two involved distinct retardation time factors. $\overline{K}$ represents the nonreversible creep. This element is rendered nonreversible by means of capillary tubes producing a head exceeding the maximum possible force in the parallel spring. The authors stated that the nonreversibility of this component is due to the following processes: (a) Water diverted from saturated to under-saturated zones is firmly bound there by the high adhesion forces, augmented by the enormous surface of the gel structure; (b) Water expelled to the atmosphere under external load, or evaporated due to a gradient of humidity between specimens and atmosphere, is not recovered on removal of the load. This precludes the restoration of the material to its original shape as meniscuses are formed at the free ends of the channels; (c) Water displaced by the external load takes part in increased hydration, i.e., in a nonreversible chemical reaction, as new ionic balances are formed. $\overline{\overline{K}}$ represents two kinds of deformation: (a) the cracking or delayed permanent set; and (b) a component of delayed elasticity in addition to $K_1$ and $K_2$.

In 1962, Glucklich and Ishai (17) proposed another model for the creep study of cement mortar on the basis of the rheological behavior of a porous elastic body with liquid in its voids. This model is shown in Fig. I. B.14. The model which they proposed was designed to represent the following behavioral response. When an external load is applied to a porous water-containing body, a certain state of stress is produced at every point of the material. Pressure differences will be found between various parts of the specimen, which will induce a slow movement of water

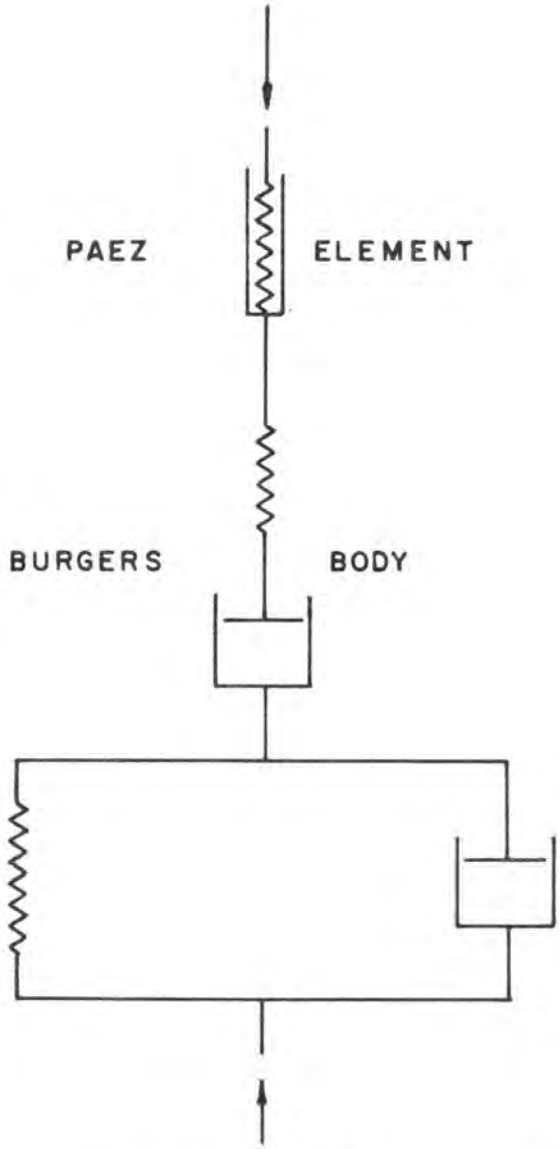


FIG. I. B.12 MODEL PROPOSED BY CONSTANTINESCU-CATUNESTI

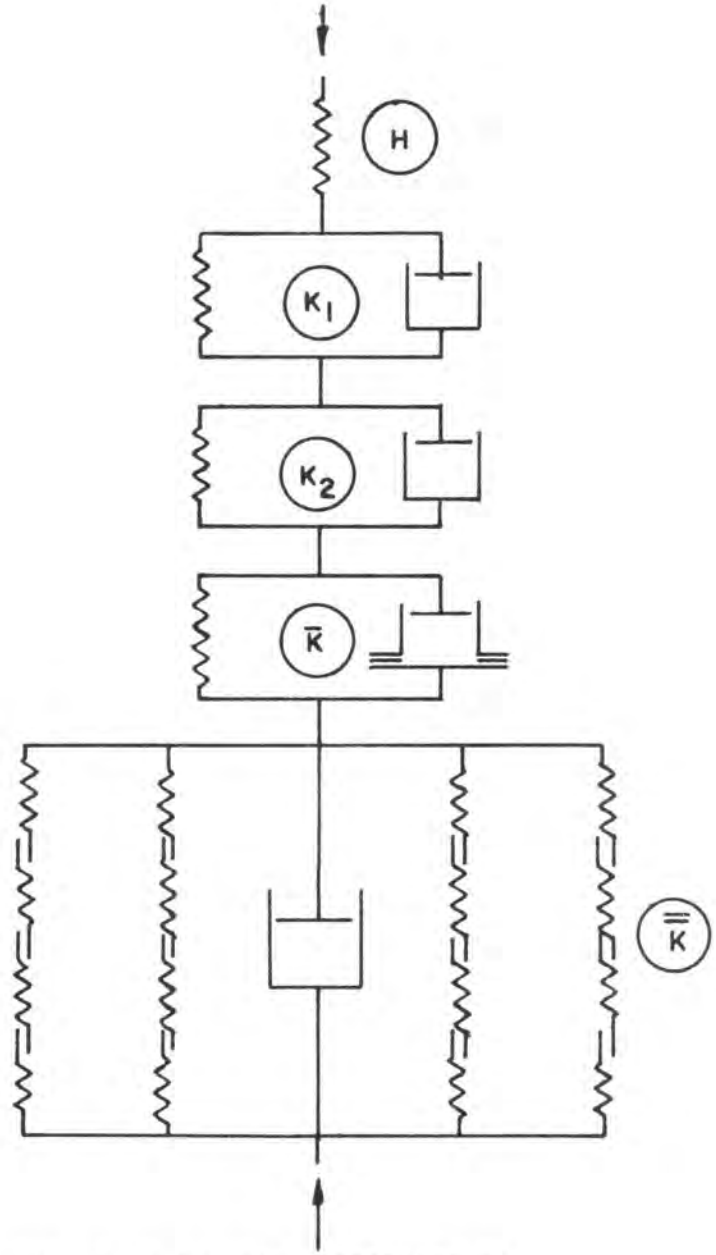


FIG. I. B.13 MODEL PROPOSED BY GLUCKLICH AND ISHAI

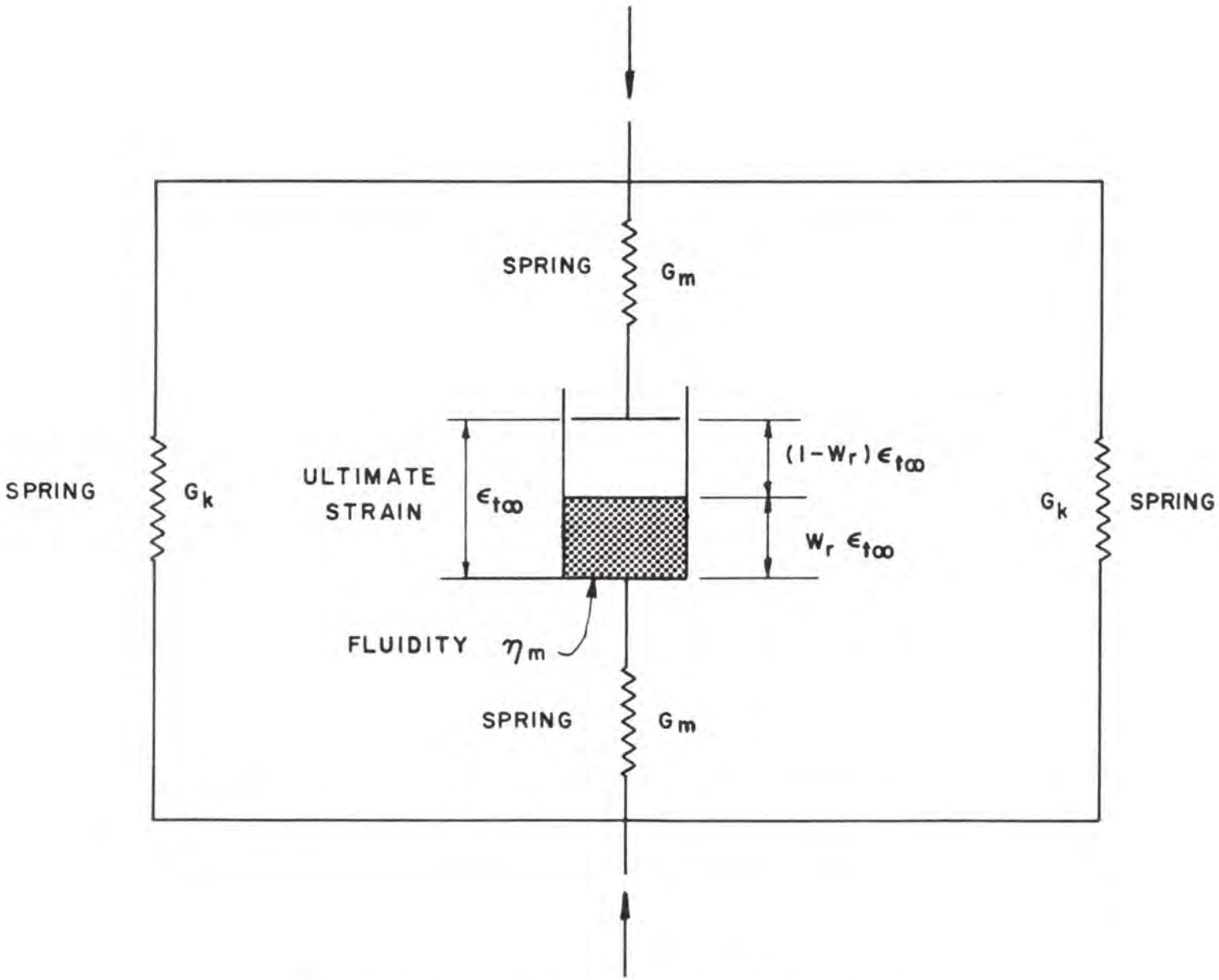


FIG. I. B.14 ANOTHER MODEL BY GLUCKLICH AND ISHAI

within the body, in accordance with the overall state of stress. The rate of this flow depends on the diameter of the voids and on the forces of adhesion between the liquid and walls of the solid.

For the model shown in Fig. I. B.14, the model constants are:

$G_m$, $G_k$, spring constants

$W_r$ = ratio of evaporable water retained during test to evaporable water content at saturation

$\eta_m$ = fluidity

$\varepsilon_{t\infty}$ = strain (at $t = \infty$)

The general tendency of the loaded body would be to change its shape elastically from the initial unloaded state to the final under load if all its voids were empty. This state would be reached by a water containing body only in a theoretically infinite time, given the whole flow process is exponential. Nevertheless, the movement will tend to a finite assymptote corresponding to the deformation of an identical elastic body with empty voids.

More recently (1962), Hansen (18, 19) has given two rheological models to represent the deformational behavior of prestressed concrete. These are shown in Fig.'s I. B.15 and I. B.16.

In 1966, Desayi and Sen (20) proposed the use of a nonlinear Maxwell model similar to the one proposed by Chang (Fig. I. B.5). This model is shown in Fig. I. B.17. The primary difference between the model of Chang and the model of Desayi and Sen is the manner in which the spring constant is related to the stress. In the model of Desayi and Sen, $E = E_0/\sigma^m$, whereas Chang assumes that $E = E_0/\sigma$.

Most of the rheological models suggested to date are based on the authors' hypothesis of the mechanism of creep. While each model appears to fit a particular set of data, no model has yet been suggested which is satisfactory under all conditions.

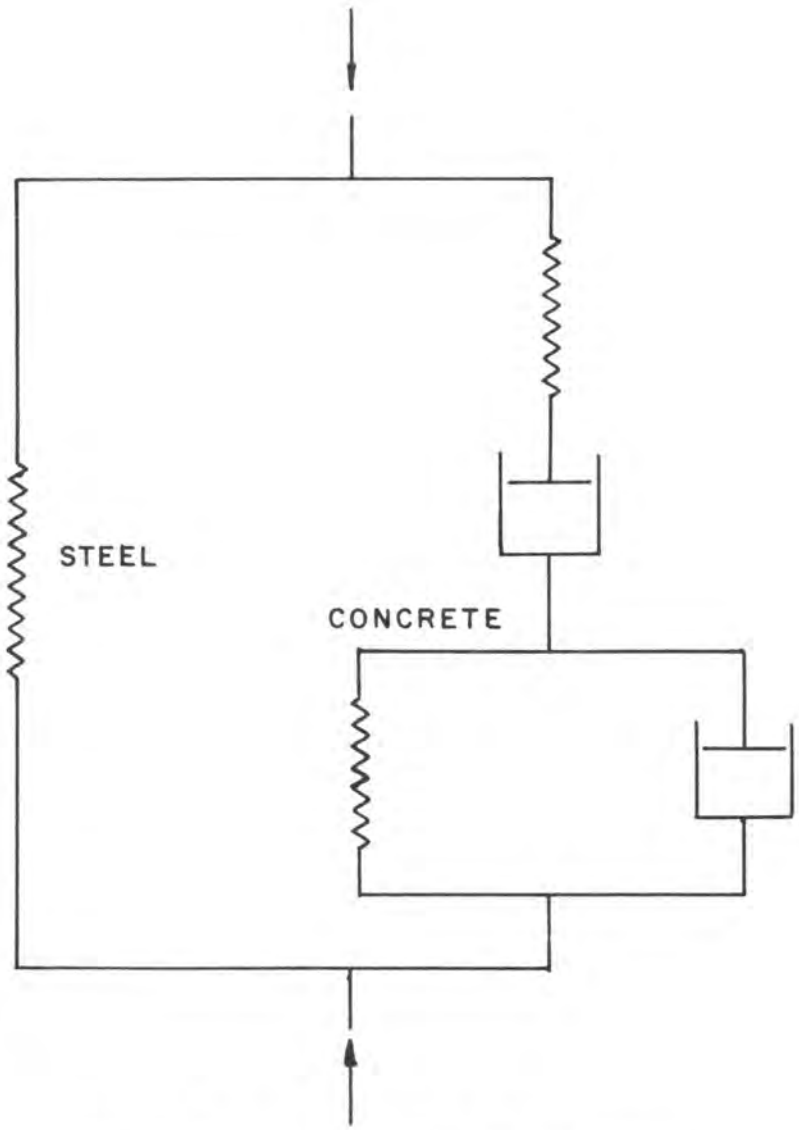


FIG. I. B.15 MODEL FOR PRESTRESSED CONCRETE (HANSEN)

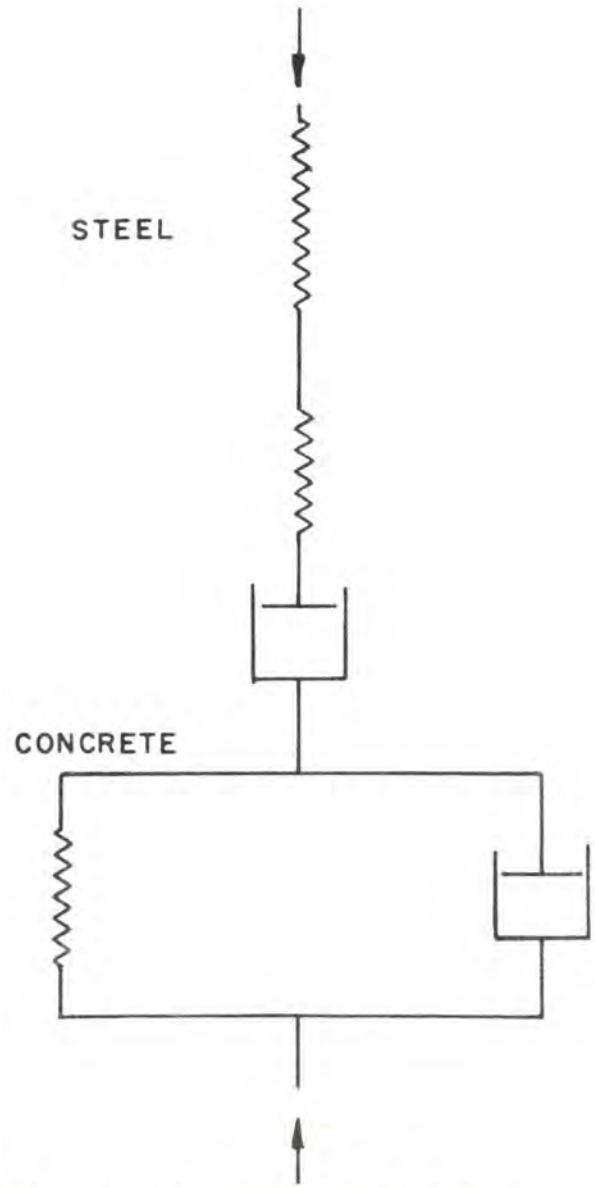


FIG. I. B.16 SECOND MODEL FOR PRESTRESSED CONCRETE (HANSEN)

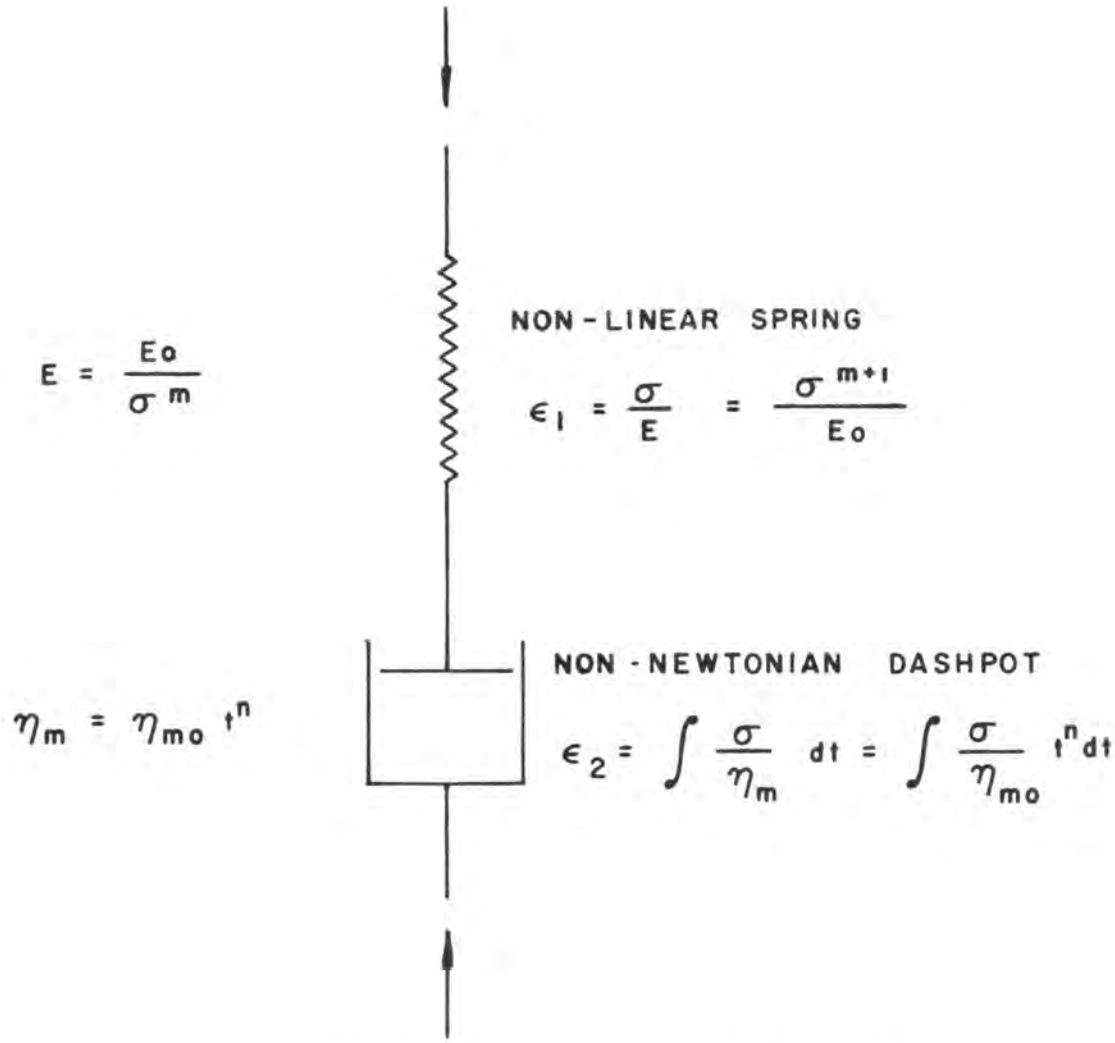


FIG. I. B.17 NON-LINEAR MAXWELL MODEL PROPOSED BY DESAYI AND SEN

# BIBLIOGRAPHY


1. Bingham, E. C. and Reiner, M. "Rheological properties of cement and cement mortar stone". Physics, March 1933. Vol. 4, pp. 88-96.

2. Burgers, I. M. and Scott Blair, G. W. "Joint Committee on Rheology of the International Council of Scientific Unions". Report on the Principles of Rheological Nomenclature. Proc. International Rheological Congress, Vol. 22. 1948. North Holland Publishing Co., Amsterdam.

3. Reiner, M. "Twelve Lectures on Theoretical Rheology." International Publishers, Inc., New York, 1949.

4. Reiner, M. "Deformation and Flow." H. K. Lewis, London, 1949.

5. Freudenthal, A. M. "The Inelastic Behavior of Engineering Materials and Structures." John Wiley and Sons, Inc., New York, 1950.

6. Flugge, W. "Mechanical models in plasticity and their use for interpretation of creep of concrete". Report No. 8, Office of Naval Research, Contract N6-ONR-251.

7. Reiner, M. "Building Materials, their Elasticity and Inelasticity." North Holland Publishing Co., Amsterdam, 1954.

8. Chang, T. S. and Kesler, C. E. "Correlation of sonic properties of concrete with creep and relaxation". Proc. A. S. T. M. 1956. Vol. 56, pp. 1257-1272.

9. Chang, T. S. and Kesler, C. E. "Prediction of creep behavior in concrete from sonic properties". Proc. Highway Res. Board, 1956, Vol. 35, pp. 436-443.

10. Ross, A. D. "Creep of concrete under variable stress". Jour. A.C.I., March 1958, Proc. Vol. 54, pp. 739-757.

11. Ross, A. D. "Creep and shrinkage of plain, reinforced and prestressed concrete - A general method of calculation", Nov. 1943. Proc. Inst. of C.E., Vol. 21, pp. 38-58.

12. Freudenthal, A. M. and Roll, F. "Creep and creep recovery of concrete under high compressive stress". Jour. A.C.I., June 1958, Proc. Vol. 54, pp. 1111-1142.

13. Hansen, T. C. "Creep of concrete - A discussion of some fundamental problems". The Swedish Cement and Concrete Res. Inst., Stockholm. Bulletin No. 33, Sept. 1958.

14. Glucklich, J. "Rheological behavior of hardened cement paste under low stresses". Jour. A.C.I., Oct. 1959. Proc. Vol. 56, pp. 327-337.

15. Constantinescu-Catunesti, S. Report presented at the Annual Meeting of the App. Mech. of the Rumanian Academy, Bucharest, 1960.

16. Glucklich, J. and Ishai, O. "Rheological behavior of hardened cement paste under low stresses". Jour. A.C.I., Feb. 1961. Proc. Vol. 57, pp. 947-964.

17. Glucklich, J. and Ishai, O. "Creep mechanism in cement mortar". Jour. A.C.I., July 1962, Proc. Vol. 59, pp. 923-948.

18. Hansen, T. C. "On rheology of hardened concrete". Proc. NR 37, 1962. The Swedish Cement and Concrete Res. Inst., Stockholm.

19. Hansen, T. C. "Creep and stress relaxation of concrete". Proc. NR 31, 1960. The Swedish Cement and Concrete Res. Inst., Stockholm.

20. Desayi, P. and Sen, B. R. "An investigation into the prediction of creep and the true ultimate strength of concrete". The Indian Concrete Journal. Vol. 40, No. 4, April 1966.

# APPENDIX II - A

# THE EFFECT OF AGGREGATE CONTENT ON THE ELASTIC AND CREEP STRAINS OF MORTAR AND CONCRETE

# APPENDIX II - A

# THE EFFECT OF AGGREGATE CONTENT ON THE ELASTIC AND CREEP STRAINS OF MORTAR AND CONCRETE

## Mechanical Model

Several investigators have suggested the use of mechanical models to predict strain behavior. All of these models essentially reduce to equivalent systems of laminations of paste and aggregate loaded both parallel and perpendicular to the plane of the lamina as shown in Fig. 8. A convenient variation is the model suggested by England (44) consisting of a cube of aggregate centered in a unit cube of paste or mortar matrix, for the mortar and concrete model, respectively. In England's model the effect of Poisson's ratio has been neglected, both for the aggregate and the paste or mortar matrix. This model has been used by Hollrah [62], in conjunction with a rheological model for the cement paste, to predict the time-dependent strain behavior of mortar and concrete.

The body centered cube of aggregate surrounded by the matrix shell shown in Fig. II. A.1 may be seen to be equivalent to a lamina of aggregate located between two lamina of matrix, with this laminar system in turn surrounded by a cylindrical shell of the matrix. For purposes of analysis, the equivalent model with the cube of aggregate shifted to one corner of the unit cube may be used. If the aggregate cube has a width of $\beta_a$, the aggregate volume ratio is

$$V_a = \beta_a^{\,3} \tag{1}$$

If the composite unit cube is subjected to an average uniaxial compressive stress $\sigma_c$, the total axial force on the cube is

$$F = \sigma_c\,(1)\;\;(1) = \sigma_c \tag{2}$$

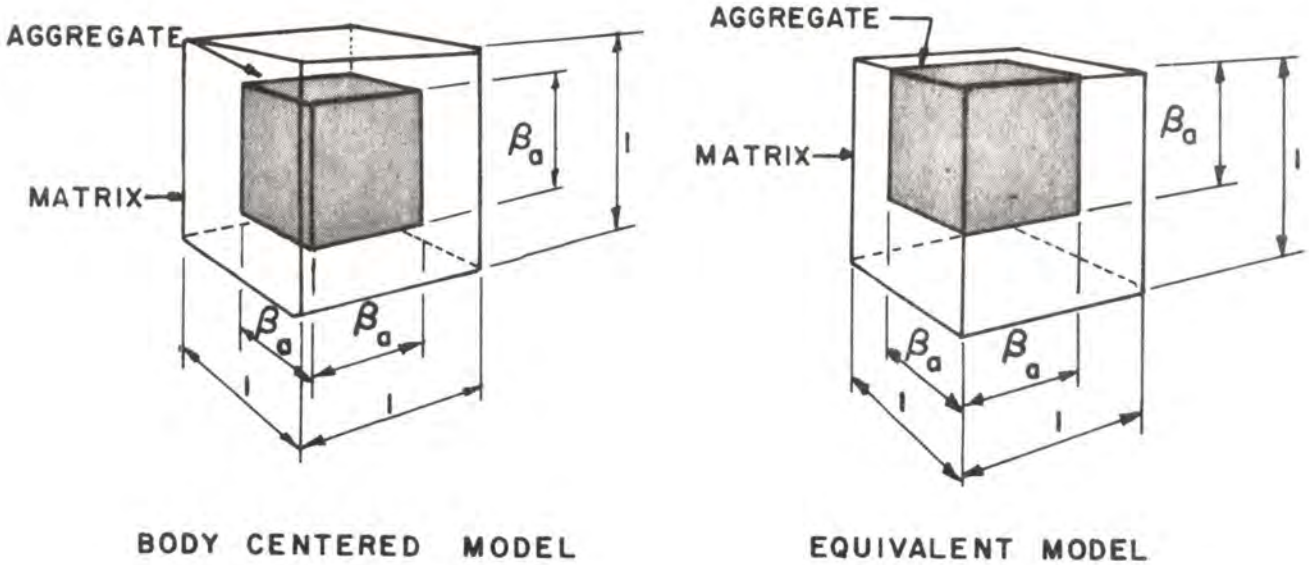


FIG. II. A.1 - ENGLAND'S MECHANICAL MODEL

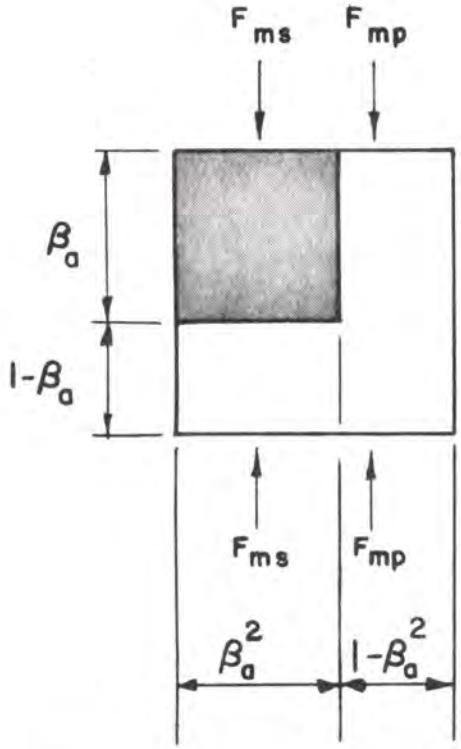


FIG. II. A.2 - FORCE SYSTEM

This force may be resolved into two components, viz. $F_{ms}$ and $F_{mp}$, acting on the cube of aggregate in series with a lamina of matrix and on the parallel lamina of matrix, respectively. From equilibrium,

$$F_{ms} + F_{mp} = F = \sigma_c \tag{3}$$

For strain compatibility

$$\frac{F_{mp}}{(1-\beta_a^2)(E_{ma})} = \frac{F_{ms}}{\beta_a^2}\left[\frac{\beta_a}{E_a} + \frac{1-\beta_a}{E_{ma}}\right] = \frac{F}{E} \tag{4}$$

where $E_a$ and $E_{ma}$ are the elastic moduli of the aggregate and the matrix, respectively, and E is the modulus of the composite system. From Eq. 4

$$F_{mp} = \frac{F}{E}(1-\beta_a^2)E_{ma} \tag{5}$$

$$F_{ms} = \frac{F}{E}\left[\frac{\beta_a^2 E_a E_{ma}}{\beta_a E_m + (1-\beta_a)E_a}\right] \tag{6}$$

Adding Eq's 5 and 6

$$F = F_{ms} + F_{mp} = \frac{F}{E}\left[(1-\beta_a^2)E_{ma} + \frac{\beta_a^2 E_a E_{ma}}{\beta_a E_{ma} + (1-\beta_a)E_a}\right]$$

hence

$$E = (1-\beta_a^2)E_{ma} + \frac{\beta_a^2 E_a E_{ma}}{\beta_a E_{ma} + (1-\beta_a)E_a} \tag{7}$$

Defining

$E_m$ = Elastic modulus of the mortar
$E_p$ = Elastic modulus of the paste (matrix)
$E_{fa}$ = Elastic Modulus of the fine aggregate
$V_{fa}$ = Ratio of volume of fine aggregate to total volume of mortar

$$\beta_{a1} = \sqrt[3]{V_{fa}} \tag{8}$$

and from Eq. 7

$$E_m = (1-\beta_{a1}^2)E_p + \frac{\beta_{a1}^2 E_{fa} E_p}{\beta_{a1} E_p + (1-\beta_{a1})E_{fa}} \tag{9}$$

Also, defining

$E_c$ = Elastic modulus of the concrete

$E_{ca}$ = Elastic modulus of the coarse aggregate

$V_{ca}$ = Ratio of volume of coarse aggregate to total volume of concrete

$$\beta_{a2} = \sqrt[3]{V_{ca}} \tag{10}$$

From Eq. 7

$$E_c = (1-\beta_{a2}^2)E_m + \frac{\beta_{a2}^2 E_{ca} E_m}{\beta_{a2}E_m + (1-\beta_{a2})E_{ca}} \tag{11}$$

Based on a limited number of tests by Hollrah (62) this model appears to satisfactorily predict the elastic properties of concrete from the mix proportions and the elastic properties of the coarse and fine aggregate and of the paste.

The model may also be used to obtain a reasonably good estimate of the total elastic and creep strain by substituting an ultimate effective or reduced modulus $E_{pu}$ for $E_p$ in Eq. 9. The reduced effective modulus of the mortar is then given by

$$E_{mu} = (1-\beta_{a1}^2)E_{pu} + \frac{\beta_{a1}^2 E_{fa} E_{pu}}{\beta_{a1}E_{pu} + (1-\beta_{a1})E_{fa}} \tag{12}$$

Similarly the reduced effective modulus of the concrete is given by:

$$E_{cu} = (1-\beta_{a2}^2)E_{mu} + \frac{\beta_{a2}^2 E_{ca} E_{mu}}{\beta_{a2}E_{mu} + (1-\beta_{a2})E_{ca}} \tag{13}$$

Since the seat of time dependent strains may be assumed to be in the paste, the same values for $\beta_{a1}$, $\beta_{a2}$, $E_{fa}$ and $E_{ca}$ may be assumed. Shrinkage strains may similarly be estimated by assuming that these strains result from an effective potential shrinkage force. Hollrah found that the elastic properties of concrete could be predicted with reasonable accuracy using this model. One difficulty arises in that the modulus of elasticity of the fine and coarse aggregate may be difficult to determine directly by test. This may be circumvented by using the model to estimate the aggregate modulus from measured modulus

values for mortar and concrete mixes. The value of the model then lies principally in its use to predict the modulus of mixes with different proportions. Table II. A.1 shows the ratio of predicted/observed modulus values for the eight concrete mixes studied by Hollrah. The elastic modulus values are in reasonably good agreement as is to be expected because the aggregate modulus values were determined using the model.

Shrinkage strains were predicted by determining the shrinkage stress potential of the paste and applying this potential as an equivalent load. As may be noted from Table II. A.1 this assumption over-estimated the shrinkage of the mix in some cases. Both for shrinkage and for creep plus shrinkage, a modified modulus value $E_{pu}$ was used for the paste. This value was determined by direct test of paste specimens.

Rheological Model

Mechanical models based on constituent properties have been used successfully to predict elastic and ultimate time-dependent strain behavior of mortar and concrete. They do not, however, provide any clue as to the rate at which these strains are developed. These time-dependent properties are usually call rheological properties. Rheological properties are commonly modeled by comparing the time-dependent strain response of a material with the deformation response of various combinations of idealized mechanical elements, such as springs and dash pots, when subjected to a force. While such models can not be expected to predict material behavior under all conditions, they do provide a useful insight into the behavior under standard environmental conditions. They are therefore useful in predicting limiting conditions of behavior. Perhaps the earliest attempts at developing such idealized models were those of Maxwell and Kelvin. Maxwell's model or the so called "Maxwell body" consists of a spring in series with a dashpot. Under a constant force, the Maxwell body is subjected to an instantaneous deformation and subsequently continues to deform at a constant rate. The instantaneous deformation of this model can be considered analogous to elastic strain, however the constant rate of strain due to the dashpot

RATIO - PREDICTED/OBSERVED VALUES

| Mix | Elastic Modulus | Shrinkage Strain | Creep plus Shrinkage Strain |
|---|---|---|---|
| 1 | 1.05 | 1.21 | 1.02 |
| 2 | 1.05 | 1.33 | 1.01 |
| 3 | .94 | 1.40 | .86 |
| 4 | 1.03 | 1.28 | 1.01 |
| 5 | .98 | 1.00 | .90 |
| 6 | 1.06 | 1.03 | .81 |
| 7 | .97 | .98 | .86 |
| 8 | .97 | 1.04 | .95 |

TABLE II. A.I COMPORATIVE MODULUS AND STRAIN VALUES

does not adequately model the creep response of cement paste, mortar or concrete.

The "Kelvin body" is a model consisting of a dashpot in parallel with a spring. Under a constant applied force this body is deformed gradually, but at a reduced rate. As the Kelvin body is deformed, the load reaction is transferred from the dashpot to the spring. Hence the force on the dashpot decreases and consequently the rate at which the body deforms. The response of the Kelvin body is therefore more closely analogous to creep strain response. The Kelvin body is reversible, since upon removal of the external force the force in the compressed spring is balanced by the reaction of the dashpot.

In 1948 Burger suggested the model shown in Fig. II. A.3 consisting of a Maxwell body in series with a Kelvin body. In the Burgers body, the Maxwell body represents the elastic deformation and the irrecoverable creep and the Kelvin body represents recoverable creep.

The Burger model represented a significant advance but still failed to adequately explain such phenomena as shrinkage, shrinkage creep or flow, and the effect on these physical properties of environmental conditions and continued hydration of the cement paste. During the decade following Burger's proposal numerous other rheological models of various degrees of sophistication have been proposed. Most of these models consisted of other combinations of the basic Maxwell and Kelvin body. Many included nonlinear elements such as friction elements, nonlinear springs and nonlinear dashpots, in an attempt to model the nonlinear physical properties due to maturization. While these models can be used to predict response for a fixed set of environmental conditions, rheological models can not be expected to predict behavior under variable conditions. At best, therefore, they are only useful as an estimate of actual response under field conditions.

Hollrah [62] has studied the response of a rheological model suggested by Pauw consisting of a linear spring in series with a Kelvin body to represent delayed elasticity and a modified Kelvin body to represent shrinkage and shrinkage creep. (Fig. II. A.4). The modified Kelvin body consists of a prestressed spring and an irreversible dashpot to represent the effect of shrinkage and flow. The prestressing force is

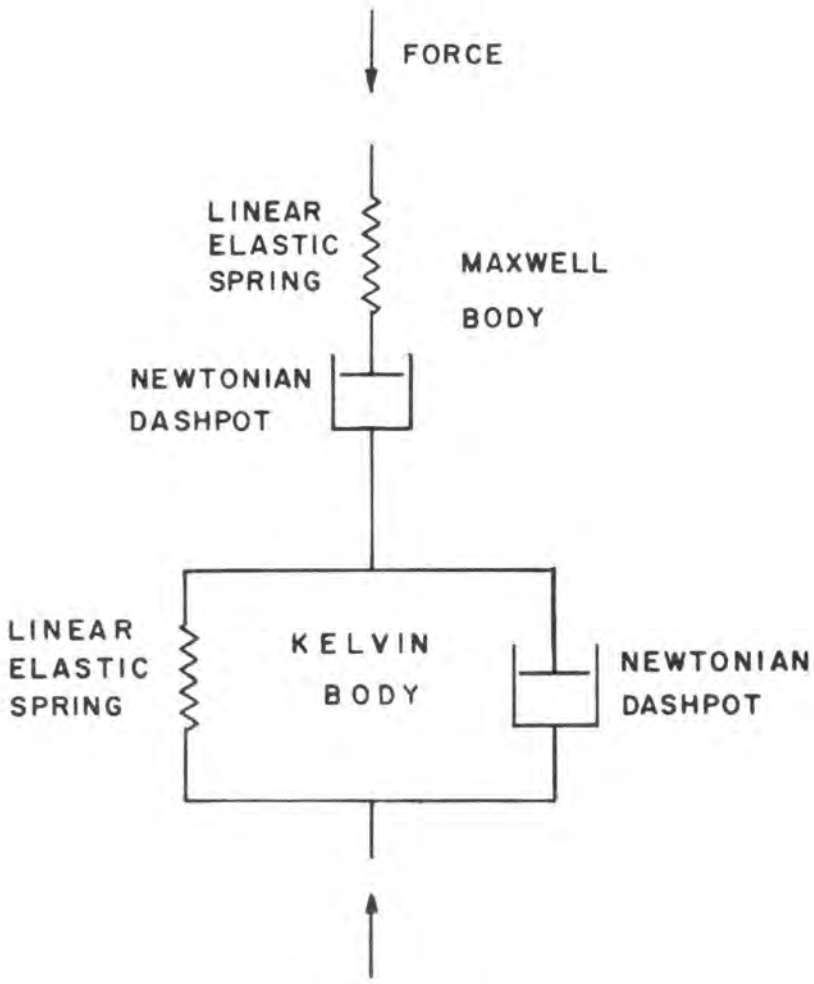


FIG. II. A.3 BURGER BODY

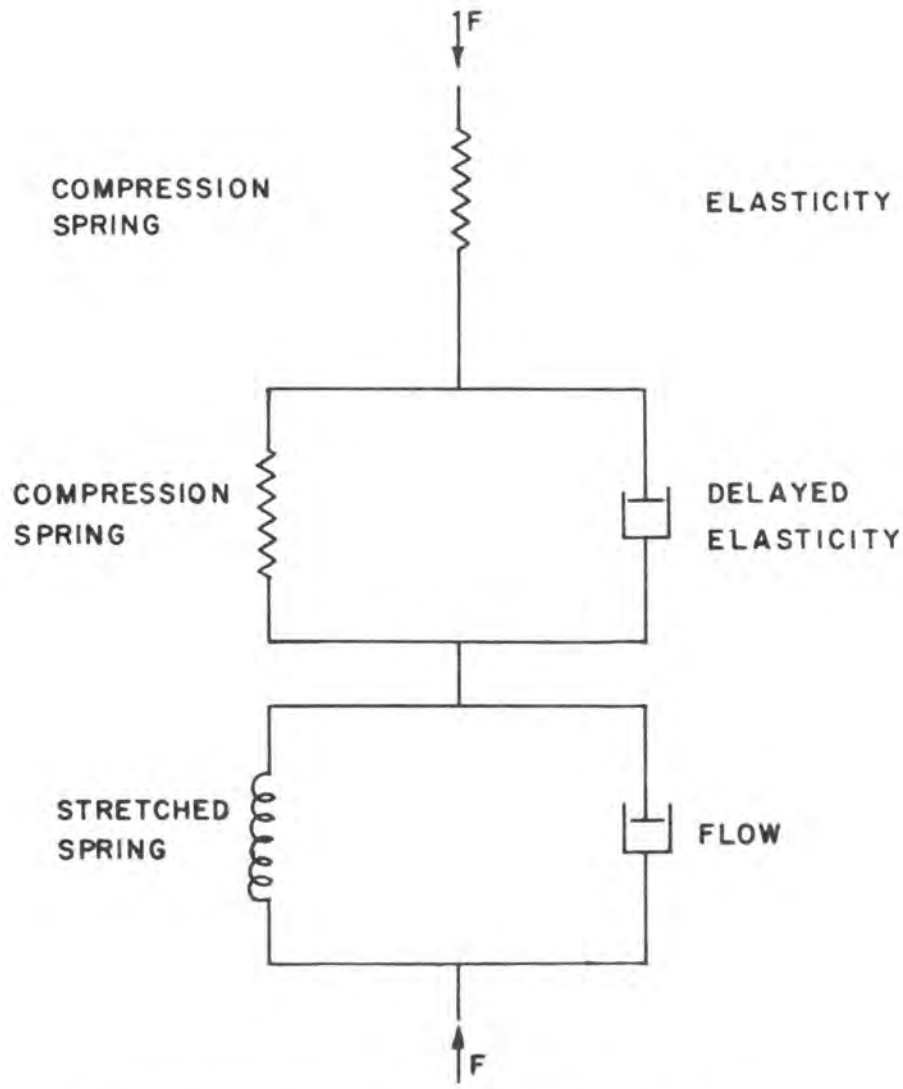


FIG. II. A.4 HOLLRAH'S RHEOLOGICAL MODEL

therefore analogous to the restrained shrinkage force potential. The compression of the spring, when this prestressing force is completely dissipated, is analogous to the ultimate shrinkage strain. Only linear springs and dashpot elements were used in this model since the increased complexity resulting from the use of nonlinear elements was not believed to be warranted by increased reliability.

The response of a unit cube of hardened cement paste subjected to constant uniform axial stress may be simulated by visualizing the cube to consist of three lamina. The deformation of top layer represents the elastic strain, that of the second layer, the delayed elastic strain; and that of the third layer, the shrinkage and flow.

The rheological constants for the paste were obtained by curve fitting to obtain the best fit for shrinkage and creep plus shrinkage data. These constants were then in turn used with the elastic modulus values for the fine and coarse aggregate in a combined model to determine the time-dependent shrinkage and creep properties of the concrete. Predicted and observed values for a typical mix are shown in Fig. II. A.5.

It may be noted that for the ages in excess of 90 days, the observed values are reasonably well-contained in a $\pm$ 10 percent scatter band. The limiting values were obtained by applying Eq. 13. Intermediate values were computed by a stepwise integration procedure using the IBM "Continuous System Modelling Program".

It may be concluded that mechanical and rheological models can be useful in extrapolating data for known mixes to similar mixes under equivalent geometrical and environmental conditions. Further experimentation would be required to establish the reliability of prediction based on these methods.

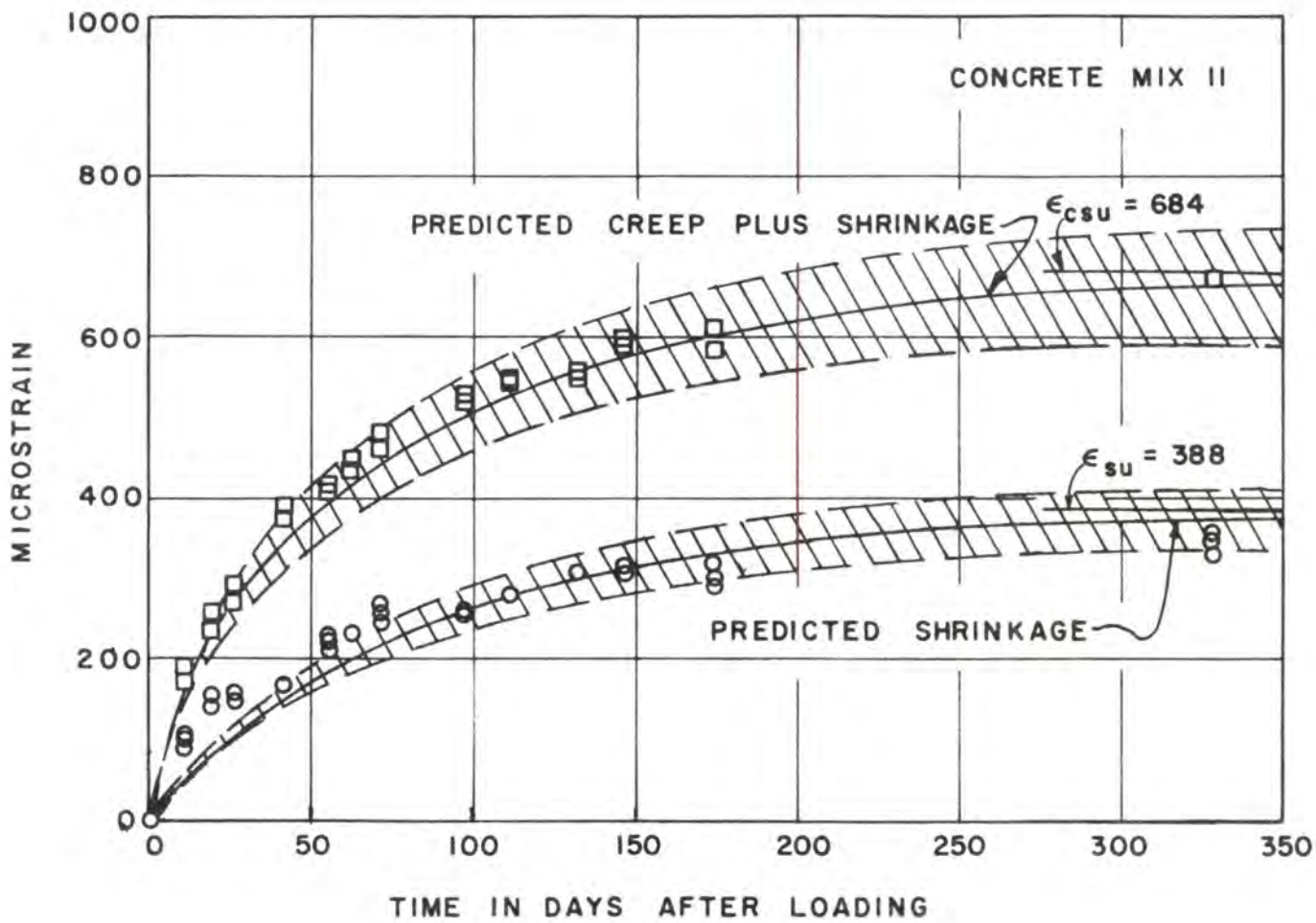


FIG. II. A.5 CREEP AND SHRINKAGE STRAIN RESPONSE

# APPENDIX II-B

# THE EFFECT OF AGGREGATE CONTENT ON THE SHRINKAGE OF CONCRETE

## APPENDIX II-B
## THE EFFECT OF AGGREGATE CONTENT ON THE SHRINKAGE OF CONCRETE

### Introduction

Pickett (43) developed a relationship between the aggregate volume ratio, the shrinkage of cement paste and the shrinkage of aggregate surrounded by a spherical shell of paste. England (44) analyzed a cubical model with the aggregate centered in the shell but assumed that the effect of Poisson's ratio of the aggregate and the paste could be neglected. The model presented herein is similar to England's model but does take into account Poisson's ratio. The final algebraic expression may be approximated to give the simple relationship given in Eq. 23, Chapter III.

### The Model

The model analyzed consists of a body-centered cube of aggregate in a shell of paste as shown in Fig. II-B-1. Thus as shown in the figure, the concrete is represented by a cube of aggregate of dimension $\beta_a$ centered in a unit cube. The volume of the aggregate therefore, is $\beta_a^3$ and, since the total volume is unity, the aggregate volume ratio is

$$V_a = \beta_a^3 \tag{1}$$

### Analysis

The analysis is made on the basis that the law of superposition may be applied. Consider first the free shrinkage, $\varepsilon_{sp}$ of an all paste cube. The cube can be restored to its original size by subjecting it to a negative hydrostatic pressure

$$\sigma_{sp} = \sigma_x = \sigma_y = \sigma_z \tag{2}$$

which will produce strains

$$\varepsilon_x = \varepsilon_y = \varepsilon_z = \varepsilon_{sp} \tag{3}$$

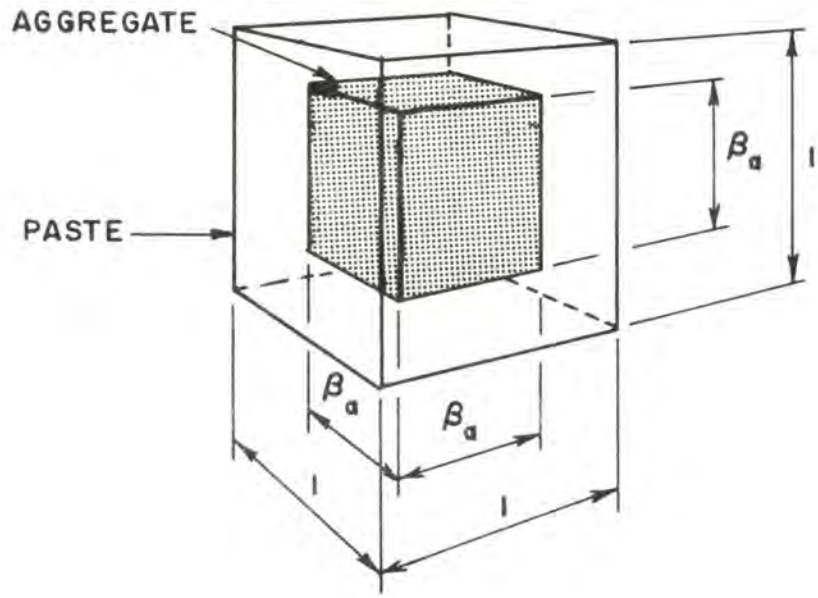


FIG. II. B.1 - BODY-CENTERED AGGREGATE-PASTE MODEL

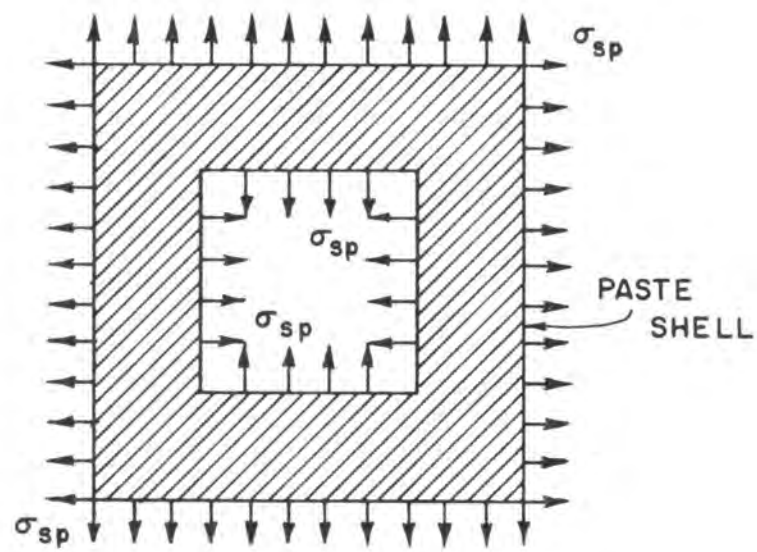


FIG. II. B.2 - FREE SHRINKAGE OF SHELL COMPENSATED BY NEGATIVE HYDROSTATIC PRESSURE

From the theory of elasticity, when Eq. 2 is satisfied

$$\varepsilon_x = \frac{1-2\nu_p}{E_p} \sigma_x , \tag{4}$$

where:

$\nu_p$ = Poisson's ratio for the paste.

Hence,

$$\sigma_{sp} = \sigma_x = \frac{E_p \varepsilon_x}{1-2\nu_p} = R_p \varepsilon_{sp} \tag{5}$$

where

$$R_p = \frac{E_p}{1-2\nu_p} \tag{6}$$

To keep the paste shell from being distorted we must apply a tensile force on both the inside and outside surface of the shell equal to

$$\sigma_{sp} = R_p \varepsilon_{sp} \tag{7}$$

as shown in Fig. II. B.2.

To restore equilibrium to the cube of concrete we must apply an equal positive hydrostatic pressure to the composite system which will induce a compressive force, $\sigma_a$, on the surface of the aggregate. Thus, the equivalent state of stress in the shell is as depicted in Fig. II. B.3.

The stresses on the left produce strains in the paste shell equal to the free shrinkage strains and the stresses on the right reduce these strains by the strains due to biaxial tension in the paste shell wall.

Consider equilibrium of a section through the middle of the cube as shown in Fig. II. B.4:

$$\sigma_a \beta_a^2 = \sigma_{pt} (1-\beta_a^2)$$

Thus, the paste shell wall is subjected to a biaxial tensile stress

$$\sigma_{pt} = \frac{\sigma_a \beta_a^2}{1-\beta_a^2} \tag{8}$$

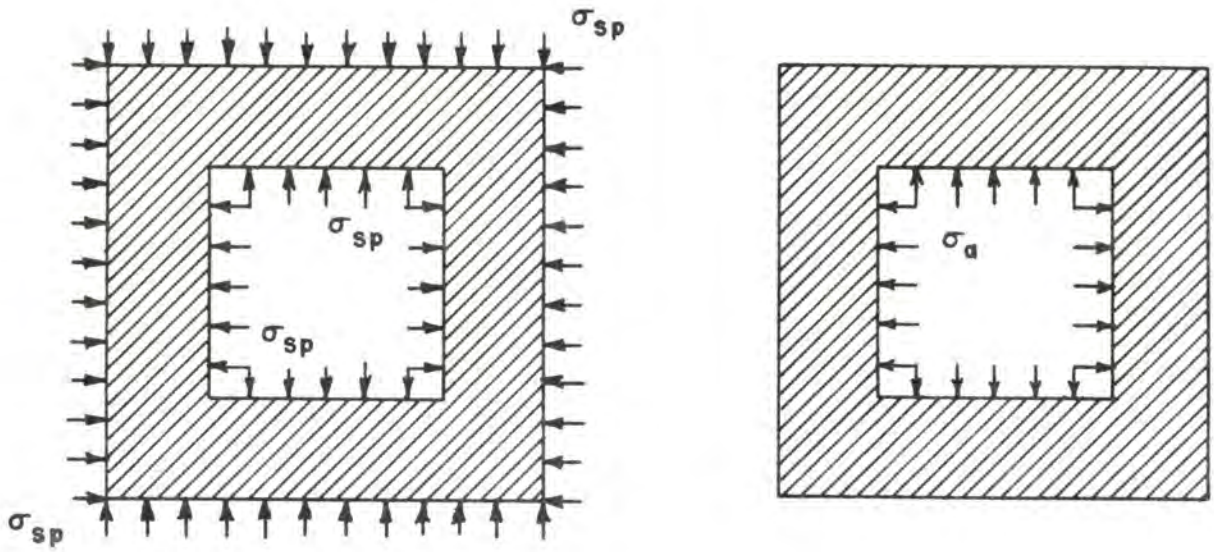


FIG. II. B.3 - EQUILIBRIUM RESTORING FORCES

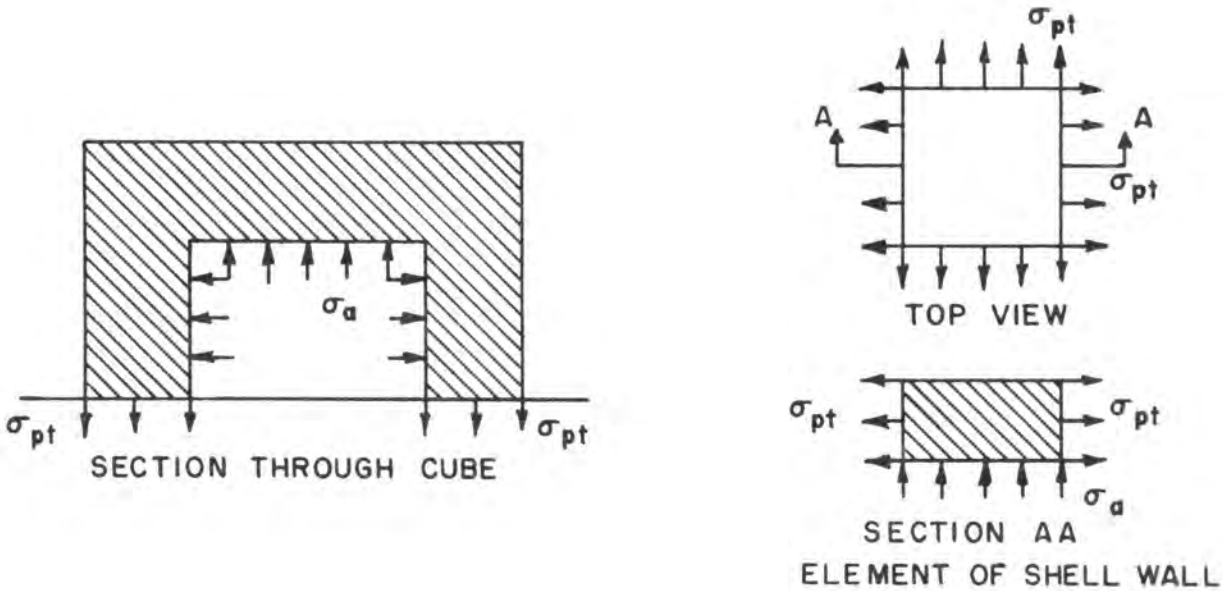


FIG. II. B.4 - EQUILIBRIUM OF PASTE SHELL

The biaxial tensile stress produces a strain in the paste shell (tangent to the shell surface)

$$\varepsilon_{pt} = \frac{\sigma_{pt}(1-\nu_p)}{E_p} = \frac{\sigma_a \beta_a^2 (1-\nu_p)}{(1-\beta_a^2)E_p} \tag{9}$$

which reduces the free shrinkage of the paste shell. For compatibility at the paste shell-aggregate interface the strain in the aggregate core must satisfy the condition

$$\varepsilon_a = \varepsilon_{sp} - \varepsilon_{pt} = \varepsilon_{sp} - \frac{\sigma_a \beta_a^2 (1-\nu_p)}{(1-\beta_a^2)E_p} \tag{10}$$

The strain in the aggregate is given by a similar relationship as Eq. 4.

$$\varepsilon_a = \frac{\sigma_a (1-2\nu_a)}{E_a} \tag{11}$$

Equating Eqs. 10 and 11

$$\varepsilon_{sp} = \sigma_a \left(\frac{\beta_a^2}{(1-\beta_a^2)} \frac{(1-\nu_p)}{E_p} + \frac{(1-2\nu_a)}{E_a}\right) \tag{12}$$

Hence,

$$\sigma_a = \frac{E_a E_p (1-\beta_a^2)\varepsilon_{sp}}{(1-2\nu_a)(1-\beta_a^2)E_p + (1-\nu_p)\beta_a^2 E_a} \tag{13}$$

and

$$\varepsilon_a = \frac{E_p\ (1-\beta_a^2)(1-2\nu_a)\varepsilon_{sp}}{(1-2\nu_a)(1-\beta_a^2)E_p + (1-\nu_p)\beta_a^2 E_a} \tag{14}$$

The biaxial stress $\sigma_{pt}$ also produces a strain normal to the shell surface which reduces the thickness of the shell.

$$\varepsilon_{pr} = -\ 2\nu_p \frac{\sigma_{pt}}{E_p}$$

$$\varepsilon_{pr} = -\ \frac{2\nu_p E_a \beta_a^2\ \varepsilon_{sp}}{(1-2\nu_a)(1-\beta_a^2)E_p + (1-\nu_p)\beta_a^2 E_a} \tag{15}$$

The total strain in the shell (normal to the surface) is therefore,

$$\varepsilon_p = \varepsilon_{sp} + \frac{2\nu_p E_a \beta_a^2 \varepsilon_{sp}}{(1-2\nu_a)(1-\beta_a^2)E_p + (1-\nu_p)\beta_a^2 E_a}$$

$$= \frac{(1-2\nu_a)(1-\beta_a^2)E_p + (1+\nu_p)\beta_a^2 E_a}{(1-2\nu_a)(1-\beta_a^2)E_p + (1-\nu_p)\beta_a^2 E_a}\varepsilon_{sp} \tag{16}$$

Finally, the total strain for the composite cube must be

$$\varepsilon_s = \beta_a \varepsilon_a + (1-\beta_a)\varepsilon_p$$

$$\varepsilon_s = \frac{(1-\beta_a^2)(1-2\nu_a)E_p + (1-\beta_a)(1+\nu_p)\beta_a^2 E_a}{(1-2\nu_a)(1-\beta_a^2)E_p + (1-\nu_p)\beta_a^2 E_a}\varepsilon_{sp}$$

$$= \frac{(1-\beta_a^2)(1-2\nu_a) + (1-\beta_a)(1+\nu_p)\beta_a^2 \frac{E_a}{E_p}}{(1-\beta_a^2)(1-2\nu_a) + (1-\nu_p)\beta_a^2 \frac{E_a}{E_p}}\varepsilon_{sp} \tag{17}$$

From Eq. 1

$$\beta_a = \sqrt[3]{V_a}$$

hence, Eq. 17 is equivalent to Eq. 21 in Chapter III.

Conclusions

As further noted in Chapter III, $E_p$ is generally much smaller than $E_a$ due to creep of the cement paste. Hence, the second term in both the numerator and denominator is dominant provided the dimension $\beta_a$ is greater than zero. Thus, for the limiting or ultimate shrinkage (17) may be approximated by:

$$\varepsilon_{su} = \left(\frac{1+\nu_p}{1-\nu_p}\right)(1-\beta_a)\,\varepsilon_{sp}\ , \quad \beta_a > 0 \tag{18}$$

Eq. 18 is equivalent to Eq. 22 in Chapter III. The above analysis does not take into account the unrestrained free shrinkage of the paste shell at the eight corners of the cube.

The total volume of these corners is

$$8\left(\frac{1-\beta_a}{2}\right)^3 = (1-\beta_a)^3$$

Hence, the shrinkage of the composite model would be increased in proportion to the total volume of the corners to the total volume and the shrinkage given by Eq. 17, reduced by the volume of the corners to the total volume. The net effect is very small in any case. For example, for an aggregate volume ratio of 0.5, $\beta_a = .794$ and $(1-\beta_a)^3 = 0.0085$. Hence, the error introduced by ignoring the effect of free shrinkage of the corners is less than one percent. It should be noted that while Eq. 18 does not give valid results as the aggregate volume ratio approaches zero, Eq. 17 yields consistent results for the full range from zero to unity.

# APPENDIX II-C

## RELEVANT PROVISIONS REGARDING CREEP AND SHRINKAGE IN THE PROPOSED REVISED CEB CODE

(Since the attached draft was translated, further revisions were incorporated at the FIP 6th Congress, Prague, June 1970. For the latest version, the reader is referred to "CEB-FIP International Recommendations for the Design and Construction of Concrete Structures - Part I. Principles and Recommendations" published by Cement and Concrete Association, 52 Grosvenor Gardens, London SW1, SBN 7210 0732 5 (CEB Information Bulletin No. 72))

## APPENDIX II-C

## RELEVANT PROVISIONS REGARDING CREEP AND SHRINKAGE IN THE PROPOSED REVISED CEB CODE

The following sections are a free translation of the French text for the proposed revised provisions for creep and shrinkage in the European Committee on Concrete (C.E.B.) "International Recommendations for Design and Execution of Reinforced Concrete Structures". The notation employed by CEB differs in many respects from that currently employed in the United States. Since work is currently underway to develop international standard notations, only such minor changes have been made as to avoid confusion with the main text.

### R12.3 Linear Deformations (Shrinkage and Creep)[1]

The coefficients indicated in R12.31 (Shrinkage) and R12.32 (Creep) give a basis for estimate and apply only to normal Portland cement concrete cured under normal conditions and subjected to a stress level of at most 35% of the compressive strength. (See Supplement M12.3) This refers to the average rupture stress on cylinders at the particular time.

### M12.3 Linear Deformations (Shrinkage and Creep)[2]

The curves shown in R12.31 (Shrinkage and R12.32) (Creep) must be used with care, since notable differences may be observed depending on the country or region, the mode of deformation of the aggregate, the nature of the cement, the amount of compaction and the nature of curing (no curing, steam curing, etc...), and finally, depending on variations of temperature and relative humidity. Elements such as thin walls and overlay road slabs are particularly sensitive to the latter.

---

[1] CEB-International Recommendations for Design and Execution of Reinforced Concrete Structures. Part 1: Analysis-Principles and Recommendations (Draft of 30 June 1969)

[2] CEB-International Recommendations for Design and Execution of Reinforced Concrete Structures. Part 1: Analysis-Manual of Application (Draft of 30 June 1969)

The coefficients indicated are given as a basis for estimation only. A degree of discretion is left to the authority in charge to adapt these coefficients to local conditions.

The coefficients given have been determined statistically for concretes subjected to normal stress levels, i.e., a maximum stress of 30-35% of $f'_c$. They do not apply without further change to steam or heat cured concretes. Creep and shrinkage strain characteristics used in computations must be determined for the actual concrete used by prior test or by examination of the behavior of structures using comparable concrete materials.

R12.31 Shrinkage

1. The shrinkage strain $\varepsilon_s$, at any given time may be determined by the relationship:

$$\varepsilon_s = \varepsilon_{su}\, \rho^*$$

where:

$\rho^*$ is a time-dependent coefficient

$\varepsilon_{su}$ is the ultimate shrinkage potential which in turn is given by the product of four coefficients

$$\varepsilon_{su} = \psi\, \alpha_s\, \beta_s\, \xi$$

$\psi$ is a function of climatic or environmental conditions,

$\alpha_s$ is a function of the dimensions of the member,

$\beta_s$ is a function of the physical composition of the concrete,

$\xi$ is a function of the geometric percentage $\rho$ of the longitudinal reinforcement:

$$\xi = \frac{1}{1+\eta\rho}$$

with $\eta$=20 to 25, to take into account the effect of creep. For general case, $\varepsilon_{su}$ as a function of $\xi$ gives the strain at the centroidal fiber for the reinforcement $\rho$ considered.

The values of $\psi$, $\alpha_s$, $\beta_s$, and $\rho^*$ as functions of the defining parameters may be estimated from the following figures.

2. Coefficient $\psi$ (Environmental Conditions)

For plain concrete (unreinforced), the mean values of $\psi$ may be estimated from the diagram below

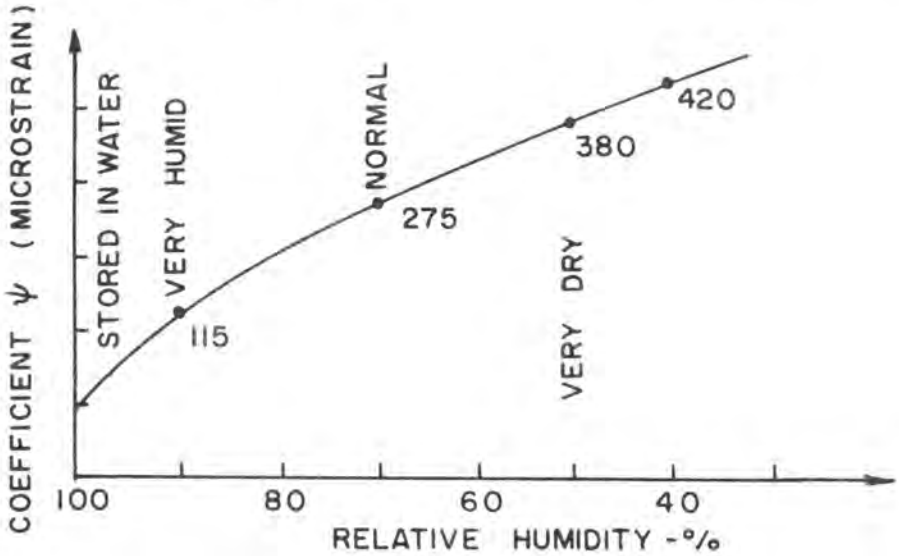


For heated floors, oven walls, etc., values of $\psi$ based on experience must be employed.

3. Coefficient $\alpha_s$ (Dimensions)

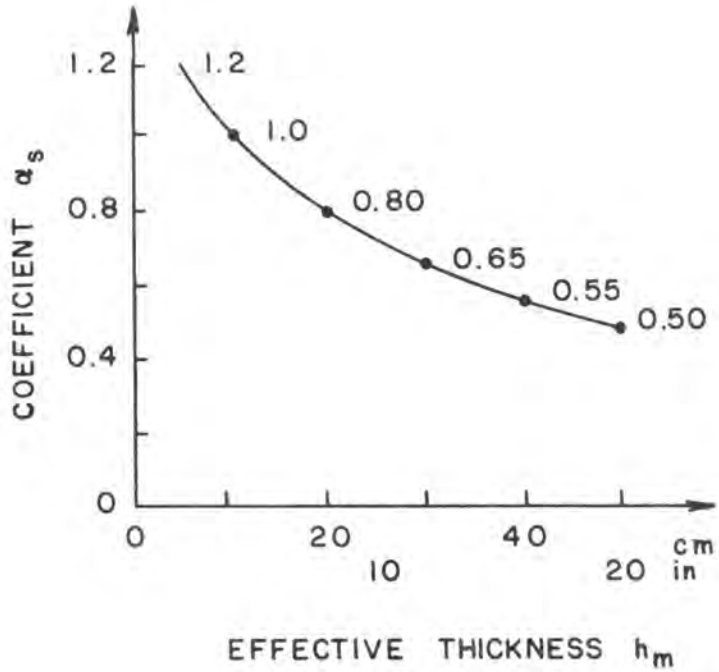

The "effective thickness" $h_m$ is the quotient of the gross area of the section and the half-perimeter, p/2, in contact with the atmosphere. This definition is derived from consideration of a circular section and can be extended to apply to other geometric sections. If one of the dimensions of the section considered is very large with respect to the other, the effective thickness corresponds very closely to the actual thickness.

The graph shows that the rate of shrinkage development is inversely proportional to the effective thickness. Nonetheless, it appears that this conclusion applies only to young concretes.

4. Coefficient $\beta_s$ (Composition of the Concrete)

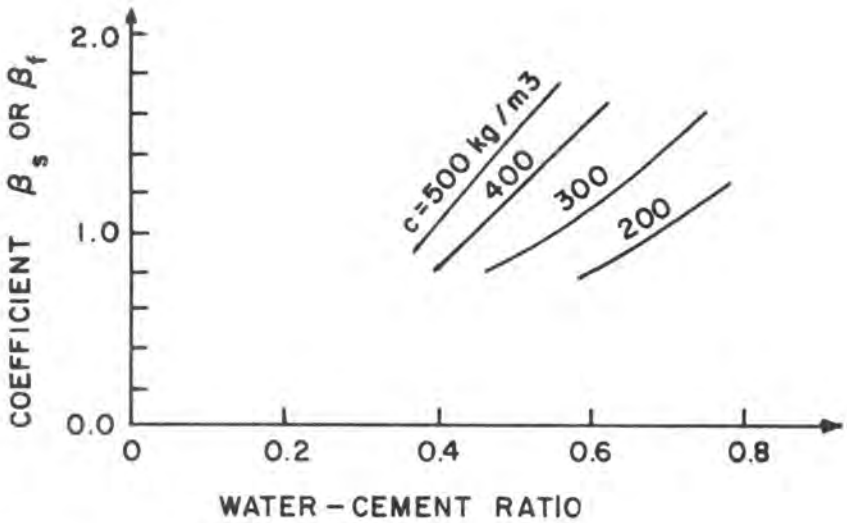


5. Coefficient $\rho^*$ (Variation as function of time)

Under constant environmental conditions, shrinkage is a function of time. In the relationship given in R12.31-1, the portion of the deformation due to shrinkage in any given time interval $(t_n - t_i)$ is equal to:

$$\varepsilon_{su} (\rho^*_{tn} - \rho^*_{ti})$$

In order to consider the influence of the dimensions of the member on the rate of shrinkage, a "fictitious age", $t_e$, is introduced to replace the real age $t_d$.

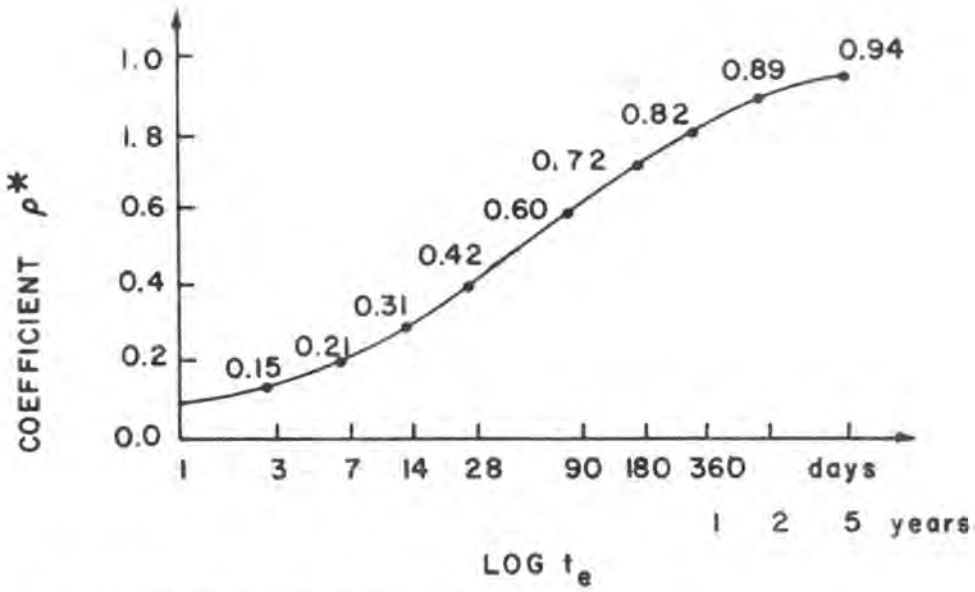


The value of $t_e$ is given by:

$$t_e = t_d\sqrt{\frac{10}{h_m}} \quad (h_m \text{ in cm})$$
$$= t_d\sqrt{\frac{4}{h_m}}$$

Exposed structures with thick walls, because of their volume and the fact that they are subjected to cyclical environmental influences, may undergo less shrinkage than laboratory test specimens.

Thus in the case of a laboratory prism specimen with 7 cm (2.75 in) sides, stored in a 50% humidity environment, shrinkage strains will reach their limiting value by the end of a year. In that case, the curve for the variable ρ* has the same configuration but is foreshortened time wise.

Curing: At early ages of the concrete, the shrinkage rate of a concrete is sensitive to the manner in which it is protected; a protected concrete shrinking only about half as much as an unprotected concrete. (This is of interest in avoiding cracking of young concretes of low strength). The difference in shrinkage decreases with age, becoming approximately 10% at the end of 4 months and eventually vanishes altogether.

R12.32 Creep

As a first approximation, a linear creep law may be assumed in evaluating the order of magnitude of creep deformations. Under this hypothesis creep deformations at any age $t_n$ subjected to a stress

applied at time $t_1$ and maintained until $t_i$ with stress changes applied in increments, may be set equal to:

$$\varepsilon_{et_1}\ \phi_n\ \zeta_{t_1}\ \rho^*(t_n-t_1) + \sum_i \Delta\varepsilon_{et_i}\ \phi_n\ \zeta_{t_i}\ \rho^*(t_n-t_i)$$

where:

$\varepsilon_{et_1}$ represents the instantaneous elastic deformation of the concrete under the effect of a stress applied at $t_1$ (which may be calculated by assuming $E_c$ has a value of 21000 $f'_{ct}$, see R12.22

$\Delta\varepsilon_{et_i}$ is the instantaneous elastic deformation (calculated in accordance with the same rules, R12.22) due to incremental changes in intensity of stress

$\phi_n$ is the ultimate creep coefficient, which in turn is the product of three coefficients

$$\phi_n = \phi_o\ \alpha_f\ \beta_f$$

$\phi_o$ is a function of climatic conditions or environment

$\alpha_f$ is a function of the dimensions of the member

$\beta_f$ is a function of the composition of the concrete

$\zeta$ is a coefficient which is a function of the age of the concrete ($t_1$, $t_i$) when an incremental stress is applied

$\rho^*$ is a coefficient which takes into account the influence of time (duration of applied load or stress)

$(t_n - t_1)$ is the interval of time between time considered and time of application of load.

$(t_n - t_i)$ is the interval of time between time considered and time of application of an incremental change in stress.

Mean values of the coefficients $\phi_o$, $\alpha_f$, $\beta_f$ as functions of defining parameters may be estimated from the following curves below.

a) In the absence of a more precise analysis for creep, it may be assumed that the creep deformation under a sustained load applied at age $t_1$ days is twice the instantaneous deformation calculated on the basis of the modulus $E_c$ (i.e., the total deformation is three times the instantaneous deformation (cf. R12, 22-2)). This simplified hypothesis

thus defines a creep strain modulus $E_{cc} = E_c/2$ which allows the calculation of the magnitude of the creep strain $\varepsilon_c$ as an elastic strain due to the stress $\sigma_c$ in the concrete adjacent to the restraining reinforcement, thus,

$$\varepsilon_c = \frac{\sigma_c}{E_{cc}}$$

b) A high percentage of plain reinforcement reduces the compressive forces in the concrete as a result of the restraining effect. This reduction can be taken into account in calculating the instantaneous deformation as well as the effect on creep.

2. <u>Coefficient</u> $\phi_o$ (Climatic Conditions)

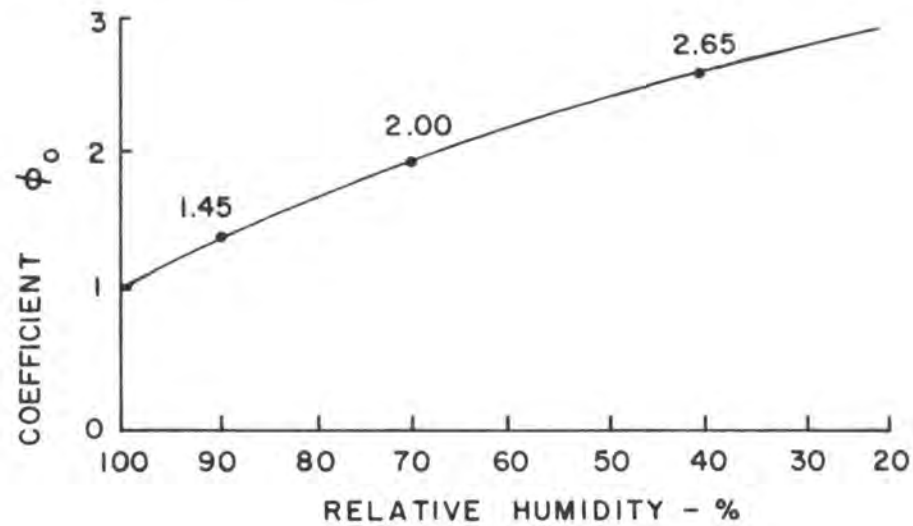


(Note $\phi_o$ can be approximated by the empirical relationship

$$\phi_o = \frac{H}{100} + \frac{6(100-H)}{200-H}$$

where H = relative humidity, expressed in per cent.)

3. Coefficient $\alpha_f$ (Effective Thickness)

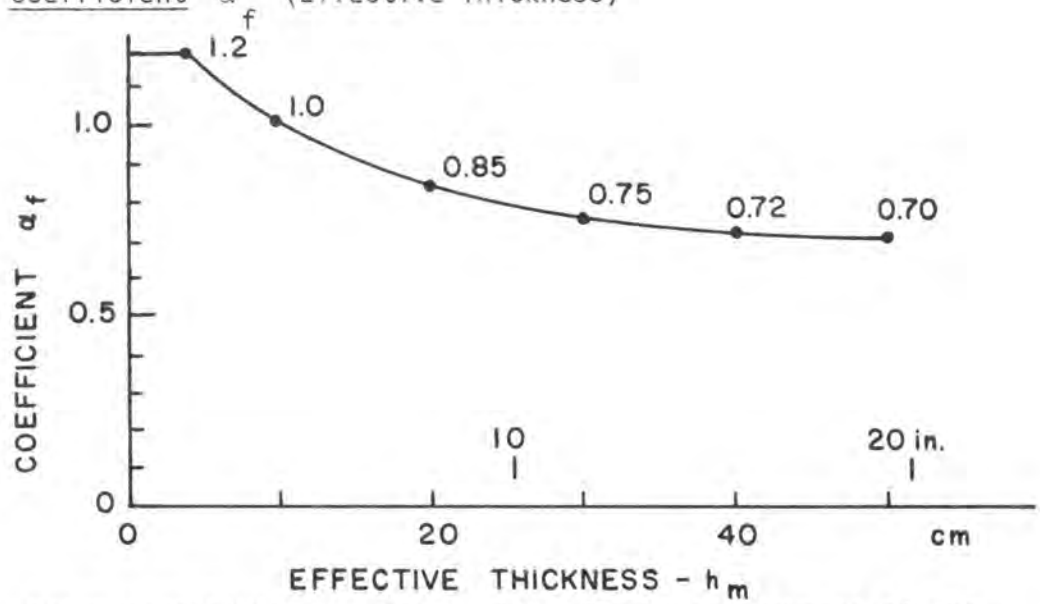


Creep sensitivity decreases with effective thickness of the element.

4. Coefficient $\beta_f$ (Composition of the Concrete)

$\beta_f = \beta_s$ as given on diagram for shrinkage.

5. Coefficient $\zeta$ (Age of Concrete at Time of Loading)

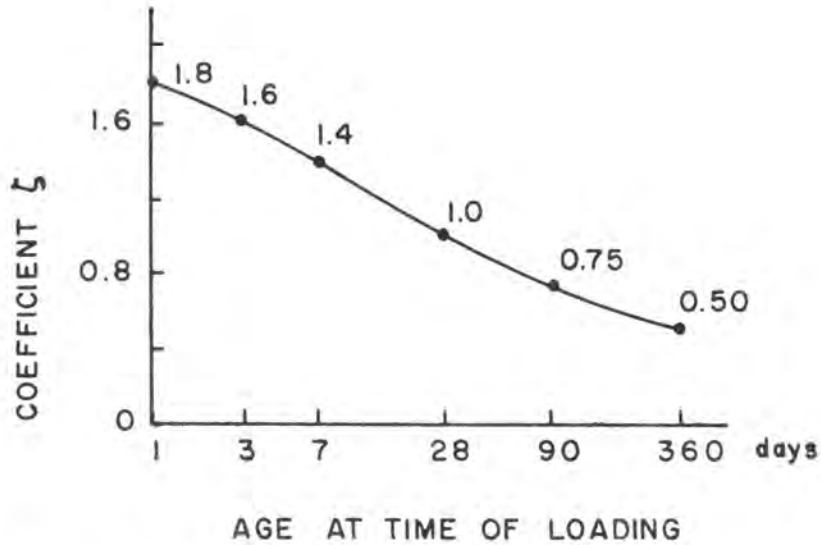


The age at time of loading has an influence at least as great as that of the environmental conditions. The values given in the

figure are for a mean ambient temperature of 20°C (68°F) under normal curing conditions. In an environment of lower temperatures than 20°C, a corrected age is assumed given by the following formula (for the range -10°C to +20°C)

$$t_r = \frac{\Sigma\Delta t(T + 10°)}{30°}$$

wherein:

$t_r$ = corrected effective age of concrete at loading, in days

$\Delta t$ = number of days during which the concrete cures (hardens) at a temperature T, expressed in degrees centigrade.

6. Coefficient $\rho^*$ (Variation as a Function of Time)

The same coefficient is used as for shrinkage, except that real time is applied. The development of creep with time is less sensitive than shrinkage to the effect of a decrease in the effective thickness of the member.

R12.33 Total Deformation

In summary, in the most general case the total deformation (elastic, shrinkage and creep) at any given time $t_n$ may be written

$$\varepsilon_{t_n} = \varepsilon_{et_1} [1 + \phi_n \zeta_{t_1} \rho^*(t_n - t_1)]$$

$$+ \sum_i \Delta\varepsilon_{et_i} [1 + \phi_n \zeta t_i \rho^*(t_n - t_i)]$$

$$+ \varepsilon_{su} (\rho^*_{t_n} - \rho^*_{t_1})$$

where the symbols are as previously defined.

Observations of the behavior of beams indicate that in practice, shrinkage affects only longitudinal displacements of the member, and creep, the rotations. For the calculation of deformations in flexural members, the effect of shrinkage may be considered negligible (except in the case of a considerable percentage of tensile reinforcement) and the term $\varepsilon_{su}(\rho^*_{t_n} - \rho^*_{t_1})$ is eliminated in the above formula. Finally the first term is valid only if the stress is constant during the period under consideration.

R12.22 Determination of Deformation Modulus for Axial Strains

1. For instantaneously applied loads or rapidly varying (dynamic) loads the axial strain of a concrete of age t days may be evaluated by the formula:

$$E_c = 21000 \quad f'_c(t)$$

applicable if the service load stress levels do not exceed 0.3 $f'_{ct}$.

In this expression, $f'_c(t)$ represents the characteristic compressive strength of the concrete at age t days. $E_c$ and $f'_c(t)$ are expressed in $kg/cm^2$.

2. The effective modulus corresponding to constant sustained loads (permanent or dead loads prestressing forces) may be deduced from the instantaneous modulus by taking into account the various strains to which the concrete is subjected. (R12.3). The effective modulus for all strains may be taken equal to

$$E_{ce} = \frac{21000 \quad f'_c(t)}{1 + \phi_n}, \ \phi_n \text{ being defined in R12.32}$$

For estimating purposes, $\phi_n$ may be assumed to be equal to 2, hence,

$$E_{ce} = 7000 \quad f'_c(t)$$

The coefficient 21000 applies only on the assumption that $f'_c$ obtained from a cylindrical specimen test (cf. R12.11 and Supplement M12.22). In the above formulas for $E_c$ and $E_{ce}$, $f'_c(t)$ is the compressive strength of the concrete at the time of the application of the loads considered; for ages greater than 28 days, the 28-day strength is assumed.

# APPENDIX III-A

## THE RATE-OF-CREEP METHOD FOR PREDICTING COLUMN STRAINS

## APPENDIX III-A

## THE RATE-OF-CREEP METHOD FOR PREDICTING COLUMN STRAINS

### Introduction

The rate of creep-method for predicting column creep and shrinkage strains appears to have been developed independently by Peabody (53) and Morsh (54). The method was modified by Holm and Pistrang and the derivation is given in their paper "Time-Dependent Load Transfer in Reinforced Lightweight Concrete Columns" (52). In a discussion of this paper, further modifications were suggested by both Illston and Leonhard to take into account the interdependence between creep and shrinkage. Pfeiffer, in his study "Reinforced Lightweight Concrete Columns" (51) used the method in the form suggested in Leonhard's discussion of Holm and Pistrang's paper. The equation suggested by Leonhard incorporates two simplifications which tend to result in a slight overestimation of the time-dependent steel stress. The error introduced is approximate proportional to the reinforcement ratio. These simplifications are not included in the development given below, but will be identified to allow comparison. The development is similar to that given by Holm and Pistrang but has been modified to use notations consistent with previously developed equations.

### Derivation of Time-Dependent Stress-Strain Equations

The initial or elastic stresses in the concrete and in the reinforcement may be obtained by the transformed area method. The average unit stress on the column is:

$$\sigma_{ave} = \frac{P}{A_g} \tag{1}$$

where:

$P$ = applied load

$A_g$ = gross area of the reinforced column

The transformed area ratio

$$\alpha_{gc} = 1 + (\eta - 1)\,\rho \tag{2}$$

where:

$\eta$ = modular ratio, $E_s/E_c$

$\rho$ = reinforcement ratio, $A_s/A_g$

The initial concrete stress is

$$\sigma_c = \frac{\sigma_{ave}}{\alpha_{gc}} \tag{3}$$

and the initial stress in the reinforcement is

$$\sigma_s = \eta\ \sigma_c \tag{4}$$

As creep and shrinkage takes place, the stress in the reinforcement increases. Since equilibrium must be maintained at all times, this increase is compensated by a decrease in the concrete stress. Equilibrium is satisfied when

$$\Delta\sigma_s\ \rho = -\ (1-\rho)\ \Delta\sigma_c$$

Hence, for any time increment $\Delta t$,

$$\Delta\sigma_s = -\ \frac{1-\rho}{\rho}\ \Delta\sigma_c \tag{5*}$$

and in the limit, as $\Delta t \to 0$

$$\frac{d\sigma_s}{dt} = \frac{-(1-\rho)}{\rho}\ \frac{d\sigma_c}{dt} \tag{6}$$

Furthermore, for any time increment $\Delta t$, the creep deformation of the concrete must be compatible with the increased strain in the reinforcement, $\Delta\sigma_s/E_s$. The creep deformation of the concrete consists of two components, the creep due to the average concrete stress, $(\sigma_c \Delta C_t)/E_c$, and the elastic recovery due to the decrease in the concrete stress occurring as creep takes place. Hence,

$$\left(\frac{d\sigma_s}{dt}\ \Delta t\right)\ \frac{1}{E_s} = \sigma_c\ \left(\frac{1}{E_c}\ \frac{dC_t}{dt}\ \Delta t\right) + \frac{1}{E_c}\ \left(\frac{d\sigma_c}{dt}\ \Delta t\right) \tag{7}$$

---

* In Leonhard's solution the ratio $(1-\rho)/\rho$ is approximated by $1/\rho$. This simplification tends to overestimate $\sigma_s$ for high reinforcement ratios.

Dividing Eq. 7 by $\Delta t/E_c$ and substituting Eq. 6:

$$-\frac{1-\rho}{\eta\rho}\frac{d\sigma_c}{dt} = \sigma_c\frac{dC_t}{dt} + \frac{d\sigma_c}{dt}$$

Hence,

$$\frac{1}{\sigma_c}\frac{d\sigma_c}{dt} = -\frac{\eta\rho}{1+(\eta-1)\rho}\frac{dC_t}{dt}$$

$$= -\frac{\eta\rho}{\alpha_{gc}}\frac{dC_t}{dt} = -\rho_e\frac{dC_t}{dt} \qquad (8)$$

where:*

$$\rho_e = \frac{\eta\rho}{\alpha_{gc}} = \frac{\eta\rho}{1+(\eta-1)\rho}$$

Integrating Eq. 8 between the limits t=0 and t, and since $C_t=0$ and $\sigma_{ct} = \sigma_c$ for t=0:

$$\ln\sigma_{ct} - \ln\sigma_c = \ln\frac{\sigma_{ct}}{\sigma_c} = \rho_e C_t$$

hence,

$$\sigma_{ct} = \sigma_c e^{-\rho_e C_t} \qquad (9)$$

The decrease in the concrete stress is

$$\Delta\sigma_c = \sigma_c - \sigma_{ct} = \sigma_c(1-e^{-\rho_e C_t})$$

hence, by Eq. 5, the increase in the steel stress is

$$\Delta\sigma_s = \frac{1-\rho}{\rho}(1-e^{-\rho_e C_t})\sigma_c$$

The stress in the reinforcement at time t is therefore,

$$\sigma_{st} = \sigma_s + \Delta\sigma_s = [\eta + \frac{1-\rho}{\rho}(1-e^{-\rho_e C_t})]\sigma_c$$

$$= [\frac{1+(\eta-1)\rho}{\rho} - \frac{1-\rho}{\rho}e^{-\rho_e C_t}]\sigma_c$$

$$= [\frac{\eta}{\rho_e} - \frac{1-\rho}{\rho}e^{-\rho_e C_t}]\sigma_c$$

---

* Leonhard uses a constant $\alpha=\eta\rho/(1+\eta\rho)$, i.e., the effect of the concrete displaced by the reinforcement is neglected.

$$\sigma_{st} = \frac{\sigma_s}{\rho_e} - \frac{1-\rho}{\rho}\sigma_{ct} = \frac{\sigma_{ave} - (1-\rho)\sigma_{ct}}{\rho} \tag{10}$$

Shrinkage

Following the suggestion of Illston and Leonhard, shrinkage is assumed to be a time-dependent function which is proportional to creep at all times. Thus,

$$\varepsilon_{st} = \sigma_{se}\,\varepsilon'_{ct} \tag{11}$$

where:

$\varepsilon'_{ct} = \frac{C_t}{E_c}$, the creep strain per unit stress.

Thus, $\sigma_{se}$ has the dimension of stress per unit area and in particular, for the limiting values of the creep coefficient, $C_u$, and the shrinkage, $\varepsilon_{su}$:

$$\sigma_{se} = \frac{\varepsilon_{su}\,E_c}{C_u} \tag{12}$$

For strain compatibility the change in strain in the reinforcement must be equal to the strain in the concrete due to shrinkage, hence,

$$\frac{1}{E_s}\frac{d(\Delta\sigma_{ss})}{dt} = \frac{d\,\varepsilon_{st}}{dt} + \frac{1}{E_c}\frac{d(\Delta\sigma_{cs})}{dt} + \frac{\Delta\sigma_{cs}}{E_c}\frac{dC_t}{dt} \tag{13}$$

where:

$\Delta\sigma_{ss}$ = change in steel stress due to shrinkage
$\Delta\sigma_{cs}$ = change in concrete stress due to shrinkage
$\varepsilon_{st}$ = shrinkage

For equilibrium, similar to Eq. 6,

$$\frac{d(\Delta\sigma_{ss})}{dt} = -\frac{(1-\rho)}{\rho}\frac{d(\Delta\sigma_{cs})}{dt}$$

and since $E_s = \eta\,E_c$, Eq. 13 may be written

$$-\frac{1}{E_c}\left(1 + \frac{1-\rho}{\eta\rho}\right)\frac{d(\Delta\sigma_{cs})}{dt} = \frac{1}{E_c}\left(E_c\frac{d\varepsilon_{st}}{dt} + \Delta\sigma_{cs}\frac{dC_t}{dt}\right) \tag{14}$$

From Eq. 11,

$$\frac{d\varepsilon_{st}}{dt} = \sigma_{se}\frac{d\varepsilon'_{ct}}{dt} = \frac{\sigma_{se}}{E_c}\frac{dC_t}{dt}$$

Substituting in Eq. 14 and multiplying by $E_c$,

$$- \left(\frac{1+(\eta-1)\rho}{\eta\rho}\right) \frac{d(\Delta\sigma_{cs})}{dt} = (\sigma_{se} + \Delta\sigma_{cs}) \frac{dC_t}{dt} \tag{15}$$

Hence,

$$\frac{1}{\Delta\sigma_{cs} + \sigma_{se}} \frac{d(\Delta\sigma_{cs})}{dt} = - \rho_e \frac{dC_t}{dt} \tag{16}$$

where $\rho_e$ is as defined for Eq. (8). Integrating between the limits t=0 to t,

$$\ln (\Delta\sigma_{cs} + \sigma_{se}) - \ln (\sigma_{se}) = - \rho_e C_t$$

hence,

$$\frac{\Delta\sigma_{cs}}{\sigma_{se}} + 1 = e^{-\rho_e C_t}$$

and hence, the change in the concrete stress due to shrinkage is:

$$\Delta\sigma_{cs} = - (1-e^{-\rho_e C_t}) \sigma_{se} \tag{17}$$

Since equilibrium must be maintained, the change in the steel stress is given by Eq. 5, hence,

$$\Delta\sigma_{ss} = - \frac{1-\rho}{\rho} \Delta\sigma_{cs} = \frac{1-\rho}{\rho} (1-e^{-\rho_e C_t}) \sigma_{se} \tag{18}$$

The corresponding strain in the reinforced member due to shrinkage of the concrete is therefore,

$$\varepsilon_{rs} = \frac{\Delta\sigma_{ss}}{E_c} = \frac{1-\rho}{E_s\rho} (1-e^{-\rho_e C_t}) \sigma_{se} \tag{19}$$

Substituting the value of $\sigma_{se}$ from Eq. (12), the limiting shrinkage strain in the column is

$$\varepsilon_{rs} = \frac{1-\rho}{\eta\rho} (1-e^{-\rho_e C_u}) \frac{\varepsilon_{su}}{C_u} \tag{20}$$

and the corresponding stresses in the concrete and reinforcement due to shrinkage are, respectively

$$\sigma_{cs} = - \sigma_{se} (1-e^{-\rho_e C_u}) \tag{21}$$

$$\sigma_{ss} = - \frac{1-\rho}{\rho} \sigma_{cs} \tag{22}$$

From Eq. 9 the limiting value of the concrete stress due to creep is

$$\sigma_{cr} = \sigma_c \, e^{-\rho_e C_u} \tag{23}$$

and of the stress in the reinforcement

$$\sigma_{sr} = \frac{\sigma_s}{\rho_e} - \frac{1-\rho}{\rho} \sigma_{cr} = \frac{\sigma_{ave} - (1-\rho) \sigma_{cr}}{\rho} \tag{24}$$

and the corresponding initial plus creep strain is

$$\varepsilon_{rc} = \frac{\sigma_{sr}}{E_s} \tag{25}$$

The final stress distribution and the strain due to the combined effects of elastic, creep and shrinkage deformation may be obtained by superposition.

# APPENDIX IV-A

## BEAMS WITH PIECEWISE CONSTANT MOMENTS OF INERTIA

## APPENDIX IV-A

## BEAMS WITH PIECEWISE CONSTANT MOMENTS OF INERTIA

### Piecewise Constant Section Approximation

In computing the deflection of continuous reinforced concrete beams, even beams of constant cross-section can not be automatically assumed to have constant section rigidity. Especially in T-beams, since the neutral axis lies closer to the extreme fiber of the flange than to the extreme fiber of the web, the section rigidity becomes very sensitive to the degree of cracking in the negative moment region. A more accurate estimate of the deflections of such beams, as well as of haunched beams, can be made if the beam is approximated by a beam with piecewise constant moments of inertia. The assumed moment of inertia in each section can then be computed as a function of the maximum moment in that section. While the latter procedure tends to underestimate the section rigidity in regions of low moment, this simplification may be shown to have a minor influence on the accuracy of the final results.

For continuous beams of constant cross-section the points of inflection (i.e., zero moment) are convenient points to delimit the regions of assumed piecewise constant rigidity as shown in Fig. IV. A.1.

For haunched beams, the assumed regions of piecewise constant rigidity may need to be determined from the geometrical properties of the haunch.

### Location of Points of Inflection

The exact location of the points of inflection can be calculated from the simple beam moment diagram if the support moments are known. For a uniformly loaded beam the centerline simple beam moment, $M_o$, is

$$M_o = \frac{w\ell^2}{8} \qquad (1)$$

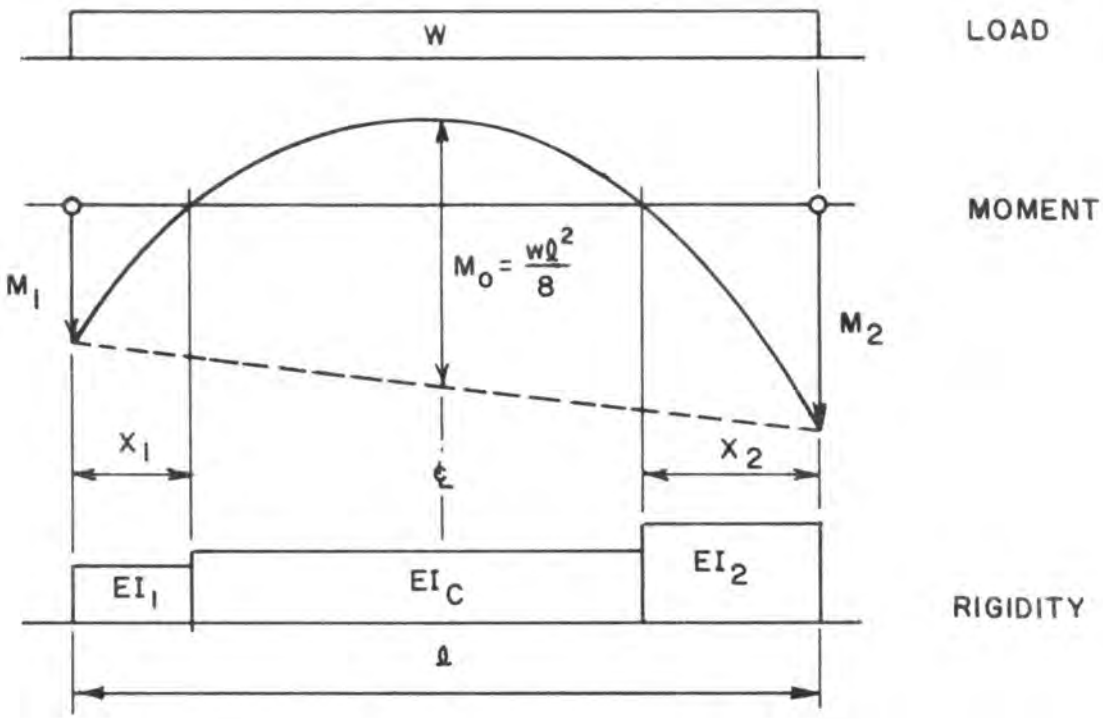


FIG. IV. A.1 ASSUMED REGIONS OF PIECEWISE CONSTANT SECTION RIGIDITY

where:

$w$ = uniformly distributed load intensity

$\ell$ = span length

Defining the dimensionless parameters

$$m_i = \frac{M_{ei}}{M_o} \qquad i=1,2 \tag{2}$$

$$X_i = \frac{x_i}{\ell} \qquad i=1,2 \tag{3}$$

where

$M_{ei}$ = the support moment

$x_i$ = distance from end of beam to point of contraflexure

Note that for the usual condition of negative support moments the parameters $m_i$ are negative. The locations of the points of inflection may then be shown to be determined by

$$X_1 = \frac{x_1}{\ell} = \frac{4 - (m_1 - m_2) - \sqrt{16 + 8\,(m_1 + m_2) + (m_1 - m_2)^2}}{8}$$

and

$$\chi_2 = \frac{x_2}{\ell} = \frac{4 - (m_2 - m_1) - \sqrt{16 + 8\,(m_1 + m_2) + (m_1 - m_2)^2}}{8} \qquad (4)$$

The values of $\chi_i$ may also be read off the graph in Fig. IV. A.2.

Centerline Deflection

The theoretical centerline deflection of the piecewise continuous beam may be computed by any appropriate method of mechanics. The calculations may be simplified somewhat by defining the following additional parameters:

$$\alpha_i = \text{relative haunch flexibility}, \quad \frac{K_c}{K_{ei}} = \frac{EI_c}{EI_i} \quad i=1,2 \qquad (5)$$

and

$$A_i = 8(1-\alpha_i)\ \chi_i^3(4-3\chi_i) \qquad i=1.2 \qquad (6)$$

$$B_i = 4(1-\alpha_i)\ \chi_i^2(3-2\chi_i) \qquad i=1,2 \qquad (7)$$

$$C_i = 8(1-\alpha_i)\ \chi_i^3 \qquad i=1,2 \qquad (8)$$

In the above definitions the subscripts i are used to denote ends 1 and 2.

With the above parameters, the centerline deflection may be shown to be given by

$$a = \frac{M_o \ell^2}{48K_c}\,[(5-A_1-A_2) + (3-B_1-C_2)m_1 + (3-B_2-C_1)m_2]^* \qquad (9)$$

The parameters A, B, and C may be conveniently evaluated by the use of the curves in Fig. IV. A.3. It may be noted that these constants are equal to zero for constant moment of inertia. For that case

$$a = \frac{M_o \ell^2}{48EI}\,[5 + 3(m_1 + m_2)] \qquad (10)$$

For a simply supported beam, $m_1 = m_2 = 0$ and Eq. 10.

---

*This equation was derived using the principle of virtual work. The details of the derivations are not given because of space limitations.

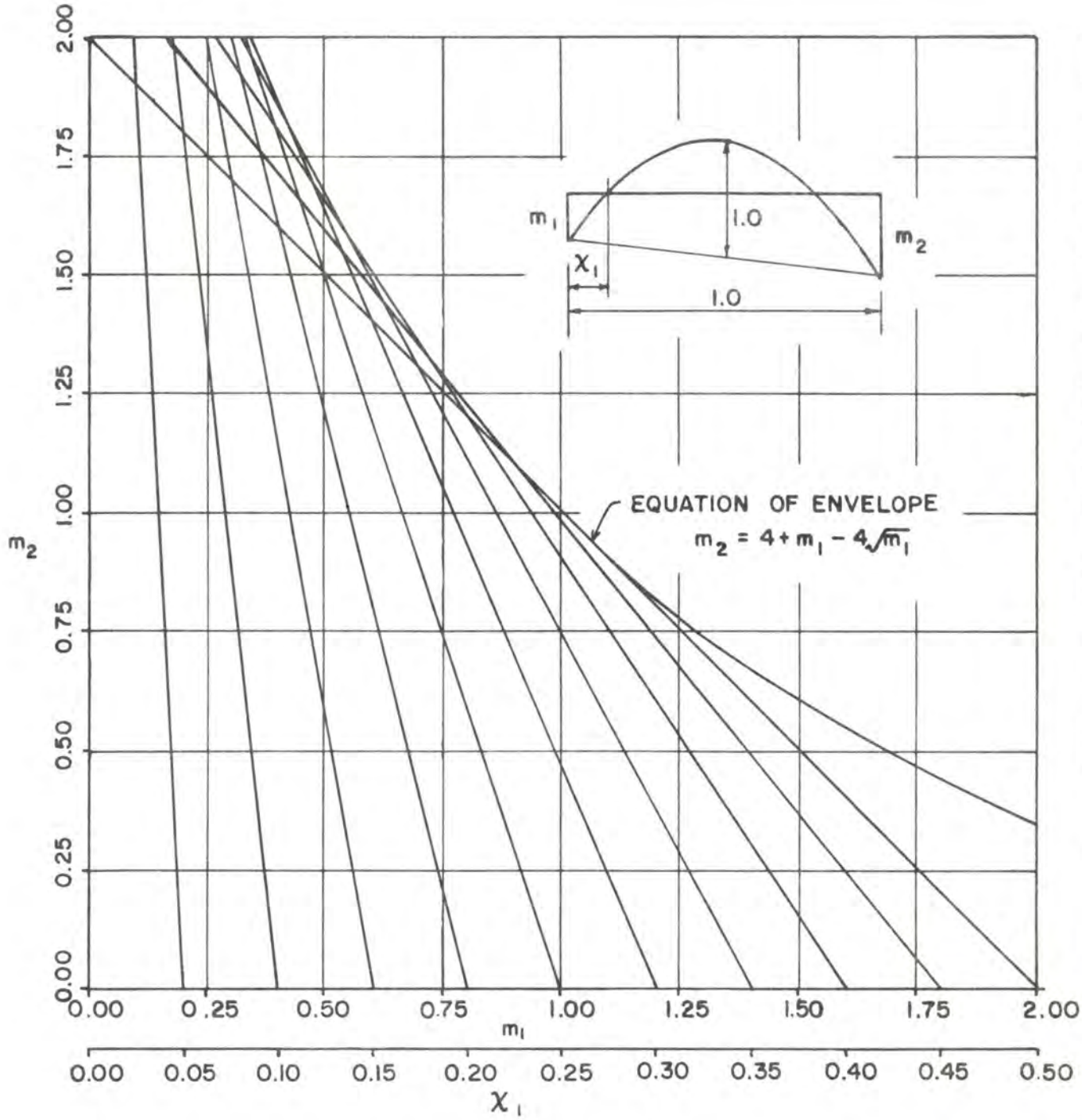


FIG. IV. A.2 LOCATION OF POINT OF CONTRAFLEXURE

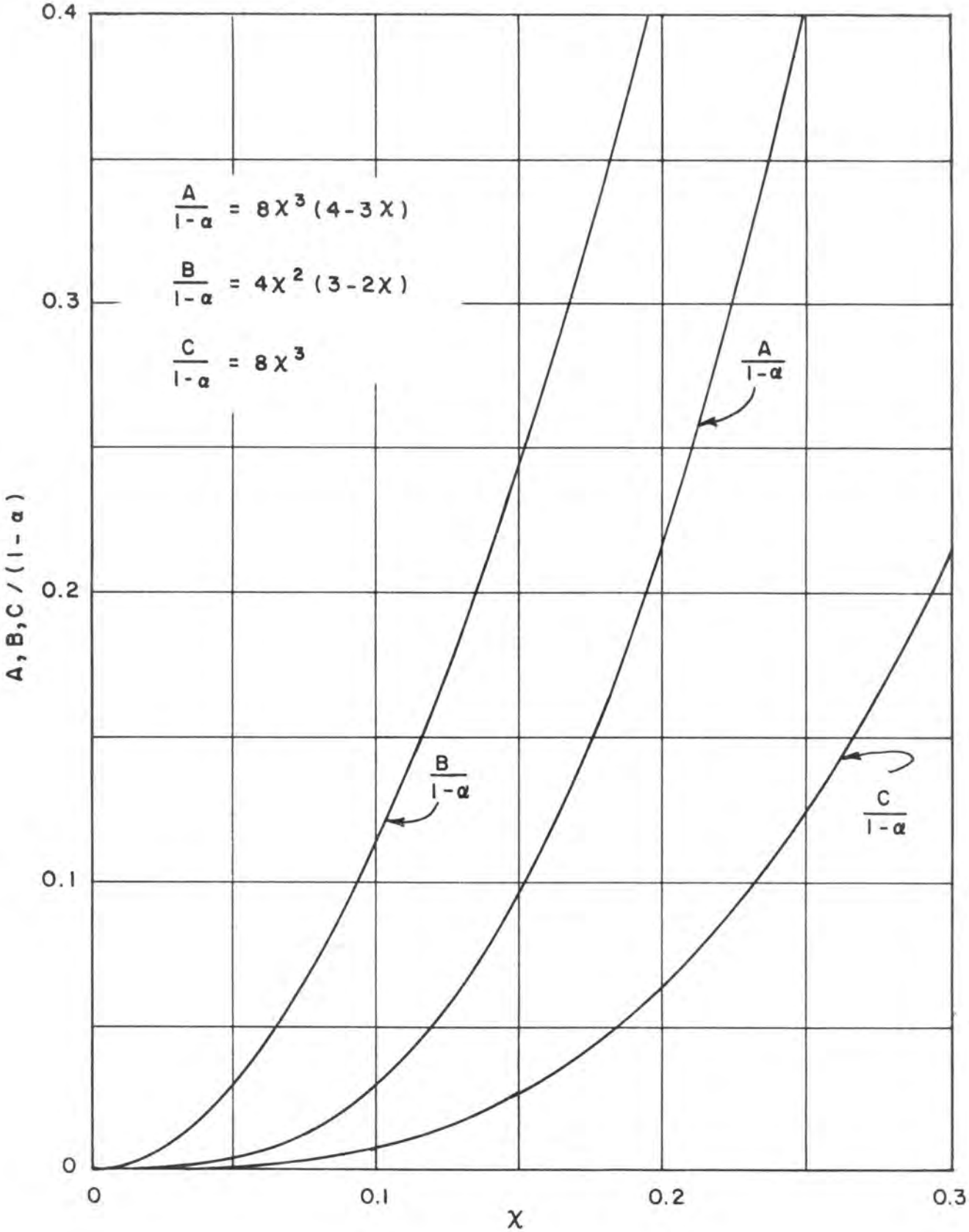


FIG. IV. A.3 STIFFNESS PARAMETERS A, B, AND C

reduces to the familiar form

$$a = \frac{5M_o\ell^2}{48EI} = \frac{5}{384}\ \frac{w\ell^4}{EI} \tag{11}$$

and for full end fixity, $m_1 = m_2 = -\frac{2}{3}$, hence

$$a = \frac{M_o\ell^2}{48EI} = \frac{w\ell^4}{384EI} \tag{12}$$

Computation of Support Moments

The support moments are a function not only of the load but also of the stiffness parameters of the members. In cracked-section analysis, the latter are in turn a function of the maximum moment in each critical region. The support moments and the effective member geometry are therefore interdependent. An iterative solution procedure may be used to compute support moments and member deflections consistent with the assumed moment-dependent section properties. To carry out these iterative steps, fixed end moments, stiffness and carry factors must be determined as a function of assumed geometry. These terms can conveniently be evaluated by the use of additional dimensionless parameters. The parameter D is defined by

$$D_i = 24(1-\alpha_i)\ \chi_i(1-\chi_i), \quad i=1,2 \tag{13}$$

and may be evaluated by the use of Fig. IV. A.4.

The three additional parameters required may be computed from combinations of parameters A, B, C and D. Thus:

$$E = 4 - (B_1 + B_2) \tag{14}$$

$$F_i = 8 - (C_1 + C_2) - D_i, \quad i=1,2 \tag{15}$$

$$G_1 = 8 + (A_1 - A_2) - 4B_1 \tag{16}$$

$$G_2 = 8 - (A_1 - A_2) - 4B_2 \tag{17}$$

Member end stiffness factor is generally defined as the moment which must be applied at the end of a member to produce unit rotation without displacement when the far end is held fixed. The carry-over factor is defined as the absolute value of the ratio of the moment induced at the

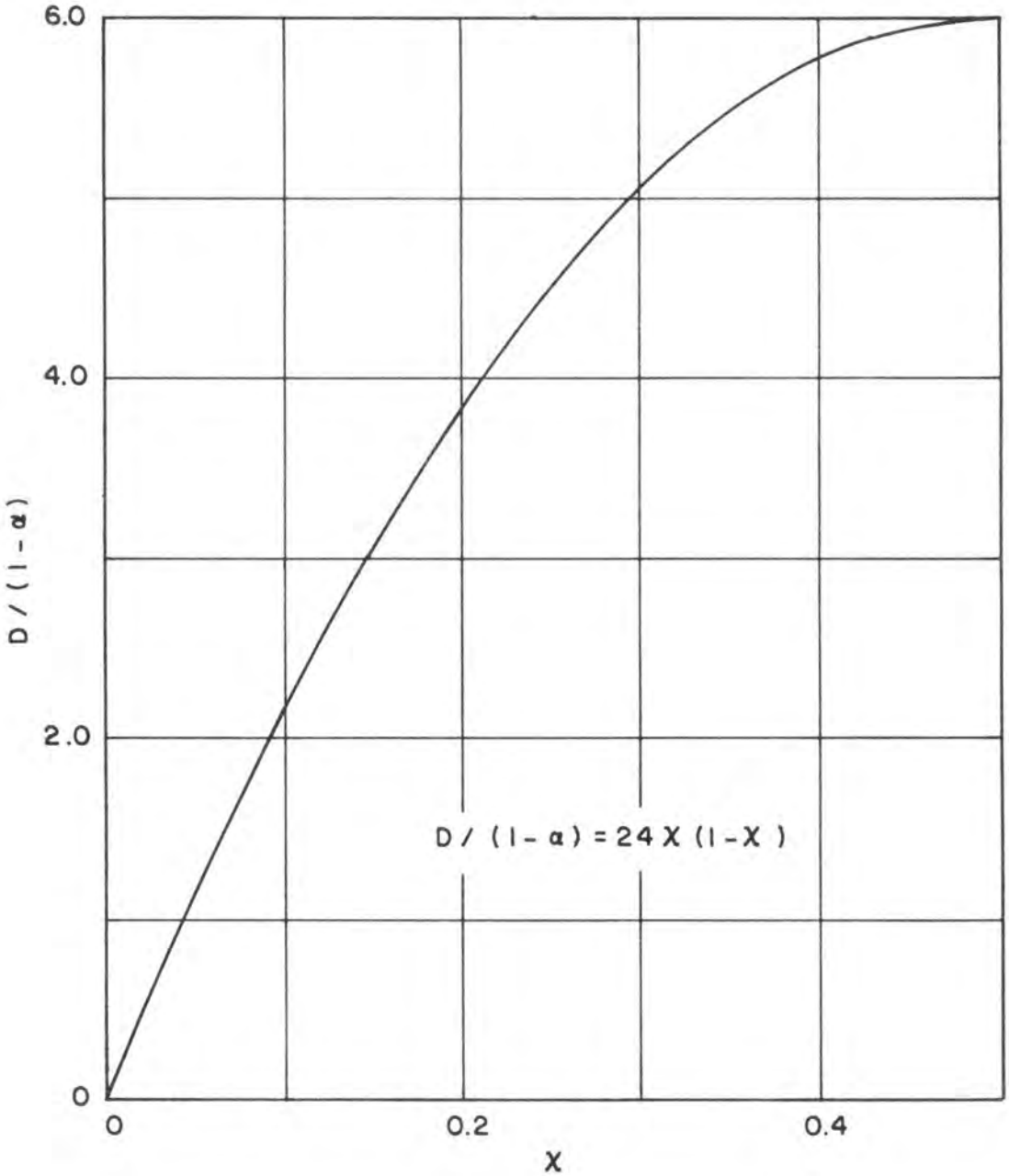


FIG. IV . A.4 STIFFNESS PARAMETER D

fixed end to the moment applied. The member stiffness factors* are then given by

$$K_1 = \frac{F_2}{F_1F_2 - E^2} \frac{24EI_c}{\ell} \tag{18}$$

and

$$K_2 = \frac{F_1}{F_1F_2 - E^2} \frac{24EI_c}{\ell} \tag{19}$$

and the corresponding carry-over factors* are

$$C_{12} = \frac{E}{F_2} \tag{20}$$

and

$$C_{21} = \frac{E}{F_1} \tag{21}$$

The fixed end moments* for a uniformly distributed load may be computed by:

$$M_1^{FE} = \frac{G_1F_2 - G_2E}{F_1F_2 - E^2} \frac{\omega\ell^2}{8} \tag{22}$$

and

$$M_2^{FE} = \frac{G_2F_1 - G_1E}{F_1F_2 - E^2} \frac{\omega\ell^2}{8} \tag{23}$$

Revised support moments may be computed by moment distribution, slope deflection or any other appropriate method of analysis. The effect of creep may be taken into account by using modified section rigidities. The deflection due to shrinkage may be computed by considering the effect of the warping moment due to restrained shrinkage.

Iterative Computation

Support moments may initially be estimated on the assumption of relative member stiffness based on gross section properties using moment distribution or other standard design analysis procedures. Section properties are next computed based on critical section moments

---

*These relationships were derived by application of the principle of virtual work. The details of these derivations are not included because of space limitations.

and the geometry of the equivalent members with piecewise constant moments of inertia is established. Fixed end moments, stiffness and carry-over moments may then be computed using the relationships given above. Revised support moments may then be computed and the geometry of the equivalent members modified. Several iterative steps may be required until the assumed geometry is consistent with revised support moments. Centerline deflections may then be computed for the assumed geometry of the members. This procedure has been found to be strongly convergent and for all practical purposes one iterative cycle should suffice. It should also be noted that the moment equations are based on the assumption of uniformly distributed loads. For other loadings, equivalent uniform loads should be used or else appropriate moment equations should be derived.

Journal Papers and Reports Related to this Project


Alcock, Donald C., and Pauw, Adrian, "Controlled-Deflection Design Method for Reinforced Concrete Beams and Slabs," Proc. Am. Conc. Inst., Title 59-22, Vol. 59, No. 5, 1962.

Pauw, A. and Meyers, B.L., "Apparatus and Instrumentation for Creep and Shrinkage Studies," Highway Research Record No. 34, Publication 1154, 1963.

Neville, Adam, M., and Meyers, Bernard L., "Creep of Concrete: Influencing Factors and Prediction," Am. Conc. Inst., Publication SP-9, Paper No. 1, 1964.

Pauw, Adrian and Meyers, Bernard L., "Effect of Creep and Shrinkage on the Behavior of Reinforced Concrete Members," Am. Conc. Inst. Publication SP-9, Paper No. 6, 1964.

ACI Committee 209, "Bibliography, Shrinkage and Creep in Concrete," Am. Conc. Inst., 1965.

Buettner, Donald R., and Hollrah, Ronald L., "Creep Recovery of Plain Concrete," Am. Conc. Inst., Journal Title No. 65-33, June, 1968.

Pauw, Adrian, "Time Dependent Deflections of a Box Girder Bridge," Am. Conc. Inst., Creep Symposium, Publication SP-27, Paper No. 6, 1970.



TE 5092.M8A3
no. 71-1
BORROW

Form DOT F 17
FORMERLY FORM

MoDOT Library
RD0016253